NEW APPROACHES IN HIGH PERFORMANCE

CAPILLARY ELECTROPHORESIS OF

BIOLOGICAL SUBSTANCES

By

WASSIM ABDEL-HAMID NASHABEH

Bachelor of Science

American University of Beirut

Beirut, Lebanon

1988

Submitted to the Faculty of the
Graduate College of the
Oklahoma State University
in partial fulfillment of
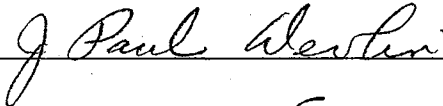the requirements for
the Degree of
DOCTOR OF PHILOSOPHY
May, 1993

NEW APPROACHES IN HIGH PERFORMANCE
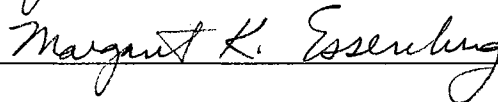
CAPILLARY ELECTROPHORESIS OF

BIOLOGICAL SUBSTANCES

Thesis Approved:

Ziad El Rami
Thesis Adviser

Horacio A Mottola

J Paul Devlin

Margaret K. Essenberg

Thomas C. Collins
Dean of the Graduate College

ACKNOWLEDGEMENTS

I would like to extend my profound and sincere appreciation to Dr. Ziad El Rassi, my research advisor, for his guidance, encouragement and friendship throughout the course of this study. His faith, patience and optimism have taught me a very valuable lesson: persistence and hard work pay off. Dr El Rassi has generously given so much of his time and effort, and for that I will be always indebted to him. As my time under his tutelage comes to an end, I am very grateful to have had the opportunity to study under him.

I would like to extend my gratitude to my committee members, Dr. Horacio A. Mottola, Dr. J. Paul Devlin and Dr. Margaret Essenberg for their support and valuable suggestions. In particular, I consider myself lucky to have had the privilege of attending courses in Analytical Chemistry presided over by Dr. Mottola and Dr. El Rassi.

Thanks are also due to the people in our research group, Daphne Tedford, Sharon Ringrose, Jianyi Cai, Jim Yu and Ying Zhang for their help and for sharing the ups and downs of doing research. Special thanks to Tim Smith for his friendship and help in the mass spectrometry experiments as well as in typing the list of symbols.

I made a number of friends while pursuing my degree at OSU. Thanks to Jamal, Imad, Marwan, Adnan, and Tracy. I am very grateful for my ex-roommate and friend, Abdel-Ghaffar, for sharing with me a long lasting friendship. Yehia, you have been a friend in the real sense of the word. It feels home being with you. I wish you every luck and happiness with Rida. I very much value you and I am so glad to have known you.

To Maria, for a wonderful time we shared together and for her continuos support and understanding.

I would like to dedicate this piece of work to the memory of my father, Abdel-Hamid, for his unconditional love and support. Jamile, my mother, you have made an enormous contribution over the years and I don't know of any way to thank you efficiently for all what you have done. You have always been my motivation and inspiration. A special thank to Amal, my lovely sister, and my brothers Mohamad and Zaher for their encouragement and for always believing in me. Mohamad, you are and always remain my intellectual guide and I will always seek your help and advice. I love you all.

Finally, I thank God for everything.

TABLE OF CONTENTS

VIII.   CAPILLARY ZONE ELECTROPHORESIS OF LINEAR AND
BRANCHED OLIGOSACCHARIDES

IX.   ENZYMOPHORESIS OF NUCLEIC ACIDS BY TANDEM
CAPILLARY ENZYME REACTOR-CAPILLARY ZONE
ELECTROPHORESIS

LIST OF TABLES

LIST OF FIGURES

Chapter III

Chapter IV

Chapter V

LIST OF SYMBOLS AND ABBREVIATIONS

a	radius of ionic solute
α	selectivity
δ	thickness of the double layer
Δh	difference in height between reservoirs
$\Delta M.I.$	group mobility index decrement
ΔP_{inj}	pressure difference across capillary
E	electric field
ε	dielectric constant
ζ	zeta potential
F-2000	fuzzy coating having PEG 2000 moieties
F-600	fuzzy coating having PEG 600 moieties
f	translational friction coefficient
g	gravitational constant
H	plate height
η	viscosity
I	ionic strength
I-200	interlocked coating having PEG 200 moieties
κ	Debye-Hückel constant
k'	capacity factor
K_M^{app}	apparent Michaelis constant
K_b	thermal conductivity of buffer
K_e	electrical conductivity

L	total length of the capillary
l	effective length of the capillary column
l_i	sample injection migration distance
μ_{app}	apparent mobility
μ_{ep}	electrophoretic mobility
μ_{os}	electroosmotic mobility
N	separation efficiency
n	peak capacity
v_{app}	apparent velocity
v_{eo}	electroosmotic velocity
v_{ep}	electrophoretic velocity
P	product
q	charge
ρ	surface charge density
R_1	capillary inter radius
R_s	resolution
σ_T^2	total variance
$\sigma_{\Delta K_e}^2$	variance induced by conductivity differences
σ_{det}^2	variance induced by detection volume
$\sigma_{\Delta h}^2$	variance induced by gravity flow
$\sigma_{i,e}^2$	variance induced by injection volume
σ_D^2	variance induced by molecular longitudinal diffusion
$\sigma_{v,h}^2$	variance induced by pressure flow
σ_w^2	variance induced by solute-wall interaction
σ_T^2	variance induced by temperature parabolic profile
S_i	substrate
t_{ads}	variance induced by residence time of adsorbed solute

t_{inj}	injection time
t_M	migration time
t_{mc}	migration time of micelle
t_o	migration time of bulk flow
t_r	retention time of solute in MECC
V	voltage
V_{max}	maximum velocity of enzymatic reaction
$W_{1/2}$	width of peak at half height
W_i	width of peak at inflection point
Ω_T	temperature coefficient of electrophoretic mobility
ψ_d	electric potential at the interface of the mobile and immobile parts of the double layer
ψ_o	electric potential at surface of the solid-liquid interface
2-AP	2-aminopyridine
6-AQ	6-aminoquinoline
ADA	adenosine deaminase
AGP	α_1-acid glycoprotein
Bu_4N^+	tetrabutylammonium bromide
CE	capillary electrophoresis
CF-LSIMS	continuous flow-liquid secondary ion mass spectrometry
CGE	capillary gel electrophoresis
CITP	capillary isotachophoresis
CZE	capillary zone electrophoresis
EDTA	ethylenediaminetetraacetic acid
EOF	electroosmotic flow
HCER	heterogeneous capillary enzyme reactor
HK	hexokinase

HPCE	high performance capillary electrophoresis
HPLC	high performance liquid chromatography
I.D.	inner diameter
IEF	isoelectric focusing
LSIMS	liquid secondary ion mass spectrometry
M.I.	mobility index
MECC	micellar electrokinetic chromatography
MES	2-[N-morpholino]ethanesulphonic acid
MS	mass spectrometry
MW	molecular weight
PEG	polyethylene glycol
PEI	polyethyleneimine
pI	isoelectric point
RSD	relative standard deviation
SDS	sodium dodecyl sulfate
TFA	trifluoroacetic acid

CHAPTER I

BACKGROUND AND RATIONALE

Introduction

Capillary electrophoresis (CE), also called high performance capillary electrophoresis (HPCE), is simply the miniaturized instrumental version of traditional electrophoresis. Electrophoresis, which was introduced more than a half century ago by Tiselius [1], is one of the separation methods based on rate processes, i.e., separations are attained *via* differences in the kinetic properties of the components of the mixture. In electrophoresis, electrically charged species are separated *via* differences in migration velocities through a supporting electrolyte under the influence of a direct-current electric field. In this sense, electrophoresis, like chromatography, is an important member of the class of differential migration methods. The major difference between both methods is that electrophoresis is a rate process separation method while chromatography is a phase equilibrium separation process.

High performance capillary electrophoresis, using sophisticated instrumentation and advanced capillary column technology, is rapidly developing into a powerful analytical technique for the high resolution separation of complex mixtures of biological, pharmaceutical and environmental significance. Unlike conventional electrophoresis, CE is amenable to automation and features high separation efficiency, small sample requirements and accurate quantitative analyses.

Free zone electrophoresis in open tubes was first demonstrated by Hjerten in 1967 [2] in rotating tubes of 3 mm inner diameter using high electric field strength and on-line

UV-detection for sensing the separated zones as they pass across the detection point. In 1974, Virtanen extended this seminal work to glass capillaries of smaller I.D. (200-500 µm) using potentiometric methods of detection [3]. Mikkers *et al* performed zone electrophoresis in instrumentation adapted from isotachophoresis employing teflon tubes of 200 µm I.D. [4]. These earlier studies did demonstrate only moderate separation efficiencies due to the relatively large injection volumes of the samples, a condition that was dictated by the poor sensitivity of detectors available at that time.

The major breakthrough in CE in terms of resolution and separation efficiency was realized when Jorgenson and Lukacs in 1981 performed the separations of amino acids and peptides in open tubes of 75 µm I.D. with on-column fluorescence detection [5,6]. This work has become the landmark for modern capillary electrophoresis. Three years later, the applicability of CE was extended to the determination of neutral species by Terabe *et al* who introduced micellar electrokinetic capillary chromatography (MECC) [7]. This important subdivision of CE allowed the separation of non-ionic compounds *via* their differential partitioning between a micellar pseudo-stationary phase and an aqueous phase. Other electrokinetic capillary chromatography methods were also reported including cyclodextrin [8], ligand exchange [9] and ion exchange [10]. These methods further extended the utility of CE to the determination of various types of species. Another major progress was accomplished by Cohen and Karger in 1987 who introduced for the first time sodium dodecyl sulfate (SDS)-polyacrylamide gel filled capillaries [11] and made significant contribution toward the utilization of these capillaries in the separation of large biomolecules and in particular oligonucleotides and DNA fragments [12,13].

These successive original works have demonstrated that HPCE is a promising new microseparation technique for the analytical determinations of ionic and neutral species. In fact, at the end of 1980's, commercial CE instruments have become available and the technique is increasingly gaining popularity as a complementary analytical tool for routine separations.

The aim of this chapter is to provide an overview of the fundamental aspects of CE and in particular capillary zone electrophoresis (CZE). First, brief accountings for the historical background, instrument set-up and different modes of contemporary CE techniques are provided. Second, an in-depth treatment is devoted to the basic mechanism of separation and solute migration in CZE. Third, the various factors contributing to band broadening in CZE are illustrated. Finally, a detailed description of the rationale, significance and scope of our study is provided at the end of this chapter. For clarity, additional backgrounds on the various research aspects of the thesis can be found in the introductory parts of the following chapters.

Instrument Set-up

One of the key advantages of HPCE is that it combines the high resolving power of traditional electrophoresis to the advanced instrumentation of HPLC. A schematic illustration of a home-made HPCE instrument is illustrated in Fig. 1. It comprises 5 major components: (i) a high voltage power supply of single or dual polarity capable of delivering 0-30 kV, (ii) a buffer filled fused-silica capillary with an inner diameter in the range 10-100 μm; the thin-walled capillary is protected from moist air or dust particles that promote the growth of fissures and cracks, making the capillary more weak and friable, by coating it with a protective polyimide film, (iii) a plexiglass safety box to protect the operator from high voltages; when opening the box to gain access to the high voltage electrode, the power supply is automatically turned off and in the meantime its output is shortened to the ground through the voltage relay, (iv) an on-column detection system, typically UV or fluorescence detector, placed near the grounded end of the capillary and (v) a read-out device. Additional features that are commonly found in commercial instruments include an automated capillary rinse and refill system to enhance system reproducibility, different methods of solute introduction e.g., pneumatic, electromigration
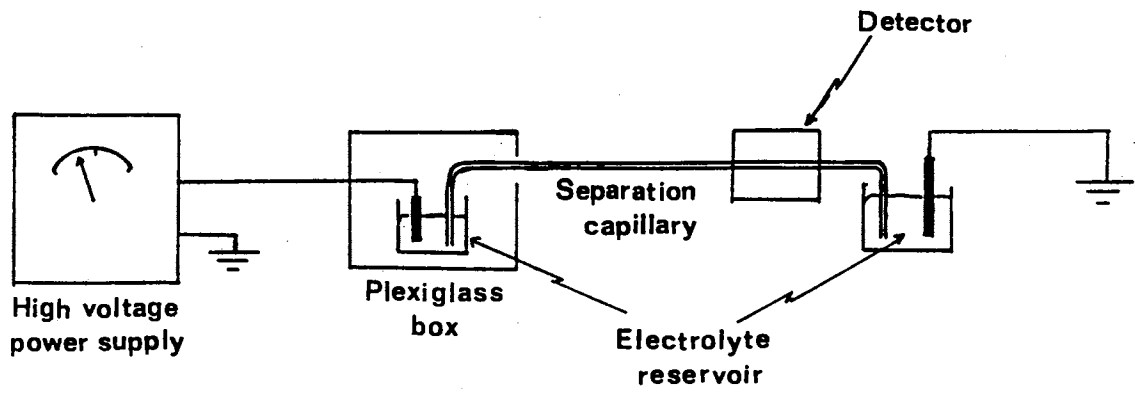
Figure 1. Instrument set-up for capillary electrophoresis

and gravity, a multiple position autosampler, a fraction collector and a computerized data acquisition system.

<center>Different Modes of CE</center>

Using the same basic instrumentation, HPCE can be performed in several modes to achieve a given separation. The origin of the different modes of separation may be attributed, in part, to the fact that CE has developed from a combination of many electrophoretic and chromatographic techniques [14]. Even though most applications have been performed using liquids as the separation media, capillary electrophoresis techniques encompass separations in which the capillary contains electrophoretic gels, various buffer additives or surfactants. The distinct modes of CE include CZE, capillary gel electrophoresis (CGE), MECC, capillary isoelectric focusing (CIEF) and capillary isotachophoresis (CITP). In all these modes, separations are achieved as the result of the unequal rate of migration of different solutes under the influence of an external electric field. This differential migration may be the result of variations in the overall charge, size, shape and/or complexation of the solutes with buffer additives.

<u>Capillary Zone Electrophoresis</u>

This mode is currently the most widely used technique in HPCE. It is analogous to elution chromatography in the sense that a narrow solute plug is introduced into a buffer filled capillary which yields discrete moving zones under the influence of an external applied field. Within the capillary tube, sample ions will migrate with a linear velocity proportional to their mobility and are thus resolved based on differences in their charge-to-mass ratio. CZE is perhaps the most universally useful mode of CE and by far the simplest electrophoretic technique due to the absence of any secondary influence, other

than the structure of the analyte and the nature of the carrier electrolyte. A detailed description of the principles of separation in CZE is provided in the next section.

Capillary Gel Electrophoresis

A powerful mode of CE for the separation of large molecular weight biopolymers is CGE. This mode is the electrophoretic analog of size exclusion chromatography. First introduced by Cohen and Karger [11], CGE has attained the highest separation efficiencies ever achieved by any analytical technique to date (up to 30 million theoretical plates per meter) [13]. The technique has several potential advantages over traditional gel electrophoresis namely, speed, high sensitivity, ease of automation and nanogram sample capabilities. As opposed to CZE, the fibrous nature of the polyacrylamide gel causes a size sieving effect in which small molecules migrate faster than larger size species, thus adding another separation mechanism. Also, the high viscosity of the gel provides an anti-convective medium particularly at the high surface area-to-volume ratios possible in narrow bore capillaries. CGE also minimizes longitudinal molecular diffusion of analytes, eliminates or greatly reduces the EOF and prevents solute-wall interactions, thus allowing higher separation efficiencies and concomitantly better resolution in shorter capillaries.

Capillary gel electrophoresis with buffer containing SDS has been introduced for the separation of peptides and proteins [11]. In this case, each SDS-solute complex has the same charge density and shape, and separation is based solely on the size or molecular weight (MW) of the solutes. A linear relationship exists between log MW of the species and their electrophoretic mobility, demonstrating that pure size separations can be achieved [11]. Gel columns have been shown to separate oligonucleotides on the basis of size or base number, a behavior that could not be achieved in free solution because mobility is roughly independent of size. High performance separations of DNA molecules have been achieved with single base resolution in short times [15].

However, the use of gel-filled capillaries is associated with several drawbacks that have greatly limited its widespread use. Most of these problems are related to the gel fabrication, reproducibility and stability of these columns as well as to bubble formations within the gel network under electrophoretic conditions. A more convenient approach has been the use of buffers containing entangled polymeric solutions acting as sieving additives [16-19]. As with CGE, these buffers provide anti-convective stabilizing media. The most important advantages of capillaries filled with entangled polymers over CGE are their flexibility and ease of operation. In addition, there is no problem of gel degradation or bubble formation. Candidate polymers need to be water soluble and preferably uncharged. Typical examples include hydroxymethylcellulose, polyethylene glycol and diethylaminoethyl-Dextran. The use of non-crosslinked polyacrylamide (liquidlike network) has been also reported for the separation of single stranded oligonucleotides [20].

Micellar Electrokinetic Capillary Chromatography

In 1984, Terabe and co-workers introduced MECC, a modified version of CZE, for the separation of neutral solutes [7]. In MECC, the separation medium consists of an electrolyte containing an ionic surfactant in an amount above its critical micellar concentration. Thus, there are two phases inside the capillary tube, an aqueous mobile phase and a micellar pseudo-stationary phase. Whereas the aqueous mobile phase moves at the velocity of electroosmosis, the micelles migrate much slower due to opposing electrophoretic forces. Analyte molecules are then separated *via* their differential migration between both phases, and they elute in the order of increasing hydrophobic character. Very polar solutes that do not interact with the micellar phase will elute first with the EOF at time t_o. On the other hand, very hydrophobic solutes that are completely solubilized by the micelles will elute last at the time t_{mc}. This produces a retention window that extends from t_o to t_{mc}. All neutral solutes are then separated between these two limits depending on their differential solubilization by the micelles. This elution range is often expressed as

the ratio t_o/t_{mc} and does influence the peak capacity n and resolution R_s in MECC through the following equations [7]:

$$n = 1 + \frac{\sqrt{N}}{4} \ln \frac{t_{mc}}{t_o} \qquad (1)$$

$$R_s = \frac{\sqrt{N}}{4} \times \frac{\alpha - 1}{\alpha} \times \frac{k'_2}{k'_2 + 1} \times \frac{1 - \frac{t_o}{t_{mc}}}{1 + \frac{t_o}{t_{mc}} k'_1} \qquad (2)$$

where α is the selectivity factor, N is the number of theoretical plates and k' is the retention factor which is calculated by the following equation:

$$k' = \frac{t_r - t_o}{t_o \left(1 - \frac{t_r}{t_{mc}} \right)} \qquad (3)$$

where t_r is the retention time of the solute. It follows then that the ability to tune the retention window to various levels can drastically improve the resolution and peak capacity of the electrophoretic system. In this regard, our laboratory has introduced micelles with adjustable surface charge density that are based on the complexation between alkylglucoside and borate ions at alkaline pH [21].

MECC has evolved into a powerful analytical tool for the separation of neutral species and chiral racemates. The ability to manipulate the micellar phase can affect the system selectivity and is analogous to changing the stationary phase in HPLC. MECC has the advantage that changing the micellar phase is very easy, requiring only that the capillary be rinsed and filled with the new micellar solution. These phases can be either anionic or cationic. Anionic surfactants include SDS [7], sodium decyl sulfate [22], sodium dodecyl sulfonate [23], sodium N-lauroyl-N-methyltaurate [24] and octylglucoside-borate complexes [21]. Cationic micelles are decyl-, dodecyl-, tetradecyl- and cetyltrimethylammonium salts [22,25-27].

Capillary Isoelectric Focusing

Another approach which has been incorporated into the capillary format is isoelectric focusing in which amphoteric molecules are separated on the basis of their isoelectric points, i.e., pI values [28-30]. This technique uses an ampholyte mixture as a background electrolyte to establish a pH gradient inside the capillary. Under the influence of an applied electric field, charged solutes migrate through the medium until the local pH is equal to their isoelectric points whereby the solutes gain neutrality and stop migrating. Consequently, zones are said to be focused. After focusing, the zones can be mobilized from the capillary *via* several approaches such as pressurized flow, salt addition to the catholyte or anolyte to produce a pH imbalance gradient or the use of electroosmotic pumping.

The resolving power in CIEF can be expressed in terms of the difference in pI, $\Delta(pI)$, of two adjacent species by [31]:

$$\Delta(pI) = 3\sqrt{\left(\frac{D_i[d(pH/dx)]}{E[-d\mu_{ep}/dpH]}\right)} \qquad (4)$$

where D_i is the mean diffusion coefficient of the solutes, μ_{ep} is the mean electrophoretic mobility, E is the applied field strength. Since the resolving power increases as $\Delta(pI)$ decreases, high resolution can be obtained for solutes with low diffusion coefficients, a high mobility slope at the isoelectric point [i.e., $d\mu_{ep}/dpH$], a shallow rate of change in pH with tube distance [i.e., $d(pH/dx)$] and a high electric field strength. CIEF has been very useful for the separation of proteins according to their isoelectric points.

Capillary Isotachophoresis

This mode is the electrophoretic analog of displacement chromatography, whereby all sample components migrate at the same velocity, a fact that gives the technique its name

(i.e., iso-tacho-phoresis = same + speed + movement). In CITP, the sample mixture is applied between two solutions of different ionic mobilities: a leading electrolyte being more mobile than any sample ion and a terminating electrolyte being the least mobile. Sample components condense between both electrolytes, producing a steady-state migrating pattern composed of consecutive zones each of which is completely separated by sharp boundaries from the preceding and the following zone. For example, in the separation of anions, a solution containing an anion of high electrophoretic mobility is placed in the anodic side and is used as the leading electrolyte. On the cathodic side of the sample, a solution containing an anion of low electrophoretic mobility is used as the terminating electrolyte. These leading and terminating electrolytes act to separate the anions of the sample from each other. The course of separation is usually monitored by the changes in absorbance or conductivity as each successive analyte reaches the detector. Unlike other CE modes where the amount of sample present can be determined from the area under the peak as in chromatography, quantitation in CITP is mainly based on the measured zone length which is proportional to the amount of sample present. In CITP, either cationic or anionic solutes can be determined but not both at once [32,33].

Principles of Separation in CZE

Since this study is a contribution to furthering the development of some aspects of capillary zone electrophoresis, the discussion in this section and thereafter will primarily cover CZE. However, many of the fundamental points addressed are also applicable to other related CE techniques.

Electrophoretic Mobility

When an external electric field E is applied to a charged solute, the solute experiences a force F_e which is equal to the product of its net charge q and the electrical field strength:

$$F_e = q \times E \tag{5}$$

This force is positive for positive ions and so it pushes them in the direction of the more negative electrode; the opposite applies to negative ions. The electrical force acting on a charged species accelerates it, but as the solute begins to move through the background buffer, it experiences a viscous drag force in the direction opposite to its direction of motion. This drag force F_d, which is proportional to the particle velocity v is given by:

$$F_d = f \times v \tag{6}$$

where f is the translational friction coefficient. It follows then that the particle is accelerated only to some limiting velocity, which depends on the strength of the applied electric field and the viscosity of the buffer solution [34]. This limiting velocity is called drift velocity or steady-state velocity and is achieved when the acceleration force is balanced by the retarding force as follows:

$$v = \frac{qE}{f} \tag{7}$$

Furthermore, the electrophoretic mobility μ_{ep} is defined as the steady-state velocity of the solute per unit field strength as:

$$\mu_{ep} = \frac{v}{E} = \frac{q}{f} \tag{8}$$

The magnitude of μ_{ep} depends on the net charge on the molecule and its frictional properties (size or shape) as well as the dielectric constant ε and the viscosity η of the running buffer. The relationship is given by [35]:

$$\mu_{ep} = \frac{2\varepsilon\zeta}{3\eta}F(\kappa a) \tag{9}$$

where ζ is the zeta potential, κ is the Debye-Huckel constant and a is the radius of the ionic solute. The parameter $F(\kappa a)$ is a constant whose value depends on the shape of the migrating species. Its value varies between 1 and 1.5. It should be emphasized that differences in the electrophoretic mobilities of the solutes form the basis for the selectivity of CZE separations.

Electroosmosis

CZE separations are exclusively performed on fused-silica capillaries, whose inner wall becomes negatively charged under most pH conditions due to the ionization of the surface silanol groups. Because of this charged surface, ionic species with similar charge sign (co-ions) are repelled from the surface, while ionic species with opposite sign (counterions) are attracted to the capillary wall. This results in the formation of an electric double layer at silica-solution interface. Part of these counterions are immobilized by electrostatic interactions with the surface, while others (due to thermal motion) reach further into the liquid forming the mobile or diffuse layer. Because of this spatial distribution of ions within the electric double layer, an electric potential gradient arises as outlined by the Stern-Gouy-Chapman theory [36].

Figure 2 illustrates the electric potential gradient at the capillary wall-liquid interface inside the capillary. ψ_o is the electric potential at the surface. The electric potential first decreases linearly in the compact region and then exponentially in the diffuse region while entering the liquid, because the space charge diminishes. The electric potential at certain
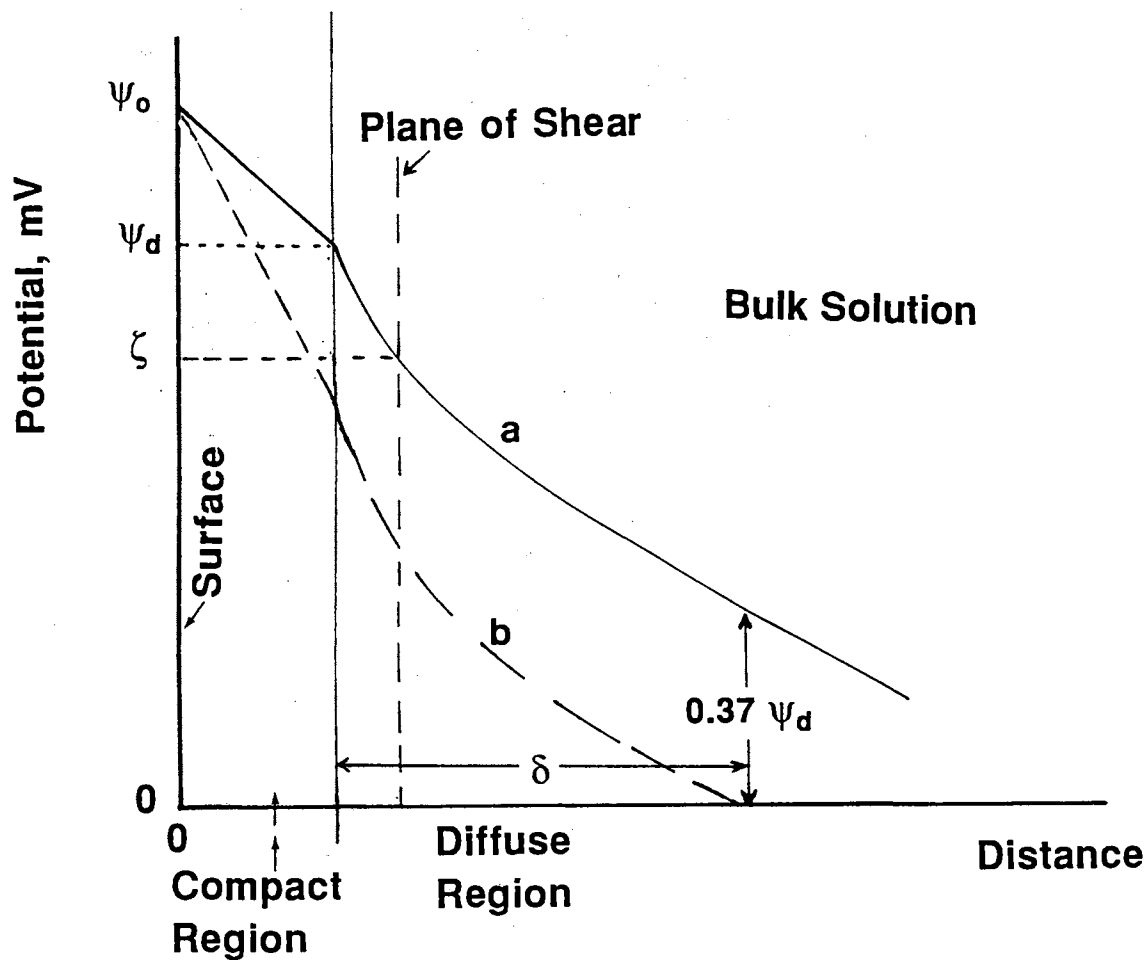
Figure 2. Stern-Gouy-Chapman model of the electric double layer. Curves a and b depict the electric potential gradient at the capillary wall-liquid interface using water and salt containing electrolytes, respectively.

planes in the liquid is used to characterize the double layer. ψ_d is the electric potential at the interface between the immobile and mobile parts of the double layer. The thickness of the double layer δ is defined as the length between the two planes where the electric potential is $(1/e)\psi_d$ and ψ_d, respectively [37]. A third characteristic electric potential is the ζ potential, which is the potential at the plane of shear occurring when the liquid is forced to move.

When an electric field is applied tangentially to the surface, it causes the hydrated counterions in the diffuse layer to migrate toward the oppositely charged electrode. The electrolyte is dragged along by these ions, which causes a liquid flow or electroosmotic flow (EOF) in the direction of the counterions. The linear velocity of the electroosmotic flow v_{eo} is given by [38]:

$$v_{eo} = \frac{\varepsilon}{4\pi\eta} E\zeta \tag{10}$$

where the zeta potential is expressed as [39]:

$$\zeta = \frac{4\pi\delta\rho}{\varepsilon} \tag{11}$$

where ρ is the surface charge density of the capillary surface. Modern electrolyte theory equates δ to $1/\kappa$. Equation 11 can thus be rearranged to:

$$\zeta = \frac{4\pi\rho}{\kappa\varepsilon} \propto \frac{1}{\sqrt{I}} \tag{12}$$

where I is the ionic strength of the medium. It follows then that increasing the ionic strength of the buffer would decrease EOF (Figure 2, curve b), while increasing the surface charge density (by increasing pH), the dielectric constant or the applied voltage would increase EOF.

The electric double layer is typically very thin (in the order of few hundred nanometers) compared to the inner diameter of the capillary. Therefore, the electroosmotic

flow can be considered to originate at the walls of the capillary. This results in a flat or plug flow profile (see Figure 3) as opposed to the parabolic flow profile observed with pressure driven flow, thus enhancing the separation efficiencies. Another advantage of the electroosmotic flow is that in most cases, it is faster than the electrophoretic mobilities of most species. It follows then that all solutes in the capillary will travel toward one end regardless of their net charge, allowing first the detection of positively charged species, followed by neutral and then negatively charged solutes. As shown in Figure 3, positively charged species are attracted towards the cathode and their speed is augmented by the EOF. Because their charge-to-mass ratio is zero, all neutral solutes migrate unresolved with the EOF and exit the capillary after the cations. Finally, the anions which are electrophoretically attracted towards the anode, are swept towards the cathode with the EOF. The EOF will add the same velocity component to all species regardless of their radial position and charge and consequently would not cause band broadening in the capillary directly. Thus, a relatively strong EOF is needed for the simultaneous determination of oppositely charged solutes in a single electrophoretic run by CZE. However, such strong flow may be detrimental to the resolution of early eluting peaks. A substantial amount of work has been carried out to introduce ways for manipulating the EOF. The various methods developed thus far, for the control of the magnitude and direction of EOF are discussed in the introductory parts of chapters 3 and 4.

Apparent Mobility

What is directly measured in a CZE experiment is an apparent mobility. This apparent mobility contains both an electrophoretic and electroosmotic components. The relationship is given by:

$$\mu_{app} = \mu_{ep} + \mu_{eo} \tag{13}$$

and similarly
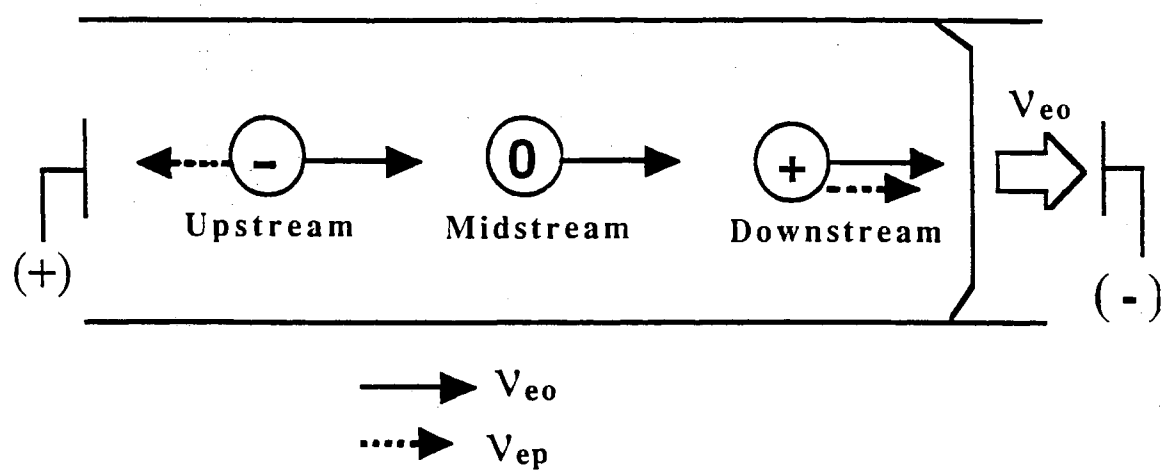
Figure 3. Separation in CZE with open tubes

$$v_{app} = v_{ep} + v_{eo} = \left(\mu_{ep} + \mu_{eo}\right)E \qquad (14)$$

where v_{app} is the apparent velocity. The migration time t_M, i.e., the time for a solute to migrate from the injection end of the capillary to the detection point, is given by [40]:

$$t_M = \frac{l}{v_{app}} = \frac{lL}{\left(\mu_{ep} + \mu_{eo}\right)V} \qquad (15)$$

where

$$\mu_{eo} = \frac{v_{eo}}{E} = \frac{lL}{t_o V} \qquad (16)$$

t_o being the migration time of a neutral species such as phenol, acetone or mesityl oxide, l is the length from the point of sample injection to the detection point and L is the total length of the capillary between the electrode reservoirs. The apparent mobility can thus be calculated directly from the electropherogram using eqn 15 that can be rearranged to:

$$\mu_{app} = \frac{lL}{t_M V} \qquad (17)$$

The magnitude of the electrophoretic mobility in the presence of EOF can also be calculated from eqns 13, 16 and 17 as:

$$\mu_{ep} = \mu_{app} - \mu_{eo} = \frac{lL}{V}\left(\frac{1}{t_M} - \frac{1}{t_o}\right) \qquad (18)$$

where it has been assumed that the direction of the electrophoretic migration is in the same direction as that of the EOF.

Optimum Separation Efficiency

Band broadening in CZE can result from a variety of factors (see below). When conditions are properly designed, the major effect controlling band width is longitudinal

molecular diffusion of the solute inside the capillary. Using Einstein's law of diffusion, the statistical equivalence of the variance of the migrating zone width is given by [5,6,41]:

$$\sigma_L^2 = 2D_i t_M = \frac{2D_i L^2}{\left(\mu_{ep} + \mu_{eo}\right)V} \tag{19}$$

where D_i is the diffusion coefficient of the solute in the background electrolyte. Under these conditions, the maximum number of theoretical plates N and minimum height equivalent to a theoretical plate H achievable in a CZE system are expressed by:

$$N = \frac{L^2}{\sigma_L^2} = \frac{\left(\mu_{ep} + \mu_{eo}\right)V}{2D_i} \tag{20}$$

and

$$H = \frac{L}{N} = \frac{2D_i L}{\left(\mu_{ep} + \mu_{eo}\right)V} \tag{21}$$

Both N and H can be readily calculated from the electropherogram by the following equation:

$$N = 5.54\left(\frac{t_M}{W_{1/2}}\right)^2 = 4\left(\frac{t_M}{W_i}\right)^2 \tag{22}$$

where $W_{1/2}$ and W_i are the width of the peak at half height and inflection point, respectively. From eqn. 20, it follows that high efficiency will be obtained by applying high voltages, i.e., by limiting the residence time of the solutes in the column. Efficiency will also be highest for large ions like proteins, as they are less diffusive (D_i in the order of 10^{-10} m^2/ sec) than small molecules (D_i in the order of 10^{-9} m^2/ sec). It is interesting to note that those analytes that would show reduced efficiency in HPLC (through the influence of D_i on mass transfer) perform best in CZE. However, due to non-diffusional band broadening (deviation from ideal behavior), lower efficiencies, although still

impressive when compared to HPLC, will generally be observed (see next section for details).

<u>Resolution</u>

While the plate height describes the dispersion of solute ions and the quality of overall separation, it is not adequate to describe the extent of separation between two adjacent species. For the latter case, the resolution R_s is used as a quantitative measure for the degree of separation of two components. In principle, the resolution is defined as the ratio of the distance between the peak maxima, Δt_M, to the mean band width of two neighboring peaks, $\overline{W}$ [42]:

$$R_s = \frac{\Delta t_M}{\overline{W}} = \frac{2(t_{M,2} - t_{M,1})}{(W_1 + W_2)} = \frac{\Delta t_M}{4\overline{\sigma_t}}$$ (23)

where $t_{M,1}$ and $t_{M,2}$ are the migration times, W_1 and W_2 are the peak widths measured by the baseline intercept, and $\overline{\sigma_t}$ is the mean standard deviation. Based on this general equation of resolution, Jorgenson and Lukacs derived the following expression for resolution in CZE [5,6]:

$$R_s = \frac{1}{4}\sqrt{N}\frac{\Delta v}{\overline{v}} = \frac{1}{4\sqrt{2}}(\mu_{ep,1} - \mu_{ep,2})\sqrt{\frac{V}{D_i(\overline{\mu_{ep}} + \mu_{eo})}}$$ (24)

where Δv is the difference in zone velocities, $\overline{v}$ is the average zone velocity, $\mu_{ep,1}$ and $\mu_{ep,2}$ are the electrophoretic mobilities for the two adjacent solutes and $\overline{\mu_{ep}}$ is their average electrophoretic mobility. When the average electrophoretic mobility becomes equal, but opposite in sign, to the electroosmotic mobility (i.e., $\overline{\mu_{ep}} = -\mu_{eo}$) resolution approaches infinity. But the same will be true for the separation time. This can be carried out by balancing EOF to be equal in magnitude and opposite in direction to the solute electrophoretic migration. Another approach to enhance the system resolution is to use

longer columns with higher applied field strength. However, as will be shown in the next section, the applied voltage cannot be increased beyond certain limits due to Joule heating effects.

Other Factors Contributing to Band Broadening
in Capillary Zone Electrophoresis

Thus far, we have considered longitudinal molecular diffusion as the only source of dispersion in CZE. If this is true, for a macromolecule electrophoresed under typical CZE conditions, one would expect separation efficiencies to be on the order of 10^6 theoretical plates. However, such high plate number is rarely achieved in routine biopolymer separations. In addition, according to eqn 20, an increase in the applied voltage should yield a monotonic increase in the efficiency. On the contrary, we [43] and other researchers [44] have found that in the separations of proteins, higher applied potential drop drastically reduced the separation efficiencies. In some instances, we have also observed solute denaturation and/or excessive peak tailing under conditions of high potential drop or sample overloading. This is because a number of additional factors contribute to band spreading in CZE. In this section, we will briefly discuss these non-diffusional contributions to zone broadening, namely Joule heating, injection volume, detection volume, conductivity differences and solute-wall interactions, and outline the optimum operating conditions for a given separation problem.

Joule Heating

In electrophoresis, the electrokinetic energy is released as heat, the Joule effect. Thus, a major limitation on the speed of CZE separations is the ability to dissipate the joule heat arising from the passage of electric current in the supporting electrolyte inside the tube. Joule heating can result in radial temperature gradient that can affect the quality of

separation in a number of ways. The heat evolved gives rise to a parabolic temperature distribution with a maximum at the axis of the tube, and consequently the system viscosity will be lower at the axis than at the wall of the capillary. Because the electrophoretic mobility is an inverse function of viscosity (see Eqn. 9), the parabolic temperature profile yields a parabolic velocity profile across the capillary [45]. Hjerten has showed that the viscosity decreases by about 2.7% per degree centigrade. Thus, if a zone has migrated 25 cm at the wall of the capillary, it has accordingly migrated 0.35 cm further at the tube axis for a temperature difference of only 0.5°C between the wall and axis of the capillary tube [41]. Such a large zone deformation can seldom be tolerated in CZE runs. Using an analogy to Taylor dispersion theory [46], Virtanen has developed an expression that describes the contribution of the temperature-induced parabolic velocity $\sigma_{\Delta T}^2$ to the total variance as [3]:

$$\sigma_{\Delta T}^2 = \frac{R_1^6 E^6 K_e^2 \Omega_T^2 \mu_{app}^2}{1536 D_i K_b^2} t_M \qquad (25)$$

where R_1 is the radius of the capillary tube, K_e is the electrical conductivity of the electrophoresis buffer, K_b is the thermal conductivity of the buffer and Ω_T is a temperature coefficient of the electrophoretic mobility defined as [47]:

$$\Omega_T = \frac{\mu_{ep,1} - \mu_{ep,2}}{\mu_{ep,1}(T_1 - T_2)} \qquad (26)$$

where $\mu_{ep,1}$ and $\mu_{ep,2}$ are the electrophoretic mobilities at temperatures T_1 and T_2, respectively. Referring to eqn 25, one should note the strong dependence of $\sigma_{\Delta T}^2$ on R_1 and E. This highlights the importance of performing CZE in capillaries with small inner diameters with efficient cooling to enable the use of high potential field. In fact, the maximized inner surface-area-to-volume ratios in small bore capillaries provide the most efficient way for heat dissipation. In this regard, our studies were exclusively carried out with fused-silica capillaries of 50 μm I.D. and the applied field strength was maintained at

moderate values in order to minimize the contribution of Joule heating variance to the observed band spreading. Also we have devised new electrophoretic methods that enabled the rapid separations of solutes at low applied field strengths, see chapters 3-5.

Injection Volume

The inherent high efficiency capabilities of CZE can be realized only when the injection system employed does not introduce significant zone broadening. It is imperative that the injection system should be capable of delivering small volume samples (typically several nanoliters) onto the column quantitatively and reproducibly. Under ideal conditions, the sample should be initially introduced as an infinitely thin zone. Obviously, this is an unrealistic assumption, since the injection zone has a finite width whose magnitude can affect the overall band dispersion. For a plug sample injection profile, Stenberg has derived a second moment or variance expression as follows [48]:

$$\sigma_i^2 = \frac{l_i^2}{12} \tag{27}$$

where l_i is the sample injection migration distance. However, this expression assumes that the solute is introduced as a rectangular plug, a condition rarely met under either hydrodynamic or electrokinetic injections.

In hydrodynamic injection, the sample is introduced into the capillary by applying a pressure difference across the capillary while one end of the capillary is immersed into the sample. Using Taylor dispersion theory and Poiseuille equation, an expression that accounts for the contribution of hydrodynamic injection $\sigma_{i,h}^2$ to the overall variance has been derived and is given by [47]:

$$\sigma_{i,h}^2 = \frac{R_l^6 \Delta P_{inj}^2}{1536 L^2 \eta^2 D_i} t_{inj} \tag{28}$$

where ΔP_{inj} is the pressure difference across the capillary tube and t_{inj} is the injection time. Alternatively, hydrodynamic injection can be performed by gravity flow through inducing a height difference between the buffer reservoirs. In this case, the pressure difference is caused by the height difference and eqn 28 can be modified to:

$$\sigma_{\Delta h}^2 = \frac{R_I^6 \Delta h}{L^2 \eta^2 D_i} t_{inj} \qquad (29)$$

In the case of electrokinetic injection, the sample is drawn to the capillary by a combination of the solute electrophoretic mobility and EOF. Thus, the amount of material is a function of the apparent mobility of the sample. The variance caused by electrokinetic injection can be deduced from eqn 25 by substituting t_{inj} for t_M [47]:

$$\sigma_{i,e}^2 = \frac{R_I^6 E^6 K_e^2 \Omega_T^2 \mu_{app}^2}{1536 D_i K_b^2} t_{inj} \qquad (30)$$

As shown in eqns 28-30, the variance induced by the injection volume decreases with decreasing the injection time. In view of this effect, we have maintained in our work the injection time of the solutes to the minimum time possible using both hydrodynamic (i.e., gravity-driven flow) and electrokinetic injections.

Detection Volume

In any detection scheme, a finite volume of the buffer is in contact with a flow cell or a sensing element (e.g., electrodes) at any given time. Therefore, the output of the detector represents a signal that is averaged over a finite volume. Stenberg derived a variance expression for the detection volume and noted that this variance is the same as that introduced by a rectangular injection plug as [48]:

$$\sigma_{det}^2 = \frac{l_j^2}{12} \qquad (31)$$

where l_j is the path length of the detector cell. Since CZE detection generally occurs on-column, the detection itself does not contribute to variance except in terms of the length of capillary segment making up the detector cell volume. Jones *et al* has shown that the detection variance is in the order of $9.52 \times 10^{-8} \, m^2$ for a typical UV detector [49]. This contribution to the total variance is usually minimal and subsequently, it will not be included in the total variance equation.

Conductivity Differences

The electrical current in an electrolyte solution is equivalent to a transport of ions. If a solute ion has the same mobility as the surrounding buffer, it will transport the current with the same efficiency as the buffer ions. The migrating solute zone will thus have the same electrical conductivity as the surrounding buffer. However, in all other cases, there will be a conductivity difference between a migrating solute zone and the surrounding medium, a phenomenon that can result in significant band broadening. Hjerten has derived a simple and approximative expression to describe conductivity-induced band broadening $\sigma^2_{\Delta ke}$ as [41]:

$$\sigma^2_{\Delta ke} = \left(\frac{\mu_{app} E t_M}{16} \right)^2 \left(\frac{\Delta ke}{ke} \right)^2 \tag{32}$$

where Δk_e is the conductivity difference between the buffer and the migrating zone and k_e is the conductivity of the buffer. Thus, to have minimum band broadening, k_e should be as small as possible and the ratio $\Delta k_e / k_e$ preferably be less than 0.5% [50]. In this regard, whenever possible, we have chosen background electrolytes whose ions have mobilities close to those of the sample ions and also used low sample concentration avoiding solute overloading that may lead to substantial loss in efficiency.

<u>Solute-Wall Interactions</u>

The tendency of silica surfaces to adsorb analyte molecules presents a potential problem in CZE, especially for macromolecules such as proteins. Adsorption of solute molecules by the capillary surface results in peak distortion and in certain cases irreversible adsorption may occur which inhibits the migration of the adsorbed species. However, upon coating the silica surface with a hydrophilic polymer, adsorption is usually minimized (see chapter 2 for details). This is because the coating is usually non-ionic and hydrophilic, and consequently reduces electrostatic interactions and engenders substantially weak hydrophobic interactions under conditions normally used in capillary electrophoresis. In addition, the polymer coating is usually dense enough to inhibit macromolecules from entering it due to sterical reasons and to the fact that electrophoretically migrating species tend to move where the hindrance to migration is the lowest [41].

However, in cases where the adsorption has not been eliminated by surface treatment or other approaches, its contribution σ_w^2 to the total variance can be determined by the following equation [51]:

$$\sigma_w^2 = 2C^2(1-C)v_{app}Elt_{ads} \tag{33}$$

where C is the concentration of free solute and t_{ads} is the mean residence time of the adsorbed solute. To diminish the variance induced by solute-wall interactions, we have introduced fused-silica capillaries with novel hydrophilic coatings that greatly minimized solute-wall interactions and enabled high separation efficiencies to be achieved.

<u>Total Variance</u>

According to statistical theory, the variance of a complex random process equals the sum of the variances generated by the individual processes, as long as they are

independent, i.e., the processes are not coupled. It follows then that for an electrophoretic peak, the observed total variance, may be expressed as:

$$\sigma_T^2 = \sum_n \sigma_n^2 \qquad (34)$$

where the sum is taken over all n contributions to the variance. In an ideal experiment, the variance arising from solute-wall interactions can be eliminated by coating the capillary surface or the appropriate choice of pH buffer. It follows then that the contributions to band broadening in CZE are molecular diffusion, parabolic temperature profile, finite injection volume and conductivity differences. Thus:

$$\sigma_T^2 = \sigma_D^2 + \sigma_{\Delta T}^2 + \sigma_i^2 + \sigma_{\Delta ke}^2 \qquad (35)$$

A comprehensive plate height equation can be written as:

$$H_T = \frac{2D_i t_M}{l} + \frac{R_1^6 E^6 K_e^2 \Omega_T^2 \mu_{app}^2}{1536 D_i K_b^2 l} t_M + \frac{R_1^6 \Delta P_{inj}^2}{1536 L^2 \eta^2 D_i l} t_{inj} + \left(\frac{\mu_{app} E t_M}{16 l}\right)^2 \left(\frac{\Delta ke}{ke}\right)^2 \qquad (36)$$

where hydrodynamic injection was assumed. In the case of electrokinetic injection, the total plate height equation is expressed by:

$$H_T = \frac{2D_i t_M}{l} + \frac{R_1^6 E^6 K_e^2 \Omega_T^2 \mu_{app}^2}{1536 D_i K_b^2 l} \left(t_M + t_{inj}\right) + \left(\frac{\mu_{app} E t_M}{16 l}\right)^2 \left(\frac{\Delta ke}{ke}\right)^2 \qquad (37)$$

Rationale, Significance and Scope of the Study

As indicated above, capillary electrophoresis is in fact an important microseparation technique. Although significant advances have been made, many aspects of the CE system still require further development and the exploitation of the full potentials of CE is yet to

come. The broad objective of this research was to contribute to the advancement of CZE methodology by providing (i) improved electrophoretic systems for the separation of important biological species (e.g., proteins, peptides, oligosaccharides and nucleic acids) and (ii) a better understanding of the underlying phenomena. Systematic studies which involved the development of inert capillary coatings and novel buffer systems as well as the enhancement of selectivity and sensitivity in CZE were pursued as a plausible route to this objective.

As mentioned earlier, the major problem encountered in CZE of biopolymers has been the pronounced affinity of polyionic macromolecules (e.g., proteins) to the negatively charged surface of fused-silica capillaries. This phenomenon often gives rise to band broadening and low recovery of the separated analytes. To provide a solution to this problem, we have developed and evaluated various hydrophilic polyether coatings on the wall of fused-silica capillaries. These coatings proved effective in shielding the silica surface toward solute-wall interactions, and consequently allowed the high separation efficiencies of proteins and their fragments (i.e., peptides, glycopeptides and glycans). Studies involving the detailed characterization of these polyether coatings are the subject of chapter 2. Their usefulness and behavior in the biological area are demonstrated in chapters 7-9.

However, the chemical modification of the capillary surface is always accompanied by a certain reduction in the electroosmotic flow (see above for description of EOF). This often leads to an increase in the separation time of the analytes, and in few instances restricts the ability of the CZE system to the determination of only similarly charged solutes. In this regard, we have investigated and introduced new ways by which the electroosmotic flow can be either tuned to any desired level or changed during the electrophoretic run independently of the applied voltage while keeping solute-wall interactions to a minimum level. The EOF control was addressed through two different approaches. In one approach, the flow was adjusted through coupled capillaries with

different magnitudes of flow. In a second approach, the electroosmotic flow was changed during analysis by using a multiport sliding valve device that permitted the switching among various set of coupled capillaries having different wall zeta potentials. Both systems were fully evaluated in terms of efficiency, electroosmotic flow velocity and reproducibility. These formats have the advantage of carrying out rapid biopolymer separations at relatively low field strength without sacrificing the high separation efficiency obtained with surface modified capillaries. The utility of the multiport sliding valve was also demonstrated and extended to fraction collection of separated analytes in short capillary segments. This simple scheme facilitated the quantitative transfer of the collected fractions to HPLC for further analysis or mass spectrometry for structural determinations. These studies are grouped in chapters 3-5.

A significant contribution of our undertakings, has been the introduction of CZE to the high resolution separation of oligosaccharides, namely the pyridylamino-derivatives of maltooligosaccharides, with naked fused-silica capillaries under electrolyte conditions whereby solute-wall interactions were minimized. In these studies (see chapter 6), we have introduced the concept of glucosyl mobility decrement, a parameter that may prove useful in correlating the mobility of derivatized oligosaccharides.

The high resolving power and reproducibility of CZE with the polyether coated capillaries enabled us (i) to enlarge the scope of applications of the technique and (ii) to study the electrophoretic behavior of biopolymers in the absence of solute-wall interactions over a wide range of conditions. We have demonstrated the potential of CZE with hydrophilic coatings in the mapping of peptide, glycopeptide and glycan fragments cleaved from glycoproteins. In addition, we have extended the utility of CZE to the separation of xyloglucan oligosaccharides from cotton cell walls. In this work, we have introduced a mobility indexing system for branched oligosaccharides with respect to well characterized linear homologous oligosaccharides. This mobility indexing system was useful in the quantitative determination of the effects of the various sugar residues on the electrophoretic

mobility of oligosaccharides. Furthermore, in these studies, we have introduced precolumn derivatization reactions that allowed the electrophoresis and sensitive detection of neutral oligosaccharides. Besides evaluating the traditionally used tagging agent, 2-aminopyridine, we have introduced a more sensitive labeling agent, 6-aminoquinoline (a UV absorbing, also fluorescent tag) in CZE of carbohydrates. These studies (see chapters 7 and 8) have provided electrophoretic systems which are expected to find general use in the biological and biomedical areas.

To conclude this research to an overall solid contribution to the advancement of capillary electrophoresis, we have also introduced a two-dimensional electrophoretic system in which short fused-silica capillaries having immobilized enzymes on the inner walls were coupled in series with capillaries having polyether hydrophilic coatings. This tandem format, which we refer to as capillary enzymophoresis, was evaluated in the area of nucleic acids to convert them to more readily separable and detectable species. Capillary enzymophoresis also proved useful in the on-line synthesis of oligonucleotides and in the on-line digestion and mapping of minute amounts of transfer ribonucleic acids. These studies are discussed in chapter 9.

The overall work has contributed to enlarging the scope of capillary electrophoresis by demonstrating its capabilities in areas that were not exploited previously and by introducing new devices and other components of the electrophoretic system that will facilitate the solution of many important analytical separation problems. The research has yielded new concepts that may path the way to increasing the utility of the technique.

References

1. A. Tiselius, *Nova Acta Regiae Soc. Sci. Ups.*, 7 (1930) 107.

2. S. Hjerten, *Chromatogr. Rev.*, 9 (1967) 322.

3. R. Virtanen, *Acta Polytech. Scand.*, 123 (1974) 1.

4. F. E. P. Mikkers, F. M. Everaerts and T. P. E. M. Verheggen, *J. Chromatogr.*, 169 (1979) 11.

5. J. W. Jorgenson and K. D. Lukacs, *Anal. Chem.*, 53 (1981) 1298.

6. J. W. Jorgenson and K. D. Lukacs, *Science,* 222 (1983) 266.

7. S. Terabe, K. Otsuka, K. Ichikawa, A. Tsuchiya and T. Ando, *Anal. Chem.*, 56 (1984) 111.

8. S. Terabe, H. Ozaki, K. Otsuka and T. Ando, *J. Chromatogr.*, 332 (1985) 211.

9. P. Gozel, E. Gossman, H. Michelsen and R. N. Zare, *Anal. Chem.*, 59 (1987) 44..

10. S. Terabe and T. Isemura, *Anal. Chem.*, 62 (1990) 650.

11. A. S. Cohen and B. L. Karger, *J. Chromatogr.*, 397 (1987) 409.

12. A. S. Cohen, D. R. Najarian, J. A. Smith and B. L. Karger, *J. Chromatogr.*, 458 (1988) 323.

13. A. S. Cohen, D. R. Najarian and B. L. Karger, *J. Chromatogr.*, 516 (1990) 49.

14. S. F. Y. Li, *J. Chromatogr. Lib.*, 52 (1992) 5.

15. A. S. Cohen, J. A. Smith and B. L. Karger, *Proc. Natl. Acad. Sci. U.S.A.*, 85 (1988) 9660.

16. A. J. C. Chen, M. Zhu, D. L. Hansen and S. Burd, *J. Cell Biol.*, 107 (1988) 241a.

17. M. Zhu, D. L. Hansen, S. Burd and F. Gannon, *J. Chromatogr.*, 480 (1989) 311.

18. A. M. Chin and J. C. Colburn, *Am. Biotech. Lab.*, Dec. (1989) 16.

19. V. Dolnik, J. F. Banks and M. Novotny, *J. Chromatogr.*, 480 (1989) 321.

20. D. N. Heiger, A. S. Cohen and B. L. Karger, *J. Chromatogr.*, 516 (1990) 33.

21. D. Burton, M. Sepaniak and M. Maskarinec, *J. Chromatogr. Sci.*, 25 (1987) 514.

22. S. Terabe, K. Otsuka and T. Ando, *Anal. Chem.*, 57 (1985) 834.

23. H. Nishi, *J. Chromatogr.*, 477 (1989) 259.

24. J. Cai and Z. El Rassi, *J. Chromatogr.*, 608 (1992) 31.

25. K. Otsuka, S. Terabe and T. Ando, *J. Chromatogr.*, 332 (1985) 219.

26. T. Tsuda, *J. High Res. Chromatogr. Chromatogr. Commun.*, 10 (1987) 622.

27. D. Crosby and Z. El Rassi, *J. Liq. Chromatogr.*, in press.

28. S. Hjerten, K. Elenbring, F. Kilar, J. L. Liao, A. J. C. Chen, C. J. Siebert and M. D. Zhu, *J. Chromatogr.*, 403 (1987) 198.

29. S. Hjerten and M. Zhu, *J. Chromatogr.*, 346 (1985) 265.

30. J. R. Mazzeo and I. S. Krull, *Biotechniques*, 10 (1991) 638.

31. P. G. Righetti, *Isoelectric Focusing: Theory, Methodology and Applications*, Elsevier, New York, 1983.

32. F. M. Everaerts and P. E. M. Verheggen in J. W. Jorgenson and M. Phillips (Editors), *New Directions in Electrophoretic Methods*, Amer. Chem. Soc. Symp., Vol 335, Washington DC, 1987, Chp. 4.

33. P. Bocek, P. Gebauer and V. Dolnik, *Anal. Isotachophoresis*, VCH Verlagsgesellschift Weinhein, 1988.

34. P. W. Atkins, *Physical Chemistry*, W. H. Freeman, CA, 1987, Chp. 25.

35. R. A. Wallingford and A. E. Ewing, *Adv. Chromatogr.*, 29 (1989) 1.

36. R. J. Hunter, *Zeta Potential in Colloid Science*, Academic Press, London, 1981.

37. A. J. Rutgers, M. de Smet and W. Rigole in H. vanOlphen and K. J. Mysels (Editors), *Physical Chenmistry: Enriching Topics from Colloid and Surface Science*, Theorex, La Jolla, CA, 1975.

38. C. L. Rice and R. Whitehead, *J. Phys. Chem.*, 69 (1965) 4017.

39. A. Adamson, *Physical Chemistry of Surfaces*, Interscience, New York, 1967, Chp.4.

40. J. W. Jorgenson and K. D. Lukacs, *J. High. Res. Chromatogr. Chromatogr. Commun.,* 4 (1981) 230.

41. S. Hjerten, *Electrophoresis,* 11 (1991) 665.

42. R. P. W. Scott, *Gas Chromatography,* Butterworth Sci. Publ., London, 1960.

43. W. Nashabeh and Z. El Rassi, *J. Chromatogr.,* 559 (1991) 367.

44. K. A. Cobb, V. Dolnik and M. Novotny, *Anal. Chem.,* 62 (1990) 2478.

45. E. Grushka, R. M. McCormick and H. H. Lauer, *Anal. Chem.,* 61 (1989) 241.

46. G. Taylor, *Proc. R. Soc. Lond.,* A219 (1953) 186.

47. P. D. Grossman in P. D. Grossman and J. C. Colburn (Editors), *Capillary Electrophoresis: Theory & Practice,* Academic Press, CA, 1992, Chp. 1.

48. J. C. Stenberg, *Adv. Chromatogr.,* 2 (1966) 205.

49. H. K. Jones, N. T. Nguyen and R. D. Smith., *J. Chromatogr.,* 504 (1990) 1.

50. H. H. Lauer and D. McManigill, *Trends Anal. Chem.,* 51 (1986) 11.

51. R. J. Wieme in E. Heftmann (Editor), *Chromatography: A Laboratory Handbook of Chromatographic and Electrophoretic Methods,* Van Nstrand Reinhold, New York, 1975, pp 228-281.

CHAPTER II

CAPILLARY ZONE ELECTROPHORESIS OF
PROTEINS WITH HYDROPHILIC
FUSED-SILICA CAPILLARIES*

Abstract

Fused-silica capillaries having surface bound hydroxylated polyether functions were developed for the separation of proteins by capillary zone electrophoresis. In one approach, the hydrophilic coatings consisted of two layers; a glyceropropylpolysiloxane sublayer covalently attached to the inner surface and a polyether top layer. In a second approach, the capillary wall was coated with polysiloxane polyether chains whose monomeric units at both ends were covalently attached to the capillary inner surface with possible interconnection. These coatings yielded capillaries with different electroosmotic flow characteristics. The relatively long polyether chains of the various coatings were effective in shielding the unreacted surface silanols, thus minimizing solute-wall adsorption. As a consequence, high separation efficiencies were obtained in the pH range 4.0 to 7.5, which allowed the separation of widely differing proteins, the characterization of heterogeneous proteins and the fingerprinting of crude protein mixtures. The various coatings were stable and exhibited reproducible separations from run-to-run, day-to-day, and column-to-column. Furthermore, a procedure was developed for restoring collapsed capillaries after prolonged use.

Introduction

Capillary zone electrophoresis (CZE) with its high resolving power and unique . selectivity is well placed to play an important role in the separation and characterization of proteins. However, since its debut [1-3], researchers have soon realized that CZE of proteins with fused-silica capillaries is hampered by solute adsorption onto the capillary inner walls, which often gives rise to band broadening and low recovery of the separated analytes.

Several attempts have been made to alleviate the problem of solute-wall interactions. The major approaches have been: (i) capillary surface treatments [4-11], (ii) the use of running electrolytes at high [12,13] or low pH [6], i.e. above or below the isoelectric points of proteins, (iii) the addition of high salt concentrations to the running electrolytes [14] using high pH, and (iv) the use of zwitterionic buffers with high salt concentrations [15]. Among all these approaches, surface modification is the method that affords the highest flexibility as far as selectivity modulation with pH changes is concerned. Indeed, approach ii limits the selectivity of the system to a narrow pH range and may result in protein denaturation at low pH or capillary degradation at high pH; approach iii may not be effective at medium pH range (5 to 7) and in addition may produce system overheating due to the high ionic strength of the running electrolyte. On the other hand, method iv, although effective in reducing solute adsorption, does not allow high sensitivity detection due to increased background in UV of most zwitterions when used at elevated concentrations.

Thus far, several coatings have been developed for CZE of proteins. These coatings are polyacrylamide [4], methylcellulose [4], glycol [5], glycerol-glycidoxypropyl [6], poly(vinylpyrrolidinone) [6], polyethylene glycol (PEG) [7], maltose [8], aryl pentafluoro (AFP) groups [9], polyethyleneimine (PEI) [10], and vinyl-bound polyacrylamide [11]. The PEI coating provided positively charged surface and was useful

for the separation of basic proteins. This mimics the idea of operating untreated fused-silica capillaries with high pH, whereby the proteins and the surface have the same charge, which then prevent adsorption by coulombic repulsion. All other coatings were of the neutral type and produced acceptable results in terms of protein separations.

This report is concerned with the investigation of surface modification procedures that yield stable and inert capillaries having moderate electroosmotic flow. The capillary surface modification reported here entails the covalent attachment of polyether chains of various length to the inner surface of fused-silica capillaries *via* siloxane bonds, either directly using polyether chains with trimethoxysilane groups at both ends or by attaching a top polyether layer to a polysiloxane sublayer already anchored to the capillary inner surface. The first type of coatings is referred to as interlocked coatings while the second as fuzzy coatings. The coated capillaries were evaluated in protein CZE and characterized in terms of efficiency and electroosmotic flow over a wide range of pH. In addition, a procedure was developed for restoration of collapsed capillaries after prolonged use.

Experimental

Instrument

The capillary electrophoresis instrument used in this study resembles that reported earlier [16,17]. It was constructed from a Glassman High Voltage (Whitehouse Station, NJ, U.S.A.) Model EHP30P3 high voltage power supply of positive polarity and a Linear (Reno, NV, U.S.A.) Model 200 UV-Vis variable wavelength detector equipped with a cell for on column detection. In all experiments, the wavelength was set at 210 nm. The electropherograms were recorded with a computing integrator interfaced with a floppy disk drive and a CRT monitor from Shimadzu (Columbia, MD, U.S.A.).

Reagents and Materials

Cytochrome c from horse heart, lysozyme from chicken egg white, ribonuclease A and α-chymotrypsinogen A, both from bovine pancreas, myoglobin from horse skeletal muscle, carbonic anhydrase from bovine erythrocytes, iron saturated transferrin from human serum, α-lactalbumin from bovine milk, and crude trypsin inhibitor and lipoxidase, both from soybean were purchased from Sigma (St. Louis, MO, U.S.A.). Table I compiles the M.W. and pI values of these proteins. γ-Glycidoxypropyltrimethoxysilane

TABLE I.

PROTEINS USED IN THIS STUDY

Proteins	M.W.	pI
Lysozyme	14,100	11.0
Cytochrome c	12,400	10.7
Ribonuclease A	13,700	9.4
α-Chymotrypsinogen A	25,500	9.5
Myoglobin	17,500	6.8-7.3
Carbonic anhydrase	31,000	5.3
Transferrin	79,550	5.2-6.1
α-Lactalbumin	14,200	4.8
Trypsin inhibitor	20,100	4.5
Lipoxidase	102,400	5.7

(Z-6040) was a gift from Dow Corning (Midland, MI, U.S.A.). Polyethylene glycol diglycidyl ether (M.W. 600) was purchased from Polysciences (Warrington, PA, U.S.A.). Polyethylene glycol (PEG) of M.W. 200, 600 and 2000, boron trifluoride etherate and phenol were obtained from Aldrich (Milwaukee, WI, U.S.A.). Reagent grade

sodium phosphate monobasic, sodium hydroxide, hydrochloric acid, dioxane, and N,N-dimethylformamide (DMF) were from Fisher Scientific (Pittsburgh, PA, U.S.A.). Fused-silica capillaries of 50 μm I.D. and 375 μm O.D. were obtained from Polymicro Technology (Phoenix, AZ, U.S.A.). Deionized water was used to prepare the running electrolyte. All solutions were filtered with 0.2 μm Uniperp Syringeless filters from Genex Corp., (Gaithersburg, MD, U.S.A.) to avoid capillary plugging.

Capillary Modification

Fused-silica capillaries of 80 cm long were treated using the following procedures.

Polyether fuzzy coatings. Fused-silica capillaries were first filled with an aqueous solution at 10% (v/v) γ-glycidoxypropyltrimethoxysilane and allowed to react at 96 °C for 40 min. This treatment was repeated four times. Subsequently, the capillary was filled with 0.01 M HCl and then heated at 95 °C for 40 min. After washing successively with water and dioxane, the capillary was flushed with a solution of dioxane at 1% (v/v) boron trifluoride. Following, the capillary was filled with an equimolar solution of polyethylene glycol diglycidyl ether (M.W. 600) and PEG 2000 or PEG 600 in dioxane. The modified capillaries were stored in HPLC grade methanol.

Polyether interlocked coatings. N,N-Dimethylformamide solutions containing PEG 200 with trimethoxysilane at both ends were introduced into the capillary and allowed to react at 100 °C for one hour. This treatment was repeated twice. All capillaries were stored in HPLC grade methanol.

Restoration of deteriorated capillaries. After prolonged use, the performance of the various hydrophilic capillaries declined due to hydrolytic degradation of some of their coatings. The feasibility of recoating a deteriorated capillary to restore its protective hydrophilic layer was assessed with polyether interlocked coatings. In this regard, the collapsed capillary was flushed with 1.0 M NaOH and then heated at 95 °C for 30 min; a

step that removed the remaining of the coating *via* nucleophilic cleavage of the siloxane bonds (Si-O-Si-C) [18]. Following, the capillary was successively washed with water, filled with 0.1 M HCl and then heated at 95 °C for 30 min. After washing with water and DMF, the capillary was filled with the coating reagent and allowed to react as described above.

Reproducibility. The coated capillaries were evaluated for the reproducibility of protein migration times from run-to-run, day-to-day and column-to-column. From run-to-run (on the same day), the relative standard deviation (% RSD) was calculated based on four successive measurements separated by 20 minutes equilibration with the running electrolyte. From day-to-day the % RSD was calculated based on a total of 9 measurements made on three different days (3 sets of 3 measurements each) and from column-to-column, the % RSD was estimated using data collected (2 sets of 6 measurements each) from two columns prepared on different days.

Results and Discussion

Surface Modification

Figures 1A and 1B depict the idealized structure of the fuzzy and interlocked hydrophilic coatings, respectively. Both types of coatings are essentially hydroxylated polyether chains covalently attached to the capillary inner surface. The fuzzy coatings (see Fig. 1A) consist of two layers: a cross-linked glyceropropylpolysiloxane sublayer covalently attached to the capillary inner-surface, and a hydrophilic polyether top layer. The fuzzy top layer is the result of the different ways in which the PEG 600 diglycidyl ether can react with the PEG 600 or 2000 leading to polyether chains of different lengths with either one end or two ends covalently attached to the sublayer. On the other hand, the interlocked coatings consist of polyether polysiloxane chains whose monomeric units at
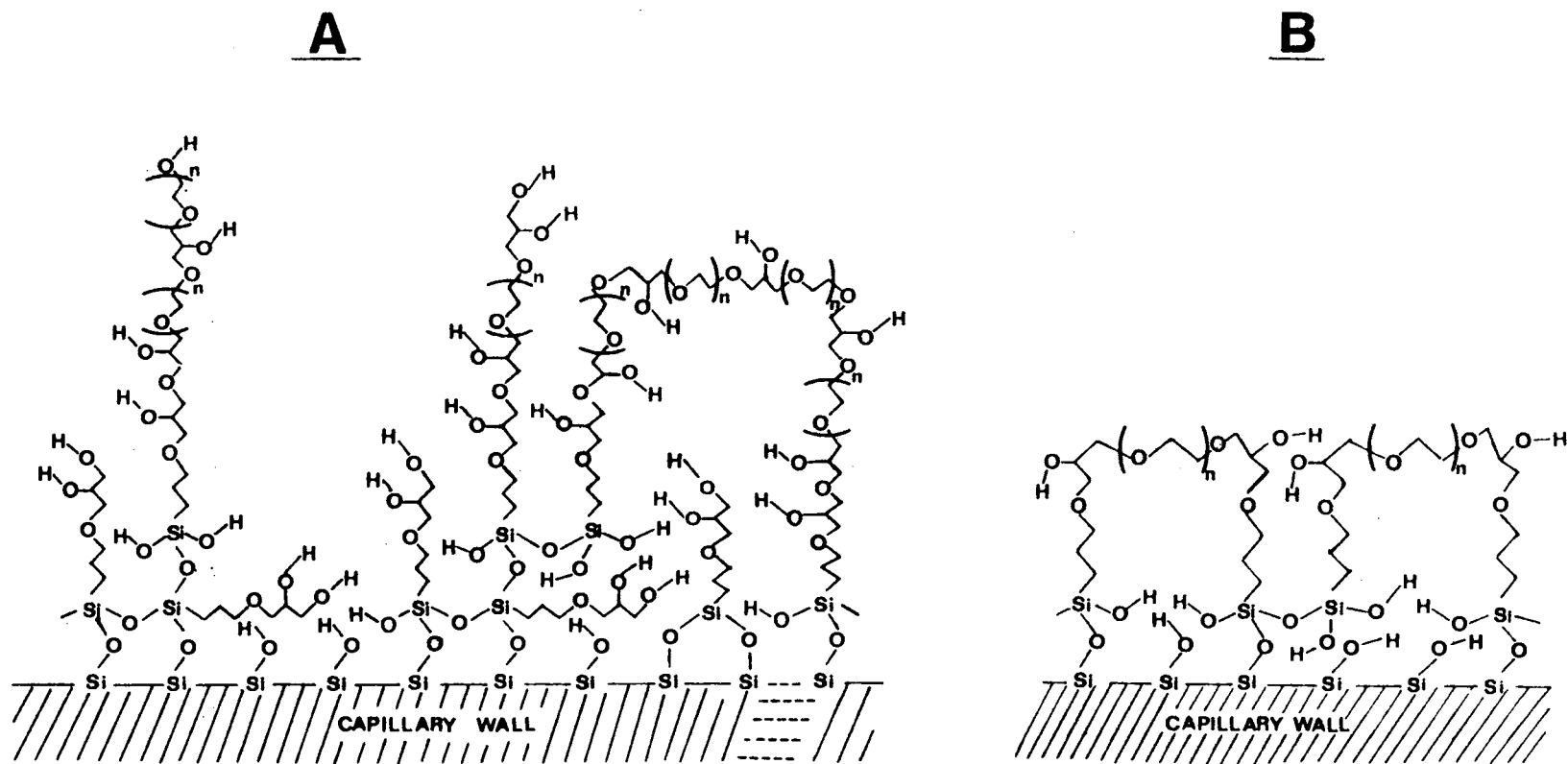
Figure 1: Schematic illustration of the idealized structures of fuzzy (A) and interlocked (B) polyether coatings of fused-silica capillaries.

both ends are covalently attached to the surface with possible interconnection. The following capillary codings will be utilized throughout the text to designate each type of coatings. F-2000 and F-600 denote capillaries with fuzzy coatings having PEG 2000 or PEG 600 moieties, respectively, whereas I-200 refers to capillaries with interlocked coatings having PEG 200 polyether chains.

Electroosmotic Flow

The above two schemes of surface modification yielded capillaries with different electroosmotic flow characteristics. Figs 2A and 2B illustrate the results obtained at 17 and 20 kV over the pH range 4.0 to 7.5 using phenol as the inert tracer. At both running voltages, the fuzzy coatings exhibited lower electroosmotic flow than the interlocked ones indicating that the concentration of unreacted surface silanols is relatively low for the capillaries with fuzzy polyether coatings. This is because the fuzzy coatings have an additional cross-linked polysiloxane sublayer that the interlocked coatings do not have. On the other hand, for the two fuzzy coatings, i.e. F-600 and F-2000, which should have the same surface concentration of unreacted silanols, F-600 exhibited a higher flow-rate than F-2000 under otherwise identical conditions. The difference in the flow-rate between the two fuzzy coatings may be related to the size of the polar top layer. The polyether chains of the polar top layer in F-600 are shorter than those in F-2000, and as a result they were less effective in masking the ionized surface silanols (i.e. unreacted silanols) toward the atmospheric binding of electrolyte cations. In view of Manning's counterion condensation theory [19], salt counterions are territorially or atmospherically bound, i.e., they are retained by the electrostatic field at the capillary surface, but remain free to move within a certain layer above it. The atmospheric binding of electrolyte cations to the negatively charged silanols generates an electric double layer adjacent to the capillary walls, which migrates toward the cathode when an electric potential is applied to the capillary.
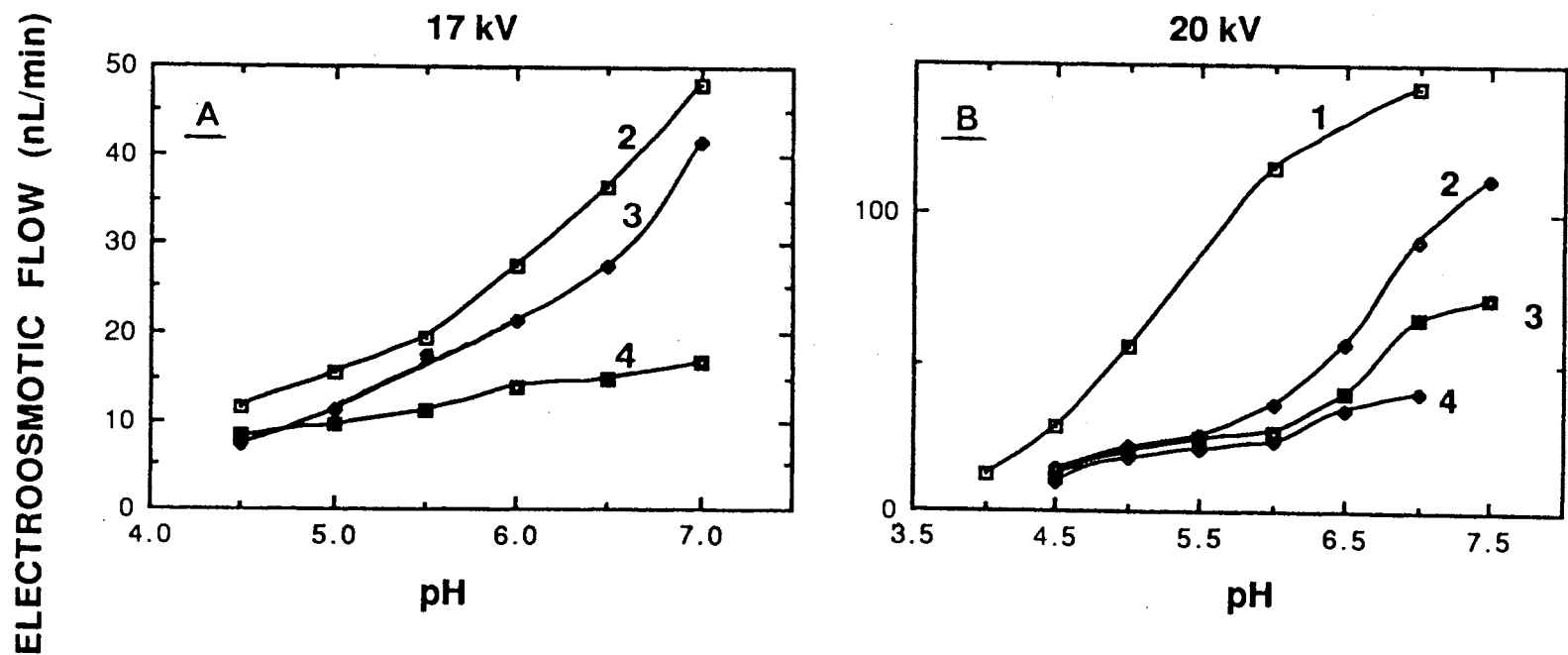
Figure 2. Plots of electroosmotic flow rates obtained on coated and uncoated capillaries versus pH of the electrolyte at 17 kV in A and 20 kV in B. Fused-silica capillaries: 1, untreated; 2, I-200; 3, F-600; 4, F-2000. All tubes were 50 cm (to the detection point), 80 cm total length x 50 μm I.D.; electrolyte, 0.1 M phosphate solutions at different pH. At 17 kV, currents were 21, 22, 23, 24, 34, and 38 μA at pH 4.5, 5.0, 5.5, 6.0, 6.5, and 7.0, respectively. At 20 kV, currents were 26, 28, 29, 30, 33, 45, 50 and 70 μA at pH 4.0, 4.5, 5.0, 5.5, 6.0, 6.5, 7.0, and 7.5, respectively. Inert tracer, phenol.

Since the cations are solvated, they pull solvent with them, thus producing the electroosmotic or bulk flow.

On the other hand, when compared to untreated fused-silica capillaries at an applied voltage of 20 kV (see Fig. 2B), the electroosmotic flow was reduced on the average by a factor of 3.6, 2.9 and 2.3 for F-2000, F-600 and I-200, respectively. It should be noted that the difference in flow-rate among the various coatings was greater in magnitude at pH 5.0 and above due to increasing ionization of the unreacted surface silanols (see Figs 2A and 2B).

In principle, changing the applied voltage should produce proportional changes in the rate of the electroosmotic flow. However, the comparison of Figs 2A and 2B shows that increasing the applied voltage by a factor of 1.17, i.e. from 17 to 20 kV, yielded a larger increase in the electroosmotic flow. On the average, the flow increased by a factor of ca. 1.5 for the coated capillaries over the pH range studied when going from 17 to 20 kV. Capillary internal temperature was found to increase in nonlinear fashion with the applied voltage [20]. On the other hand, solvent viscosity decreases exponentially with increasing temperature and since the electroosmotic flow is inversely proportional to viscosity, this decrease in viscosity may have caused the jump in flow at 20 kV when compared to 17 kV.

Evaluation of Coated Capillaries with Basic Proteins

Figures 3, 4 and 5 depict typical electropherograms of four model basic proteins performed on F-2000, F-600, and I-200 coated capillaries, respectively, at an applied voltage of 17 kV using 0.1 M phosphate solutions as the running electrolyte at different pH. The average plate count per meter, N_{av}, is indicated on each electropherogram. These efficiency values may indicate that interaction between the proteins and the inner surface proper of the capillaries has been greatly reduced. Based on the results of electroosmotic flow with the various capillaries (see Fig. 2), some unreacted silanols remained on the
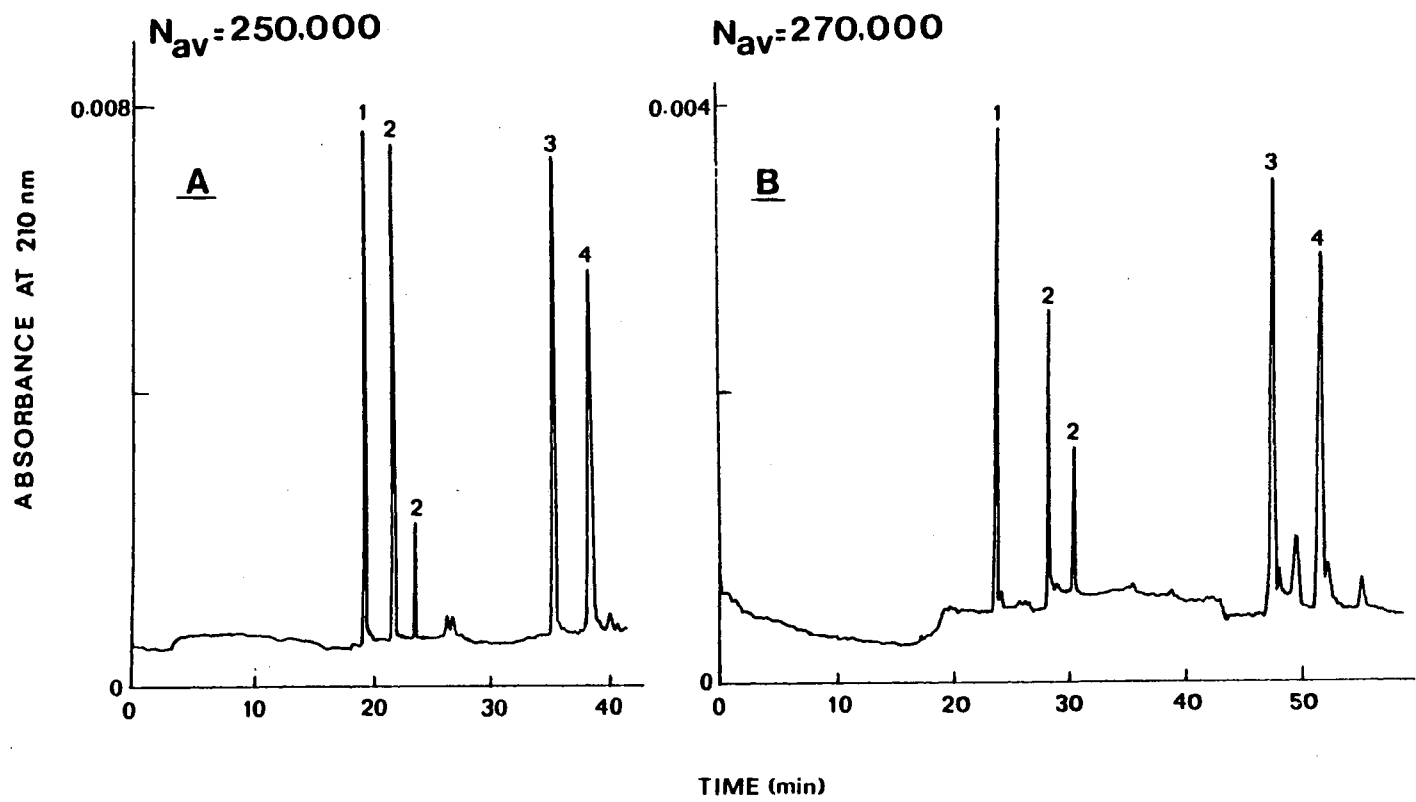
Figure 3. Electropherograms of basic proteins obtained on the fuzzy 2000 coated capillary. Capillary, 50 cm (to the detection point), 80 cm total length x 50 μm I.D.; electrolyte, 0.1 M phosphate solutions at pH 6.0 in A and 7.0 in B; running voltage, 17 kV; currents were 24 and 38 μA at pH 6.0 and 7.0, respectively. Proteins: 1, lysozyme; 2, cytochrome c; 3, ribonuclease A; 4, α-chymotrypsinogen A.
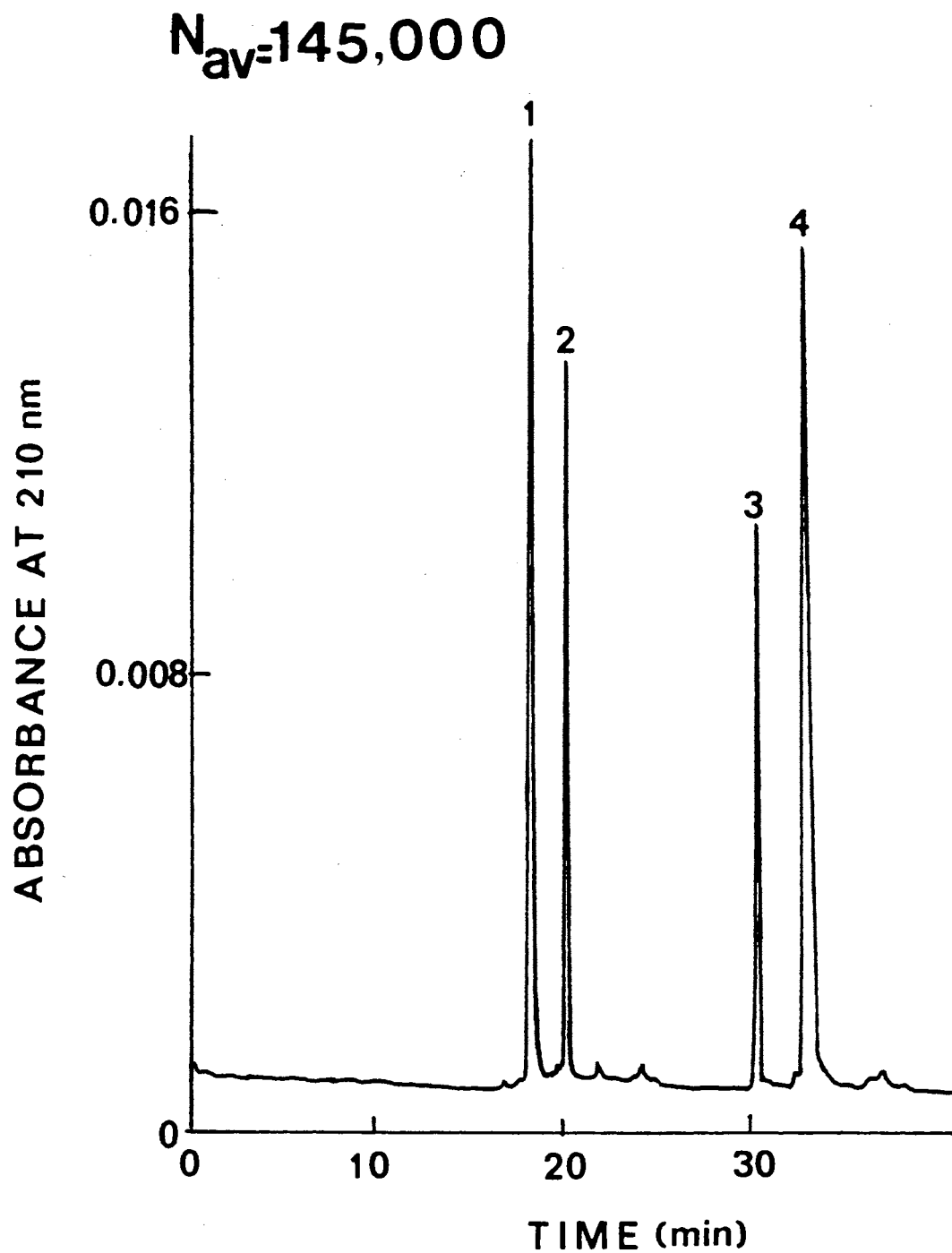
Figure 4. Electropherogram of basic proteins obtained on fuzzy 600 coated capillary at pH 6.0. All other conditions are the same as in Figs 2 and 3.
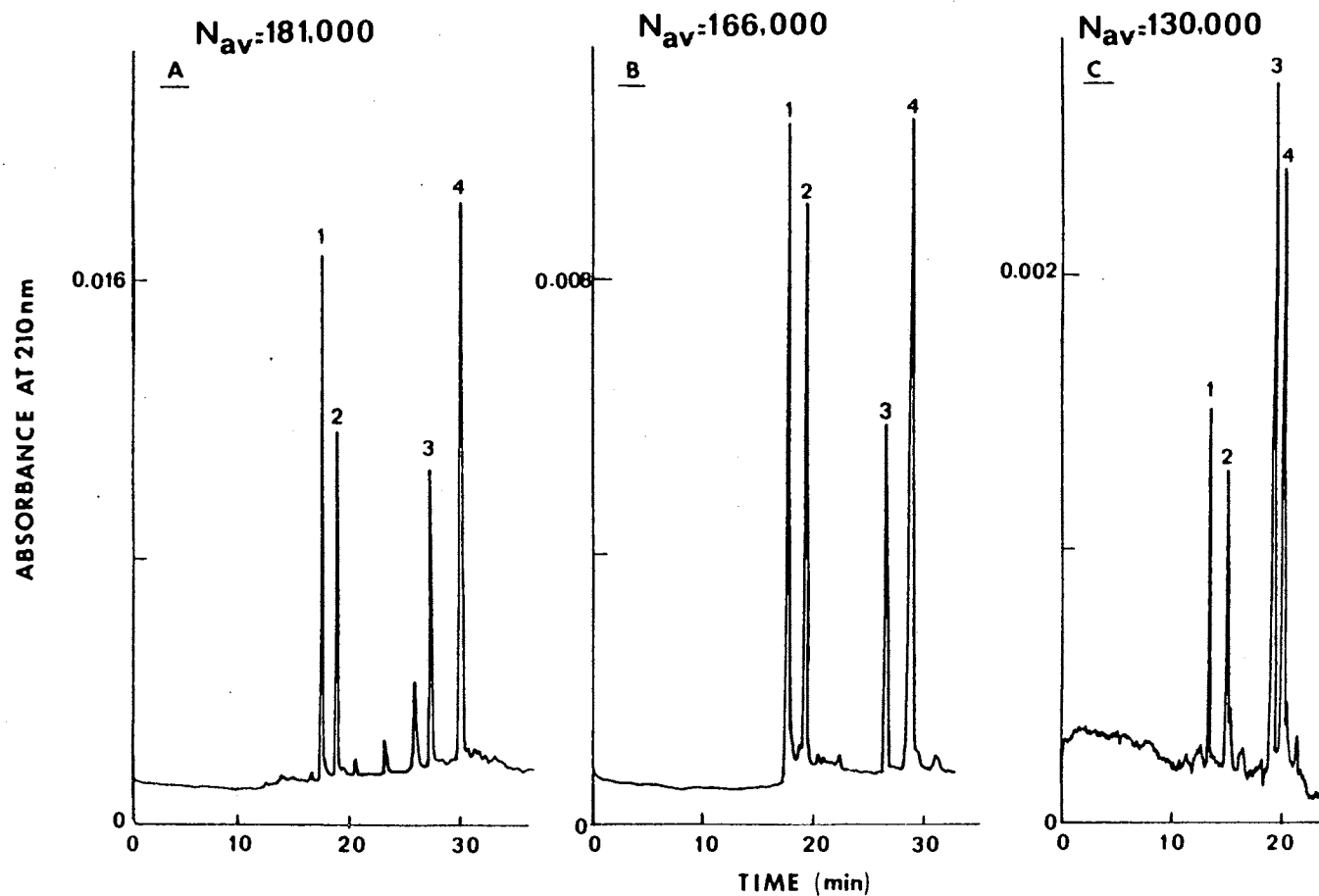
Figure 5. Electropherograms of basic proteins obtained on interlocked 200 coated capillary at pH 5.0 (A), pH 6.0 (B) and pH 7.0 (C). All other conditions are the same as in Figs 2 and 3.

capillary inner surface. These silanols which were accessible for the atmospheric binding of small counterions, may be less exposed for the territorial binding of large polyionic solutes such as proteins. The relatively long polyether chains of the various coatings are believed to hinder the access of macromolecules to the unreacted silanols. Indeed, according to Manning's counterion condensation theory [19], charges must be within the Bjerrum length in order to undergo electrostatic interactions. This length is defined as the distance at which two unit charges interact with an energy of $k_B T$ (k_B is Boltzman's constant and T is absolute temperature) in the relevant dielectric medium and its value is 7.14 Å in water at 25 °C.

Referring to Fig. 5, the N_{av} obtained on I-200 was slightly lower at pH 7.0 than at pH 5.0; a trend that was also observed on F-600 and F-2000. This may be due to increasing ionization of unreacted surface silanols and/or Joule heating with increasing pH. Raising the electrolyte pH from 5.0 to 7.0 would lead to increasing protein interactions with the residual ionized silanols, which in turn would cause lower separation efficiencies. On the other hand, due to increasing the ionic strength of the running electrolyte with increasing pH, the current almost doubled when the pH of phosphate solution was raised from 5.0 to 7.0. Higher currents lead to increasing center-to-wall temperature difference, thereby producing a more pronounced radial viscosity gradient inside the capillary. As a result, radial variations in the overall velocity profiles (i.e., the sum of electrophoretic and electroosmotic velocity) of the separated proteins would also increase in magnitude at high currents. These perturbations in the velocity profiles may produce mass transfer resistances that broaden the migrating solute zones and cause lower separation efficiencies. The effect of temperature gradients on CZE separation efficiency is well documented [21,23].

The values of N_{av} obtained on F-600 and I-200 capillaries were quite comparable, but lower than those obtained on F-2000 under otherwise identical conditions (see Figs 3, 4, and 5). This may be due to the higher electroosmotic flow with F-600 and I-200 when

compared to F-2000. Under these conditions, mass transfer resistances due to heat-induced perturbations in the overall velocity profiles are amplified. Another possible explanation is that the F-600 and I-200 coatings are not as effective as F-2000 coatings in shielding the unreacted surface silanols toward the protein solutes. It has been shown that a slight solute-wall adsorption can cause separation efficiency to decline [24].

In CZE of proteins, capillary internal Joule heating due to passage of current through the electrolyte inside the tube, could also denature the biomacromolecules. Increasing the voltage from 17 to 20 kV using 0.1 M phosphate solutions at pH 6.0, 6.5 and 7.0 resulted in increasing the current from 24 to 33 μA, from 34 to 45 μA and from 38 to 50 μA, respectively. At this higher voltage, and independently of the nature of the coating, α-chymotrypsinogen A did not elute from the capillary when pH 6.5 or 7.0 were used, while the peaks of cytochrome c and lysozyme, and to a lesser extent that of ribonuclease A, exhibited a significant drop in efficiency. At pH 6.0, increasing the voltage from 17 to 20 kV did only result in lowering the separation efficiency. This may be due to the binding of proteins to the coating proper by hydrophobic interactions. It has been shown in liquid chromatography of proteins that hydrophobic interactions are induced and/or increased with increasing temperature due to heat-induced conformational changes[25,26]. These interactions which are the result of temperature effects arising from Joule heating can be viewed as the major contributors to band broadening at elevated voltage.

To examine the influence of the running voltage on separation efficiencies, the four basic proteins (i.e. lysozyme, cytochrome c, ribonuclease A, and α-chymotrypsinogen A) were analyzed on an I-200 capillary at different voltages using 0.1 M phosphate, pH 7.0. The results are illustrated in Fig. 6 by a plot of average plate count per meter versus applied voltage. As in the preceding experiment, α-chymotrypsinogen A did not elute from the capillary at an applied voltage of 20 kV. It is seen that an applied voltage in the range 10-13 kV yields higher efficiency than at elevated voltage. However, the tradeoff is longer
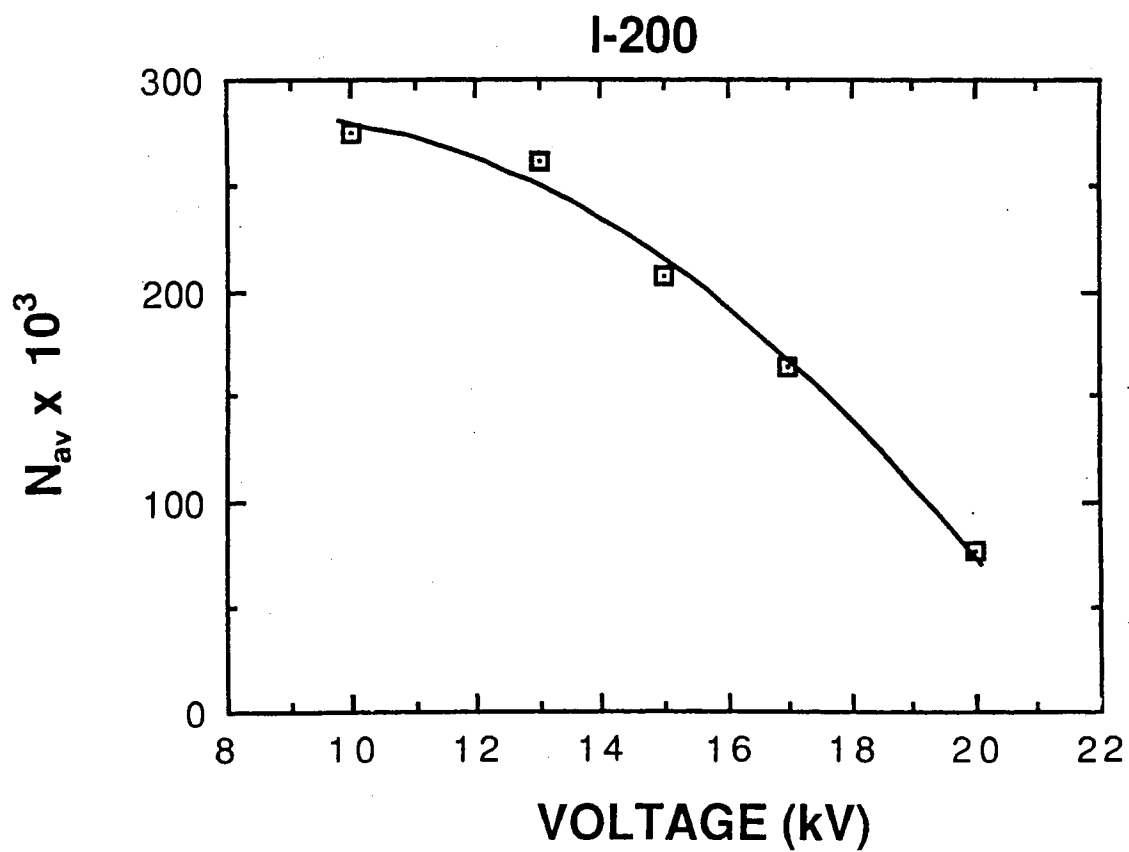
I-200

Figure 6. Plot of average plate count per meter versus applied voltage obtained on an I-200 capillary. Electrolyte, 0.1 M phosphate solution, pH 7.0; currents were, 7, 20, 28, 38, and 50 µA at 10, 13, 15, 17, and 20 kV, respectively. All other conditions are the same as in Figs 2 and 3.

analysis time. A running voltage of 16-17 kV seems to be a compromise, whereby protein separation can be carried out relatively fast without sacrificing separation efficiencies. The relatively high separation efficiency obtained at lower running voltage may result from diminished Joule heating of the system. Similar observations were recently reported by Cobb *et al* [11] with capillaries having polyacrylamide coatings.

To evaluate the effect of ionic strength on separation efficiencies, the voltage was kept low (i.e. 10 kV) so that a wide range of phosphate concentrations in the running electrolyte can be investigated without overheating the system. This set of experiments was performed on an I-200 capillary at pH 7.0. The results are depicted in Fig. 7 by a plot of N_{av} versus the phosphate concentrations in the running electrolyte. As can be seen in Fig. 7, N_{av} first increased, passed through a maximum and then decreased with increasing phosphate concentrations. Again, the sharp decrease in separation efficiency at high ionic strength (i.e., at 0.25 M; see Fig. 7) can be related to effects associated with system heating. At this lower voltage, i.e. 10 kV, and using 0.25 M phosphate, α-chymotrypsinogen A eluted from the capillary despite that the current was as high as with 0.1 M phosphate and 20 kV (i.e. 50 μA); conditions under which the same protein was tightly bound to the capillary (see above). It seems that for the same current passing through the running electrolyte, a higher ionic strength would stabilize protein structure, and consequently protein hydrophobic interaction with the coating due to heat-induced conformational changes would be reduced.

To compare the three types of coatings, the peak capacity, *n*, was calculated for each capillary based on the following assumptions: (i) all capillaries can generate 100,000 theoretical plates per column on the average over the pH range 4.5-7.0, (ii) the hypothetical proteins differ among each others by their pI values, which span 4-11, (iii) lysozyme is the first eluting peak, and (iv) the analysis time is set arbitrarily to 150 min, time at which the center of the last eluting peak appears in the detector. The peak capacity, *n*, was calculated using the equation:
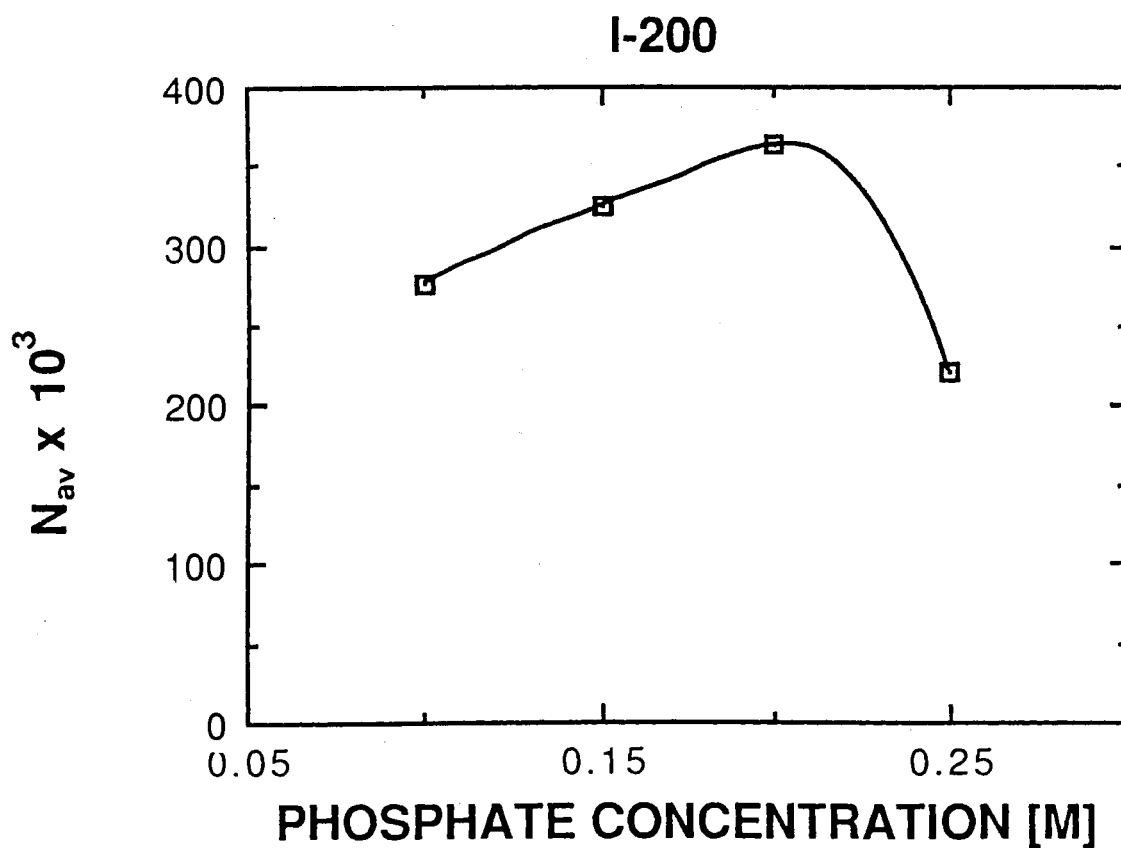
Figure 7. Plot of average plate count per meter versus the ionic strength of the running electrolyte obtained on an I-200 capillary. Electrolytes, phosphate solutions at different ionic strength, pH 7.0; running voltage 10 kV; currents were, 7, 18, 35 and 50 μA at 0.1, 0.15, 0.2 and 0.25 M phosphate, respectively. All other conditions as in Figs 2 and 3.

$$n = 1 + \sqrt{\frac{N_{av}}{16}} \times ln\frac{t_f}{t_i}$$

and the results are depicted in Fig. 8 for the pH range 4.5 to 7.0. In this equation, t_i is the migration time of lysozyme and t_f is that of phenol (i.e. the inert tracer); a migration time interval within which the elution of basic and slightly acidic proteins may take place. On the other hand, the migration times of acidic proteins are assumed to lie between the migration times of phenol, t_i , and that of the last eluting peak, t_f, set arbitrarily to 150 minutes. The migration times of lysozyme and phenol used in calculating peak capacity were those obtained from experiments performed on the various capillaries with a migration distance of 50 cm (i.e. distance from injection end to detection point) using 0.1 M phosphate solutions at pH ranging from 4.5-7.0, and a running voltage of 17 kV. Referring to Fig. 8, it can be seen that F-2000 capillaries require an electrolyte of pH 7.0 to elute an equal number of positively and negatively charged proteins, whereas this situation is reached at pH 5.5 for I-200 and F-600 capillaries. Due to the oversimplifications in the calculations, the peak capacity may not be realistic. Nevertheless, to obtain similar behavior in terms of peak capacity, it seems wise to state that a tube with relatively low electroosmotic flow requires the use of an electrolyte pH that is two or more units higher in value than with a capillary having 2.5 to 3 times higher electroosmotic flow. Another difference is that at any pH the peak capacity for positively charged proteins on the F-2000 capillary is always greater than that with F-600 and I-200. On the other hand, the peak capacity for the negatively charged proteins is higher with F-600 and I-200 than with F-2000.

Figure 9 illustrates the overall and the electrophoretic mobilities of two model proteins (i.e., lysozyme and ribonuclease A) as well as the electroosmotic mobility of neutral solutes over the pH range studied with F-2000, F-600 and I-200 coated capillaries. In all cases (see Fig. 9), the electrophoretic mobility of the two test proteins decreased sharply between pH 5.5 and 6.0 indicating the deprotonation of an imidazole and/or the
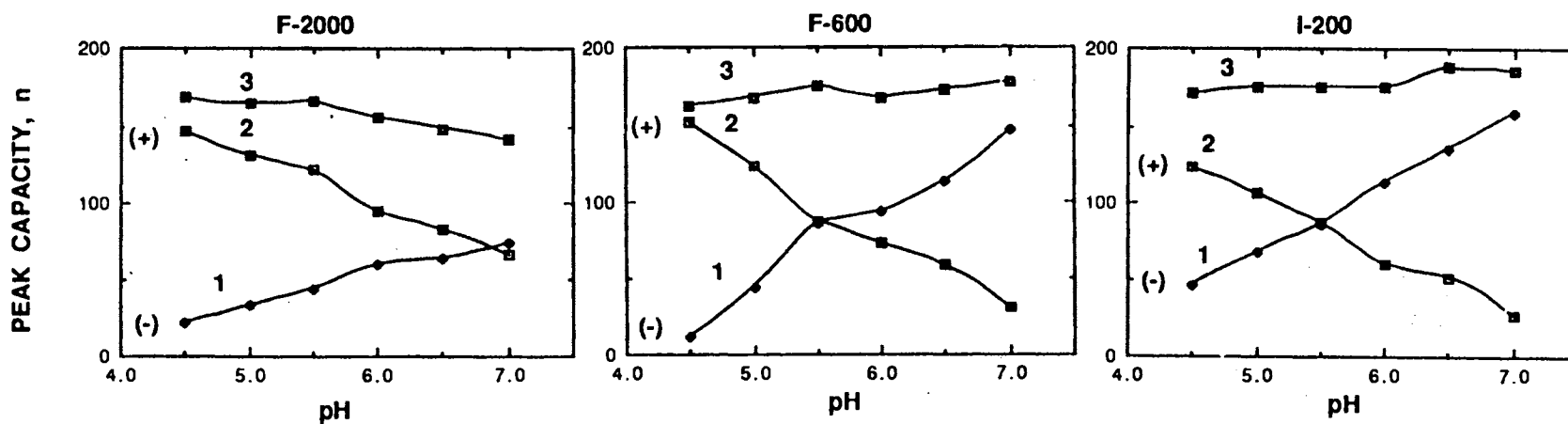
Figure 8. Comparison of peak capacity, n, of the different coatings over the pH range 4.5 to 7.0 using lysozyme and phenol migration times at 17 kV (see text for details). 1, n for negatively charged proteins; 2, n for positively charged proteins; 3, total n.
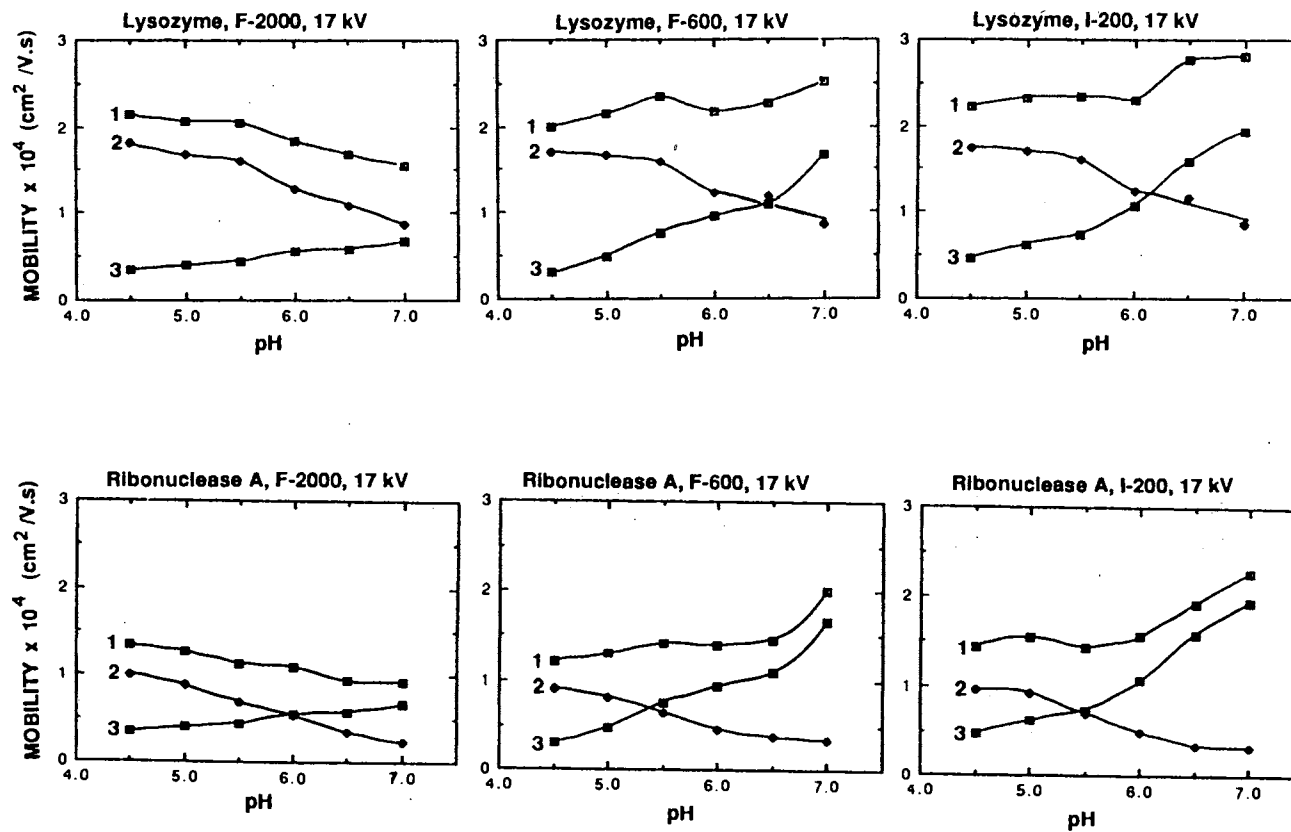
Figure 9. Plots of overall and electrophoretic mobilities of lysozyme and ribonuclease A as well as electroosmotic mobility versus pH on the different coatings. Electrolytes, 0.1 M phosphate solutions at different pH. 1, overall mobility; 2, electrophoretic mobility; 3, electroosmotic mobility. All other conditions are the same as in Figs 2 and 3.

dissociation of a carboxylic side chain group. Furthermore, the electrophoretic mobility of proteins was virtually independent of the nature of the coatings under otherwise identical conditions. This is an indication of quasi-homosystems; meaning that the various coatings are quite effective in shielding the surface proper of the capillary toward the protein solutes. On the other hand, the overall mobility, $\mu_{overall}$, which is the sum of electroosmotic and electrophoretic mobilities, varied from one coating to another. The electroosmotic flow was relatively low with F-2000 capillary, and since this flow increased slightly with the pH at 17 kV, the overall mobility of the proteins almost paralleled their electrophoretic mobility (see Fig. 9). This may represent an advantage when dealing with unknown substances in the sense that their basicity or acidity can be assessed from simple $\mu_{overall}$-pH plot. On the other hand, the overall mobility of the same proteins followed different patterns on F-600 and I-200 mainly due to their higher electroosmotic flow. For lysozyme, the overall mobility increased between pH 4.5 and 5.5, decreased at pH 6.0 and then increased between pH 6.0 and 7.0. For ribonuclease A, a sharp increase in the overall mobility occurred in the pH range 6.0-7.0.

Reproducibility and Stability of the Coatings

These studies were carried out on F-600 and I-200 capillaries that are representative of fuzzy and interlocked coatings, respectively. Table II summarizes the run-to-run, day-to-day and column-to-column migration reproducibility expressed in terms of percent relative standard deviation (%RSD) with four basic proteins at pH 6.5. It should be noted that the column-to-column reproducibility reflects columns made on two different days. It can be seen that the interlocked 200 is slightly more reproducible than the fuzzy coatings simply because the surface modification is accomplished in a single step in the former, whereas it takes three steps to make the latter.

The different coatings were quite stable. In fact, the various columns exhibited constant performance for several weeks when operated at pH 6.0 or below, and for more than 80 hours when used in the pH range 6.5 to 7.0.

TABLE II.

REPRODUCIBILITY OF MIGRATION TIMES OF PROTEINS ON F-600 AND I-200 CAPILLARIES

Capillary, 50 cm (to the detection point), 80 cm total length x 50 μm I.D.; electrolyte, 0.1 M phosphate, pH 6.5; applied voltage, 17 kV; current, 38 μA (see experimental for details).

Protein	%RSD					
	F-600			I-200		
	Run to run	Day to day	Column to column	Run to run	Day to day	Column to column
Lysozyme	1.6	1.4	4.2	0.9	1.6	1.5
Cytochrome c	0.2	0.6	6.7	0.9	1.8	2.2
Ribonuclease A	1.5	1.2	5.4	1.0	1.9	2.8
α-Chymotrypsinogen A	1.8	2.3	4.5	1.0	2.0	2.3

Restoration of Capillary Coatings

After prolonged use, the various capillaries lost some of their coatings by hydrolytic degradation, and consequently they exhibited strong interactions with the

A

$N_{av} = 140,000$

0.003

0.002

0.001

0

ABSORBANCE AT 210 nm

ORIGINAL

1
2
3
4 5 6 7
8

0   20   40

B

$N_{av} = 140,000$

0.016

0.008

0

COLLAPSED

3
4
1 2 5 6,7
8

0   20   40

TIME (min)

C

$N_{av} = 140,000$

0.006

0.004

0.002

0

RESTORED

2
1
3
4 5 6
7
8

0   20   40
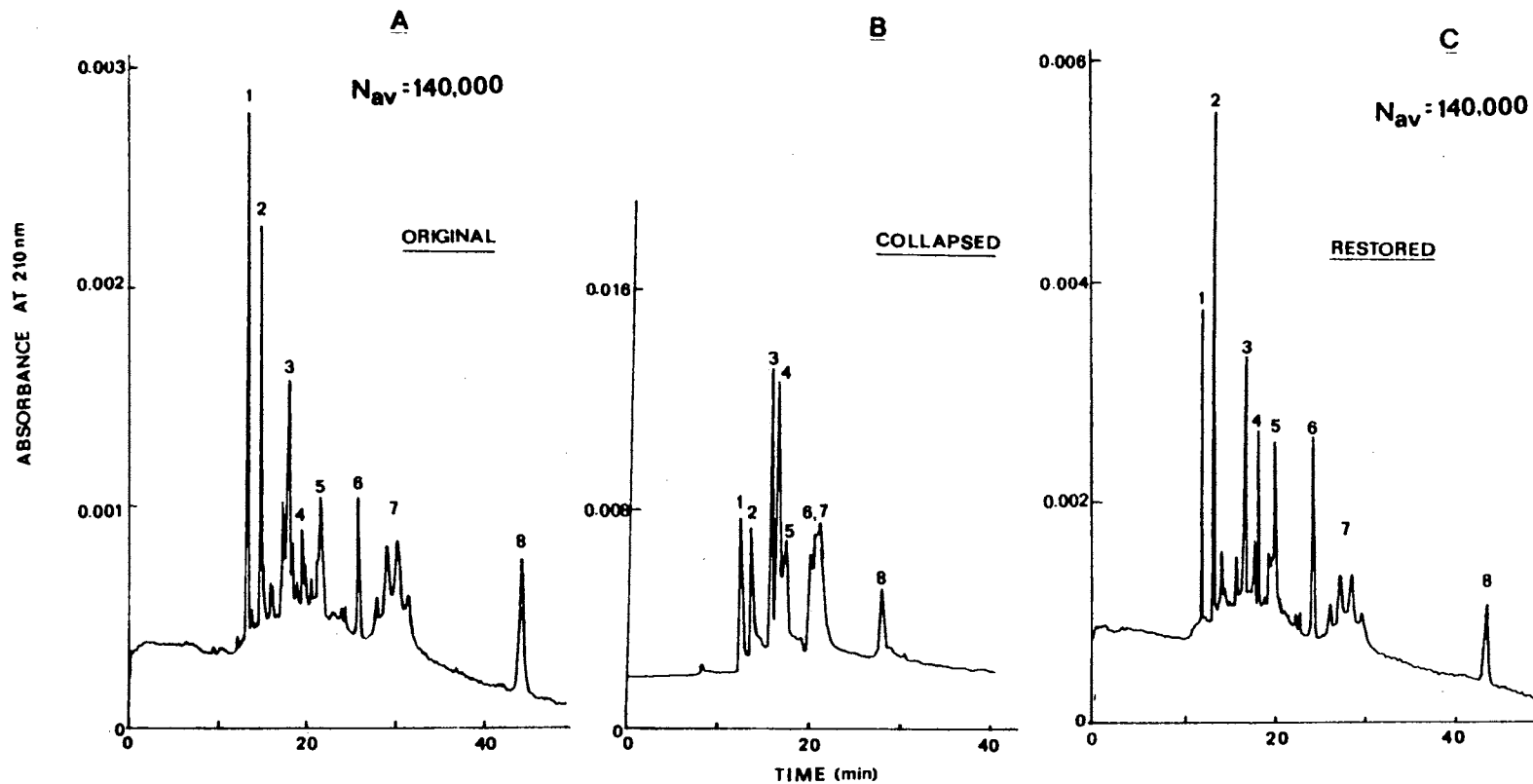
Figure 10. Electropherograms of basic and acidic proteins obtained on original (A), collapsed (B) and restored (C) I-200 capillaries. Electrolyte, 0.1 M phosphate solution, pH 7.0; running voltage, 17 kV. All other conditions as in Fig. 3. Proteins: 1, lysozyme; 2, cytochrome c; 3, ribonuclease A; 4, α-chymotrypsinogen A; 5, myoglobin; 6, carbonic anhydrase; 7, transferrin; 8, α-lactalbumin. In both cases N_{av} was calculated on the well defined peaks, i.e. peaks 1, 2, 4, 6, and 8.

proteins and high electroosmotic flow nearing that obtained with uncoated capillaries. Figure 10 A illustrates the separation of 8 acidic and basic standard proteins spanning a wide range of molecular weights. This electropherogram is typical of what can be obtained on an original I-200 coating that is still exhibiting constant performance in terms of efficiency, resolution and electroosmotic flow characteristics. We have chosen several proteins to better assess the feasibility of restoring a collapsed capillary. Figure 10 B represents a typical electropherogram obtained on the same capillary after it has lost some of its coating, whereby a significant drop in efficiency and resolution as well as a pronounced increase in electroosmotic flow can be noticed.

In an attempt to restore the performance of the capillary, the remaining of the coating was stripped of the inner wall of the collapsed capillary column by treatment with aqueous solutions of sodium hydroxide. The naked capillary thus obtained was then recoated as described in the experimental section. It can be seen from Fig. 10 C that the column can be restored to its original performance in every regard. To assess the reproducibility of this procedure, we have performed the restoration several times on collapsed I-200 capillaries and each time obtained similar results to those reported in Fig. 10 C. The procedure developed here for restoring capillary coatings is expected to be applicable to other type of coatings provided that they are attached to the capillary inner surface *via* siloxane bonds.

Referring to Figs 10 A and 10 C, It should be noted that human serum transferrin is a heterogeneous glycoprotein consisting of at least five isoforms [27,28] that differ among each other in sialic acid content. It can be seen that the present electrophoretic system is capable of separating these isoforms. Furthermore, most of the commercial standard proteins are somewhat microheterogeneous or not highly pure as manifested by the presence of small peaks that elute before or after the main peaks when the selectivity of the electrophoretic system is adequate (e.g. myoglobin, cytochrome c, etc.; *cf* Figs 4, 5, 6 and 10).

Applications

As discussed above, the I-200 capillaries exhibited relatively higher electroosmotic flow than F-600 and F-2000 capillaries, and similarly to the fuzzy coatings they showed no significant solute-wall interactions over a wide range of pH. In capillary zone electrophoresis, the primary goal of surface modification of fused-silica capillaries is to minimize protein-wall interactions without completely inhibiting the electroosmotic flow. A reduction in the flow by a factor of 2.0 to 2.5 with respect to the untreated capillary is ideal in order to analyze both positively and negatively charged species in the positive polarity mode. This characteristic added to the "neutrality" of the inner wall is advantageous in capillary electrophoresis with on-line detection. As in slab gel electrophoresis the electropherogram, which is the written record of the experiment, should contain the maximum information about a given mixture. The presence of a moderate electroosmotic flow in capillary zone electrophoresis with coated capillaries permits the achievement of this goal. For a crude mixture whereby the pI values of all the components are not known, the presence of electroosmotic flow is essential to analyze and characterize (fingerprinting) the mixture. This is in part the advantage of I-200 capillaries over the fuzzy capillaries.

Figure 11 represents a typical electropherogram of crude soybean trypsin inhibitor (Sigma # T-9128) performed on I-200 capillaries. It can be seen that the mixture contains at least 23 minor components and one major component. Another example of the usefulness of I-200 in analyzing complex protein mixture is shown in Fig. 12, which illustrate the electropherogram of commercial lipoxidase (Sigma # L-8383), the unsaturated-fat oxidase. The microheterogeneity of lipoxidase was recently assessed by others [29] using several high performance liquid chromatography techniques. The
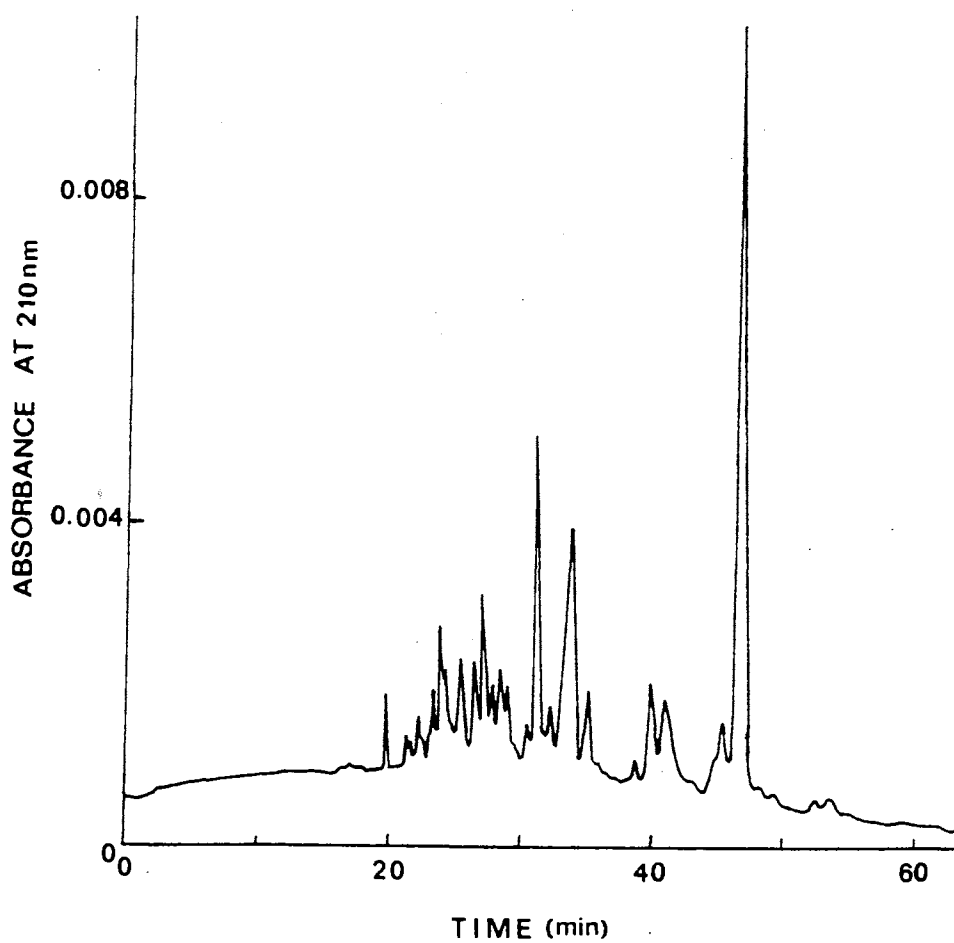
Figure 11. Electropherogram of crude soybean trypsin inhibitor. Capillary, I-200; electrolyte, 0.1 M phosphate solution, pH 6.5; running voltage, 17 kV. All other conditions as in Figs 2 and 3.
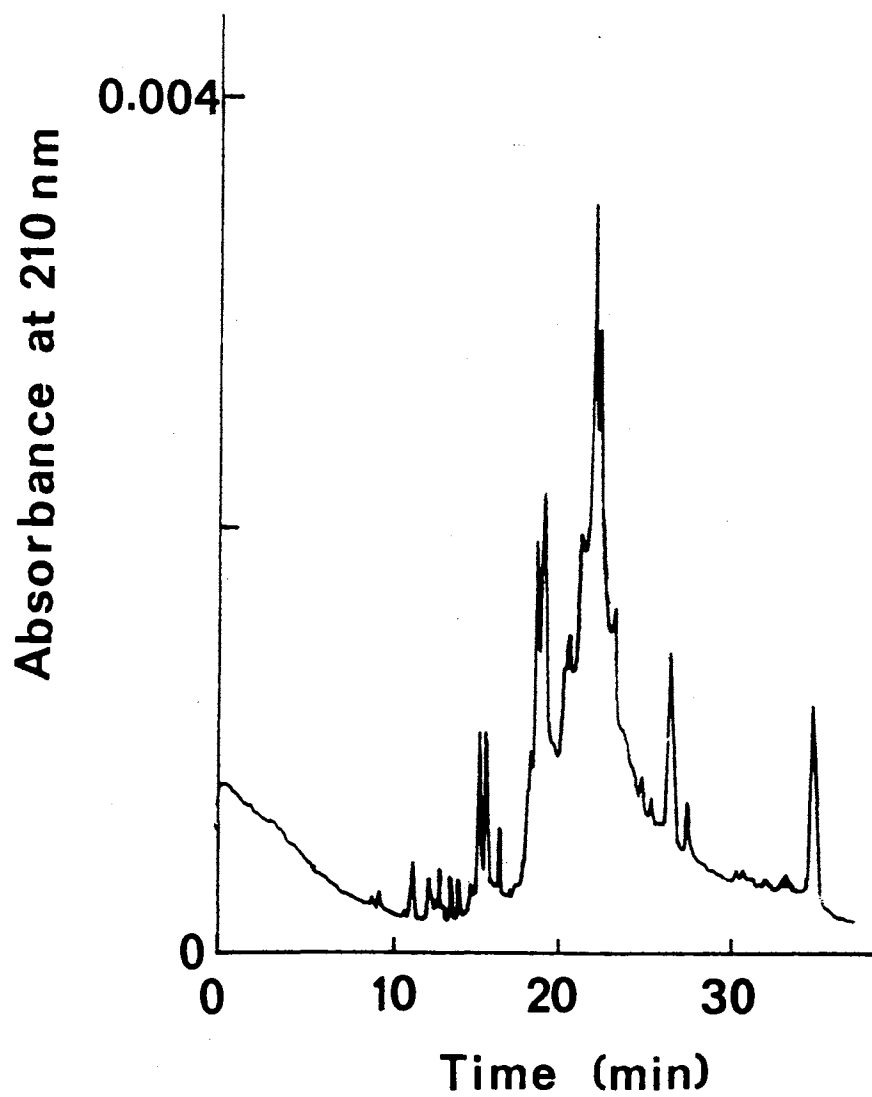
Figure 12. Electropherogram of commercial soybean lipoxidase. Capillary, I-200, 0.1 M phosphate solution, pH 7.0; running voltage 17 kV. All other conditions as in Figs 2 and 3.

commercial protein gave also multiple peaks when chromatographed by reversed-phase, anion exchange or metal chelate interaction chromatography [29].

The F-600 capillaries would also be useful in the above applications; however, longer analysis time would be expected under otherwise identical conditions. In a recent publication from our laboratory [17], F-2000 capillaries were used successfully at high voltage for the tryptic mapping of glycoproteins and the separation of oligosaccharide chains cleaved from glycoproteins. On the other hand, F-2000 capillaries may prove useful in isoelectric focusing or isotachophoresis whereby the presence of low electroosmotic flow may not be deleterious and good resolution of the solute bands could still be achieved.

Acknowledgement

References

1. F.E.P. Mikkers, F.M. Everaerts and T.P.E.M. Verheggen, *J. Chromatogr.*, 169 (1979) 11.

2. S. Hjerten, *J. Chromatogr.*, 270 (1983) 1.

3. J.W. Jorgenson and K.D. Lukacs, *Anal. Chem.*, 53 (1981) 1298.

4. S. Hjerten, *J. Chromatogr.*, 347 (1985) 191.

5. J.W. Jorgenson, *Trends Anal. Chem.*, 3 (1984) 51.

6. R.M. McCormick, *Anal. Chem.*, 60 (1988) 2322.

7. G.J.M. Bruin, J.P. Chang, R.H. Kuhlman, K. Zegers, J.C. Kraak and H. Poppe, *J. Chromatogr.*, 471 (1989) 429.

8. G.J.M. Bruin, R. Huisden , J.C. Kraak and H. Poppe, *J. Chromatogr.*, 480 (1989) 339.

9. S. A. Swedberg, *Anal. Biochem.*, 185 (1990) 51.

10. J.K. Towns and F.E. Regnier, *J. Chromatogr.*, 516 (1990) 69.

11. K.A. Cobb, V. Dolnik and M. Novotny, *Anal. Chem.*, 62 (1990) 2478.

12. H.H. Lauer and D. McManigill, *Anal. Chem.*, 58 (1986) 166.

13. Y. Walbroehl and J.W. Jorgenson, *J. Microcolumn Sep.*, 1 (1989) 41.

14. J.S. Green and J.W. Jorgenson, *J. Chromatogr.*, 478 (1989) 63.

15. M. Bushey and J.J. Jorgenson, *J. Chromatogr.*, 480 (1989) 301.

16. W. Nashabeh and Z. El Rassi, *J. Chromatogr.*, 514 (1990) 57.

17. W. Nashabeh and Z. El Rassi, *J. Chromatogr.*, 536 (1991) 31.

18. K.K. Unger, *"Porous Silica,"* Elsevier Scientific Publishing, Co., New York, 1979, p. 86

19. G.S. Manning, *Q. Rev. Biophys.*, 11 (1978) 179.

20. J.W. Jorgenson, *ACS Symp. Ser.*, 335 (1987) 182.

21. J.H. Knox and I.H. Grant, *Chromatographia,* 24 (1987) 135.

22. F. Foret, M. Deml and P. Bocek, *J. Chromatogr.,* 452 (1988) 602.

23. E. Grushka, R.M. McCormick and J.J. Kirkland, *Anal. Chem.,* 61 (1989) 241.

24. M. Martin and G. Guiochon, *Anal. Chem.,* 56 (1984) 614.

25. S. Hjerten, *J. Chromatogr.,* 87 (1973) 325.

26. Z. El Rassi, A.L. Lee and Cs. Horvath, in J.A. Asenjo (ed), *"Separation Processes in Biotechnology,"* Marcel Dekker, Inc., 1990, p. 447.

27. S. Petren and O. Vesterberg, *Biochim. Biophys. Acta,* 994 (1989) 161.

28. F. Kilar and S. Hjerten, *J. Chromatogr.,* 480 (1989) 351.

29. Y. Kato, K. Nakamura and T. Hashimoto, *J. Chromatogr.,* 354 (1986) 511.

CHAPTER III

COUPLED FUSED SILICA CAPILLARIES FOR RAPID
CAPILLARY ZONE ELECTROPHORESIS
OF PROTEINS*

Abstract

A novel two-dimensional electrophoretic system for the control of electroosmosis in capillary zone electrophoresis has been developed and evaluated for rapid separations of proteins. The system comprises uncoated and polyether-coated fused silica capillaries coupled in series. An equation relating the average electroosmotic flow velocity in the coupled capillaries to the intrinsic electroosmotic velocities of the connected segments and their corresponding lengths has been derived and verified experimentally. This approach has the advantage of enabling the electroosmotic flow to be tuned independently of the applied voltage. As a consequence, rapid protein separations at relatively low field strength was achieved without sacrificing the high separation efficiencies obtained with surface modified capillaries.

Introduction

Capillary zone electrophoresis (CZE) is rapidly becoming an important microseparation tool in many areas of the life sciences and biotechnology. The success of the technique in the separation of biopolymers, and in particular proteins, has in part been a

---

64

result of recent advances in surface treatment which have yielded capillaries which are more inert and less-adsorptive towards biomacromolecules than untreated fused-silica [1-5]. Most procedures for surface modification have, however, resulted in complete [1,2] or partial inhibition [3-5] of the electroosmotic flow; this has led to an increase in the analysis time of proteins.

The search for a system which would provide fast yet efficient protein analysis is still, therefore, a priority and several attempts have been made to control the direction and magnitude of the electroosmotic flow in fused silica capillaries. Typical examples include chemical modification of the capillary surface [1-5], addition of surface-active species to the running electrolyte [6,7], use of mixed buffer systems [8], and the superimposition of an external field across the capillary wall [9,10].

In a recent report from our laboratory [5], we have demonstrated the high separation efficiencies and potentials of fused-silica capillaries having surface-bound hydroxylated polyether functions in CZE of proteins. This publication introduces a simple two-dimensional electrophoretic system in which a hydrophilic polyether capillary is connected in series with an untreated fused-silica capillary past the detection point. Such coupling has reduced the analysis time by a factor of three without sacrificing separation efficiency.

The effect of the fractional length of the untreated capillary portion on the magnitude of the average electroosmotic flow in the coupled capillaries was investigated. A simple model was developed to calculate the average electroosmotic velocity throughout the tandem capillary columns. The methodology described here can be applied to other tandem electrophoretic systems we have previously reported, including those used for on-line preconcentration [11] and capillary enzymophoresis [6].

Theory

In capillary zone electrophoresis, a charged solute migrates within the bulk electroosmotic flow with an apparent velocity, v_{app}, given by:

$$v_{app} = v_{eo} + v_{ep} \qquad (1)$$

where v_{eo} and v_{ep} are the electroosmotic and electrophoretic velocities, respectively. Under a given set of conditions, the electrophoretic velocity of the analyte is a predetermined characteristic and cannot be manipulated easily. Instead, the electroosmotic velocity, the magnitude of which is proportional to the zeta potential, ζ, at the silica-water interface, can in some instances be adjusted independently to suit a given separation problem.

For a given capillary where the zeta potential of the wall is constant throughout the column, the electroosmotic velocity is expressed as :

$$v_{eo} = \frac{\varepsilon \zeta}{4 \pi \eta} E \qquad (2)$$

where ε and η are the dielectric constant and viscosity, respectively, of the medium and E is the electric field strength. When two or more capillary columns for which the magnitudes of the zeta potentials are different, i.e., for which the magnitudes of intrinsic electroosmotic velocities are different, the principle of conservation of matter for a noncompressible fluid (i.e., continuity principle) implies that the net outflow of mass from the volume be equal to the decrease of mass within the volume [12,13]. Therefore, for any particular section i of the coupled capillaries, the volumetric flow-rate, Q, should be constant and can be expressed as follows [13]:

$$Q = A_i \times v_{eo,i} = constant \qquad (3)$$

where A_i and $v_{eo,i}$ are the cross-sectional area and average velocity of the section i, respectively. A uniform bulk electroosmotic flow velocity should, therefore, be established throughout the whole capillary column provided that all the coupled columns have the same inner diameter. For a system of n coupled capillaries having the same inner diameter, the bulk flow would have an average velocity which is a weighted average of the intrinsic electroosmotic flow velocities of the tandem capillary columns, as follows:

$$v_{eo} = \sum_{i=1}^{n} \frac{v_{eo,i} l_i}{l_t} \qquad (4)$$

For the coupled capillaries system described in this report whereby two columns having different surface characteristics, i.e., polyether interlocked coating (denoted as I-200, see experimental) and untreated fused-silica, are connected in series, the average electroosmotic flow velocity can be expressed as:

$$v_{eo} = \frac{v_{eo,1} l_1}{l_t} + \frac{v_{eo,2} l_2}{l_t} \qquad (5)$$

or

$$v_{eo} = \frac{\varepsilon}{4\pi\eta} \left(\frac{\zeta_1 l_1}{l_t} + \frac{\zeta_2 l_2}{l_t} \right) E \qquad (6)$$

where l_t is the total length of the connected capillaries, $v_{eo,1}$ and $v_{eo,2}$ are the intrinsic electroosmotic velocities obtained on separate lengths of the I-200 and untreated fused silica capillaries, respectively, and l_1 and l_2 are the corresponding lengths of the capillaries.

Equation (5) can be also expressed in term of the electroosmotic mobilities as follows:

$$\mu_{eo} = \frac{\mu_{eo,1} l_1}{l_t} + \frac{\mu_{eo,2} l_2}{l_t} \qquad (7)$$

which can be rearranged into the following form:

$$\mu_{eo} = \left(\mu_{eo,1} - \mu_{eo,2} \right) \frac{l_1}{l_t} + \mu_{eo,2} \qquad (8)$$

A plot of μ_{eo} versus l_1/l_t gives a straight line with a slope of $\mu_{eo,1} - \mu_{eo,2}$ and an intercept of $\mu_{eo,2}$. Furthermore, Eqn. 8 is valid irrespective of the direction of the electroosmotic flow. It can be envisioned from this concept, that by connecting equal. lengths of two capillaries having intrinsic electroosmotic mobilities of same magnitude but of opposite sign, a tandem electrophoretic system with zero flow can be achieved. It is also possible to yield zero flow by coupling appropriate lengths of capillaries which have different flow magnitudes which are opposite in direction.

Experimental

Instrument and Capillary Columns

Capillary electrophoresis was performed on an instrument assembled in-house from commercially available components; it resembled that already reported [5,11]. Polyimide-coated fused-silica capillaries of 50-μm I.D. and 365-μm O.D. were obtained from Polymicro Technology (Phoenix, AZ, U.S.A.). Untreated and polyether coated capillaries were used in this study. Capillaries coated with surface-bound interlocked polyether moieties of average molecular weight 200, i.e., poly(ethyleneglycol) 200, were prepared according to previously described procedures [5] and coded as I-200.

Reagents and Materials

Carbonic anhydrase from bovine erythrocytes, α-lactalbumin and β-lactoglobulin B both from bovine milk were purchased from Sigma (St. Louis, MO, U.S.A.). Phenol which was used as an inert tracer for measuring the electroosmotic flow was obtained from J.T. Baker Inc (Phillipsburg, NJ, USA). All other reagents were of analytical grade and were from Fisher Scientific (Pittsburgh, PA, U.S.A.).

Methods

In all experiments, the capillary columns were connected butt-to-butt using a PTFE tube the inner diameter of which matched the outer diameters of the two capillary columns. The total length of the coupled capillaries was kept constant and was equal to 80 cm; the separation distance, i.e., the distance between the points of injection and detection, was 30 cm. The lengths of the individual capillaries were, however, varied to encompass various proportions of the differently coated columns. Solutes were introduced hydrodynamically by raising the inlet reservoir for a certain height above the outlet reservoir for a given period of time. The detection wavelength was set at 210 nm for sensing the various protein solutes as well as the neutral marker, phenol.

Results and Discussion

Tunable Electroosmosis

The electrophoretic system with coupled capillaries was first characterized in terms of its average electroosmotic flow, using phenol as an inert tracer. The results obtained are depicted in Figure 1 by a plot of the electroosmotic mobility as a function of the fractional length of the untreated portion of the capillary: the applied potential was 20 kV and the running electrolyte 0.1 M sodium phosphate solution, pH 6.5. As shown in this plot, the electroosmotic mobility increased linearly with increasing the length of the untreated capillary (i.e., that which had the highest intrinsic electroosmotic velocity in the tandem system). The experimental electroosmotic mobility data points fitted quite well Eqn 8 with a correlation coefficient of 0.997. Thus, by simply variation of the fractional length of either capillary column, the electroosmotic mobility can be tuned to any desired level within the upper and lower limits set by the intrinsic electroosmotic mobilities of the individual capillaries.
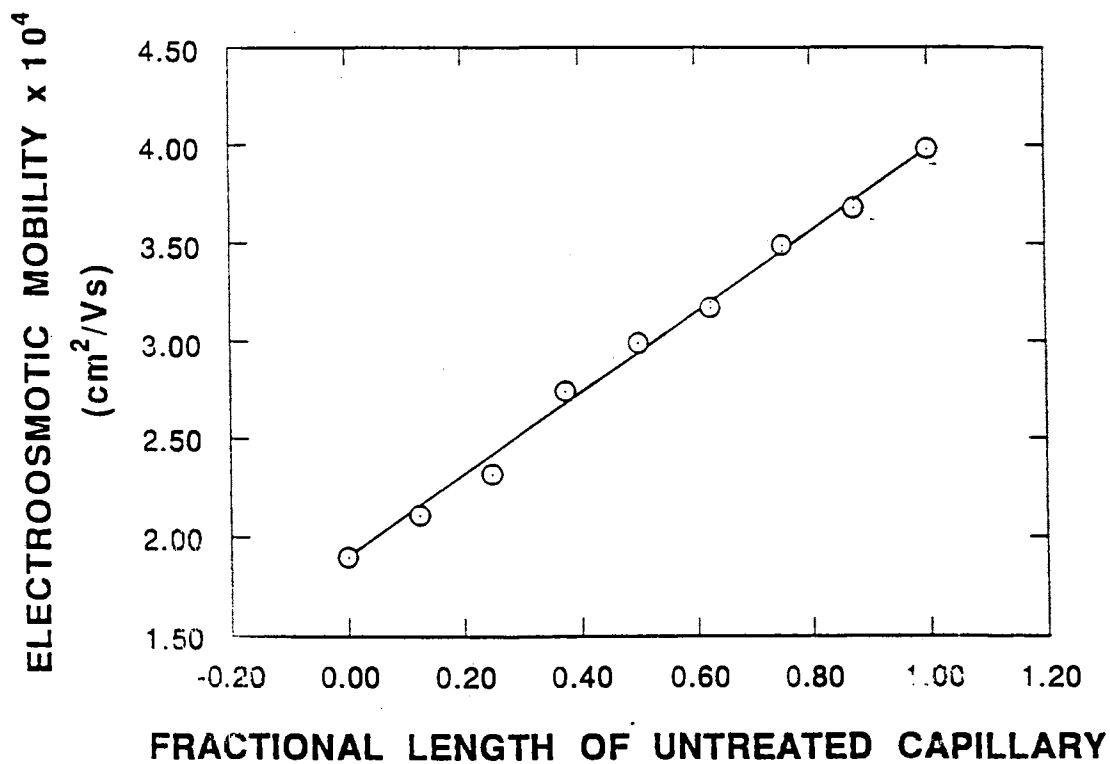
Figure 1. Dependence of electroosmotic mobility on the fractional length of the untreated capillary segment in coupled I-200 → untreated capillaries. Tandem capillaries, 30 cm (to the detection point), 80 cm (total length) x 50 μm I.D., length of individual capillaries varied to span the various fractional lengths investigated; running voltage, 20 kV; background electrolyte, 0.1 M sodium phosphate solution, pH 7.0. Inert tracer: phenol.

Rapid Separation of Proteins

The usefulness of the tandem electrophoretic system for the rapid separation of proteins was also evaluated. Figure 2a illustrates a typical electropherogram of three model proteins performed on an I-200 coated capillary, again using an applied voltage of 20 kV with 0.1 M sodium phosphate solution as the running electrolyte. Figure 2b-e demonstrate the electropherograms obtained from the same protein mixture on tandem I-200 → untreated capillary combinations; the lengths of the component columns were in different proportions, but otherwise the conditions were identical. It can be seen from these electropherograms that the apparent mobility of the model proteins increased monotonically with increasing the fractional length of the untreated capillary portion. This is further illustrated in Figure 3 which represents typical plots of the apparent and electrophoretic mobilities of α-lactalbumin, and the electroosmotic mobility of the neutral marker, as a function of the fractional length of the untreated capillary in the tandem system; the conditions used were as described above. As expected, the apparent mobility, which is the sum of electroosmotic and electrophoretic mobilities, increased linearly (correlation coefficient of 0.996) in the range studied, and almost paralleled the electroosmotic mobility, whereas the electrophoretic mobility remained unchanged. Similar behavior to that shown in Figure 3 was observed for carbonic anhydrase and β-lactoglobulin B. These findings demonstrate the suitability of the tandem I-200 → untreated capillary system for the analysis of acidic proteins which would be electrostatically repulsed from the negatively charged fused silica capillaries. Other tandem systems that will suit the analysis of basic, neutral and acidic proteins in a single electrophoretic run are currently under development (see chapters 4 and 5).

The tandem electrophoretic system was also evaluated in terms of separation efficiencies. The average plate height per meter (H_{av}) is indicated on each electropherogram in Figure 2. From these measurements, it can be seen that the tandem
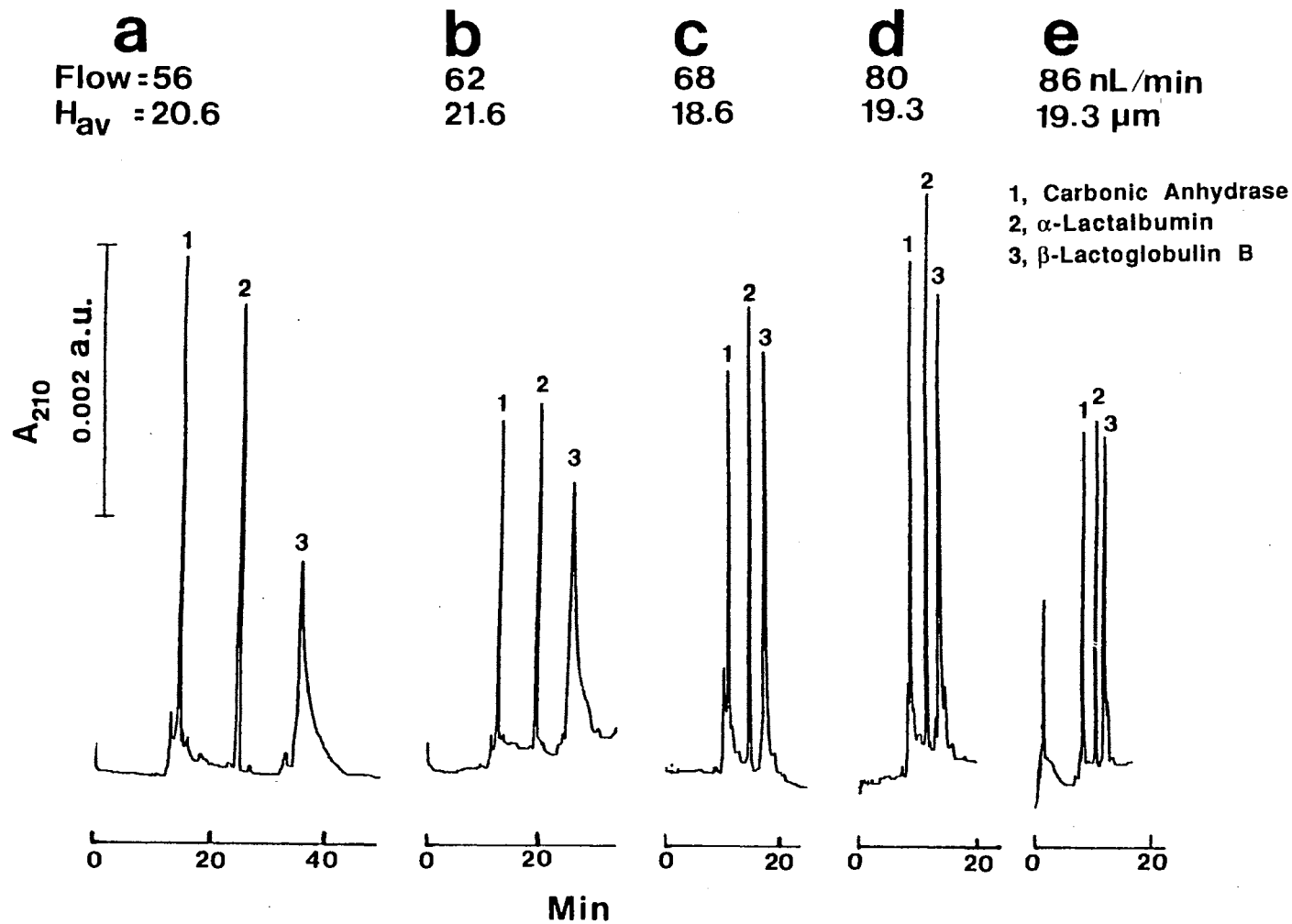
Figure 2. Typical electropherograms of proteins obtained on (a) I-200 coated capillary and (b-e) tandem I-200 → untreated capillaries with 0.125, 0.25, 0.375, and 0.5 fractional lengths of the untreated segment, respectively. Proteins: 1, carbonic anhydrase; 2, α-lactalbumin; 3, β-lactoglobulin B.
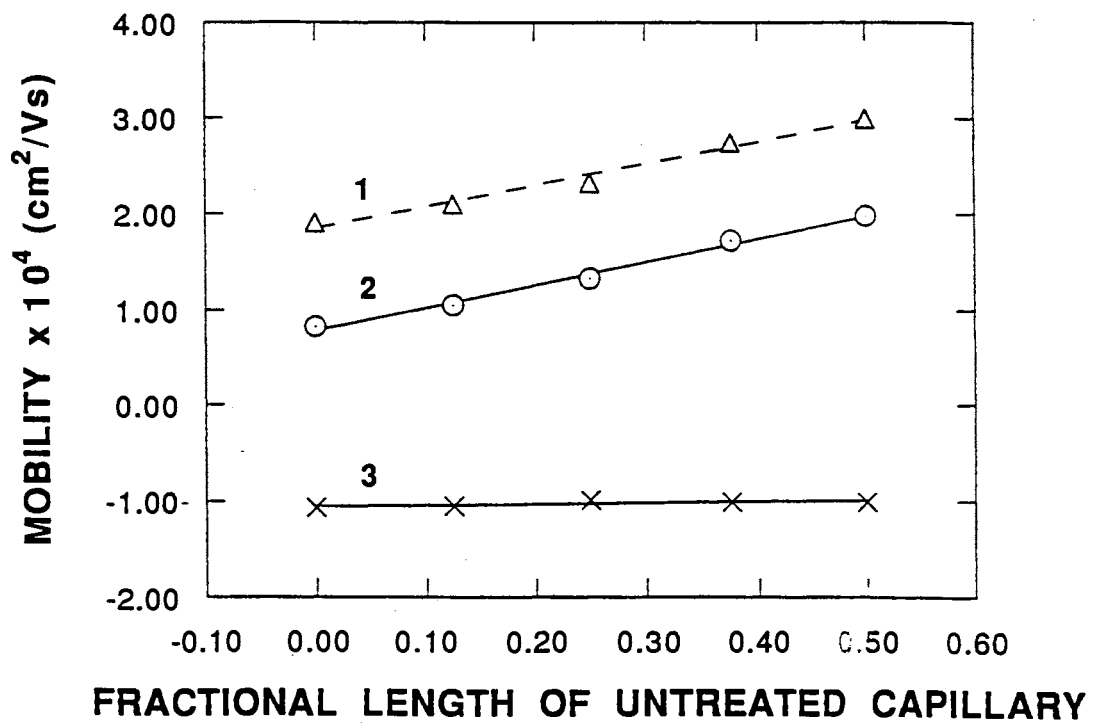
Figure 3. Dependence of electroosmotic mobility (1) and apparent and electrophoretic mobilities (2 and 3, respectively) of α-lactalbumin on the fractional length of the untreated capillary segment in coupled I-200 → untreated capillaries.

operation has no adverse effects on the separation efficiencies. Comparison of Figures 2a and 2e reveals that H_{av} decreased slightly from 20.6 to 19.3 μm, while the migration time for carbonic anhydrase, α-lactalbumin and β-lactoglobulin B decreased by a factor of 2.0, 2.4 and 2.9, respectively. This demonstrates the advantage of being able to perform rapid protein analysis with high separation efficiencies without the need to apply high potential drop, which may result in increased joule heating; it has, in fact, been shown that the separation efficiencies of proteins decreased sharply with increasing the applied voltage [2,5].

Conclusion

A simple tandem system has been developed which enables rapid protein analysis to be performed without sacrificing separation efficiency. The study has, in addition, revealed interesting fundamental points concerning the operation in series of coupled capillaries having surfaces with different zeta potentials. Other systems which enable the electroosmotic flow to be manipulated independently of the applied voltage during analysis are currently under investigation (see chapters 4 and 5).

Acknowledgement

References

1. S. Hjerten, *J. Chromatogr.*, 347 (1985) 191.

2. K. A. Cobb, V. Dolnik and M. Novotny, *Anal. Chem.*, 62 (1990) 2478.

3. S. A. Swedberg, *Anal. Biochem.*, 185 (1990) 51.

4. J. K. Towns and F. E. Regnier, *Anal. Chem.*, 63 (1991) 1126.

5. W. Nashabeh and Z. El Rassi, *J. Chromatogr.*, 559 (1991) 367.

6. W. Nashabeh and Z. El Rassi, *J. Chromatogr.*, 596 (1992) 251.

7. A. Emmer, M. Jansson, and J. Roeraade, *J. Chromatogr.*, 547 (1991) 544.

8. R.-L. Chien and J. C. Helmer, *Anal. Chem.*, 63 (1991) 1354.

9. C. S. Lee, W. C. Blanchard, and C.-T. Wu, *Anal. Chem.*, 62 (1990) 1550.

10. C. S. Lee, D. McMaginill, C.-T. Wu, and B. Patel, *Anal. Chem.*, 63 (1991) 1519.

11. J. Cai and Z. El Rassi, *J. Liq. Chromatogr.*, 15 (1992) 1179.

12. R. H. Sabersky and A. J. Acosta, *"Fluid Flow"*, The Macmillan Company, New York (1964) 16-19.

13. R. C. Binder, *"Fluid Mechanics"*, 2nd Edition, Prentice Hall, New York (1949) 41-43.

CHAPTER IV

FUNDAMENTAL AND PRACTICAL ASPECTS OF COUPLED CAPILLARIES FOR THE CONTROL OF ELECTROOSMOTIC FLOW IN CAPILLARY ZONE ELECTROPHORESIS OF PROTEINS*

Abstract

This article represents an extension to a new approach, which was introduced very recently by our laboratory (see chapter 3), for the control of the magnitude of electroosmotic flow in capillary zone electrophoresis. In this new approach, short fused silica capillaries having different ζ potentials were coupled in series, and the amount of the electroosmotic flow was conveniently varied by changing the lengths of the individual capillary segments. The different coupled capillary systems evaluated in this study comprised various combinations of untreated fused silica capillaries and polyether coated capillaries having various electroosmotic flow characteristics. A general equation relating the average electroosmotic flow velocity in the coupled capillaries to the intrinsic electroosmotic velocity of the connected segments and their corresponding lengths has been derived and verified experimentally. The rate of the electroosmotic flow in a given system of coupled capillaries could be tuned over a range bordered by the lowest and highest intrinsic flow rates of the connected capillary segments. In addition, a system of

---

coupled capillaries that permitted a stepwise change in the rate of the electroosmotic flow during analysis was introduced and evaluated. These elution schemes were useful in the rapid separation of oppositely charged proteins in a single electrophoretic run and in the rapid analytical determination of the various components of heterogeneous proteins.

Introduction

In capillary zone electrophoresis (CZE), the observed migration behavior of charged species is determined by the electroosmotic flow (EOF) of the bulk solution inside the capillary and the electrophoretic mobilities of the analytes. While separation in CZE is based on differences in the electrophoretic mobilities of the analytes, the amount of time the solutes spend in the capillary is affected by the direction and magnitude of the EOF, which contribute to the migration of all analytes to the same extent regardless of their charges. While a relatively low level of electroosmotic flow is advantageous for the separation of closely related positively or negatively charged species, the analysis of basic, neutral and acidic solutes in a single electrophoretic run would require a relatively strong electroosmotic flow velocity.

Recently, Lee et al [1, 2] demonstrated that the direction and velocity of the EOF can be changed by the application of an external electric potential across a buffer-filled sheath capillary surrounding the separation capillary. More recently, Hayes and Ewing [3] proposed the use of a radial voltage with capillaries having an external film of conductive polymer for the control of EOF in CZE. However, the control of the electroosmotic flow by virtue of electronic means, i.e., application of an external electric field, is only effective at low pH or with the use of surface modified capillaries whereby the concentration of the ionized surface groups are quite low and thus can be overcome by the electrostatic charges induced by the external potential.

Very recently, we have introduced a new electrophoretic system for the control of EOF in CZE. In this system, two capillaries having different wall ζ potential were coupled in series beyond the detection point [4]. When fused-silica capillaries with polyether coatings were connected to untreated fused-silica capillary tubes, the average electroosmotic flow velocity throughout the tandem capillary system was found to be a linear function of the fractional length of the individual connected capillary segments. This enabled the tuning of the rate of EOF independently of the applied voltage within the upper and lower limits of the intrinsic electroosmotic mobilities in the individual connected capillaries. The tandem operation allowed the rapid analysis of acidic proteins that would repulse electrostatically from the negatively charged fused-silica surface.

The aim of the present article is to investigate the potentials of other coupled capillary systems in the control of EOF and to extend the utility of the new approach to the rapid analysis of oppositely charged proteins in a single electrophoretic run with minimum solute-wall interaction. This was accomplished by connecting in series fused-silica capillaries of different intrinsic electroosmotic flow characteristics whose inner surfaces were either naked or modified with polyether chains of various length. Such coupling has reduced the separation time of model proteins by a factor of 2 on the average. In addition, a configuration of coupled capillaries which allowed a stepwise increase in the electroosmotic flow during analysis was introduced. This elution scheme permitted a 3 fold decrease in the analysis time of model proteins without sacrificing the high separation efficiencies that can be achieved with surface-modified capillaries.

Experimental

Apparatus

The instrument for capillary electrophoresis used in this study was assembled in-house from commercially available components, and resembled that reported earlier [4,5].

It comprised two high-voltage power supplies of positive and negative polarity Models MJ30P400 and MJ30N400, respectively, from Glassman High Voltage (Whitehouse Station, NJ, U.S.A.) and a Linear (Reno, NV, U.S.A.) Model 200 UV-Vis variable wavelength detector equipped with a cell for on-column capillary detection. The electropherograms were recorded with a Shimadzu computing integrator Model C-R6A (Columbia, MD, U.S.A.) equipped with a floppy disk drive and a cathode-ray tube (CRT) monitor.

<u>Reagents and Materials</u>

Lysozyme from chicken egg white, ribonuclease A from bovine pancreas, carbonic anhydrase from bovine erythrocytes, α-lactalbumin and β-lactoglobulin B both from bovine milk and albumin from chicken egg were purchased from Sigma (St. Louis, MO, U.S.A.). Table I compiles the molecular weights (M_r) and isoelectric points (pI) of these proteins. Reagent grade sodium phosphate monobasic, hydrochloric acid, sodium hydroxide and HPLC grade methanol were obtained from Fisher Scientific (Pittsburgh, PA

TABLE I

PROTEINS USED IN THIS STUDY.

Proteins	M_r	pI
Lysozyme	14,100	11.0
Ribonuclease A	13,700	9.40
Carbonic anhydrase	31,000	6.20
α-lactalbumin	14,200	4.80
β-lactoglobulin A	35,000	5.23
Albumin, egg	45,000	4.63

U.S.A.). Phenol which was used as an inert tracer for measuring the electroosmotic flow (EOF) was obtained from J.T. Baker Inc (Phillipsburg, NJ, USA).

Capillary Columns

Polyimide-coated fused-silica capillary columns of 50-μm I.D. and 365-μm O.D. were obtained from Polymicro Technology (Phoenix, AZ, U.S.A.). Both untreated and coated capillaries were used in this study. The coated capillaries were modified in-house with surface-bound hydroxylated polyether chains of various length according to previously described procedures [6]. The capillary coding I-200 and F-2000 are used to denote capillaries with interlocked coatings having polyethylene glycol 200 chains and capillaries having fuzzy coatings with polyethylene glycol 2000 moieties, respectively.

Other Procedures

The capillary segments of the tandem capillary systems were connected butt-to-butt using PTFE tubes the inner diameter of which matched the outer diameter of the connected capillary columns. In all cases the connection was made beyond the detection point. While the length of the individual capillaries having different surface characteristics was varied to span a wide range of fractional length, the total length of the coupled capillaries was kept constant at 80 cm with a detection window at 30 cm from the inlet reservoir. It has to be noted that in all experiments, the background electrolyte was 0.1 M sodium phosphate, pH 6.50. Solute introduction was by hydrodynamic flow (i.e., by gravity flow) at a differential height of 5 cm between the electrolyte reservoirs for 10 seconds. The detection wavelength was set at 210 nm for sensing the various proteins as well as the inert tracer.

To ensure reproducible separations the capillary column was flushed successively with fresh buffer, water, methanol, water, and again running buffer. In addition, the

running electrolyte was renewed after each run and the capillary was allowed to equilibrate with the new buffer for 10 minutes before each injection.

<center>Results and Discussion</center>

Control of Electroosmotic Flow by Coupled Capillaries

We have previously shown [4] that for a system of n coupled capillaries having the same inner diameter but differing in their ζ potentials, the average electroosmotic mobility, μ_{eo}, across the tandem system is a weighted average of the intrinsic or local electroosmotic mobilities in the individual connected segments as follows [4]:

$$\mu_{eo} = \frac{\sum_{i=1}^{n} \mu_{eo,i} l_i}{l_t} \qquad (1)$$

where l_i is the length of the individual capillary segment, i, l_t is the total length of the connected capillaries and $\mu_{eo,i}$ is the intrinsic electroosmotic mobility in each capillary segment, i, measured on a separate length l_i. Equation 1 can be rearranged as a linear function of the fractional length of a given capillary segment, i, in the tandem capillaries as follows:

$$\mu_{eo} = (\mu_{eo,i} - \sum_{j=1,j\#i}^{n} \mu_{eo,j}) \frac{l_i}{l_t} + \sum_{j=1;j\#i}^{n} \mu_{eo,j}[1 - \frac{\sum_{k=1;k\#i,j}^{n} l_k}{l_t}] \qquad (2)$$

where j and k are random variables. It follows then that the electroosmotic flow can be in principle controlled to any desired value bordered by the lowest and highest intrinsic electroosmotic mobilities in the individual capillaries.

Due to the differences between the intrinsic electroosmotic flows in the connected segments and the uniform bulk flow across the tandem capillary system, a compensating

hydrostatic pressure would develop. Consequently, a deviation from a plug flow profile towards a laminar or Poiseuille profile would result. As the difference between the intrinsic electroosmotic flow and the bulk flow increases, the laminar flow profile would become more pronounced. Although a purely pressure driven laminar flow is known to introduce band broadening, it has been shown recently that the superposition of a Poiseuille flow on an electroosmotic flow may not necessarily deteriorate the separation efficiencies [7]. In addition, under conditions whereby the pressure driven flow opposes the bulk flow, the electrokinetic dispersion coefficient may be even reduced [7]. A detailed treatment concerning the effects of superposed laminar and electroosmotic flow profiles on electrokinetic dispersion in CZE can be found in Ref. 7.

Equation 2 was verified experimentally by measuring the EOF in 3 different tandem capillary systems, i.e., F-2000 $\rightarrow$ I-200, F-2000 $\rightarrow$ untreated and I-200 $\rightarrow$ untreated, using phenol as the inert tracer. The results are shown in Fig. 1 by plots of the electroosmotic mobility versus the fractional length of the capillary segment having the highest intrinsic EOF. This will be the untreated capillary segment in the F-2000 $\rightarrow$ untreated and I-200 $\rightarrow$ untreated tandem capillaries, and I-200 capillary in the F-2000 $\rightarrow$ I-200 coupled capillaries (see legend of Fig.1 for details). As expected, the EOF changed linearly with the fractional length of the coupled capillaries and fitted quite well to Eqn. 2 with correlation coefficients of 0.997 on the average. The data points in Fig. 1 show clearly that the EOF can be changed in a predictable manner by varying the length of the connected capillary segment(s). The slope of these curves, $\mu_{eo,i} - \sum_{j=1,j\#i}^{n} \mu_{eo,j}$, is indicative of the range over which the EOF can be varied. The higher the slope, the wider is the range of variation. For instance, and at the voltage of the experiments of Fig. 1, the F-2000 $\rightarrow$ untreated coupled capillaries with the highest slope allowed the tuning of the EOF to any value between 28 and 115 nL/min, while with the F-2000 $\rightarrow$ I-200 tandem capillary system the change in the EOF was limited to the interval 28 to 58 nL/min.
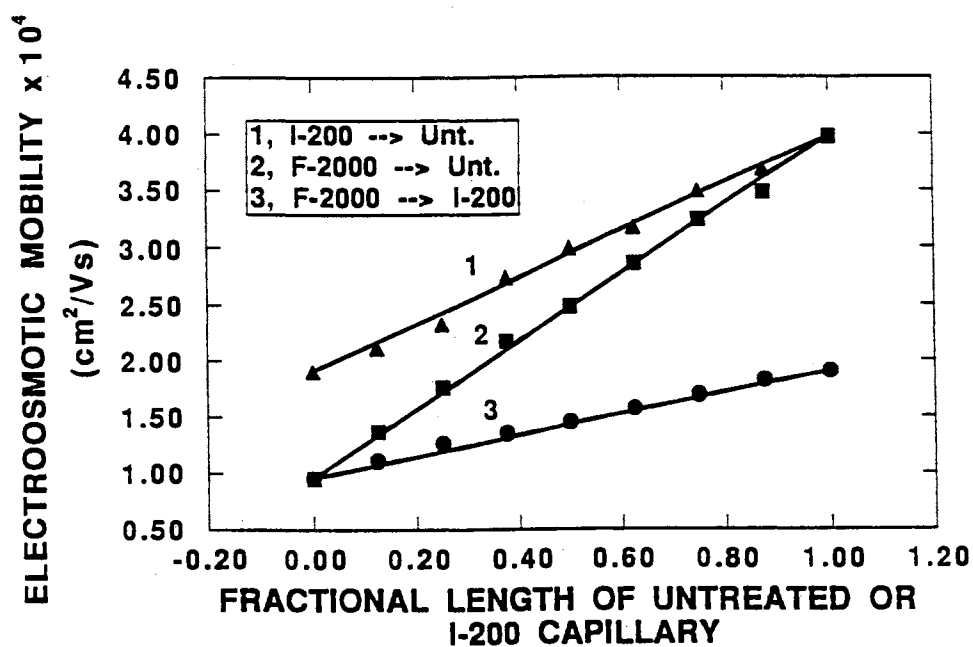
Figure 1. Plots of the electroosmotic mobility versus the fractional length of the untreated capillary segment in (1) and (2) or versus the fractional length of the I-200 capillary segment in (3). (1) I-200 → untreated, (2) F-2000 → untreated, (3) F-2000 → I-200. Tandem capillaries, 30 cm (to the detection point), 80 cm (total length) x 50 μm I.D.; running voltage, 20 kV; background electrolyte, 0.1 M sodium phosphate solution, pH 6.50. Inert tracer, phenol. Unt. stands for untreated fused-silica capillary.

Evaluation of the F-2000 → I-200 Coupled Capillaries with Proteins

An important feature of coupled capillaries is their ability to adjust the separation time to suit a particular separation problem. To realize this attractive advantage, the tandem system should meet three major criteria: (i) solute-wall interactions must be absent, (ii) the coupled capillaries should not introduce band broadening and (iii) the connected capillary segments should allow the tuning of the EOF over a wide range to accommodate the electrophoresis of a broad range of analytes.

Although, our initial studies with the I-200 → untreated capillaries showed promise in the rapid and efficient analysis of acidic proteins [4], this system was not suitable for the simultaneous separation of both acidic and basic proteins. In fact, as the basic proteins entered the untreated segment of the I-200 → untreated tandem system, the EOF started to decrease during the electrophoretic run due to solute adsorption on the inner surface of the capillary, and concomitant decrease in the magnitude of the negative ζ potential of the capillary wall. This phenomenon drastically delayed, and in some instances inhibited, the elution of the later eluting acidic proteins.

A better approach that would permit the analysis of oppositely charged species in the absence of solute-wall interactions is the use of the F-2000 → I-200 coupled capillaries. The polyether chains of these coated capillaries have been shown effective in minimizing solute-wall interaction [6]. Furthermore, due to the difference in the length and the way in which the polyether chains are attached to the capillary inner surface, the F-2000 and I-200 capillaries possess different levels of electroosmotic flow [6]. Therefore, their coupling would allow the tuning of the EOF so that oppositely charged solutes could be analyzed in a single electrophoretic run with high separation efficiencies.

The feasibility of the F-2000 → I-200 tandem capillaries in the rapid analysis of biopolymers was demonstrated by using a mixture of 5 model proteins the pI values of which ranged from 5.2 to 11.0 (see table I). Figure 2a depicts a typical electropherogram
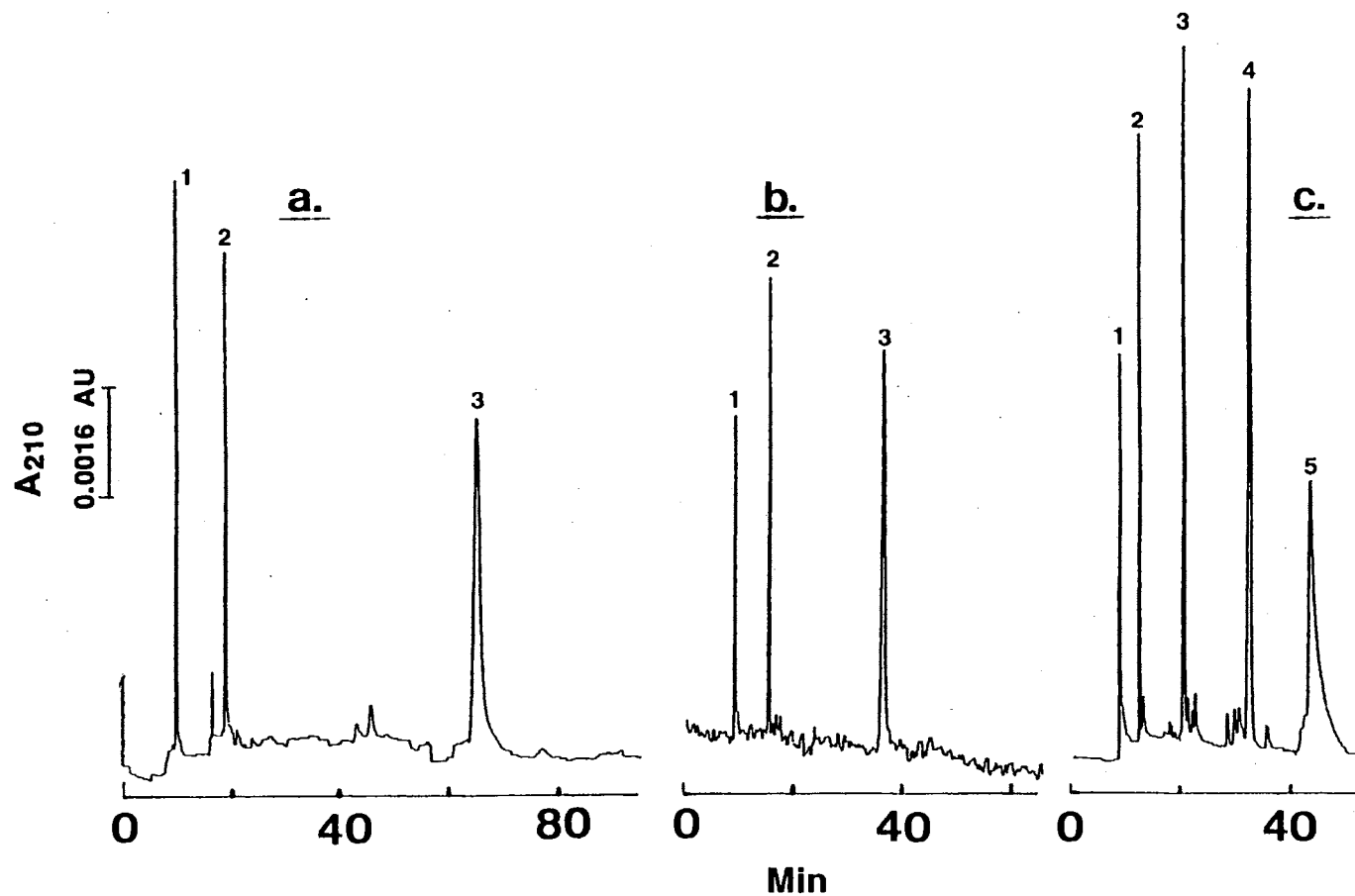
Figure 2. Typical electropherograms of proteins obtained on F-2000 coated capillary in (a) and on tandem F-2000 → I-200 capillaries with 0.25 and 0.5 fractional length of the I-200 capillary segment in (b) and (c), respectively. Proteins: 1, lysozyme; 2, ribonuclease A; 3, carbonic anhydrase; 4, α-lactalbumin; 5, β-lactoglobulin A. All other conditions are as in Fig. 1.

of this protein mixture performed on an F-2000 capillary at an applied voltage of 20 kV using 0.1 M sodium phosphate solution, pH 6.50, as the running electrolyte. Due to the low electroosmotic flow obtained with the F-2000 capillary (*ca.* 28 nL/min), carbonic anhydrase was eluted after ca. 65 min while the elution of a-lactalbumin would require 235 min as calculated from the EOF and the electrophoretic mobility of this solute. On the other hand, β-lactoglobulin A, having an electrophoretic mobility greater in magnitude and opposite in direction than the electroosmotic flow, would leave the F-2000 capillary and enter the inlet buffer reservoir after introducing the sample by gravity driven flow. Although high separation efficiencies could be achieved, the F-2000 capillary can only be used for the analysis of basic and moderately acidic solutes. Figure 2b and c illustrates the electropherograms of the same protein mixture performed on the F-2000 → I-200 coupled capillaries with 0.25 and 0.5 fractional length of the I-200 capillary segment, respectively, under otherwise identical conditions as in Fig. 2a. It can be seen from these electropherograms that the analysis time of the model proteins decreased as the fractional length of the I-200 capillary increased. At 0.5 fractional length of the I-200 capillary, the EOF generated (43 nL/min) by the tandem capillaries was enough to bring about the analysis of all 5 proteins within 50 min.

Figure 3 illustrates typical plots of the overall and electrophoretic mobilities of two proteins as well as plots of the electroosmotic mobility versus the fractional length of the I-200 capillary segment in F-2000 → I-200 coupled capillaries. In both cases, the electrophoretic mobility of the two test proteins remained practically unchanged while the overall and electroosmotic mobilities increased linearly and paralleled each other. This observation indicates that the variation in the analysis time of the model proteins is solely due to the change in the EOF, and no significant interaction between the proteins and the inner surface proper of the capillaries was present.

The effect of the tandem system on the bandwidth of the separated proteins was also investigated. Table II summarizes the plate height obtained with three model proteins

a.

b.
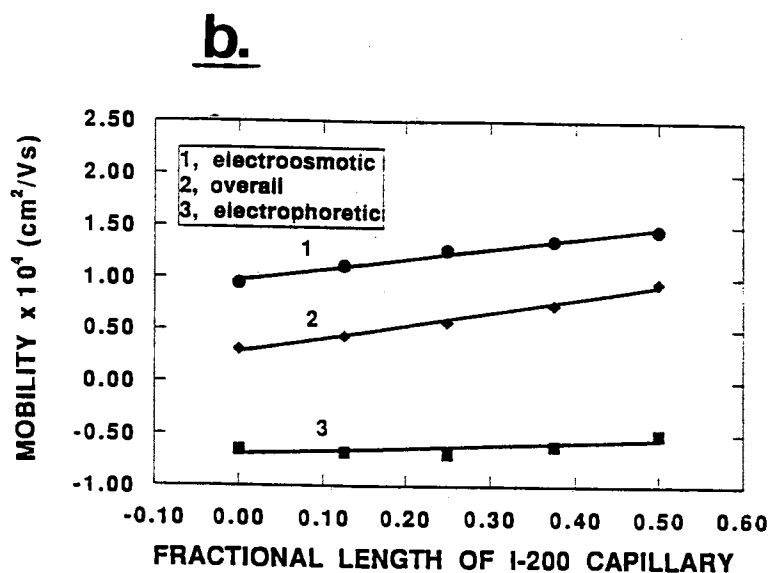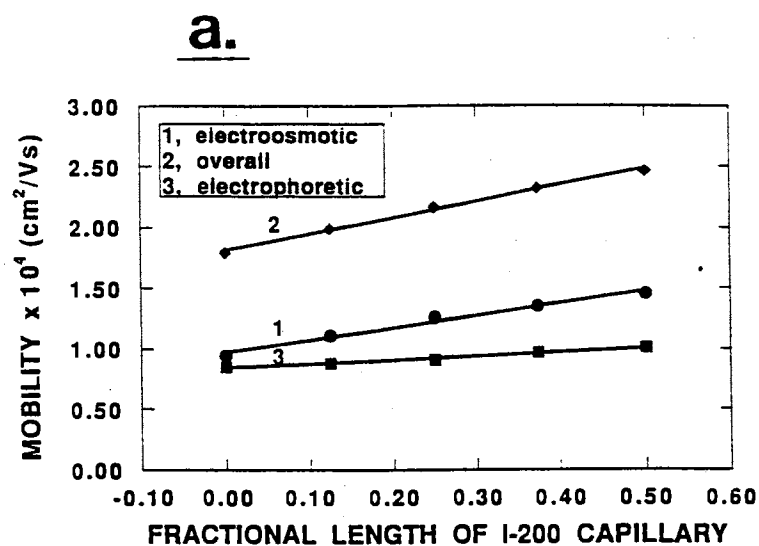
Figure 3. Plots of overall and electrophoretic mobilities of lysozyme in (a) and carbonic anhydrase in (b) as well as plots of the electroosmotic mobility of phenol versus the fractional length of the I-200 capillary segment in the F-2000 → I-200 tandem system. All other conditions are as in Fig. 1.

TABLE II

VALUES OF PLATE HEIGHT (H) MEASURED FROM SELECTED PROTEIN PEAKS

Protein	H (μm)				
	Fractional length of I-200 capillary in the F-2000 $\rightarrow$ I-200 system				
	0.00	0.125	0.25	0.375	0.50
Lysozyme	7.05	6.12	6.70	7.59	7.50
Ribonuclease A	3.50	4.10	5.00	5.80	6.67
Carbonic anhydrase	20.4	18.8	15.2	16.5	19.2
Average plate height *	10.3	9.67	8.97	9.96	11.1

at each fractional length studied. It can be seen from Table II that while the average plate

height of the three model proteins remained almost the same, the analysis time decreased

by a factor of *ca.* 2.0 at 0.5 fractional length of each of the connected capillaries. It is

believed that shortening the residence time of the separated analytes has decreased the

amount of molecular diffusion, and subsequently may have compensated for band

broadening caused by the laminar flow profile.

Separation of Ovalbumin Components

Ovalbumin, the major protein constituent of egg white, is a heterogeneous protein

due to the variation in its phosphate content [8]. About 75% of this protein possesses two

phosphate groups per mole of the protein, and is designated A_1. The remaining of

ovalbumin largely consists of another component, A_2, having only one phosphate group

per molecule. In addition, small amounts of a phosphate-free component, A_3, are also

present. Obviously, when ovalbumin was analyzed by electrophoresis, it showed different bands [9].

Therefore, ovalbumin was a good example to evaluate the effect of the magnitude of EOF as far as the quality of the analytical information generated during CZE separation is concerned. In other words, the goal was to determine whether there would be a loss in the analytical information when the speed of separation was increased. On this basis two tandem capillary systems of moderate and relatively high EOF were evaluated. As demonstrated in Fig. 1, F-2000 → I-200 offers a tunable flow over a moderate range whereas F-2000 → untreated allows a higher EOF to be realized. Figure 4a and b represents typical electropherograms of ovalbumin performed on the F-2000 → I-200 and F-2000 → untreated tandem capillaries, respectively. Similarly to previous observations in free-boundary electrophoresis [9], this protein showed different electrophoretic components due to the variation in its phosphorous content. Comparison of Fig. 4a and b reveals that both electropherograms clearly show all the differently phosphorylated components of ovalbumin; the only difference is that the separation time on the F-2000 → untreated system was decreased by a factor of ca. 4.0. Thus, while drastically decreasing the separation time, the analytical information remained almost the same when going from low to high EOF by the use of coupled capillaries.

Rapid Separation of Proteins by Stepwise Increase in the EOF

The separation time of oppositely charged proteins was further decreased by increasing the EOF during the electrophoretic run. This was carried out by switching manually from one tandem capillary system of relatively low EOF to another set of coupled capillaries of higher EOF. In the beginning of the run, the tandem system consisted of three capillary segments connected in series and containing F-2000, I-200 and untreated capillary at 0.5, 0.25 and 0.25 fractional lengths, respectively. Thereafter, a stepwise increase in EOF was carried out by connecting in series F-2000 and untreated capillary at
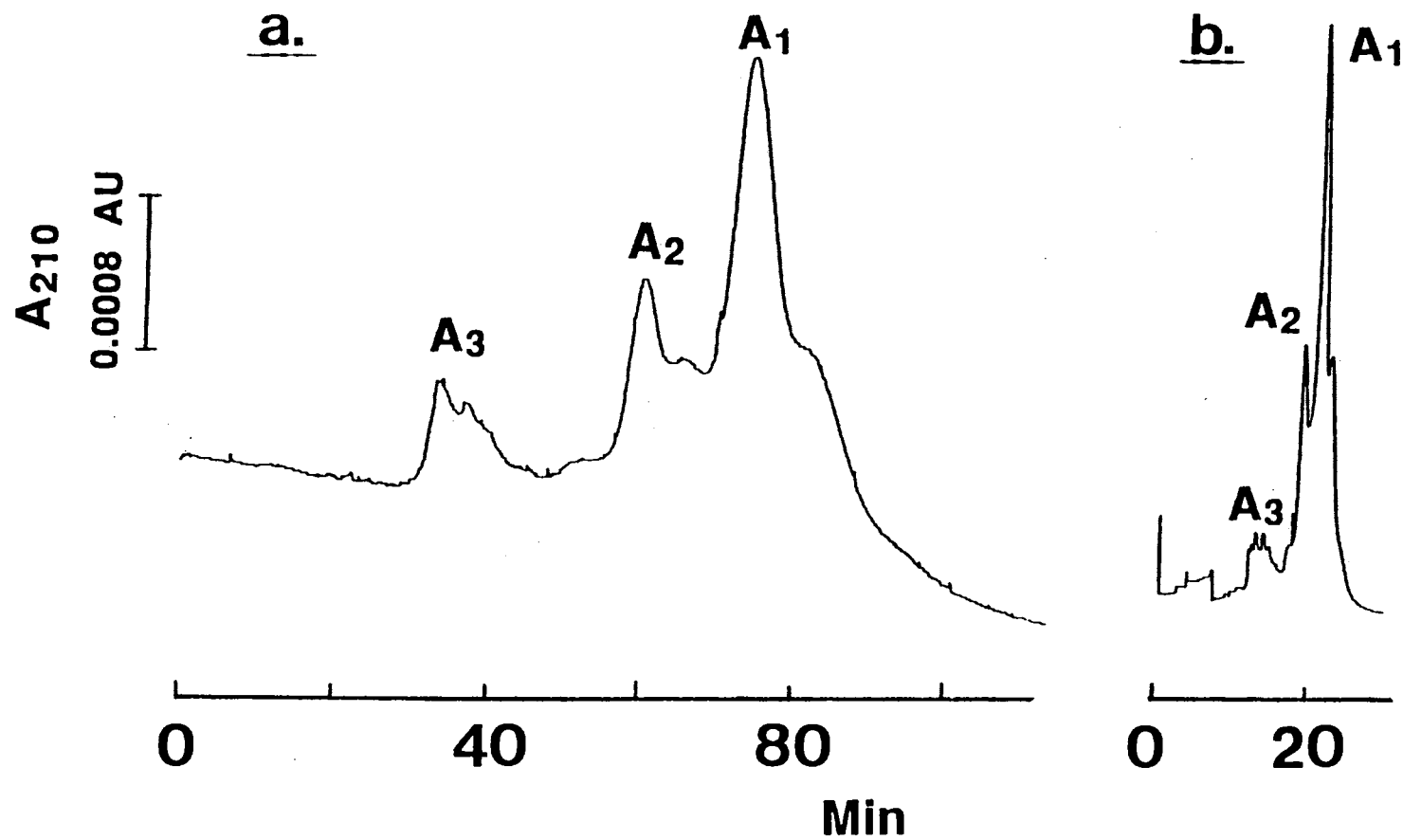
Figure 4. Typical electropherograms of ovalbumin obtained on F-2000 → I-200 in (a) and F-2000 → untreated in (b) at 0.5 fractional length of the I-200 and untreated capillary, respectively. All other conditions are as in Fig. 1.

0.5 fractional length each. In both tandem capillary systems, the F-2000 capillary having the most inert surface toward proteins, was selected as the separation capillary. Under these conditions, the EOF increased stepwise from 58.2 to 72.5. Figure 5 is a typical electropherogram of the 5 model proteins using the stepwise increase in the EOF. The arrow in Fig. 5 indicates the time at which the stepwise increase in EOF was performed. It should be noted that the voltage was turned off at the time the first set of coupled capillaries was disconnected and replaced by the untreated capillary segment. This manual operation required less than 20 sec.

As can be seen in Fig. 1, a relatively high level of EOF can only be achieved with the incorporation of an untreated capillary segment in the tandem capillaries. But, any basic solute should not come into direct contact with the inner surface of the untreated fused-silica capillary to avoid solute-wall interactions, and in turn the unpredictable change in the level and polarity of EOF. For this reason, the length of the I-200 segment in the first set of coupled capillaries was adjusted to trap all the basic proteins as they elute from the fuzzy capillary after being separated and detected. Thus, while the I-200 segment provided the shielding from wall interaction, its presence in conjunction with the untreated segment afforded a moderate EOF. Once all basic solutes entered the I-200 capillary, a stepwise increase in EOF was performed whereby both the I-200 and untreated capillaries were disconnected and replaced by one untreated segment at 0.5 fractional length to speed the net migration of the acidic solutes.

The above elution schemes involving two-step coupled capillaries yielded an increase in the EOF by a factor of 1.35 in I and 1.69 in II (see Fig. 5), when compared to the F-2000 → I-200 tandem capillary system at 0.5 fractional length of the I-200 capillary segment in Fig. 2c. Furthermore, comparison of Figs 2a and 5 reveals that the average plate height for lysozyme, ribonuclease A and carbonic anhydrase increased slightly from 10.3 to 12.5 μm, a factor of 1.2, while the migration time for these proteins decreased by factors of 1.9, 2.4 and 4.7, respectively. The slight increase in the olate height may be
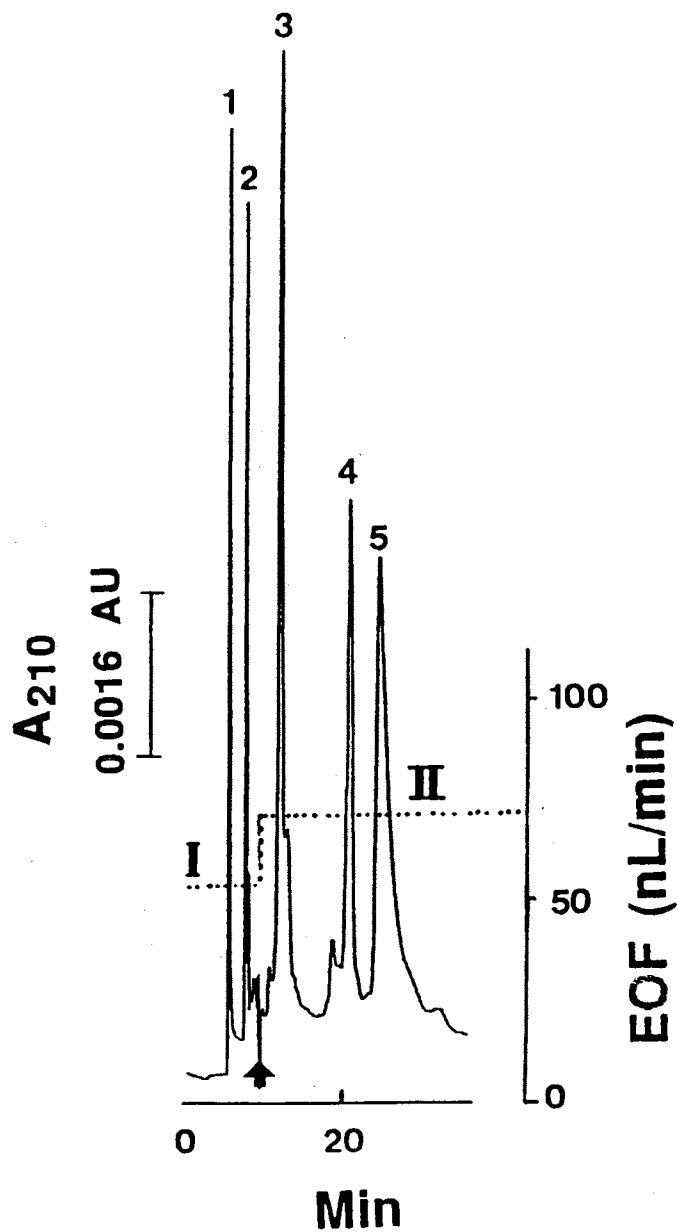
Figure 5. Rapid capillary zone electrophoresis of proteins with stepwise increase in the electroosmotic flow. Initial flow I: F-2000 → I-200 → untreated coupled capillaries at 0.5, 0.25 and 0.25 fractional length of the F-2000, I-200 and untreated capillaries, respectively. II: F-2000 → untreated capillaries at 0.5 fractional length each. All other conditions are as in Fig. 1. The arrow is to indicate the time at which the stepwise increase in EOF has occurred.

attributed to the presence of more pronounced laminar flow resulting from the large difference in the bulk flow and the intrinsic EOF in the F-2000 capillary segment.

To further develop this concept and permit the realization of several stepwise increases in the EOF during analysis, a multiple capillary device which will allow the switching between several coupled capillary systems having different electroosmotic flow characteristics is under development [10], see chapter 5.

The two-step tandem capillaries provided the rapid analysis of proteins at relatively moderate applied voltage. To obtain nearly the same EOF (i.e., 65.0 nL/min) with the F-2000 capillary as with the two-step coupled capillaries, the F-2000 capillary had to be operated at an applied voltage of 28 kV whereby the current was relatively high (155 μA). Fig. 6 illustrates a typical electropherogram of the protein mixture obtained at high voltage with F-2000 capillary. As can be seen in Fig 6, with the exception of ribonuclease A the proteins underwent severe sample degradation. The peak of β-lactoglobulin A disappeared, lysozyme eluted as a tailing peak and only short peaks were observed for carbonic anhydrase and α-lactalbumin. These observations may be attributed to system overheating [11-12] and/or to the binding of the proteins to the coating proper by hydrophobic interactions at elevated temperatures due to heat-induced conformational changes as previously shown in liquid chromatography [13,14]. Very recently, it has been shown that capillary temperature can dramatically affect the electrophoretic patterns of proteins in CZE *via* the reduction of the structural metal in metalloproteins and by inducing conformational changes [15].
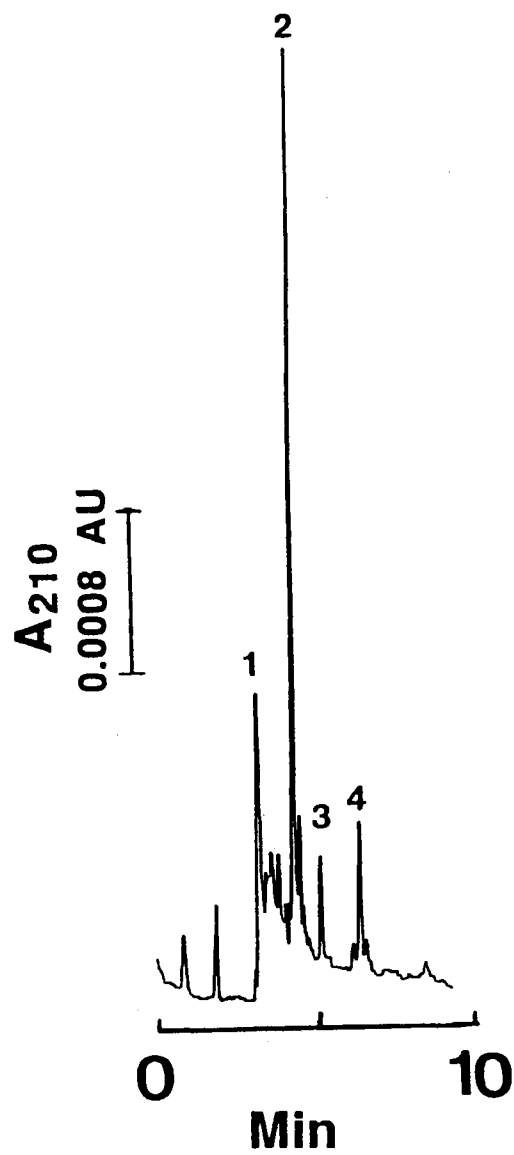
Figure 6. Electropherogram of model proteins on fuzzy 2000 coated capillary at an applied voltage of 28 kV. All other conditions are as in Fig. 2a.

References

1. C. S. Lee, W. C. Blanchard, and C.-T. Wu, *Anal. Chem.,* 62 (1990) 1550.

2. C. S. Lee, D. McManigill, C.-T. Wu and B. Patel, *Anal. Chem.,* 63 (1991) 1519.

3. M. A. Hayes and A. G. Ewing, *Anal. Chem.,* 64 (1992) 512.

4. W. Nashabeh and Z. El Rassi, *J. High Res. Chromatogr.,* 15 (1992) 289.

5. W. Nashabeh and Z. El Rassi, *J. Chromatogr.,* 596 (1992) 251.

6. W. Nashabeh and Z. El Rassi, *J. Chromatogr.,* 559 (1991) 367.

7. R. Datta and V. R. Kotamarthi, *AIChE Journal,* 36 (1990) 916..

8. A. Gottschalk and E. R. B. Graham in H. Neurath (Editor), *The Proteins: Composition, Structure and Function,* Academic press, New York, Vol. IV, 1966, p. 113-115.

9. G. E. Perlmann, *J. Gen. Physiol.,* 35 (1952) 711.

10. W. Nashabeh, J. T. Smith and Z. El Rassi, *Electrophoresis,* in press.

11. K. A. Cobb, V. Dolnik and M. Novotny, *Anal. Chem.,* 62 (1990) 2478.

12. J. S. Green and J. W. Jorgenson, *J. Chromatogr.,* 478 (1989) 63.

13. S. Hjerten, *J. Chromatogr.,* 87 (1973) 325.

14. Z. El Rassi, A. L. Lee and Cs. Horvath, in J. A. Asenjo (Editor), *Separation Processes in Biotechnology,* Marcel Dekker, New York, 1990, p.477.

15. R. S. Rush, A. S. Cohen and B. L. Karger, *Anal. Chem.,* 63 (1991) 1346.

CHAPTER V

STUDIES IN CAPILLARY ZONE ELECTROPHORESIS WITH A
POST-COLUMN MULTIPLE CAPILLARY DEVICE FOR
FRACTION COLLECTION AND STEPWISE
INCREASE IN THE ELECTROOSMOTIC
FLOW DURING ANALYSIS*

Abstract

A new approach involving the stepwise increase in electroosmotic flow during analysis in capillary zone electrophoresis has been introduced and evaluated in the rapid separations of proteins and peptides. The stepwise increase in electroosmotic flow is based on the principle of coupled capillaries in series having different flow characteristics, a concept that was introduced recently by our laboratory. To produce stepwise changes in electroosmotic flow during analysis, a post-column multiple capillary device, which allowed the switching between several coupled capillary systems, was designed and constructed in-house. The utility of the multiple capillary device was also demonstrated and extended to fraction collection of separated analytes in short capillary segments. The fraction collection in capillaries facilitated the quantitative transfer of the collected fractions to high performance liquid chromatography (HPLC) for further analysis or to mass spectrometry (MS) for structural determination. The off-line combination of capillary zone

electrophoresis with an HPLC or with a MS utilized commercial instruments without the need of expensive interfacing designs.

Introduction

Gradients in solvent composition and temperature are widely used in liquid and gas chromatography, respectively. These gradients are capable of changing the equilibrium distribution of solutes, thus greatly affecting the chromatographic selectivity. The concept of gradients has been exploited recently in capillary electrophoresis (CE) to improve the overall separation. Typical examples include gradients of organic solvent in micellar electrokinetic capillary chromatography [1]; dynamic programming of pH [2] and its application to capillary zone electrophoresis (CZE) of proteins [3]; the transient ionic matrix method [4] and its variant [5] in which the analytes upon encountering an ionic pulse migrating in the opposite direction will undergo changes in migration velocities; temperature programming in CZE with buffers of large temperature coefficient which induce pH and viscosity changes [6]; and the so called non uniform electrical field effect whereby the electrolyte inside the capillary is replaced continuously with an electrolyte of the same species but with different concentrations [7]. These gradient approaches have led to significant changes in selectivity, which resulted in improved separations.

On the other hand, flow programming which was applied in liquid chromatography to improve resolution and speed of separations [8], has not been yet introduced to CZE despite the strong need for means to solve the elution problem of oppositely charged species. Recently, this problem has been alleviated by two different approaches that provided relatively strong and constant electroosmotic flow (EOF) [9-12]. In one approach, coupled capillary tubes in series having different intrinsic EOF enabled the control of the overall velocity of the bulk flow in the coupled capillaries format, and consequently permitted the rapid and efficient analysis of proteins [9,10]. In another

approach, the direction and velocity of the EOF were altered by the application of an external potential across the separation capillary [11,12]. However, elevated and constant EOF could result in some instances in decreasing the resolution of early eluting peaks. This fact underscores the need for programming the EOF during analysis to allow adequate resolution of early eluting peaks and fast separation of strongly retarded zones.

Another area of growing interest in CE has been the development of efficient ways for the collection of the separated analytes. Rose and Jorgenson introduced an automated fraction collector with microcones containing small amounts of the background electrolyte into which the capillary outlet end is submerged [13]. Also, Cohen *et al.* [14] employed a similar approach for collecting DNA fragments. Since in both cases collection requires a microcone or microcentrifuge tube containing a small volume of the background electrolyte, a significant dilution of the sample may occur. Also, sample loss can result from solute adsorption to the walls of the collection cone or tube.

Recently, a series of collection methods that are continuous in operation have been introduced and evaluated in CZE. In these continuous approaches, the collection end of the capillary is electrically isolated by completing the electric circuit at a point situated at a short distance from the capillary outlet. A porous glass joint [15,16] or an on column frit [17] or a tee [18,19] or a fracture [20] served as the means for maintaining the electrical connection. These interrelated approaches were triggered by the porous glass joint arrangement which was originally introduced by Wallingford and Ewing [21] for electrochemical detection. In all these methods, the separation potential is applied only over the first segment, and due to the strong EOF, the analytes are transported across the electrically isolated capillary segment where they can be collected at the outlet. The porous glass sleeve or the fracture or the frit permitted ion movement but not bulk electrolyte flow. While the production of a fracture in a capillary tube or connecting capillary segments through a porous glass sleeve required inexpensive tools, the frit design necessitated the use of a high power carbon dioxide laser to delicately drill a hole in the capillary wall, a

fact that may limit its widespread use. In the tee assembly, two fused-silica capillaries of large I.D. were coupled together, while a third fused-silica capillary of smaller I.D. provided the connection to the ground. Owing to the high flow resistance in the direction of the cathodic end (i.e., small I.D. capillary), the majority of the solutes is forced into the electrically isolated capillary segment of large I.D. that served as the collecting column outlet. However, one disadvantage of using the tee assembly is that part of the solute is lost through the narrow capillary. Nevertheless, this approach allowed the micropreparative collection of CZE analytes by using a bundle of capillaries which were merged into a single column containing the tee assembly *via* a link tube [19].

In the above continuous approaches (i.e., without interrupting the current flow), sample collection may be accomplished directly in a dry microcentrifuge tube [17], onto a flat surface [22] or into nitrocellulose-coated aluminum foils [16]. However, these techniques are self-diluting in the sense that a small droplet must form (ca. 1.4 µL, i.e. 50 times dilution [17]) in order to become collectable or in some instances extensive mixing of the separated analytes may occur [17].

In another approach [22], continuous sample collection has been achieved in capillary devices containing short segments packed with controlled-pore glass beads having surface-bound antibodies. This selective collection and/or concentrating method was shown useful in collecting urinary constituents for up to 350 ng of purified materials. Very recently, a micropreparative CE apparatus was described in which solutes were adsorbed onto a moving blotting membrane as they migrate electrophoretically out of the capillary [23]. However, in both cases the subsequent elution of the collected solutes from the membrane or the glass beads for further analyses will introduce severe dilution and possible sample loss through sample handling.

The aim of the present article is to investigate the potentials of a multiple-capillary device, referred to as a multiport sliding valve, in the stepwise increase in EOF during analysis. As a natural extension of the utility of the valve, we have evaluated this

instrument in collection of solutes in capillary tubes after CZE separations. The stepwise increase in EOF is based on the principle of controlling EOF through coupled capillaries, a concept that was recently introduced by our laboratory [9,10]. The stepwise increase in EOF was accomplished through the sliding valve by switching between several coupled capillary systems having different EOF characteristics. This enabled the rapid and efficient analysis of proteins and peptides. In addition, as a fraction collector in capillary tubes, the multiport sliding valve facilitated the quantitative transfer of the analytes to high performance liquid chromatography for further analysis or to mass spectrometry for structural determinations.

Experimental

Reagents and Materials

Lysozyme from chicken egg white, ribonuclease A from bovine pancreas, carbonic anhydrase from bovine erythrocytes, α-lactalbumin and β-lactoglobulin A both from bovine milk, bradykinin, hydroxyproline bradykinin ([Hyp^3]-bradykinin), bradykinin potentiator C, Des-Asp^1-angiotensin I, Thr-Phe-Gln-Ala-Tyr-Pro-Leu-Arg-Glu-Ala, Val-Gly-Ser-Glu and Phe-Leu-Glu-Glu-Val were purchased from Sigma (St. Louis, MO, U.S.A.). Reagent grade sodium phosphate monobasic, phosphoric acid, sodium hydroxide and trifluoroacetic acid (TFA) were obtained from Fisher Scientific (Pittsburgh, PA, U.S.A.). Glycerol and thioglycerol were purchased from Fluka (Ronkonkoma, NY, U.S.A.). Phenol which was used as an inert tracer for measuring the EOF was obtained from J.T. Baker Inc (Phillipsburg, NJ, USA).

<u>Capillary Electrophoresis Instrument.</u>

The instrument for capillary electrophoresis used in this study is illustrated in Fig. 1. It comprised of two high-voltage power supplies of positive and negative polarity Models MJ30P400 and MJ30N400, respectively, from Glassman High Voltage (Whitehouse Station, NJ, U.S.A.), a Linear (Reno, NV, U.S.A.) Model 200 UV-Vis variable wavelength detector equipped with a cell for on-column capillary detection, and an on-line multiport sliding valve for changing the magnitude of EOF during analysis as well as for fraction collection in capillary tubes after CZE separations. The electropherograms were recorded with a Shimadzu computing integrator Model C-R6A (Columbia, MD, U.S.A.) equipped with a floppy disk drive and a cathode-ray tube (CRT) monitor.

The multiport sliding valve was designed and constructed in-house from plexiglass and delrin materials. The valve consisted of two major parts: a U shaped stator or body (1) that holds the separation capillary, and a slider (2) to which all other capillary segments of higher EOF are attached. The capillaries were tightly held in both parts with vinyl nuts and flat PTFE ferrules (3). The various capillary segments were firmly inserted into holes (designated 4 and 5) of 360 μm I.D. and 2.38 mm deep at the interfaces of the body and slider. The highly polished interfaces were covered with a thin layer of silicon grease to ensure a smooth frictional contact and avoid electrolyte leakage. The sliding valve permitted the alignment of the separation capillary with another capillary segment(s) (see Fig. 1), one at a time, through a locating pin (6). The alternation of different capillaries through the sliding part of the valve produces various sets of coupled capillaries in which the nature and length of the separation capillary are conserved. In this arrangement, the coupled capillaries are connected butt-to-butt with zero dead volume. The switching of the capillaries was ensured by a brass allthread (7), which moved the slider in the forward or backward direction. The multiport sliding valve was constructed in the Physics and
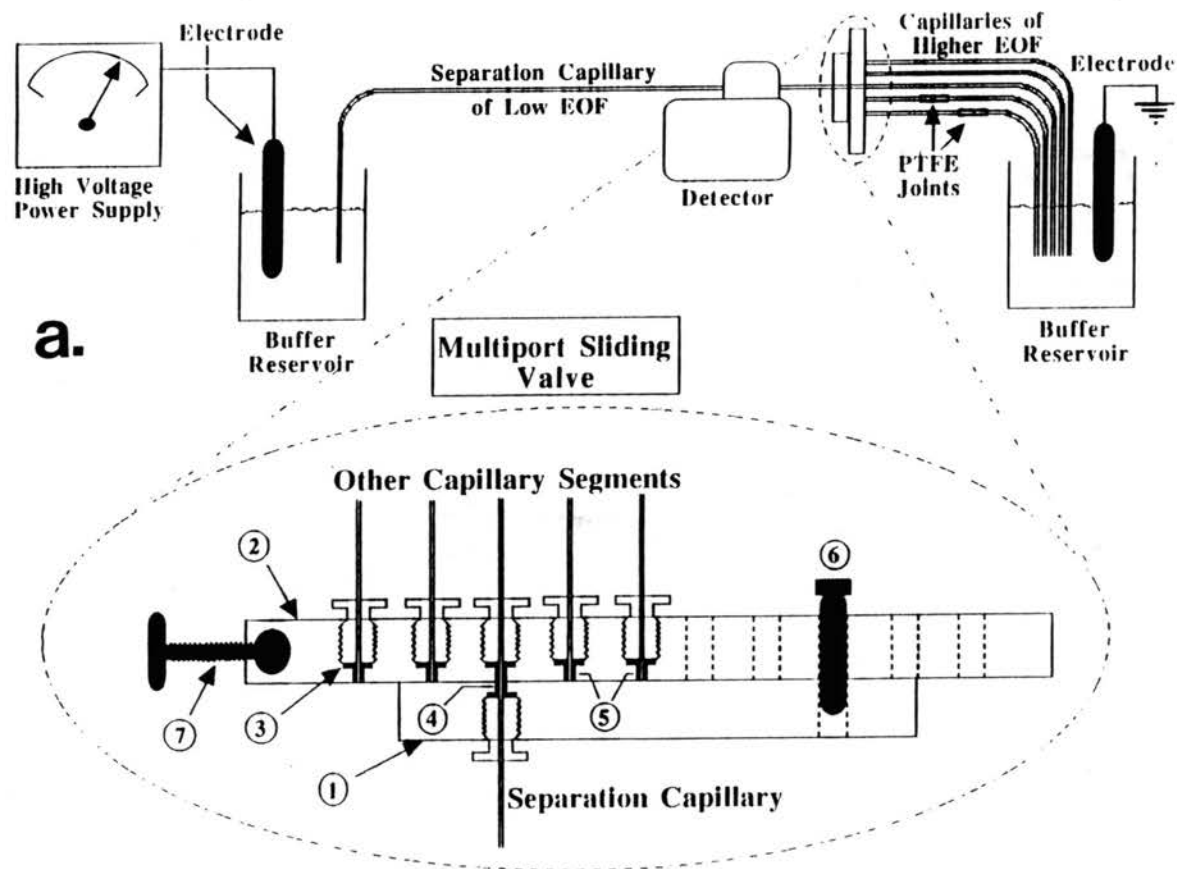
Figure 1. Schematic illustration of the capillary electrophoresis system with the multiport sliding valve. The separation capillary was 45 cm total length with an effective length of 30 cm. The length of the other capillary segments was 45 cm each. The valve was positioned 15 cm past the detection window. The separation capillary can be aligned with only one of the other capillary segments at a time. 1, U shaped body; 2, slider; 3, PTFE flat ferrule; 4, one hole of 365 μm I.D. and 2.38 mm deep at the interface of the stator; 5, corresponding holes in the slider (a total of 5 holes); 6, locating pin; 7, brass allthread.

Chemistry Instrument Shop at Oklahoma State University by Mike Lucas at a cost of $ 20.00 for materials.

High Performance Liquid Chromatography Instrument

The chromatograph was assembled from an LDC/Milton Roy (Riviera Beach, FL, U.S.A.) Model CM4000 multiple solvent delivery pump and a dual beam variable-wavelength detector Model Spectro Monitor 3100. A Rheodyne (Cotati, CA, U.S.A.) Model 7125 sampling valve was used for sample introduction. For standard HPLC injections, a 20-μL sample loop was used. In HPLC analysis of collected fractions after CZE separations, the collection capillary column of 45 cm total length and 50 μm I.D. was first disconnected from the multiport sliding valve and then mounted directly as a loop on the sampling valve using Mini-tight fittings from Upchurch Scientific (Oak Harbor, WA, U.S.A.). Chromatograms were recorded with a Shimadzu (Columbia, MD, U.S.A.) Model C-R5A integrator. A Bakerbond wide-pore octadecyl-silica column (250 x 4.6 mm) having mean particle and pore diameters of 5 μm and 300 Å, respectively, was a gift from J.T. Baker (Phillipsburg, NJ, U.S.A.).

Mass Spectrometry Instrumentation

All mass spectra were acquired with a VG ZAB2-SE instrument (VG Analytical Ltd., Manchester, UK). The instrument is equipped with a VG II-250 data acquisition system. Liquid secondary ion mass spectrometry (LSIMS) was performed with a cesium ion gun operated at 32 kV. The positive secondary ions were accelerated at 8 kV in the case of static LSIMS and at 6 kV when using the continuous-flow system (CF) with a source potential operated in the positive polarity. The mass range scanned was 600 to 1200 m/z at a rate of 15 s/decade. An instrument resolution of approximately 1500 was used in acquiring the spectra. Calibration was made using cesium iodine on the probe tip.

In the case of static LSIMS, spectra were obtained by signal adding five scans with the use of the multichannel analysis software of the data system. The sample matrix was 1:1 mixture of glycerol and thioglycerol with 1% (v/v) TFA added to enhance the ionization of the peptides. The matrix (1 µL) was applied to the stainless steel probe tip, and the content of the collection capillary was emptied onto the probe tip using a microsyringe.

For CF-LSIMS, the spectra were obtained by a single scan, and no signal averaging was applied. The mobile phase was a 1:1 mixture of water and methanol containing 2.5% (v/v) glycerol and 0.1% (v/v) TFA. A flow rate of 4 µL/min was supplied to the source by a µLC-500 syringe pump (ISCO, Inc., Lincoln, NE, USA). The mobile phase was delivered by a 75 µm fused silica capillary, that was approximately 80 cm in length from the microinjector to the source. The content of collection capillary was drawn into a microsyringe and introduced into the loop (2 µL) of the microinjector (Valco, Houston, TX, USA), located between the µLC-pump and the inlet of the mass spectrometer.

Capillary Columns

Polyimide-coated fused-silica capillary columns of 50-µm I.D. and 365-µm O.D. were obtained from Polymicro Technology (Phoenix, AZ, U.S.A.). Both untreated and coated capillaries were used in this study. The coated capillaries were modified in-house with surface-bound polyether chains (i.e., polyethylene glycol, PEG) of various length according to previously described procedures [24]. The hydroxylated polyether capillaries are coded as I-200 and F-2000 to designate capillaries with interlocked coatings having PEG 200 polyether chains and capillaries having fuzzy coatings with PEG 2000 moieties, respectively.

Other Procedures.

Unless otherwise stated, the separation capillary was an F-2000 polyether coated capillary of 45 cm total length with a detection window at 30 cm from the inlet reservoir. The multiport sliding valve was positioned at 15 cm beyond the detection point. The total length of all coupled capillaries (including the separation capillary) was kept constant at 90 cm (refer to legend of Fig. 1 for more details). All capillaries were first filled and then equilibrated with the running electrolyte. During the switching between several coupled capillary systems, the voltage was first turned off in order to avoid a back flow of the electrolyte which may induce a vacant space at the connection tip of the separation capillary. Following, the slider was adjusted to the desired position and electrophoresis resumed. Such operation required between 5-10 seconds. It should be noted that in all experiments the background electrolyte was 0.1 and 0.01 M sodium phosphate, pH 7.0, for the separation of proteins and peptides, respectively. Solute introduction was by electromigration for 5 sec at 18 kV. The amounts of solutes introduced into the separation capillary (Q) was estimated from the following equation [25]:

$$Q = \frac{(\mu_e + \mu_{eo})V_i \pi r^2 C t_i}{L}$$

where μ_e is the solute electrophoretic mobility, μ_{eo} is the electroosmotic mobility, V_i is the injection voltage, r is the inner radius of the capillary, C is the solute concentration, t_i is the injection time and L is the total length of the capillary. In both CZE and HPLC, the detection wavelength was set at 210 nm for sensing the various solutes.

Results and Discussion

Stepwise Increase in Electroosmosis During Analysis

Principles. In this study, the stepwise increase in EOF during CZE analysis is based on the principle of coupled capillary tubes in series with different magnitude of intrinsic EOF. The fundamental and practical aspects of coupled capillaries for the control of EOF in CZE have been recently introduced and evaluated by our laboratory [9,10]. We have shown that the average electroosmotic mobility, μ_{eo}, across a given tandem capillary system is a weighted average of the intrinsic or local electroosmotic mobilities in the individual connected segments as follows:

$$\mu_{eo} = \frac{\sum_{i=1}^{n} \mu_{eo,i} l_i}{l_t}$$

where l_i is the length of the individual capillary segment, i, l_t is the total length of the connected capillaries and $\mu_{eo,i}$ is the intrinsic electroosmotic mobility in each capillary segment, i, measured on a separate length l_t. We have also shown that the EOF in the coupled capillaries is a linear function of the fractional length of any given capillary segment. Thus, by varying the fractional length of the connected capillary columns, the EOF can be conveniently tuned to any desired level that is bordered by the lowest and highest intrinsic electroosmotic mobilities of the connected segments.

An important feature of the concept of manipulating the EOF with coupled capillaries is that the EOF can be increased during analysis independently of the applied voltage. This can be accomplished through the use of the multiport sliding valve, described in Experimental, by simply switching between several coupled capillary systems having different EOF characteristics. In this arrangement, the separation starts at low EOF to provide adequate resolution of initially eluting zones, then increasing the EOF stepwise to allow fast separation of slow migrating species. In other words, the separation begins

with a set of coupled capillaries of low EOF, and at successive time intervals, other sets of coupled capillaries of higher EOF are assembled by moving the slider of the multiport sliding valve in the forward direction. In these successive events, the separation capillary is aligned with the next capillary segment(s) of higher EOF than in the preceding set of coupled capillaries. In all the coupled capillary systems, the capillary segment with the lowest EOF makes up the separation capillary, which stays unchanged throughout the entire separation. The segment of higher EOF can be either a single capillary column or 2 or more capillary segments coupled in series *via* PTFE tubes the inner diameters of which match the outer diameters of the connected segments, see Fig. 1. The separation capillary is chosen to be the one with the most inert surface toward proteins in order to minimize electrostatic interaction between the solutes and the capillary wall. The choice of the other capillary segments of higher EOF in the tandem systems is mainly dictated by the nature of the separated analytes and the desired level of EOF.

Since acidic solutes undergo electrostatic repulsion from negatively charged capillaries, the analysis of acidic proteins can be carried out with coupled capillaries containing untreated segments. Under these conditions, a relatively strong EOF is produced, and as a result, rapid analyses can be achieved. In the analysis of basic analytes, the various sets of coupled capillaries employed in the stepwise elution can also contain untreated segments. However, basic proteins should not come into direct contact with the inner surface of untreated fused-silica capillary to avoid solute-wall adsorption, and consequently abrupt and unpredictable changes in EOF. These elution schemes are illustrated below in the separations of proteins and bioactive peptides.

Proteins. Figure 2a illustrates a typical electropherogram of a mixture of 5 standard proteins the isoelectric points of which range from 4.8 to 11.0. It was performed on an F-2000 polyether coated capillary using an applied voltage of 222 V/cm with 0.1 M sodium phosphate, pH 7.0, as the running electrolyte. Although high separation efficiencies could
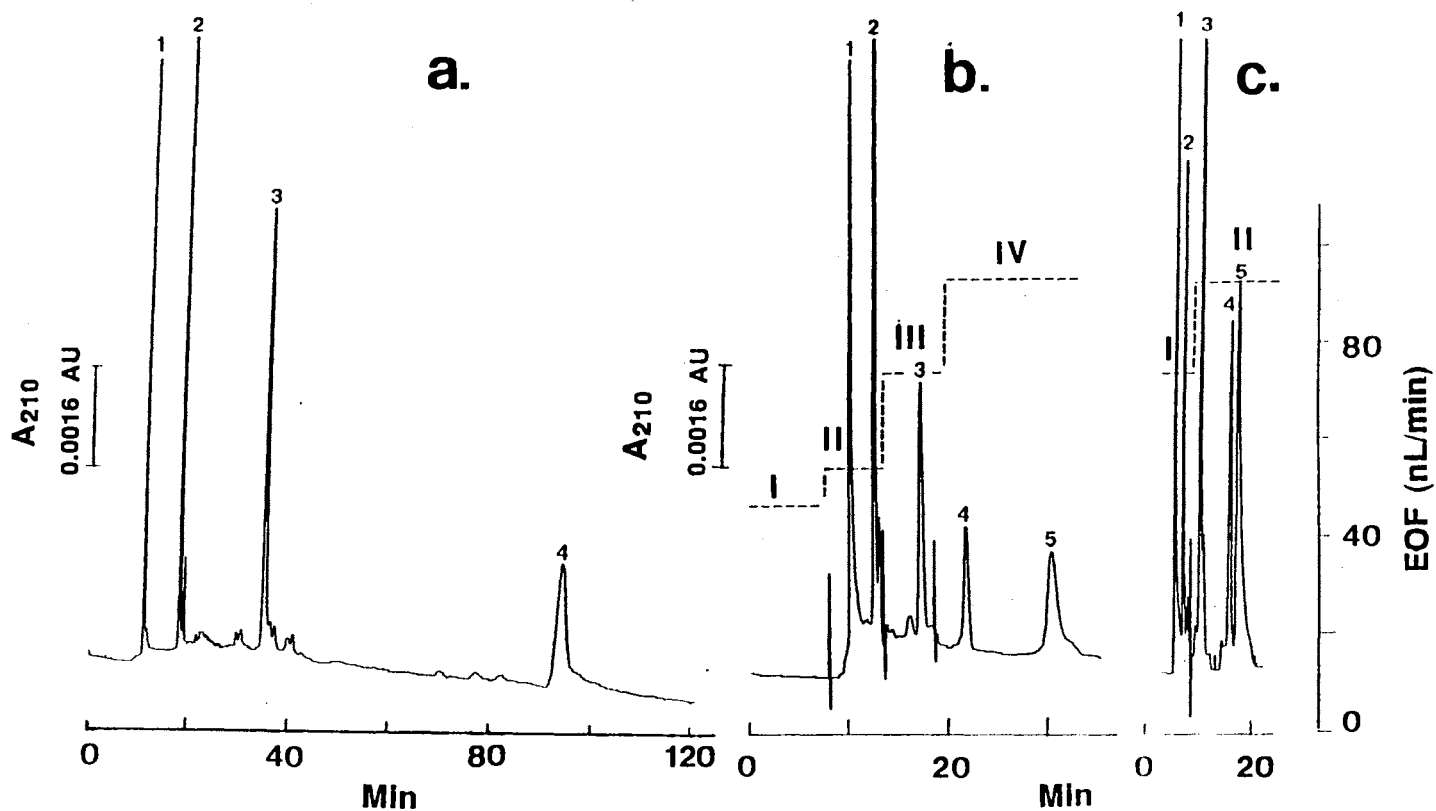
Figure 2. Typical electropherograms of model proteins obtained on F-2000 coated capillary in (a) and on different combinations of F-2000, I-200 and untreated capillaries with either a three or one steps increase in the electroosmotic flow in (b) and (c), respectively. In (b): I, initial flow, F-2000 → I-200 capillaries at 0.75 and 0.25 fractional length, respectively; II, F-2000 → I-200 capillaries at 0.5 fractional length each; III, F-2000 → I-200 → untreated coupled capillaries at 0.5, 0.25 and 0.25 fractional length of the F-2000, I-200 and untreated capillaries, respectively; IV, F-2000 → untreated capillaries at 0.5 fractional length each. In (c): I, initial flow, identical to III in (b); II, identical to IV in (b). Tandem capillaries, 30 cm (to the detection point), 90 cm (total length) x 50 μm I.D.; running voltage, 222 V/cm; background electrolyte, 0.1 M sodium phosphate solution, pH 7.0. Proteins: 1, lysozyme (pI = 11.0); 2, ribonuclease A (pI = 9.4); 3, carbonic anhydrase (pI = 6.2); 4, α-lactalbumin (pI = 4.8); 5, β-lactoglobulin A (pI = 5.2).

be achieved, this electrophoretic system does not allow the analysis of all the components of the mixture under investigation. In fact, due to the low EOF on the F-2000 capillary (ca. 37 nL/min), only basic proteins could be eluted in reasonable time while acidic proteins such as β-lactoglobulin A which have an electrophoretic mobility greater in magnitude but opposite in sign to the EOF, did not migrate toward the detection end. Figure 2b illustrates the electropherogram of the same protein mixture obtained with 3 consecutive stepwise increases in the EOF using the multiport sliding valve. At the beginning of separation, the coupled capillaries were F-2000 and I-200 at 0.75 and 0.25 fractional lengths, respectively, which insured a relatively moderate EOF that was slightly higher than that obtained on the F-2000 alone. Following, the two basic solutes (i.e., lysozyme and ribonuclease A) were eluted in a first step using an F-2000 → I-200 tandem electrophoretic system at 0.5 fractional length each. This step was sufficiently prolonged to allow basic proteins to exit the separation capillary and be trapped in the I-200 segment. In a second elution step, the tandem system consisted of three capillary segments connected in series and containing F-2000, I-200 and untreated capillaries at 0.5, 0.25 and 0.25 fractional lengths, respectively. The relatively higher EOF achieved (74 nL/min) was sufficient to bring about the elution of carbonic anhydrase, a moderately acidic solute, within 17 minutes. Finally, in a third elution step, a higher level of EOF was obtained using F-2000 → untreated tandem capillaries at 0.5 fractional length each, which allowed the elution of the retarded acidic protein, i.e., β-lactoglobulin A. In total, the EOF was increased stepwise by factors of 1.17, 1.61 and 2.02, consecutively, with respect to the initial flow condition. When compared to the EOF generated by the F-2000 alone, the EOFs of the successively used coupled capillaries were higher by factors of 1.24, 1.45, 2.0 and 2.5.

The analysis time of oppositely charged proteins was further decreased by affecting one step increase in EOF by switching from one coupled capillary system of relatively high EOF to another system of much higher EOF, see Fig. 2c. Under this elution condition, the

EOF was increased from 74 to 93 nL/min which corresponds to the second and third elution steps in Fig. 2b. As shown in Fig. 2c, this single step increase in the EOF enabled the rapid analysis of widely differing proteins with base line resolution and narrow band widths.

Peptides. The methodology of stepwise changes in the EOF during analysis was also evaluated in the rapid separation of bioactive peptides. Again, the F-2000 capillary was selected as the separation capillary while the other capillary segments consisted of various combinations of F-2000, I-200 and untreated capillaries. As can be seen in Fig. 3a, only basic, neutral and moderately acidic peptides were eluted on the F-2000 capillary within 2 hours using 0.01 M sodium phosphate, pH 7.0, as the background electrolyte at an applied field strength of 222 V/cm. However, with the use of the multiport sliding valve, all peptides were analyzed within 25 to 30 min. This is illustrated in Fig. 3b and c which depicts typical electropherograms of the same peptide mixture performed with either a one or two steps increase in the EOF, respectively. Referring to Fig. 3c, the separation started with an F-2000 → I-200 tandem system at 0.75 and 0.25 fractional length, respectively, that generated an EOF of 67 nL/min. This initial flow condition permitted the rapid elution of basic peptides. Following, neutral and slightly negatively charged peptides were analyzed at an EOF of 82 nL/min. Finally, an EOF of 138 nL/min, an increase by a factor of 2.37 as compared to F-2000, enabled the rapid and efficient analysis of acidic peptides. As can be seen in Fig. 3, the apparent mobility of the model peptides increased with increasing the EOF. This is further illustrated in Table 1 which provides the values of the electrophoretic and electroosmotic mobilities of the analyzed solutes on the F-2000 capillary as well as on the various combinations of the F-2000, I-200 and untreated capillaries. As expected, the electrophoretic mobility of the selected peptides remained practically unchanged. This is an indication that the variation in the apparent mobility is
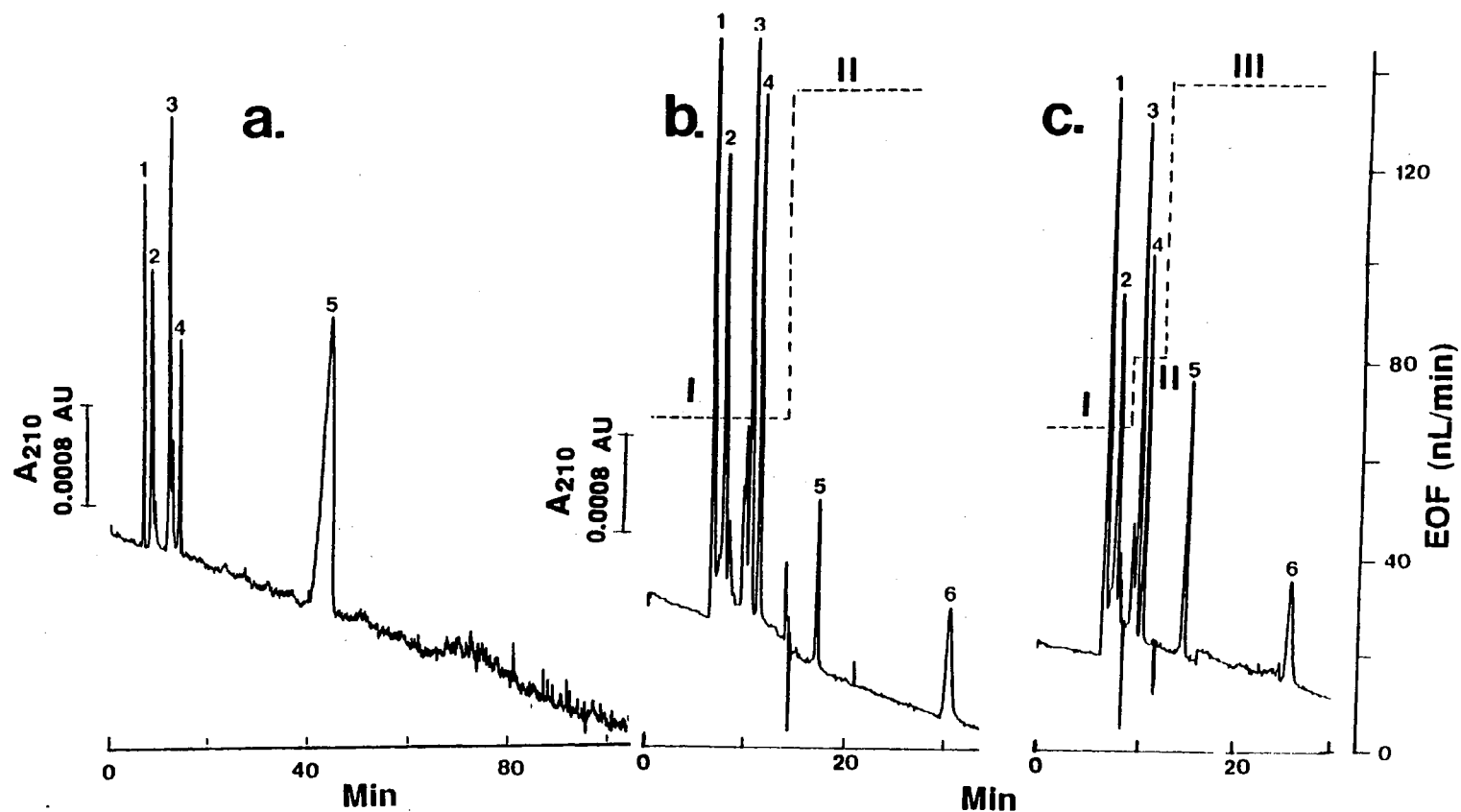
Figure 3. Typical electropherograms of bioactive peptides obtained on F-2000 coated capillary in (a) and on different combinations of F-2000, I-200 and untreated capillaries with either a one or two steps increase in the electroosmotic flow in (b) and (c), respectively. In (b): I, initial flow, F-2000 → I-200 capillaries at 0.75 and 0.25 fractional length, respectively; II, F-2000 → untreated capillaries at 0.5 fractional length each. In (c): I, initial flow, identical to I in (b); II, F-2000 → I-200 capillaries at 0.5 fractional length each; III, identical to II in (b). Tandem capillaries, 30 cm (to the detection point), 90 cm (total length) x 50 μm I.D.; running voltage, 222 V/cm; background electrolyte, 0.01 M sodium phosphate solution, pH 7.0. Peptides: 1, bradykinin; 2,

TABLE I

ELECTROPHORETIC (μ_{ep}) AND ELECTROOSMOTIC (μ_{eo}) MOBILITIES OF SELECTED PEPTIDES ON F-2000 AND F-2000, I-200 AND UNTREATED TANDEM SYSTEMS

Peptide	Capillary type					
	F-2000		1) F-2000→I-200 (0.75:0.25) 2) F-2000→Untreated (0.5:0.5)		1) F-2000→I-200 (0.75:0.25) 2) F-2000→I-200 (0.5:0.5) 3) F-2000→Untreated (0.5:0.5)	
	μ_{ep} $\times 10^4$	μ_{eo} $\times 10^4$	μ_{ep} $\times 10^4$	μ_{eo} $\times 10^4$	μ_{ep} $\times 10^4$	μ_{eo} $\times 10^4$ (cm^2/V.s)
Arg-Pro-Pro-Gly-Phe-Ser-Pro-Phe-Arg	1.22	2.14	1.12	2.58	1.09	2.58
Arg-Val-Tyr-Ile-His-Pro-Phe-His-Leu	0.60	2.14	0.58	2.58	0.50	2.58
Thr-Phe-Gln-Ala-Thr-Pro-Leu-Arg-Glu-Arg	-0.22	2.14	-0.22	2.58	-0.24	2.65
pGlu-Gly-Leu-Pro-Pro-Gly-Pro-Pro-Ile-Pro-Pro	-0.54	2.14	-0.54	2.58	-0.52	2.71
Val-Gly-Ser-Glu	-1.64	2.14	-1.70	3.02	-1.69	3.22
Phe-Leu-Glu-Glu-Val	NE[a]	2.14	-3.28	4.03	-3.12	4.01

a) No elution within two hours

solely due to the increase in the EOF and that the tandem operation do not introduce solute-wall interactions or any other adverse effects.

This demonstrates the advantage of being able to perform rapid biopolymer analysis with good separation efficiencies without the need to apply high potential drop. Furthermore, the use of stepwise elution improves the overall separation process by allowing a better modulation of front- and back-end relative migration of the analytes. This feature of the tandem system is advantageous for the analysis of crude mixtures whereby the pI values of all the components are not known or vary over a wide range, so that maximum analytical information about a given mixture can be achieved in a single electrophoretic run.

Fraction Collection in Capillary Tubes

A challenging area in CE is the collection of minute amounts of analytes so that further analyses can be performed on the collected fractions. An ideal fraction collection methodology should in principle meet the following criteria: (i) the collection device should not cause significant dilution of the samples which may hinder their subsequent analyses, (ii) the collection method should not denature or alter the chemical nature of the analytes, (iii) the collection procedure should minimize any loss in material so that quantitative transfer is possible, (iv) the fraction collector should enable the collection of several solutes in a continuous fashion and (v) the collection method should be convenient involving simple instrumentation and that can be readily automated.

As a fraction collector in capillary tubes, the multiport sliding valve meets most of the above criteria. The collection of the sample in capillary segments is fully quantitative and the possibility of sample mixing is minimized. This is facilitated by the fact that after collecting a peak, the separation capillary is aligned with another capillary segment for the collection of the next eluting zone. Also, the capillary format provides a convenient

transfer of the collected fractions to other separation methods such as HPLC or spectroscopic techniques, e.g, mass spectrometry. These characteristic features of the collection *via* the multiport sliding valve are illustrated in the analysis and structural determinations of bioactive peptides.

Figure 4a illustrates a typical electropherogram of the separation of three bioactive peptides namely, bradykinin, [Hyp³]-bradykinin, bradykinin potentiator C. Both bradykinin and [Hyp³]-bradykinin differing among each other by only one hydroxyl substitution at the proline residue, were not resolved by CZE on an I-200 capillary at an applied field strength of 200 V/cm using 10 mM sodium phosphate, pH 7.0, as the running electrolyte. This is because these peptides have approximately the same charge-to-mass ratio. However, both peptides were well separated from the slightly acidic bradykinin potentiator C. Thus, the electrophoretic system fails to provide complete analytical information about the peptide mixture in the sense that its components could not be fully resolved. However, these components are likely to be separated by other techniques having different selectivity. Thus, the ability to collect CZE fractions can be advantageous for determining the presence of interfering species before attempting any quantitative analysis by CZE.

Transfer of collected fractions to an HPLC system. Figure 4b illustrates a chromatogram of the above peptide mixture obtained by RPC, which was performed on a Bakerbond wide-pore octadecyl-silica column. The peptides were eluted using a 15 min linear gradient of increasing acetonitrile concentration in the eluent from 20 to 50 % (v/v). The presence of an extra hydroxyl group in [Hyp³]-bradykinin imparted more hydrophilic character to the peptide and consequently was less retarded on the RPC column than bradykinin. The RPC tracing of the collected fractions after CZE separations using the sliding valve fraction collector is shown in Fig. 4c and d. In this study, the capillary segment was first removed from the sliding valve and then mounted as a micro-loop on the
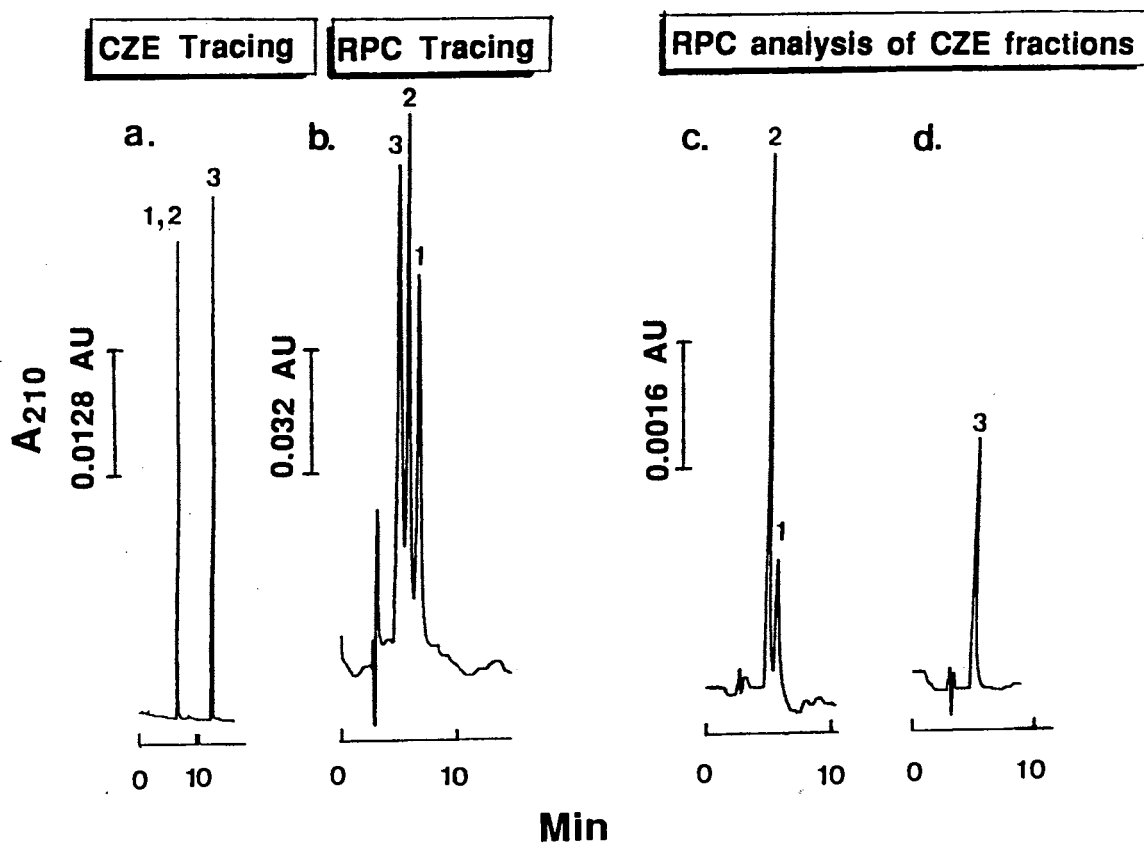
Figure 4. (a), Typical electropherograms of bioactive peptides performed on an I-200 polyether coated capillary; (b), RPC of bioactive peptides; (c) RPC of the first collected peak obtained in (a); (d), RPC of the second collected peak obtained in (a) . (a): Other conditions are as in Fig. 3 except running voltage was 200 V/cm. (b), (c) and (d): Column, Bakerbond wide pore octadecyl-silica column, 250 x 4.6 mm I.D.; linear gradient of increasing acetonitrile in water from 20 % to 50% (v/v) at 0.05% (v/v) TFA within 15 min; flow rate, 1.0 mL/min. Peptides: 1, bradykinin; 2, [Hyp^3]-bradykinin; 3, bradykinin potentiator C. See text for other experimental details.

sampling valve of the HPLC system. Thereafter, the valve was switched from the load position to the injection position for 5 sec. A delay of 30 sec was necessary to stabilize the pressure difference arising from the flow restriction in the capillary column. Following, gradient elution similar to that in Fig. 4b was performed. As anticipated, the RPC analysis of the first CZE peak revealed the presence of two peptides (compare Fig. 4a, b and c) while that of the second CZE fraction confirmed the purity of the bradykinin potentiator C solute (compare Fig. 4a, b and d). While the separation in CZE is based on differences in the charge density of the analytes, RPC separates primarily on the basis of differences in the hydrophobic character of the solutes. Thus, the off-line combination of both techniques can provide the most advanced analytical information about a given mixture. In addition, this transfer is quantitative since the full amount of the CZE analyte is trapped in the capillary segment. The solute is then introduced without dilution as a thin plug into the RPC column. This transfer can be either micropreparative or of analytical nature. Shown in Fig. 4c is the micropreparative transfer of 50 ng of bradykinin collected from the electrophoretic run. For analytical transfer, the limit of detection will be dictated by that of CZE, which was in the range of 200 pg for bradykinin.

Transfer of the collected fractions to mass spectrometry. The collected fractions after CZE separations were also transferred to an MS whereby both static and continuous flow LSIMS analyses were performed. Figure 5a and b represents typical static-LSIMS spectrum of the first and second CZE peaks of Fig. 4a, respectively. In this mode of operation, the capillary segment containing the collected solute(s) was first disconnected from the sliding valve. Following, its content was emptied on the probe tip of the MS. It can be seen from Fig. 5a that the analysis of the first CZE peak revealed the presence of both coeluting peptides as manifested by the $[M+H]^+$ adducts of both bradykinin and $[Hyp^3]$-bradykinin while the $[M+H]^+$ peak in Fig. 5b corresponded to bradykinin potentiator C. However, the use of static LSIMS is hampered by the large sample quantity
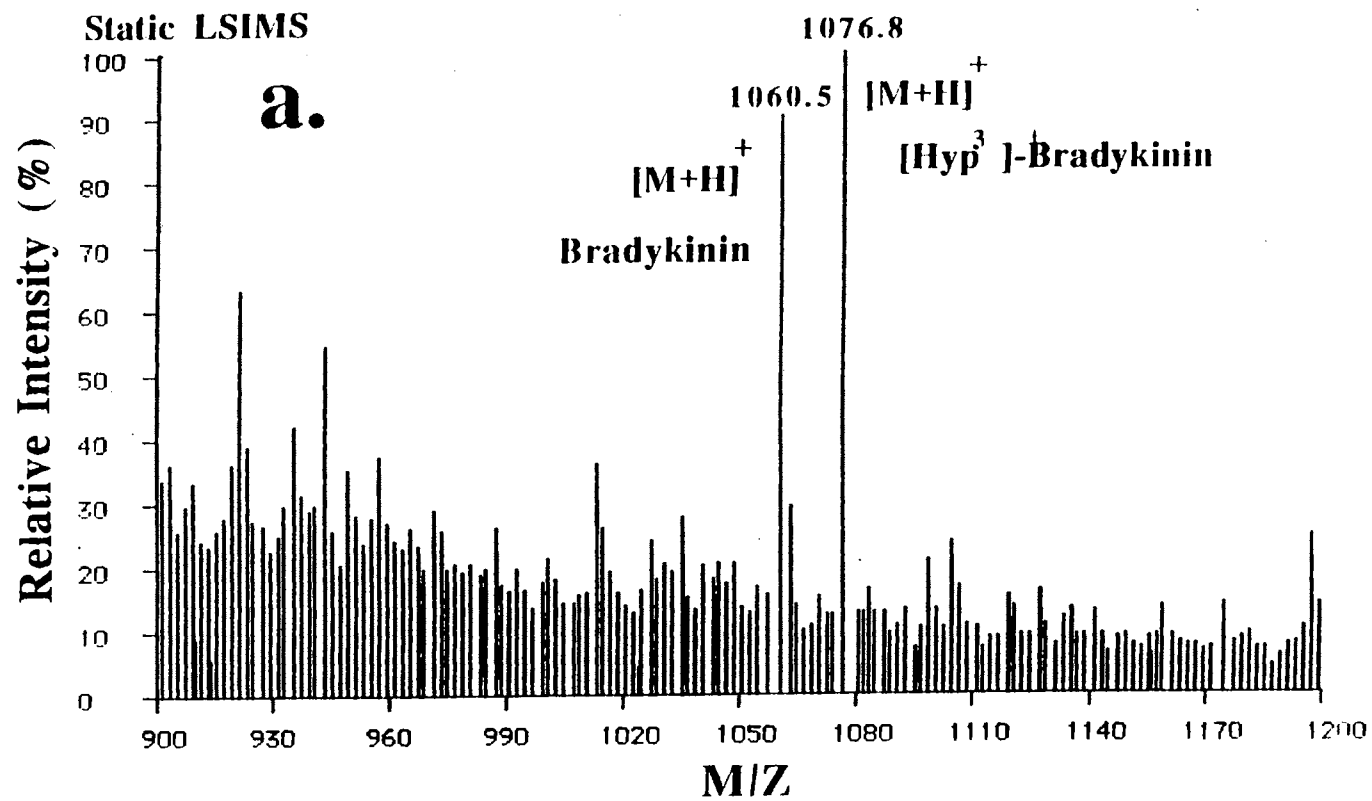
Figure 5a. Static liquid secondary mass spectrometry analysis of the first collected fractions after CZE analysis. See Experimental for details.
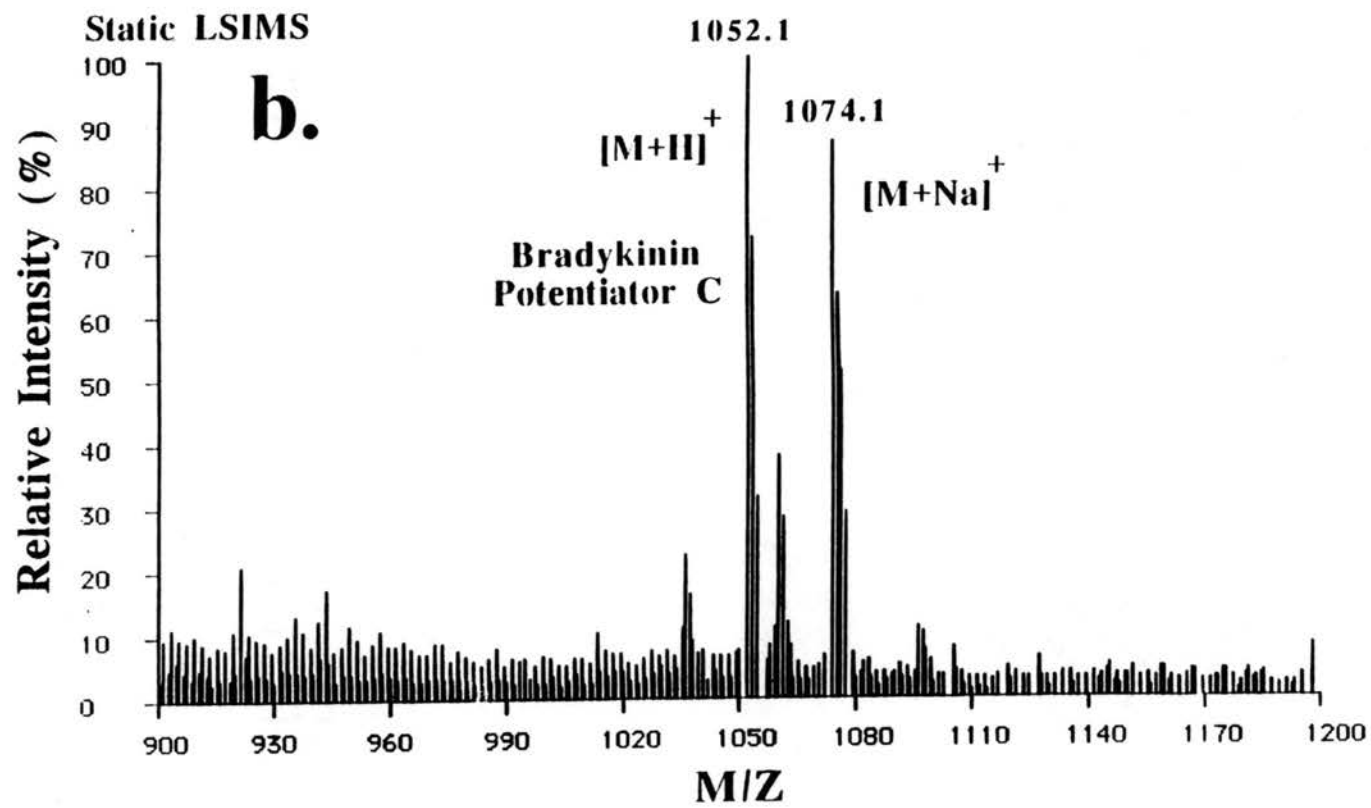
Figure 5b. Static liquid secondary mass spectrometry analysis of the second collected fractions after CZE analysis. See Experimental for details.

required for analysis. The limit of detection was ca. 1ng for bradykinin, a reduction by 5 fold with respect to that obtained in UV detection, see above. To enhance the sensitivity of the off-line combination of CZE and MS, CF-LSIMS was employed using bradykinin as a model analyte. In such transfer, the content of the capillary segment was first sucked into a microsyringe and thereafter injected into the MS. CF-LSIMS is a dynamic process in which the matrix/sample surface is continuously renewed; this significantly enhances the signal to noise ratio and consequently allows lower detection limits to be achieved [26]. Figure 6 displays the spectrum of 40 pg of bradykinin that was collected during the electrophoretic run. Note that in UV absorbance no detection signal was observed for this amount, and the collection of the sample required prior knowledge of its migration time. Under optimized conditions, near 1pg of bradykinin (slightly less than 1 fmole) could be detected using CF-LSIMS with a signal to noise ratio of 2:1.

The off-line combination of CZE and LSIMS clearly demonstrates its potentials in providing valuable structural information of the CZE analytes as well as revealing the presence of overlapping solutes or impurities. It should be also noted that the off-line transfer procedure is very simple and can be used with commercial MS instruments without the need of expensive interface design.

Conclusion

In summary, the multiport sliding valve enabled the control of electroosmosis as well as the collection of the analytes after CZE separations. The EOF was increased stepwise during the electrophoretic run independently of the applied voltage by switching between several coupled capillaries having different wall ζ potentials. This approach can be used for the rapid analysis of widely differing biopolymers and the separations of unknown crude mixtures. In another aspect, the multiport sliding valve permitted the collection of the analytes after CZE separations in capillary tubes. This collection was fully
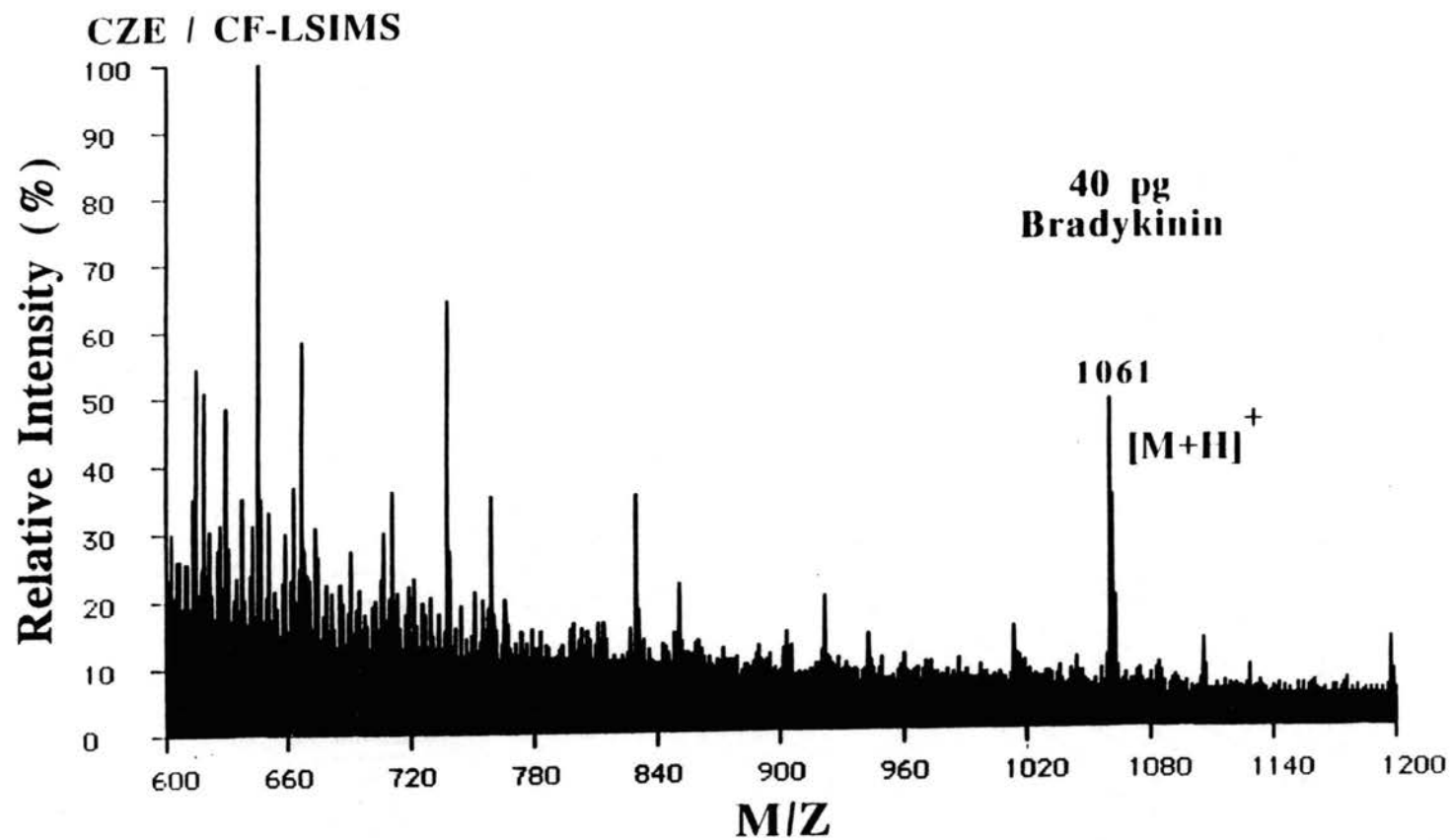
Figure 6. Continuous-flow Liquid secondary mass spectrometry spectrum (CF-LSIMS) obtained with 40 pg of bradykinin collected after CZE separation. See Experimental for details.

quantitative and did not involve significant dilution of the analytes. In addition, the collection in capillary tubes enabled the convenient and quantitative transfer of the solutes to HPLC and MS for further analysis and identification of the collected fractions. Our initial studies in static and CF-LSIMS showed that the off-line combination of CF-LSIMS and CZE was a 1000 fold more sensitive than static-LSIMS.

Acknowledgment

References

1. M.J. Sepaniak, D. F. Swaile, and A. G. Powell, *J. Chromatogr.*, 480 (1989) 185

2. P. Bocek, M. Deml, J. Pospichal, and J. Sudor, *J. Chromatogr.*, 470 (1989) 309.

3. F. Foret, S. Fanali, and P. Bocek, *J. Chromatogr.*, 516 (1990) 219.

4. P. Bocek, M. Deml, J. Pospichal, and J. Sudor, *J. Chromatogr.*, 500 (1990) 673.

5. J. Sudor, J. Pospichal, M. Deml, and P. Bocek, *J. Chromatogr.*, 545 (1991) 331.

6. C.-W. Whang, and E. S. Yeung, *Anal. Chem.*, 64 (1992) 502.

7. X. Huang, and J. I. Ohms, *J. Chromatogr.*, 516 (1990) 133.

8. L. R. Snyder, and J. J. Kirkland, *Introduction to Modern Liquid Chromatography*, 2nd Edit., Wiley Interscience, New York, 1979, pp. 712-713.

9. W. Nashabeh and Z. El Rassi, *J. High Res. Chromatogr.*, 15 (1992) 289.

10. W. Nashabeh and Z. El Rassi, *J. Chromatogr.*, 1993, 632 (1993) 157.

11. C. S. Lee, D. McManigill, C.-T. Wu and B. Patel, *Anal. Chem.*, 63 (1991) 1519.

12. M. A. Hayes and A. G. Ewing, *Anal. Chem.*, 64 (1992) 512.

13. D. J. Rose, and J. W. Jorgenson, *J. Chromatogr.*, 438 (1988) 23.

14. A. S. Cohen, D. R. Najarian, A. Paulus, A. Guttman, J. A. Smith, and B. L. Karger, *Proc. Natl. Acad. Sci. U.S.A.*, 85 (1988) 9660.

15. N. A. Guzman, L. Hernandez, and B. G. Hoebel , *Biopharm.*, January (1989) 23.

16. R. Takigiku, T. Keough, M. P. Lacey,. and R. E. Schneider, *Rapid Commun. Mass Spectrom.*, 4 (1990) 24.

17. X. Huang and R. N. Zare, *Anal. Chem.*, 62 (1990) 443.

18. C. Fujimoto, Y. Muramatsu, M. Suzuki and K. Jinno, *J. High Resol. Chromatogr.*, 14 (1991) 178.

19. N. A. Guzman, M. A. Trebilcock and J. P. Advis, *Anal. Chim. Acta,* 249 (1991) 247.

20. C. Fujimoto, T. Fujikawa and K. Jinno, *J. High Resol. Chromatogr.*, 15 (1992) 201.

21. R. A. Wallingford and A. G. Ewing, *Anal. Chem.*, 60 (1988) 258.

22. N. A. Guzman, M. A. Trebilcock and J. P. Advis, *J. Liq. Chromatogr.*, 14 (1991) 997.

23. K.-O. Eriksson, A. Palm. and S. Hjerten, *Anal. Biochem.*, 201 (1992) 211.

24. W. Nashabeh and Z. El Rassi, *J. Chromatogr.*, 559 (1991) 367.

25. R. A. Wallingford and A. G. Ewing, *Adv. Chromatogr.*, 29 (1989) 1.

26. R. M. Capricoli, T. Fan. and J. S. Cortell, *Anal. Chem.*, 58 (1986) 2949.

CHAPTER VI

CAPILLARY ZONE ELECTROPHORESIS OF
PYRIDYLAMINO DERIVATIVES OF
MALTOOLIGOSACCHARIDES*

Abstract

Maltooligosaccharides derivatized with 2-aminopyridine were separated by capillary zone electrophoresis in the pH range 3.0 to 4.5 using 0.1 M phosphate solutions as the running electrolyte. The inclusion of small amounts of tetrabutylammonium bromide in the electrolyte solution facilitated the separation at pH 5.0 and yielded high separation efficiency. The separated zone of pyridylamino derivatives of maltooligosaccharides migrated across the fused silica capillary and passed the detection point in the order of increasing size. The "overall mobility" was a linear function of the number of glucose residues in the homologous series.

Introduction

Capillary zone electrophoresis (CZE) is increasingly employed for the separation and analysis of a wide variety of compounds ranging in size from small ions and molecules [1-7] to high molecular weight substances such as proteins [8-10] and nucleic acid fragments [11,12]. However, the potential of the technique has not been yet exploited

---

in many areas including carbohydrates. This may be due to the lack of charges and chromophores in the carbohydrate molecules.

Indeed, neutral carbohydrates are not directly amenable to electrophoresis. However, they may become charged as the result of complex formation with other ions. The complex formation equilibria, e.g., borate complexes, have been exploited in traditional paper electrophoresis [13,14]. Very recently, the sugar-borate complexes at pH 10 have been utilized in capillary zone electrophoresis for the separation of reducing monosaccharides [15] tagged with 2-aminopyridine.

On the other hand, pre-column derivatizations to produce a chromophore or fluorophore have been extensively used in HPLC of carbohydrates to allow their sensitive detection [16,17] (for review see Refs. 18 and 19). It is expected that many of these detection schemes will also be applied to carbohydrate detection in CZE.

In the present report, we extend the potential of CZE to the separation of pyridylamino (PA) derivatives of maltooligosaccharides. The derivatization of mono- and oligosaccharides with 2-aminopyridine is well documented [15,20] and was used for HPLC analysis of carbohydrates by UV [21] or fluorescence detection [17]. The tagging of maltooligosaccharides with 2-aminopyridine provides the homologs with a positive charge, which allowed their analysis by paper electrophoresis [20]. Indeed, the pK_a value of the derivatives has been found to be 6.7 [20], a value equal to that found for free 2-aminopyridine [22].

This paper presents the results of a study of the electrophoretic conditions for the separation of PA derivatives of maltooligosaccharides by CZE. High separation efficiencies were obtained in the pH range 3.0 to 4.5, which is ideal for the operation of fused silica capillary columns as far as the stability of the column and the reproducibility of the separations are concerned. In addition, the inclusion of small amounts of tetrabutylammonium bromide in the running electrolyte was a useful adjunct to effect full separation of the homologous series at pH 5.0. The PA derivatives of the

maltooligosaccharides eluted in the order of increasing size. The "overall mobility" was a linear function of the number of glucose residues in the homologous series. The slope of the lines, which we refer to as "overall mobility" decrement, is expected to facilitate the identification of oligosaccharides at large.

Experimental

Electropherograph

The instrument for capillary electrophoresis used in this study resembled that reported by others [3,4]. It was constructed from a Glassman High Voltage (Whitehouse Station, NJ, U.S.A.) Model EH30P3 high-voltage power supply and a Linear (Reno, NV, U.S.A.) Model 200 UV-Vis variable wavelength detector equipped with a cell for on-column capillary detection. The detection wavelength was set at 240 nm. The electropherograms were recorded with a Kipp and Zonen Model BD 40 strip chart recorder. The high-voltage output and the ground were connected to platinum electrodes, which were placed in 2.0 mL electrolyte reservoirs. The ends of the fused silica capillary were dipped in both reservoirs and that completed the circuit. The separation and sample introduction were carried out in the positive polarity mode, i.e. the anodic reservoir served as the high voltage output (injection end) and the cathodic reservoir was at the ground potential (detection end).

Capillary Columns

Fused silica capillary columns of 50-μm I.D. and 365-μm O.D. having polyimide-clad were obtained from Polymicro Technology (Phoenix, AZ, U.S.A.). The total column length was 80 cm while the separation distance was 50 cm, i.e. from the injection end to the detection point. The polyimide-clad of the capillary was burned off at the detection point and the exposed quartz tubing was placed in the detector cell.

Reagents and Materials

The following PA derivatives of maltooligosaccharides: PA-maltotetraose (PA-G$_4$), PA-maltopentaose (PA-G$_5$), PA-maltohexaose (PA-G$_6$), and PA-maltoheptaose (PA-G$_7$) were a gift by Dr. A. Mort from the Biochemistry Department at Oklahoma State University. The covalent attachment of 2-aminopyridine to the reducing end of the maltooligosaccharides was carried out using the procedure of reductive amination [20]. Reagent grade sodium phosphate monobasic and dibasic, phosphoric acid, hydrochloric acid, sodium hydroxide, phenol, tetrabutylammonium bromide were obtained from Fisher Scientific (Pittsburgh, PA, U.S.A.). Distilled water was used to prepare the running electrolyte as well as the solutions used in column cleaning and pretreatment. All solutions were filtered with 0.2-μm UniPrep syringeless filters obtained from Genex Corporation (Gaithersburg, MD, U.S.A.) to avoid column plugging.

Procedures

In all experiments (except where indicated) the voltage drop across the capillary during electrophoresis was fixed at 20 kV, while injection was made by electromigration at 18 kV for 15 seconds.

All experiments were carried out with uncoated fused silica capillaries. The untreated silica capillary column was flushed with 1 N NaOH followed by water and the running electrolyte. The running electrolyte was renewed after 5-6 runs, and the capillary column was flushed with fresh buffer before each injection in order to ensure reproducible separations [23].

The electroosmotic flow rate was measured by the ratio of the volume of the capillary (volume of a cylinder in 50 cm length and 50 μm i.d.) and the time required for phenol, an inert tracer [9], to migrate the 50 cm distance between the injection end and the detection point.

Results and Discussion

The electrophoretic behavior of each PA-maltooligosaccharide was examined using 0.1 M aqueous phosphate solutions at different pH. The results are depicted in Fig. 1 in terms of migration time versus pH of the electrolyte solution. As expected, the migration time of the different homologs from the injection to the detection point decreased with increasing pH. This behavior is primarily due to the increase in electroosmotic flow [24], because higher electrolyte pH produces an increase in the ionization of silanol groups on the surface of fused silica capillaries. Indeed, as can be seen in Figs 1 and 2, phenol which is believed to migrate with the electroosmotic or bulk flow [9] clearly demonstrated this trend. In the pH range from 3.0 to 5.5 the positively charged PA-maltooligosaccharides migrated ahead of phenol and were separated according to their size. At pH 6.0 and 7.0, the derivatives practically coeluted at approximately the same migration time as phenol (see Fig. 1). Obviously in this pH range the PA-maltooligosaccharides become less positively charged. Under these circumstances neutral and quasi-neutral solutes are swept with the electroosmotic flow (bulk flow).

Figure 3 illustrates the high separation efficiency obtained with a 50 cm (separation distance) untreated fused silica capillary tube at 20 kV using 0.1 M phosphate, pH 4.0, as the running electrolyte. As can be seen in Fig. 3, base line resolution is obtained in less than 25 minutes.

Figure 4 illustrates the "overall mobility" of PA-maltooligosaccharides at different pH as a function of the number of glucose residues in the homologous series. The slope of the lines, which is the "overall mobility" decrement, δ, was relatively constant over the pH range 3.0 to 4.5 (see Table I). On the other hand, δ dropped sharply at pH 5.0, and
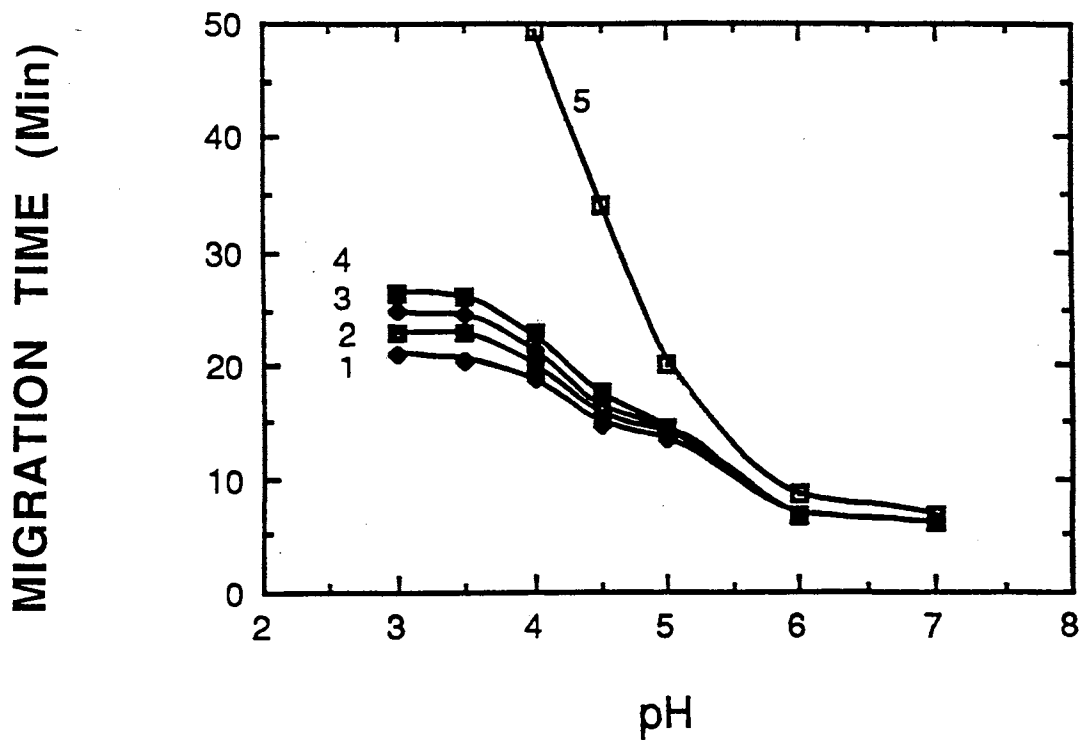
Figure 1. Migration times of PA-maltooligosaccharides and phenol as a function of electrolyte pH. Capillary, fused silica tube, 50 cm (to the detection point) x 50-μm I.D.; electrolytes, 0.1 M phosphate solutions at different pH; voltage, 20 kV; current was ca. 60 μA; injection by electromigration for 15 sec at 18 kV; temp., 25 C. 1, PA-G_4; 2, PA-G_5; 3, PA-G_6; 4, PA-G_7; 5, phenol.
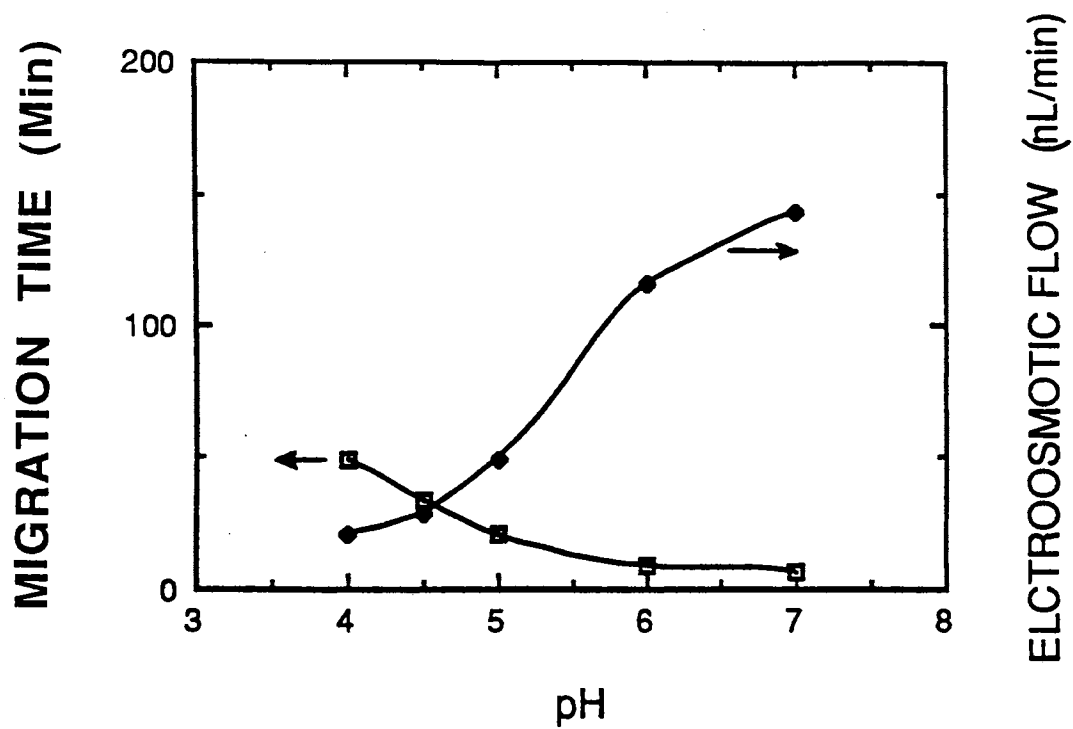
Figure 2. Migration times for phenol and electroosmotic flow as a function of electrolyte pH. Other conditions as in Fig. 1.
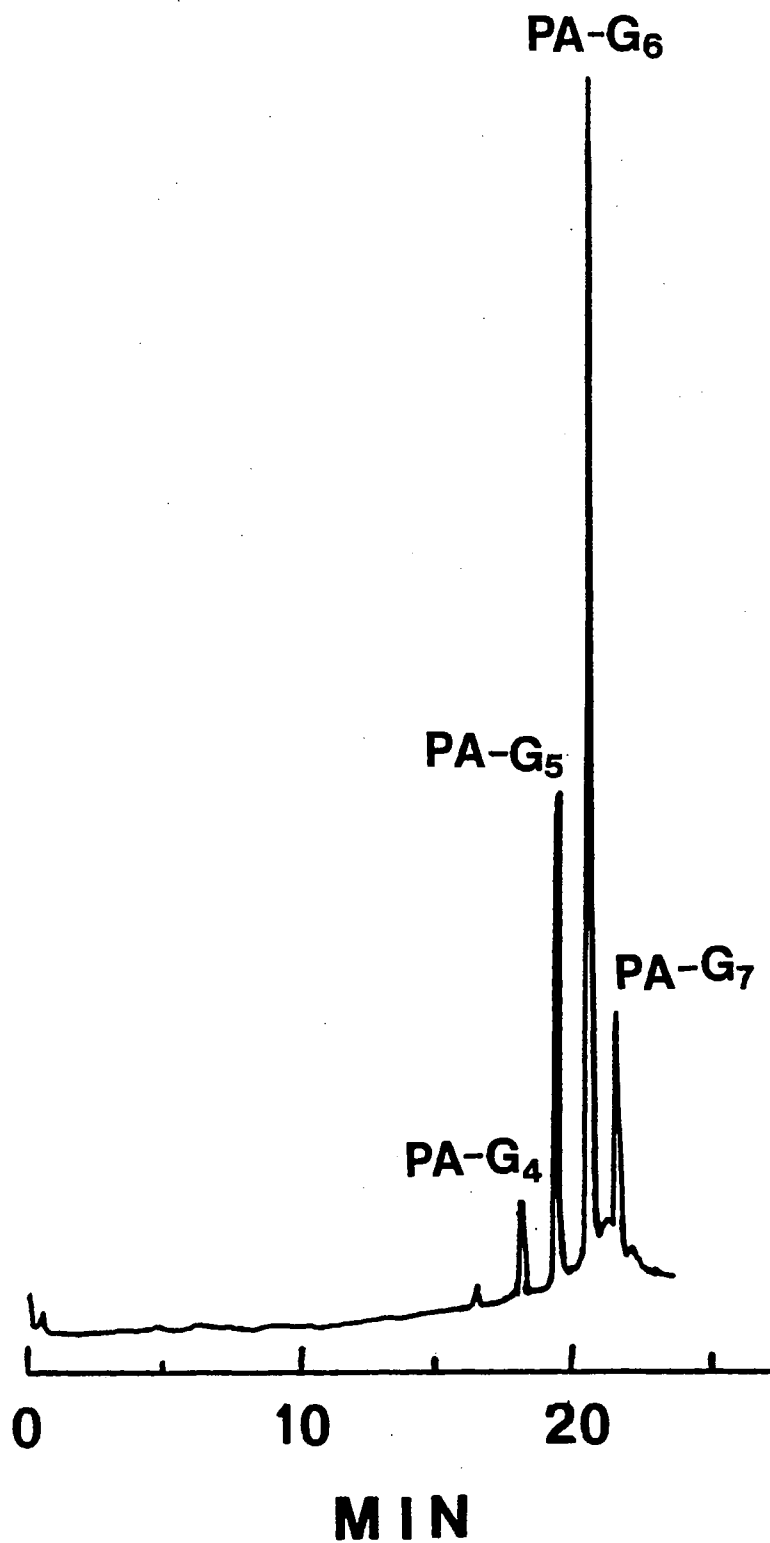
Figure 3. Separation of PA-maltooligosaccharides. Electrolyte: 0.1 M phosphate, pH 4.0. UV detection at 240 nm. Other conditions as in Fig. 1.
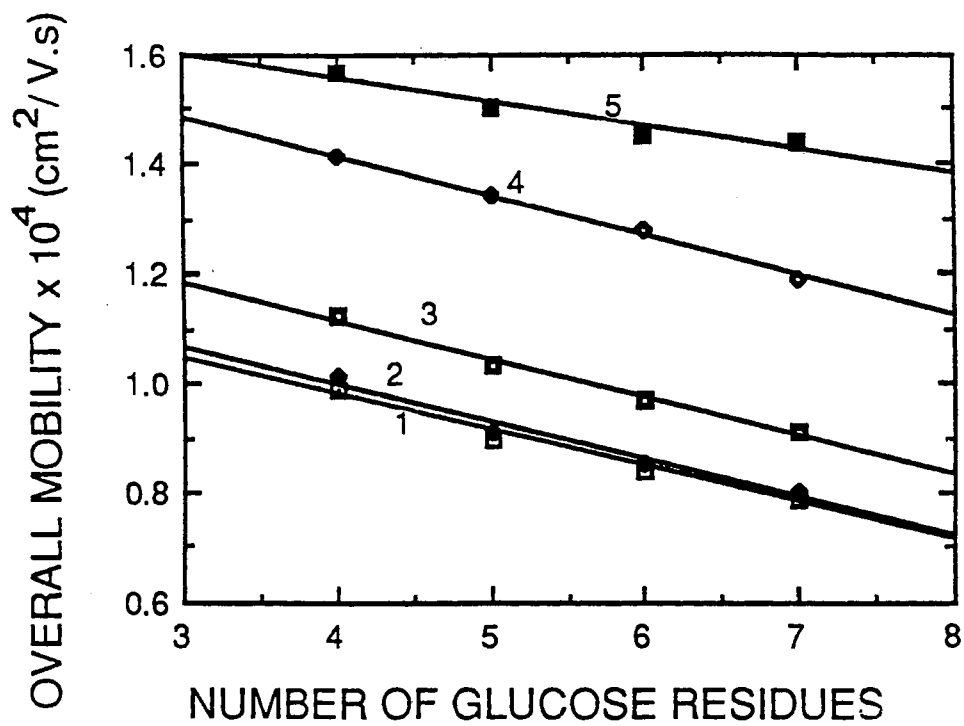
Figure 4. "Overall mobility" as a function of the number of glucose residues in the homologous series at different pH. Other Conditions as in Fig. 1. 1, pH 3.0; 2, pH 3.5; 3, pH 4.0; 4, pH 4.5; 5, pH 5.0.

TABLE I.

OVERALL MOBILITY DECREMENT, δ, AS ESTIMATED FROM THE SLOPE OF THE PLOTS OF OVERALL MOBILITY *VERSUS* THE NUMBER OF GLUCOSE RESIDUES IN THE HOMOLOGOUS SERIES.

Electrolytes: 0.1 M phosphate solutions at different pH values.

pH	$\delta \times 10^6 \, cm^2/V.s$	Correlation coefficient
3.0	-10.6	0.98
3.5	-11.5	0.97
4.0	-10.6	0.99
4.5	-11.4	0.99
5.0	-6.5	0.92

reached almost zero at pH 6.0 and 7.0 whereby the PA-maltooligosaccharides moved virtually together with the bulk flow.

The effect of electrolyte concentration on the electrophoretic behavior of the homologs was studied at pH 4.0 using 0.025, 0.05, 0.075 and 0.1 M phosphate solutions. The results are depicted in Fig. 5 in terms of "overall mobility" versus the molar concentration of the running electrolyte. As expected, the "overall mobility" decreased with increasing phosphate concentration in the running electrolyte solution. This is due to the reduction in electroosmotic flow [25], as a consequence of an increase in the viscosity of the electrolyte solution and a decrease in both the thickness of the double layer and the zeta potential of the capillary wall [26]. It has to be noted that a concentration of 0.075 to 0.1 M phosphate in the running electrolyte yielded sharper peaks and consequently higher resolution than a lower phosphate content. This may be due to the salt shielding effect of
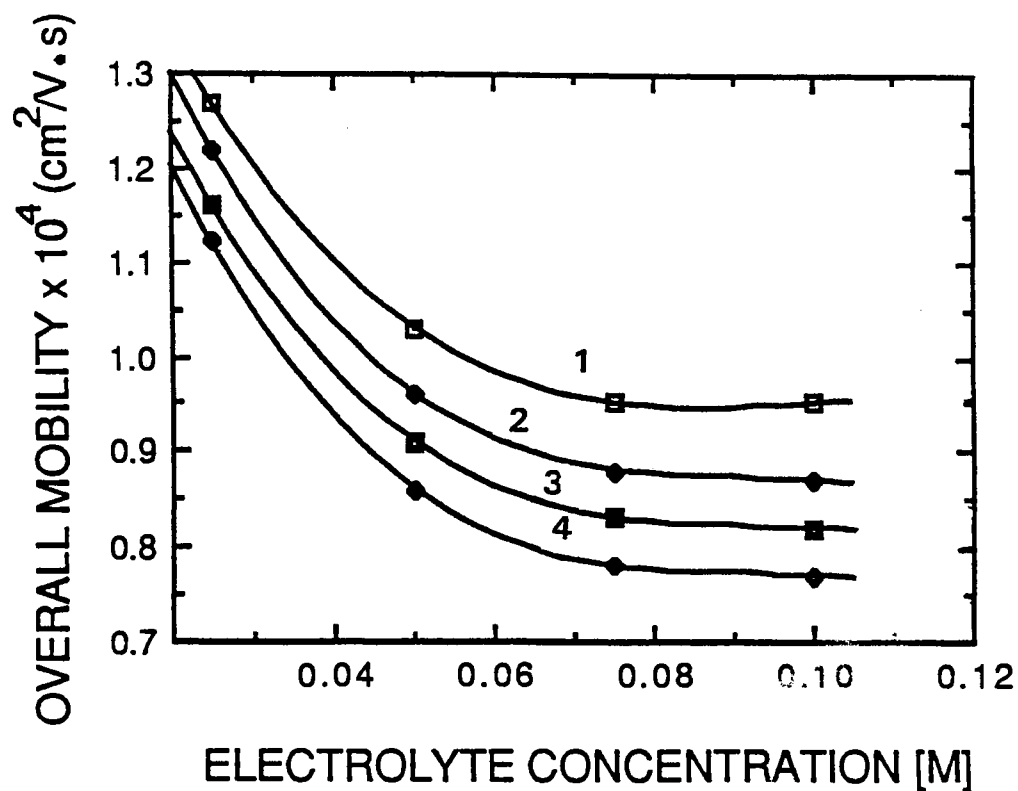
Figure 5. "Overall mobility" as a function of electrolyte concentration. Electrolytes: phosphate solutions at different concentrations, pH 4.0. Currents: 15 μA, 25 μA, 40 μA, and 60 μA at 0.025, 0.05, 0.075, and 0.1 M, respectively. Other conditions as in Fig. 1. 1, PA-G_4; 2, PA-G_5; 3, PA-G_6; 4, PA-G_7.

silanol groups on the capillary walls, which minimizes wall interaction with the positively charged PA-maltooligosaccharides.

For each electrolyte concentration, the "overall mobility" data from the preceding experiments are plotted in Fig. 6 versus the number of glucose residues in the homologous series. Straight lines are obtained with a correlation coefficient equal or greater than 0.99 (see Table II). The "overall mobility" decrement, δ, for the homologs increased slightly with the electrolyte concentration by a factor of 1.15 when going from 0.025 to 0.1 M phosphate.

TABLE II.

OVERALL MOBILITY DECREMENT, δ, AS ESTIMATED FROM THE SLOPE OF THE PLOTS OF OVERALL MOBILITY *VERSUS* THE NUMBER OF GLUCOSE RESIDUES IN THE HOMOLOGOUS SERIES.

Electrolytes: solutions at different phosphate concentrations, pH 4.0.

Phosphate concentration, [M]	δ x 10^6 cm^2/V.s	Correlation coefficient
0.025	-8.4	0.99
0.05	-8.6	0.99
0.075	-8.8	0.99
0.1	-9.5	0.99

As indicated above, the resolution between the homologs decreased with increasing pH. Fig. 7 shows the separation of PA-maltooligosaccharides at pH 5.0 with and without tetrabutylammonium bromide in the running electrolyte solution. The inclusion of 50 mM
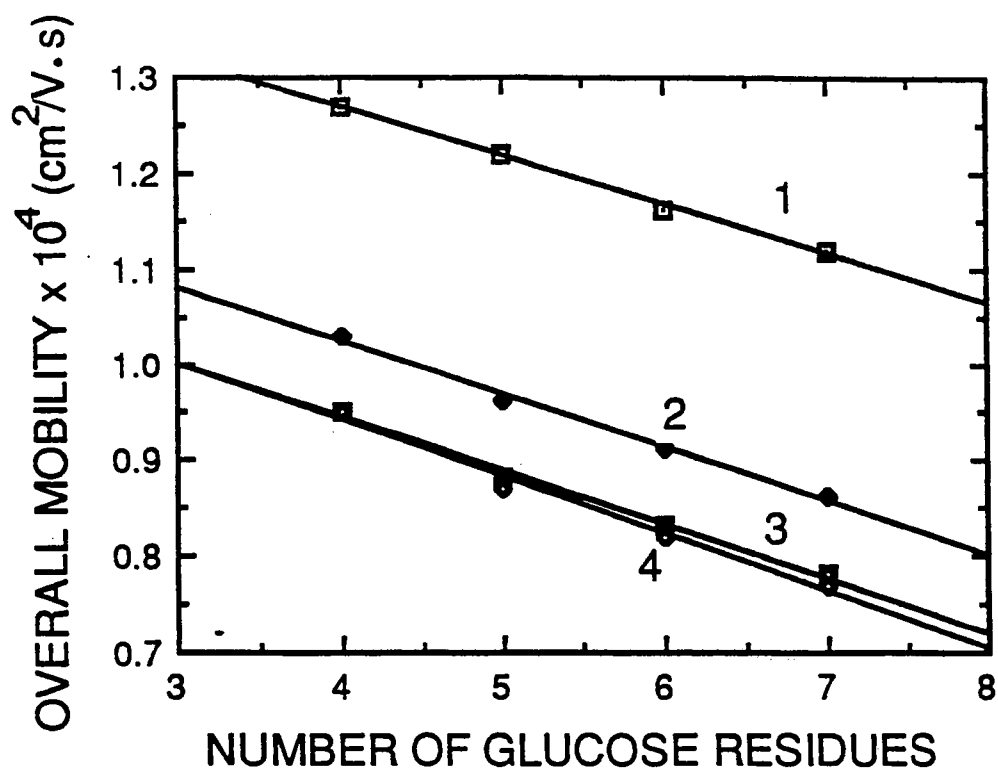
Figure 6. "Overall mobility" as a function of glucose residues in the homologous series at different phosphate concentration in the electrolyte. 1, 0.025 M; 2, 0.05 M; 3, 0.075 M; 4, 0.1 M. Other conditions as in Fig. 5.
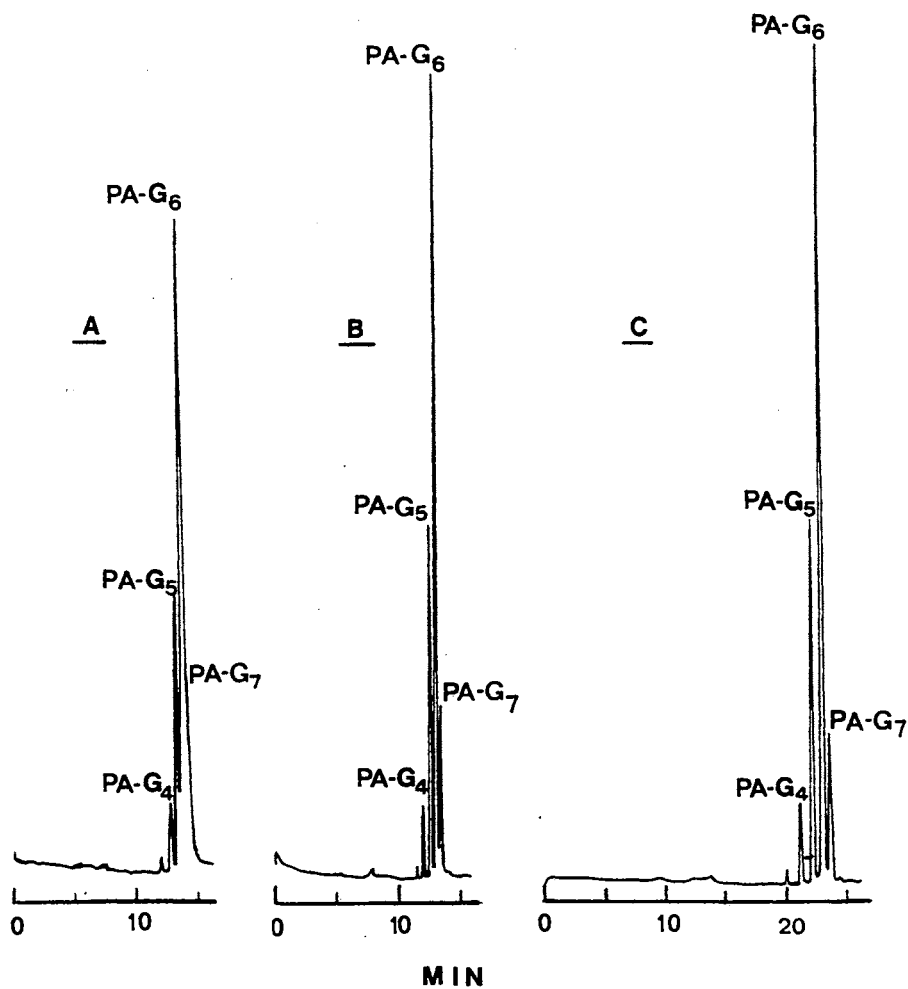
Figure 7. Separation of PA-maltooligosaccharides. Electrolytes, 0.1 M phosphate, pH 5.0, without and with 50 mM tetrabutylammonium bromide in A and B, respectively. In both cases the voltage was 20 kV and the corresponding currents were 60 and 125 µA. In C as in B except voltage was 15 kV and current was 60 µA. Other conditions as in Fig. 1.

tetrabutylammonium bromide in the electrolyte solution yielded higher separation efficiency and concomitantly higher resolution. A further increase in resolution was achieved by using 15 kV instead of 20 kV. This may be due to a lesser heat overload of the system and decreased electroosmotic flow at the lower voltage.

To study the effect of tetrabutylammonium bromide on separation, 50 mM of this organic salt were added to 0.1 M phosphate solutions at different pH. The results are summarized in Table III in terms of migration modulus, η, which is the ratio of the migration time of the solute in the presence to that in the absence of tetrabutylammonium

TABLE III.

MIGRATION MODULUS, η, OF PYRIDYLAMINO DERIVATIVES OF MALTOOLIGOSACCHARIDES AT DIFFERENT pH.

Electrolytes: 0.1 M phosphate solutions with or without 50 mM tetrabutylammonium bromide.

PA-maltooligosaccharide	Migration Modulus, η		
	pH 3.0	pH4.5	pH 5.0
PA-G_4	1.8	1.5	0.96
PA-G_5	2.0	1.5	0.96
PA-G_6	2.3	1.5	0.96
PA-G_7	2.5	1.5	0.96

bromide. At pH 5.0 and above, η is almost equal to unity, whereas at pH 4.5 and 3.0 η is greater than 1 and 2, respectively. In the pH range 5.0 to 7.0, the small changes in the migration of PA-maltooligosaccharides upon adding tetrabutylammonium bromide to the

electrolyte solution may be viewed as the result of two opposing effects: increased overall mobility due to attenuation in wall interaction of the positively charged derivatives versus a reduction in the electroosmotic flow as a consequence of increasing the ionic strength of the electrolyte solution. At pH 3.0 and 4.5, where wall interaction is less pronounced, the enhancement in migration time upon adding the organic salt (see Table III) may be explained by the decrease in the electroosmotic flow resulting from an increase in the ionic strength of the running electrolyte.

Acknowledgments

References

1. F. E. P. Mikkers, F. M. Everaerts and T. P. E. M. Verheggen, *J. Chromatogr.,* 169 (1979) 11.

2. S. Hjerten, *J. Chromatogr.,* 270 (1983) 1.

3. J. W. Jorgenson and K. D. Lukacs, *Anal. Chem.,* 53 (1981) 1298

4. J. W. Jorgenson and K. D. Lukacs, *Science,* 222 (1983) 266.

5. E. Gassmann, J. E. Kuo and R. N. Zare, *Science,* 230 (1985) 813.

6. S. Fujiuwara and S. Honda, *Anal. Chem.,* 58 (1986) 1811.

7. R. A. Wallingford and A. G. Ewing, *Anal. Chem.,* 61 (1989) 98.

8. H. H. Lauer and D. McManigill, *Anal. Chem.,* 58 (1986) 166.

9. R. M. McCormick, *Anal. Chem.,* 60 (1988) 2322.

11. A. S. Cohen, D. Najarian, J. A. Smith and B. L. Karger, *J. Chromatogr.,* 458 (1988) 323.

12. S. Compton and R. Brownlee, *BioTechniques,* 6 (1988) 5.

13. S. J. Angyal and J. A. Mills, *Aust. J. Chem.,* 32 (1979) 1993.

14. B. Bettler, R. Amado and H. Neukom, *J. Chromatogr.,* 498 (1990) 213.

15. S. Honda, S. Iwase, A. Makino and S. Fujiwara, *Anal. Biochem.,* 176 (1989) 72.

16. W.T. Wang, N.C. LeDone, B. Ackerman and C.C. Sweely, Anal. Biochem., 141 (1984) 366.

17. N. Tomiya, J. Awaya, M. Kurono, S. Endo, Y. Arata and N. Takahashi, *Anal. Biochem.,* 171 (1988) 73

18. S. Honda, *Anal. Biochem.,* 140 (1984) 1.

19. K. B. Hicks, *Adv. Carbohydr. Chem. Biochem.,* 46 (1988) 17.

20. S. Hase, S. Hara and Y. Matsushima, *J. Biochem.,* 85 (1979) 217.

21. N. O. Maness and A. Mort, *Anal. Biochem.,* 178 (1989) 248.

22. A. E. Martell and R.M. Smith, *"Critical Stability Constants,"* Vol. 2, Plenum Press, New York, N.Y., 1975, p. 205.

23. R. G. Nielsen, G. S. Sittampalam and E. C. Rickard, *Anal. Biochem.,* 177 (1989) 20.

24. K. D. Lukacs and J.W. Jorgenson, *J. High Res. Chromatogr. Chromatogr. Commun.,* 8 (1985) 407.

25. M. M. Bushey and J. W. Jorgenson, *J. Chromatogr.,* 480 (1989) 301.

26. C. J. van Oss, *Sep. Purif. Methods,* 8 (1979) 119.

CHAPTER VII

CAPILLARY ZONE ELECTROPHORESIS OF α_1-ACID GLYCOPROTEIN FRAGMENTS FROM TRYPSIN AND ENDOGLYCOSIDASE DIGESTIONS*

Abstract

Capillary zone electrophoresis with fused-silica tubes having hydrophilic coating on the inner walls was evaluated in the separation of peptide and glycopeptide fragments from trypsin digestion of α_1-acid glycoprotein. Submapping of glycosylated and nonglycosylated tryptic fragments of the glycoprotein by capillary electrophoresis was facilitated by selective isolation of the glycopeptides on concanavalin A silica-based stationary phases prior to the electrophoretic run. In addition, the electrophoretic map and submaps of the whole tryptic digest and its concanavalin A fractions, respectively, allowed the elucidation of the microheterogeneity of the glycoprotein. Also, capillary zone electrophoresis proved suitable for the mapping of the oligosaccharide chains cleaved from the glycoproteins by endoglycosidase digestion. The oligosaccharides cleaved from human and bovine α_1-acid glycoprotein were analyzed after derivatization with 2-aminopyridine, which allowed their sensitive detection by on-column UV absorption. The separation was best achieved when 0.1 M phosphate solution, pH 5.0, containing 50 mM teterabutylammonium bromide was used as the running electrolyte. The effect of the

---

organic salt on separation was attributed to ion-pair formation and/or hydrophobic interaction.

Introduction

High performance capillary electrophoresis (HPCE) is rapidly developing and becoming an important tool for the separation of a wide variety of biological substances including peptides [1-3], proteins [4-6], nucleic acid fragments [7-9] and recently oligosaccharides [10]. The recent advances in instrumentation and the many sound features of HPCE, e.g. various modes of separation, high resolving power, and small sample requirement, have made it possible for the technique to play this role.

This study is concerned with investigating the potential of capillary zone electrophoresis (CZE) in the separation and characterization of glycoprotein fragments, i.e. peptides, glycopeptides and oligosaccharide chains. In this regard, we have selected human α_1-acid glycoprotein (AGP) as a model protein for the evaluation of CZE in analytical glycoprotein chemistry and analytical biotechnology. Besides being one of the best physicochemically characterized glycoproteins [11], human AGP is an attractive model because of its relatively high content of carbohydrates. Indeed, this single polypeptide chain of 181 amino acids has five glycosylation sites at asparagine residues in positions 15, 38, 54, 75, and 85 in the N-terminal of the molecule [12] . The N-linked oligosaccharide chains, which are of complex types at different degree of branching and sialylation (see Fig. 1), make up 45% of the total weight of the protein [11] (approx. M.W. = 41,000).

As will be shown in this report, CZE with its high resolving power and unique selectivity is well suited for the separation and characterization of peptide and glycopeptide fragments from the tryptic digest of human AGP, especially when combined with lectin affinity chromatography. For the selective isolation of glycopeptides prior to CZE analysis

Fucα(1→3)

Galβ(1→4)GlcNAcβ(1→4)

Galβ(1→4)GlcNAcβ(1→2)Manα(1→3)
★

CF BF B A C

Manβ(1→4)GlcNAcβ(1→4)GlcNAcβ1–Asn

Galβ(1→4)GlcNAcβ(1→2)Manα(1→6)
★

Galβ(1→4)GlcNAcα(1→6)
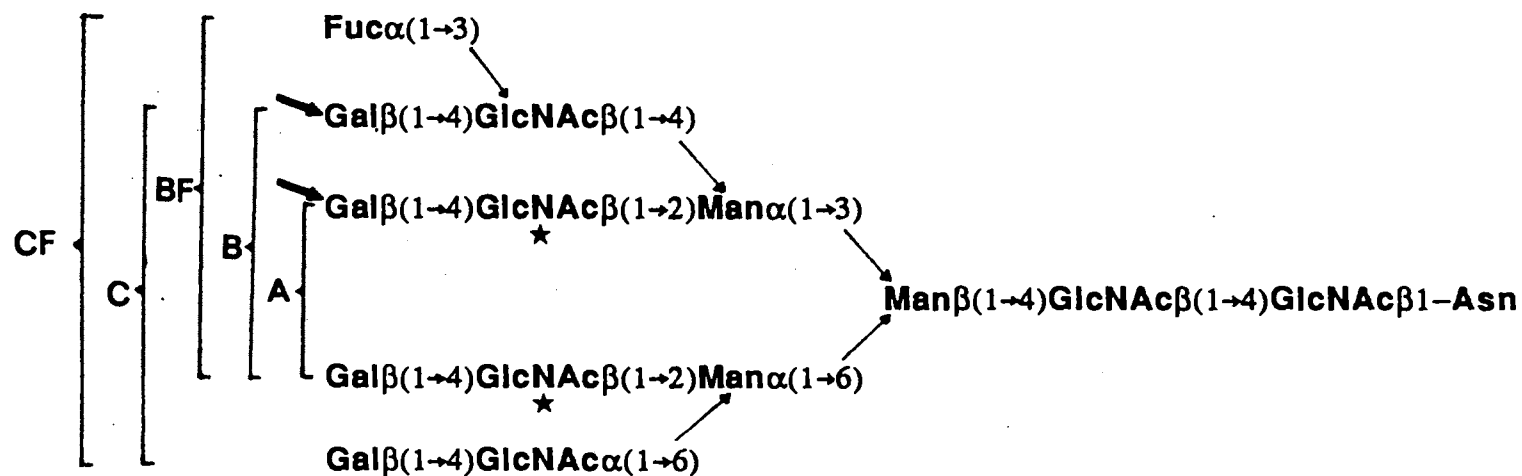
Figure 1. Primary structures of the five carbohydrate classes as elucidated by Schmid *et al.*[12]. Classes A, B, and C are the bi-, tri-, and tetraantennary complex N-linked glycans, respectively, whereas BF and CF are the fucosylated B and C structures. Two additional glycans having the tetranatennary basic structure like class C were also reported [24]. One has two additional fucose each linked to the outer chain at the GlcNAC residues marked with a star, while the second one has an outer chain prolonged by Gal β (1 - 4) GlcNAc at either of the Gal residues marked with an arrow.

we have used concanavalin A silica-based stationary phases. This arrangement allowed CZE tryptic mapping of the whole digest as well as CZE submapping of glycosylated and non-glycosylated fragments. In addition, the usefulness of the technique in mapping the carbohydrate units of the protein liberated by endoglycosidase digestion is also demonstrated. The CZE methodology that generated the fingerprint for an endoglycosidase digest of human AGP, was also applied to the glycans of bovine AGP . In both cases the oligosaccharides were derivatized with 2-aminopyridine, which provides the carbohydrates with a positive charge and a UV-absorbing (also fluorescent) tag [13].

Experimental

CZE Instrument

The instrument for capillary electrophoresis used in this study resemble that reported earlier [10]. It was constructed from a Glassman High Voltage (Whitehouse Station, NJ, U.S.A.) Model EH30P3 high-voltage power supply of positive polarity and a Linear (Reno, NV, U.S.A.) Model 200 UV-Vis variable wavelength detector equipped with a cell for on-column capillary detection. In all experiments, sample injection was made by electromigration at a voltage and for a duration that varied from one mixture to another, and are indicated in the figure legends. The detection wavelength was set at 200 nm or 240 nm for sensing the polypeptides or derivatized oligosaccharides, respectively. The electropherograms were recorded with a Shimadzu computing integrator (Columbia, MD, U.S.A.) equipped with a flopyy disk drive and a CRT monitor.

Capillary Columns

Fused-silica capillary columns of 50–μm I.D. and 365-μm O.D. having polyimide-cladding were obtained from Polymicro Technology (Phoenix, AZ, U.S.A.). All capillaries (except where indicated) used in this study were modified in house with a

hydrophilic coating on the inner walls. The inert coating, which consisted essentially of hydroxy-polyether will be evaluated in CZE of proteins in an upcoming article (see Chp. 2 [14]). It was prepared by allowing the capillary to react first with γ-glycidoxypropyltrimethoxysilane and then with a mixture of polyethylene glycol (M.W. 2000) and polyethylene glycol diglycidyl ether (M.W. 600). The running electrolyte was renewed after 5-6 runs and the capillary column was flushed successively with fresh buffer, water, methanol, water, and again running buffer before each injection in order to ensure reproducible separations.

HPLC Instrumentation and Columns

The chromatograph was assembled from an LDC/Milton Roy (Riviera Beach, FL, U.S.A.) Model CM4000 solvent delivery pump with dual beam variable-wavelength detector Model Spectro Monitor 3100. A Rheodyne (Cotati, CA, U.S.A.) Model 7125 sampling valve with a 100-μL sample loop was used for injection. Chromatograms were recorded with a Shimadzu (Columbia, MD, U.S.A.) Model C-R5A integrator.

A home made concanavalin A-silica (ConA-silica) column (100x4.6 mm) was prepared by attaching Con A to Zorbax silica gel (Du Pont, Willmington, DE, U.S.A.) using a procedure similar to that described by Larsson et al [15]. Zorbax is a spherical silica with 300 Å and 7-μm pore and particle diameters, respectively. A bakerbond wide pore octadecyl-silica column (250x4.6 mm) having mean particle and pore diameters of 5 μm and 300 Å, respectively, was a gift from J.T. Baker (Phillipsburg, NJ, U.S.A.).

Reagents and Materials

Human and bovine $α_1$-acid glycoproteins, TPCK-treated trypsin, mannose (Man), galactose (Gal), N-acetylglucosamine (GlcNAc), N-acetylgalactosamine (GalNAc), N-acetylneuraminic acid (NeuNAc), methyl-α-D-mannopyranoside, 2-aminopyridine, Brij 35 and Tris were obtained from Sigma (St. Louis, MO, U.S.A.). Peptide-N-glycosidase F

(PNGase F) from *Flavobacterium meningosepticum* was obtained from Boehringer Mannheim (Indianapolis, IN, U.S.A.). Reagent grade sodium phosphate monobasic and dibasic, boric acid, phosphoric acid, hydrochloric acid, acetic acid, sodium hydroxide, and HPLC grade methanol and acetonitrile were obtained from Fisher Scientific (Pittsburgh, PA, U.S.A.). Mercaptoethanol, sodium cyanoborohydride, polyethylene glycol and γ-glycidoxypropyltrimethoxysilane, and tetrabutylammonium bromide were from Aldrich (Milwaukee, WI, U.S.A.). Distilled water was used to prepare the running electrolyte as well as the solutions used in column cleaning and pretreatment. All solutions were filtered with 0.2-μm UniPrep syringeless filters obtained from Genex Corporation (Gaithersburg, MD, U.S.A.) to avoid column plugging.

Tryptic Digest

The digestion of AGP with TPCK-treated trypsin was carried out in a 10 mM Tris buffer containing 100 mM ammonium acetate and 0.1 mM calcium chloride, pH 8.3, at a trypsin substrate ratio of 1:100 and a temperature of 37 C [16]. Trypsin was added again after 2 hours and the digestion was stopped after a total of 4 hours by addition of 10% (v/v) phosphoric acid. Thereafter, the whole digest was desalted by passing it on a Bakerbond wide pore octadecyl-silica column (250x4.6 mm) equilibrated with water at 0.05% (v/v) trifluoroacetic acid (TFA). The bound fragments were eluted stepwise with 80% acetonitrile in water (v/v) at 0.05 % TFA (v/v). In this desalting process, single amino acids in the tryptic digest are lost but no major peak showed in the dead volume of the column. The pooled fraction was evaporated to dryness using a SpeedVac Concentrator (from Savant Instrument Co., Farmingdale, NY, USA). The dried materials were dissolved in the appropriate buffer used in the subsequent experiments.

Part of the dried materials was used for the CZE tryptic mapping, another part was fractionated on Con A-silica column into groups of peptide and glycopeptide fragments

which were employed to produce CZE submaps of glycosylated and nonglycosylated peptides, and a third part was incubated with PNGase F to generate the oligosaccharides.

Cleavage of Oligosaccharides

The whole digest, which was desalted on the RPC column as described above was then dissolved in 20 mM phosphate buffer containing 2 mM EDTA, 1 % (v/v) mercaptoethanol, and 0.1 % (w/v) Brij 35, pH 7.5. To this solution 3 units of peptide-N-glycosidase F were added, and the incubation was maintained at 37 C for 24 hours [17]. Thereafter, the mixture was evaporated to dryness with a Savant SpeedVac Concentrator. The dried materials containing the cleaved oligosaccharides, the peptide fragments, and other reagents employed in the incubation step was used as is without a sample clean up prior to the derivatization of its oligosaccharide components.

Derivatization of Mono-and Oligosaccharides

Commercially available standard monosaccharides such as Man, Gal, GalNAc, GlcNAc, and NeuNAc, which are the constituents of the carbohydrate chains of glycoproteins as well as the oligosaccharides cleaved from the glycoprotein were tagged with 2-aminopyridine (2-AP) at their reducing termini as described by Hase *et al* [13]. The mixtures containing the pyridylamino (PA) derivatives of the various sugars were first evaporated to dryness using SpeedVac concentrator. Subsequently, the dried materials were dissolved in water and then applied to capillary electrophoresis without any sample clean up from excess derivatizing agent and other components of the reaction mixture.

Results and Discussion

CZE Tryptic Mapping and Submapping

All CZE tryptic mapping and submapping of human α_1-acid glycoprotein were performed on a capillary with hydrophilic coating on the inner walls, and using 0.1 M phosphate solution, pH 5.0, as the running electrolyte. The hydrophilic coating minimized solute-wall interactions and also permitted the electrophoresis of basic proteins in the pH range 2.0 to 7.0 with high separation efficiencies [14]. Furthermore, with the coated capillaries, the electroosmotic flow decreased by a factor of ca. 3.5 when compared with the uncoated capillary.

Fig. 2 illustrates the CZE mapping and submapping of peptide fragments from the tryptic digest of human AGP. The electropherogram of the whole digest has an elution pattern characteristic of a mixture whose peptide fragments are widely different in size and net charge. Three areas, with different peak capacity, denoted by A, B and C can be distinguished on the electropherogram of the whole digest. They are separated by two quasi peakless areas (see whole digest, Fig. 2). Obviously, small and positively charged peptide fragments are likely to be present in area A, slightly neutral peptides may be located in area B, and large and negatively charged tryptic fragments may be seggregated in area C. The values of the nominal "overall mobility", for areas A, B and C are 2.94×10^{-4}, 1.7×10^{-4} and 0.88×10^{-4} cm^2/Vs, respectively.

As seen in Fig. 2, the map for the whole tryptic digest of human AGP demonstrates the high resolving power of CZE and reveals the microheterogeneities of the glycoprotein as manifested by the excessive number of peaks for a protein of 181 amino acid residues with 20 trypsin cleavage sites (8 lysine and 12 arginine residues) [11,18]. In fact, by neglecting all sources of heterogeneity in the protein, the tryptic digest should result only into 12 peptide and 5 glycopeptide fragments, and three single amino acids (two
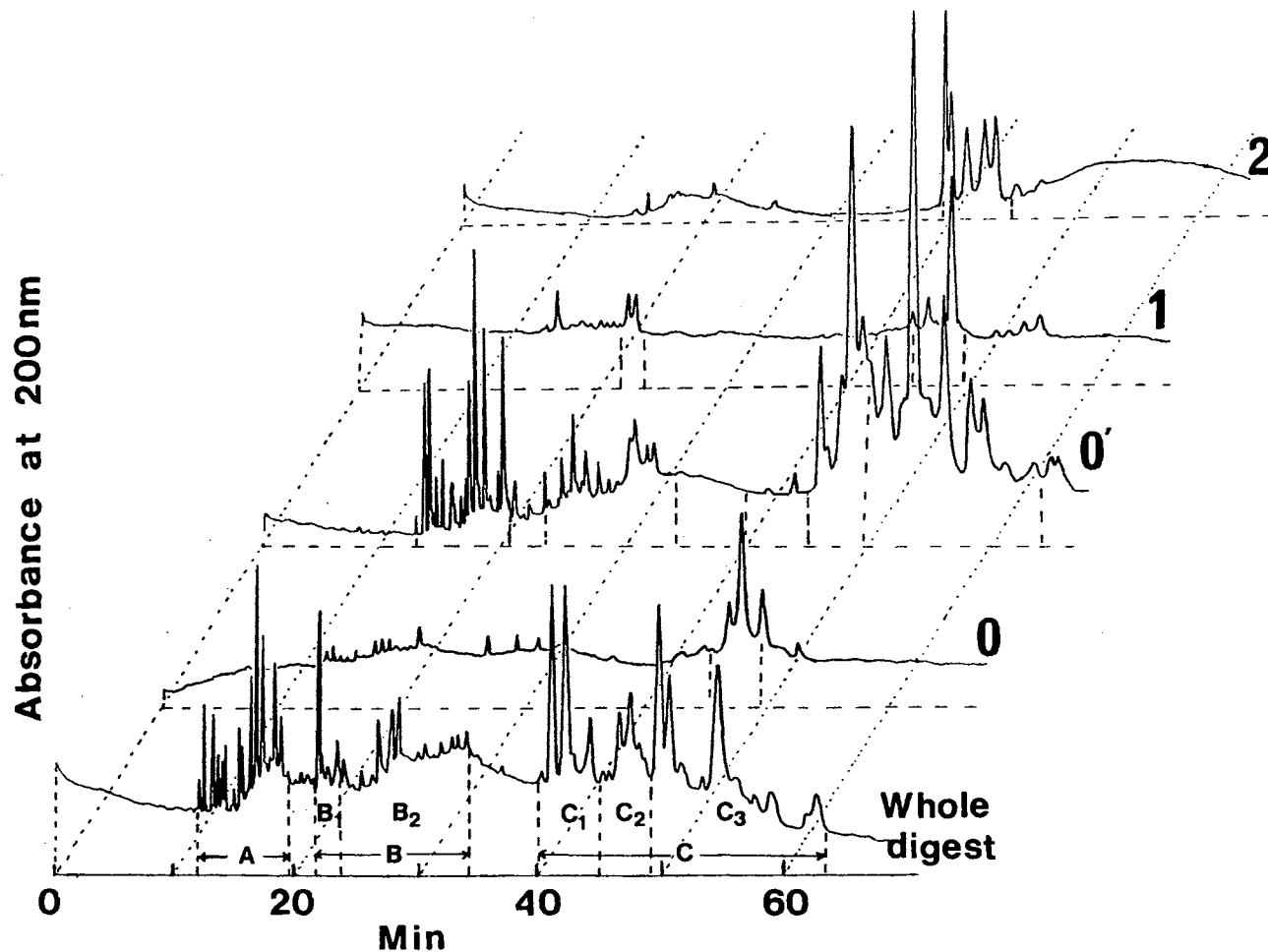
Figure 2. Capillary zone electrophoresis tryptic mapping and submapping of human AGP. Capillary, fused-silica tube with hydrophilic coating on the inner walls, 45 cm (to the detection point), 80 cm total length x 50 μm I.D.; electrolyte, 0.1 M phosphate solution, pH 5.0; running voltage, 22.5 kV; current was ca. 55 μA; injection by electromigration for 4 s at 22.5 kV. Symbols: fraction 0, con A non-reactive (excluded from the column); fraction 0', Con A non-reactive (unretained by the column); fraction 1, Con A slightly reactive (eluted with buffer); fraction 2, Con A strongly reactive (eluted with the haptenic sugar).

lysine and one arginine). However, more than any other serum glycoproteins, AGP is a highly heterogeneous protein [11,18,19]. One of the unique aspects of the primary structure of polypeptide chain of pooled human AGP is its peculiar structural polymorphism [11]. Substitutions were found at 21 of the 181 amino acids in the single polypeptide chain, which is responsible in part for multiple peptide and glycopeptide fragments in the tryptic digest. More details concerning the primary structure of the protein can be found in Refs. 11 and 18). Another source of multiple fragments in the tryptic digest is the microheterogeneities of the oligosaccharide chains attached [11,19,20]. Indeed, the variation in the terminal sialic acid causes charge heterogeneity in the glycopeptide fragments cleaved at the same location by trypsin, the differences in the extent of glycosylation among a population of the protein molecules lead to fragments having the same peptide backbone but with or without carbohydrate chains, and the variation in the nature of the oligosaccharide chains at each location yields several glycopeptides that have the same peptide backbone, but differ in their oligosaccharide structures.

To further elucidate the microheterogeneity of the glycoprotein and to generate CZE submaps for the tryptic digest, i.e., maps of groups of peptide or glycopeptide fragments, we have combined high performance lectin affinity chromatography and capillary electrophoresis. Figure 3 shows affinity chromatography group separation of the peptide fragments from human AGP performed on silica-bound concanavalin A column. The pooled fractions labeled 0 and 0' contain the Con A non reactive species, whereas those labeled 1 and 2 have the Con A slightly and strongly reactive fragments, respectively. Whereas the components of fraction 1 were slightly retained by Con A and eluted from the column with the equilibrating buffer (binding buffer), the components of fraction 2 interacted strongly with Con A and eluted from the column with the heptanic sugar; methyl-α–D-mannopyranoside.

The different Con A fractions were first desugared and/or desalted on an RPC column (see experimental section) and then analyzed by CZE. The results are depicted in
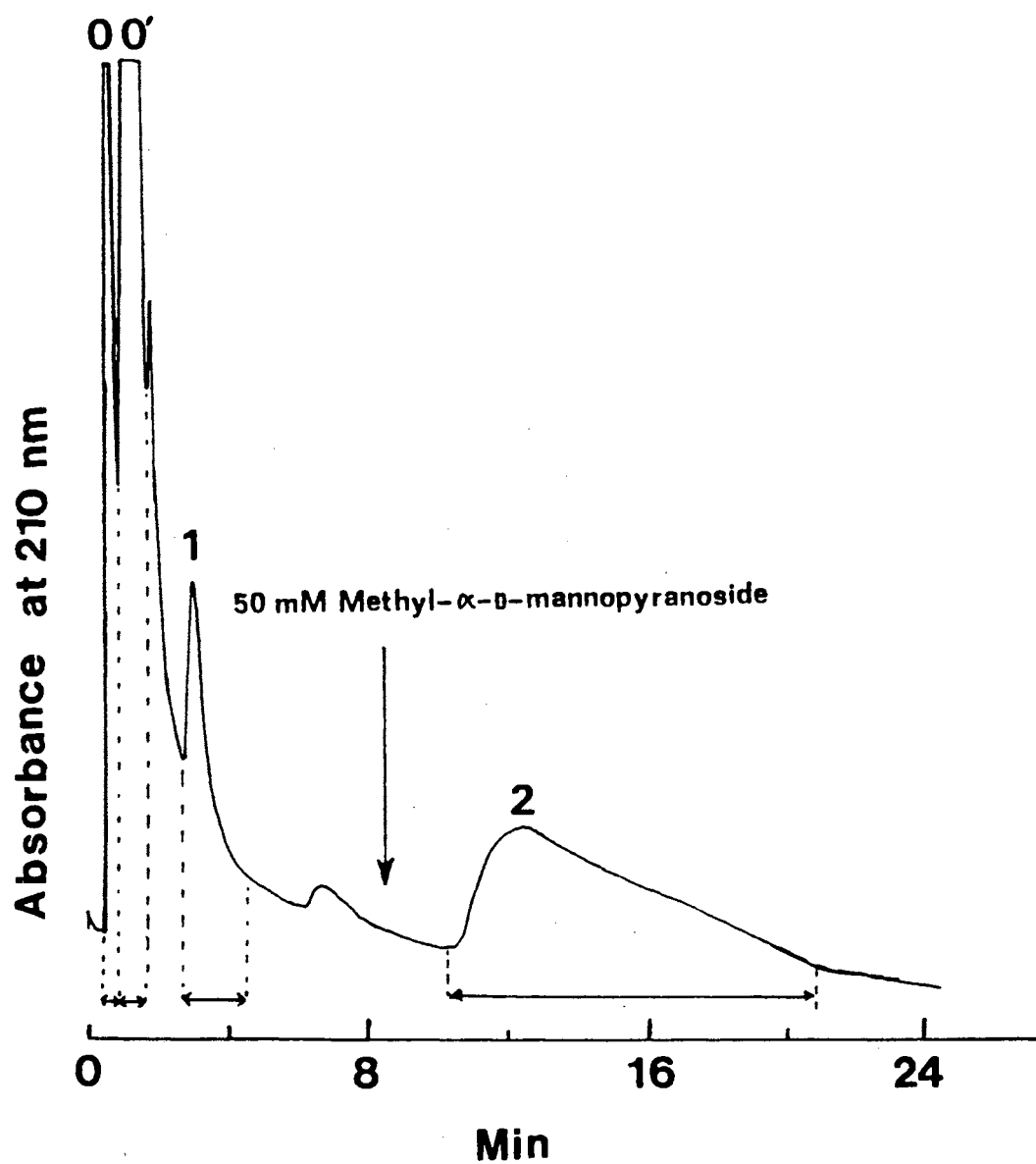
Figure 3. High performance lectin affinity chromatography of human AGP tryptic digest. Column, silica-bound concanavalin A, 100x4.6 mm; flowrate, 1 mL/min; temp., 25 C. Binding buffer, 20 mM phosphate, pH 6.5 containing 0.1 M NaCl; debinding buffer, 50 mM methyl-α-D-mannopyranoside in the binding buffer.

Fig. 2, and are referred to as submaps denoted by 0, 0', 1 and 2. The tryptic fragments of fraction 0 were excluded from the Con A column, possibly due to electrostatic repulsion between the peptides of the fraction and the Con A surface of same charge at pH 6.5 (pI value of ConA is ca. 4.5-5.5; Ref. 21). Indeed, the CZE submap 0 exhibited peaks eluting late from the capillary, and corresponding to area C_2 on the whole map, which is mainly populated by negatively charged peptide fragments as reflected from the value of its nominal overall mobility (μ_{app}= 1.0 x 10^{-4} cm^2/Vs). Fraction 0', whose peptide fragments did not interact with the Con A and eluted in the column void volume, yielded the CZE submap 0' containing most peaks that are in the map of the whole digest except those in areas B_1 and C_1. The two submaps 0 and 0' are mostly populated by nonglycosylated fragments, since their components are repulsed from or not retained by the Con A column.

Concanavalin A fraction 1 produced a CZE submap containing glycopeptide fragments with tri- and tetraantennary glycans that are known to interact weakly with ConA [22]. The submap 1 has some of the fragments that are missing in submap 0' (area B_1), but has fragments from area C_2 and minor peaks from area C_3 on the whole map. Fraction 2 produced a CZE submap with peaks corresponding to area C_1 on the whole map that are missing from submaps 0, 0', and 1. They are believed to be the glycopeptides with biantennary glycans that strongly bind to a Con A affinity column [22,23]. An area on the whole map worth mentioning is area C_2 whose components are found in submaps 0, 0' and 1. The components of this area on submaps 0, 0', and 1 are likely to be different from each others but overlap in the whole digest due to insufficient selectivity.

The approach tested and developed here is capable of elucidating the microheterogeneity of the protein, and is convenient for CZE submapping of tryptic fragments of interest, e.g. glycopeptides. This methodology is expected to work also with other glycoproteins, and the CZE submapping of all the glycosylated tryptic fragments

with different type of glycans may require the use of more than one lectin column in the prefractionation step.

CZE Mapping of Oligosaccharide Chains from AGP

Human AGP oligosaccharides were cleaved form the glycopeptide fragments of the tryptic digest using peptide-N-glycosidase F (PNGase F), an endoglycosidase that cleaves all types of N-linked oligosaccharide chains between the asparagine and the carbohydrate units [17]. The CZE mapping of the PA derivatives of these oligosaccharides is portrayed in Fig. 4a. It was performed on a coated capillary using 0.1 M phosphate solution, pH 5.0, containing 50 mM tetrabutylammonium bromide as the running electrolyte. As can be seen in Fig. 4a, the electropherogram shows six well defined peaks and a few minor peaks, eluting after the excess 2-aminopyridine (2-AP) and some spikes. The glycans of AGP (see Fig. 1) are known for their microheterogeneities caused mainly by variation in their terminal sialic acid. This may explain the presence of several peaks in the CZE map. The spikes indicated the presence of undissolved matters in the sample, since they were more numerous when applying the mixture to CZE without centrifugation.

Based on the above results, CZE can play an important role in the field of glycan separation and characterization. In addition, it holds promise for rapidly monitoring the extent of deglycosylation. Indeed, in another set of experiments, the oligosaccharides were cleaved directly from the glycoprotein using the same amount of protein starting materials as in the preceding experiment and keeping other conditions identical, i.e. pH, temperature, number of PNGase F units, and the time of digestion. The extent of deglycosylation from the whole protein decreased when compared to that from the glycopeptide fragments. This was ascertained from the disappearance of three major peaks from the CZE map (indicated by asterisks in Fig. 4a). This can be explained by the better accessibility of the endoglycosidase to the cleaving site in the glycopeptides than in the intact glycoprotein.
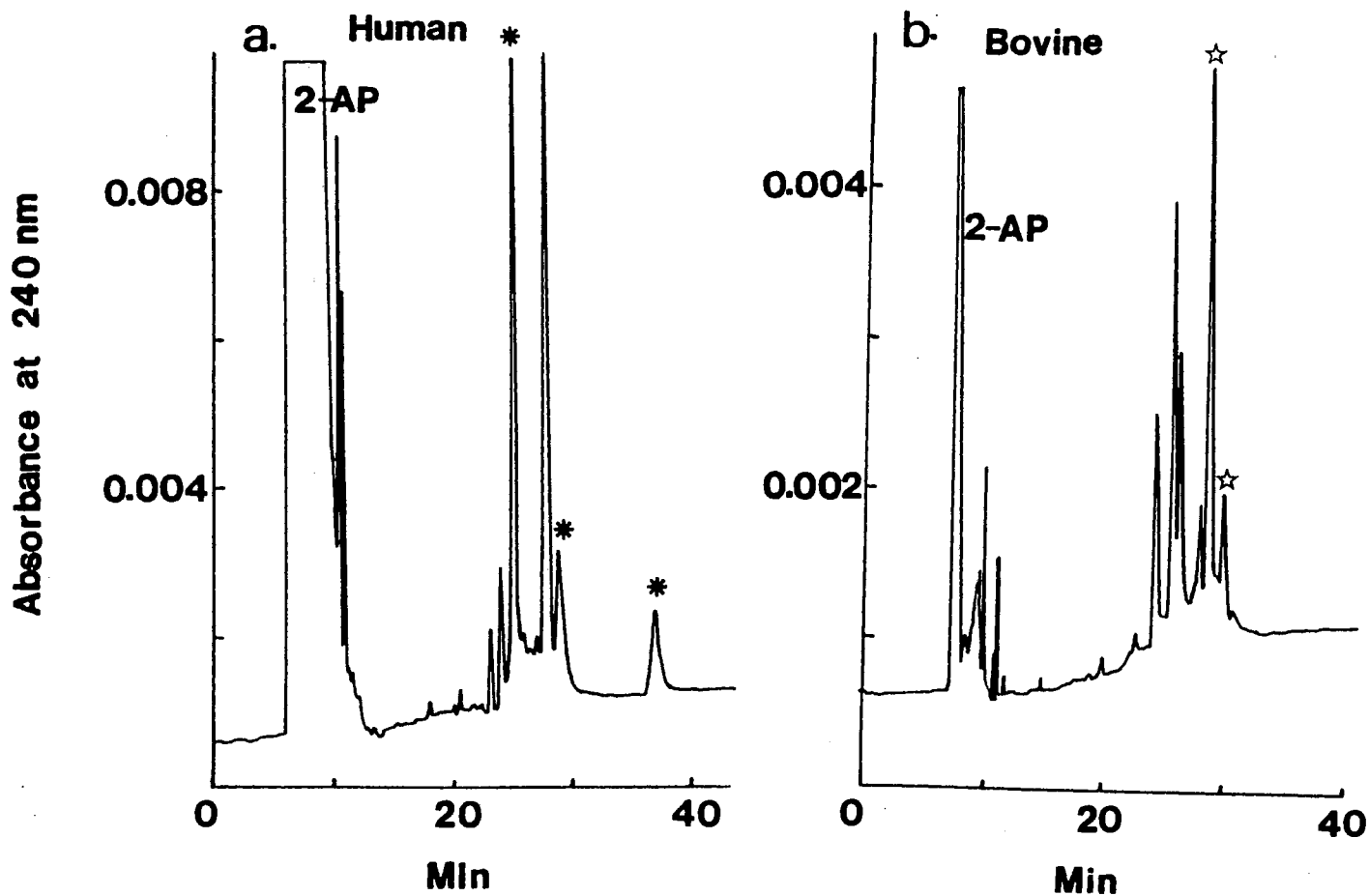
Figure 4. Capillary zone electrophoresis mapping of pyridylamino derivatives of human (a) and bovine (b) α_1-AG oligosaccharides. Capillary, fused-silica tube with hydrophilic coating on the inner walls, 45 cm (to the detection point), 80 cm total length x 50 m I.D.; electrolyte, 0.1 M phosphate solution, pH 5.0, containing 50 mM tetrabutylammonium bromide; running voltage, 18 kV; current 80 μA; injection by electromigration for 2 s at 18 kV.

To evaluate the potential of CZE in elucidating the difference in glycan structures, the oligosaccharides from bovine AGP were cleaved from the glycopeptides and derivatized with 2-AP as in the case of human glycoprotein. Subsequently, the derivatized bovine AGP oligosaccharides were analyzed by CZE using the same electrophoretic conditions as in Fig. 4a, and their corresponding CZE map is depicted in Fig. 4b. The map shows an elution pattern different from that of the oligosaccharides derived from the human glycoprotein. Both human and bovine AGPs have been found to have the same sialic acid, galactose and mannose content [25]. The major differences are such that 50% of the sialic acid in bovine AGP are N-glycolylneuraminic acid and the fucose content is very low [25]. These differences are accentuated by CZE mapping of both types of glycans; compare Figs. 4a and 4b.

In a recent report from our laboratory [10], we have demonstrated the capability of CZE in the separation of the PA derivatives of maltooligosaccharides. This study has shown the effectiveness of tetrabutylammonium bromide in affecting full separation of the oligomers. The organic salt was also useful in the separation of glycans. The comparison of Figs. 5a and 5b demonstrates the high selectivity and high resolution attained upon adding tetrabutylammonium bromide to the running electrolyte. Indeed, in the absence of the organic salt (Fig. 5a), the glycans were separated as two minor peaks and one large peak, whereas upon adding tetrabutylammonium bromide to the running electrolyte several additional peaks appeared in the map (Fig. 5b). The improvement in selectivity upon adding the organic salt to the running electrolyte can be explained by ion pair formation between the quaternary ammonium salt and the sialic acid of the carbohydrate chains and/or by hydrophobic interaction between the alkyl chains of the organic cation and the PA-oligosaccharides. On the other hand, the addition of tetrabutylammonium bromide increased the ionic strength of the running electrolyte, and as expected the residence time of the separated glycans increased. This is due to the reduction in electroosmotic flow [26], as a consequence of a decrease in both the thickness of the double layer and the ζ potential
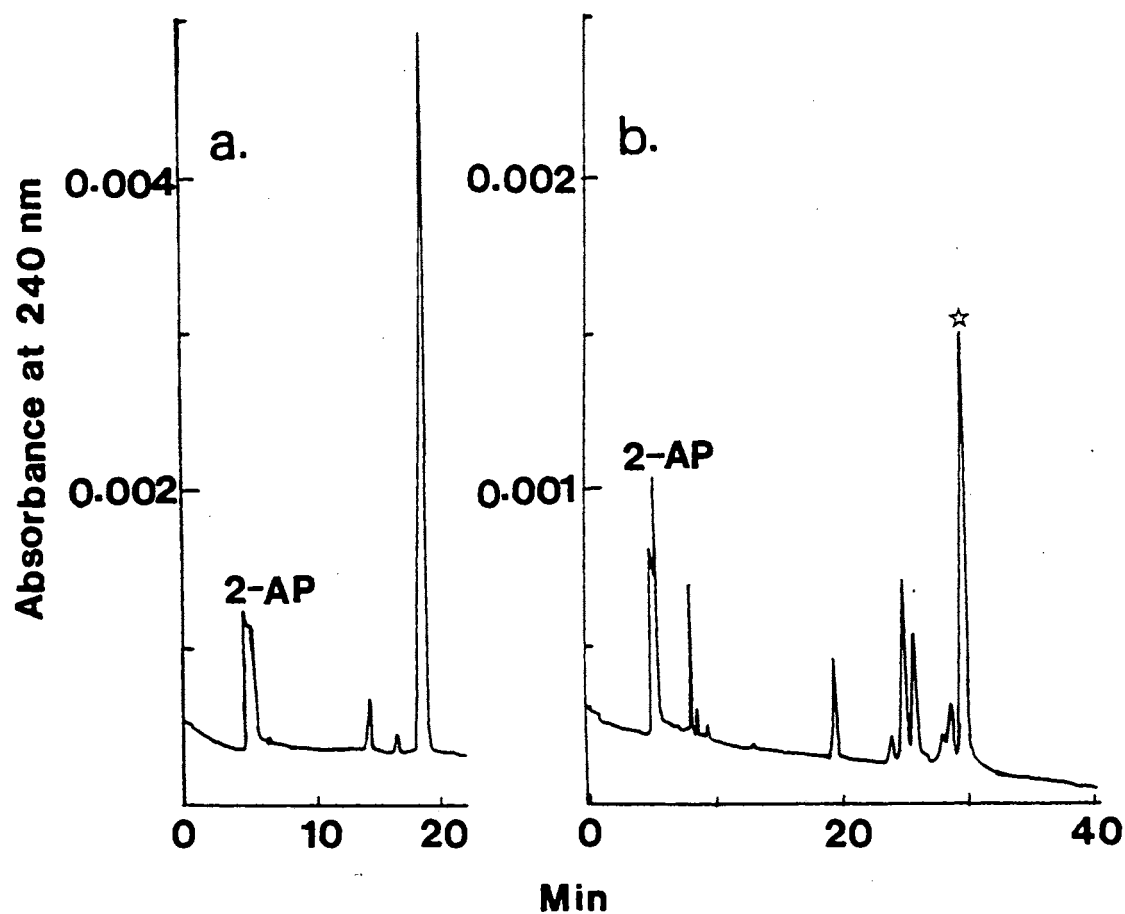
Figure 5. Capillary zone electrophoresis mapping of pyridylamino derivatives of bovine AGP oligosaccharides without (a) or with (b) 50 mM tetrabutylammonium bromide in the running electrolyte. Capillary, fused-silica tube with hydrophilic coating on the inner walls, 35 cm (to the detection point), 70 cm total length x 50 μm I.D.; electrolyte, 0.1 M phosphate solution, pH 5.0; running voltage, 15 kV; currents were ca. 55 μA in (a) and 90 μA in (b); injection by electromigration for 8 s at 15 kV.

of the capillary wall [27]. The decrease in the rate of the flow is more reflected on the late eluting zones than 2-AP. The migration time of 2-AP increased slightly by a factor of 1.08.

The comparison of electropherograms in Figs. 4b and 5b reveals the influence of the effective capillary length, i.e. the distance from the injection end to the detection point, on the separation of glycans at approximately the same field strength. The difference between these two electropherograms is such that the former was performed on a capillary of 80 cm total length and 45 cm effective length whereas the latter was obtained with a capillary of 70 cm total length and 35 cm separation distance. Although a better selectivity was obtained in Fig. 5b, especially for the fast migrating zones, the peaks of the electropherogram in Fig. 4b are sharper and concomitantly complete resolution was obtained for the last two peaks (indicated by stars in Figs. 4b and 5b).

As pointed out in the experimental section, the derivatization of the oligosaccharides was carried out in the presence of the protein or the peptide fragments without an isolation step of the cleaved oligosaccharides. Also the mixture containing the derivatized oligosaccharides, excess derivatizing agent and other components of the reaction mixture (see experimental) was applied directly to CZE. Since the remaining protein, peptides, and other components of the reaction mixture do not form an interference at the wavelength of detection (240 nm) and the excess 2-aminopyridine elute first in the electrophoretic run, solid phase extraction or other isolation procedures were not needed prior to CZE analysis. This represents an advantage for the method established here in terms of reduced time and labor. In addition, since no extraction step is involved, the approach used here eliminates sample loss.

The results of the above study demonstrate the effectiveness of the technique in the area of glycoconjugate research. In addition, since CZE uses nanoliter quantities for several runs, the small sample size most often encountered in the domain of glycans is not

a limiting factor and the technique can be explored further in the separation and analysis of carbohydrate chains of glycoproteins provided that authentic standards are available.

CZE Analysis of Monosaccharide Constituents of Glycoproteins

The above electrophoretic systems were also employed in the separation of the constituents of carbohydrate chains of glycoproteins using coated capillaries. The following standards: galactose, mannose, N-acetylglucosamine, N-acetylgalactosamine, and N-acetylneuraminic acid, were first derivatized with 2-aminopyridine. Following, the PA-sugars were electrophoresed on a coated capillary, using 0.1 M phosphate solution, pH 5.0, with or without tetrabutylammonium bromide. In the presence of 50 mM tetrabutylammonium bromide in the running electrolyte (see Fig. 6a), the PA derivatives of the monosaccharides were only separated into groups whereby, Man and Gal separated from GalNAc and GlcNAc and the PA derivative of NeuNAc being a zwitterion at pH 5.0 migrated at slower paste. In the absence of tetrabutylammonium bromide in the running electrolyte the acetylated (GlcNAc and GalNAc) and nonacetylated (Man and Gal) monosaccharides coeluted. The migration modulus, η, which is the ratio of the migration times in the presence to that in the absence of tetrabutylammonium bromide were 1.13 for Gal and Man, 1.16 for GlcNAc and GalNAc, and 1.04 for NeuNAc. Although, only group separation can be obtained when tetrabutylammonium bromide is added to the running electrolyte, the method established here may prove useful in the analysis of sugar residues of glycans cleaved by sequential exoglycosidases.

The full resolution of the PA derivatives of the standard monosaccharides was brought about by using uncoated capillary and borate-sugar complexes at high pH (see Fig. 6b), an electrophoretic system exploited earlier by Honda *et al* [28] for a series of monosaccharides and by Wallingford and Ewing for cathecolamines [29]. The anionic borate-sugar complexes created the charge for electrophoretic separation, as shown in Fig. 6b. It is well known that compounds containing *cis*-oriented hydroxyl groups form
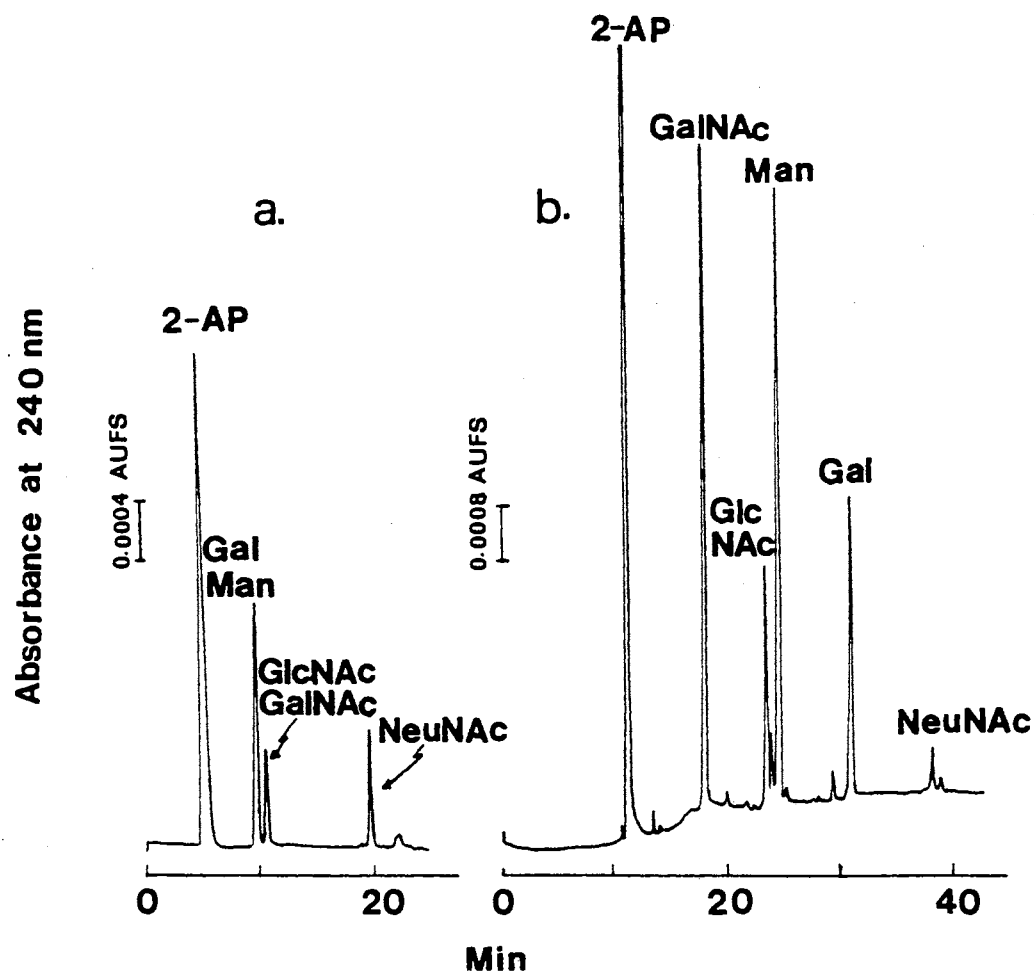
Figure 6. Capillary zone electrophoresis of pyridylamino derivatives of standard monosaccharides. Panel a: Capillary, fused-silica tube with hydrophilic coating on the inner wall, 35 cm (to the detection point), 70 cm total length x 50 μm I.D.; electrolyte, 0.1 M sodium phosphate solution, pH 5.0, containing 50 mM tetrabutylammonium bromide; running voltage, 15 kV; current was ca. 55 μA; injection by electromigration for 8 s at 15 kV. Panel b: Capillary, uncoated fused-silica tube, 50 cm (to the detection point),80 cm total length x 50 μm I.D.; electrolyte, 0.2 M sodium borate, pH 10.5; running voltage, 18 kV; current was 75 μA; injection by electromigration for 1 s at 10 kV.

stronger complexes with borate than those having *trans*-oriented diols [30]. Mannose has *trans*-diols at C3/C4 position, and therefore migrated faster than galactose which has *cis*-diols at the same location. This trend does not follow for GalNAc and GlcNAc, may be due to the presence of N-acetyl group which may affect the binding of borate. NeuNAc is a negatively charged species at high pH and the binding of borate to this molecule slows even further its migration.

Acknowledgement

References

1. P. D. Grossman, J. C. Colburn, H. H. Lauer, R.G. Nielsen, R. M. Riggin, G. S. Sittampalam and R. C. Rickard, *Anal. Chem.*, 61 (1989) 1186.

2. Z. Deyl, V. Rohlicek and M. Adam, *J. Chromatogr.*, 480 (1989) 371.

3. J. Frenz, S.-L. Wu and W. S. Hancock, *J. Chromatogr.*, 480 (1989) 379.

4. H. H. Lauer and D. McManigill, *Anal. Chem.*, 58 (1986) 166.

5. R. M. McCormick, *Anal. Chem.*, 60 (1988) 2322.

6. M. Bushey and J. W. Jorgenson, *J. Chromatogr.*, 480 (1989) 301.

7. A. S. Cohen, D. Najarian, J. A. Smith and B. L. Karger, *J. Chromatogr.*, 458 (1988) 323.

8. A. Cohen, D. Najarian, A. Paulus, A. Guttman, J. Smith and B. L. Karger, *Proc. Natl. Acad. Sci., U.S.A.,* 85 (1988) 9660

9. H. Drossman, J. A. Luckey, A. J. Kostichka, J. D'Cunha and L. M. Smith, *Anal. Chem.,* 62 (1990) 900.

10. W. Nashabeh and Z. El Rassi, J. Chromatogr., 514 (1990) 57.

11. K. Schmid in F.W. Putnam (Editor), *"The Plasma Proteins"*, 2nd edition, Vol. 1, Academic Press, New York, 1975, pp. 183-228.

12. K. Schmid, J.P. Binette, L. Dorland, F.G. Vliegenhart, B. Fourmet, and J. Montreuil, *Biochim. Biophys. Acta,* 581 (1979) 356.

13. S. Hase, S. Hara and Y. Matsushima, J. Biochem., 85 (1979) 217.

14. W. Nashabeh and Z. El Rassi, *J. Chromatogr.,* 559 (1991) 367.

15. P. O. Larsson, M. Glad, L. Hansson, M.-D. Hansson, S. Ohlson and K. Mosbach, *Adv. Chromatogr.*, 21 (1982) 41.

16. C. B. Kasper, in S. B. Needleman (Editor), *"Protein Sequence Detrmination"*, Spring Verlag, Berlin, New York, 1975, p. 114.

17. A. L. Tarentino, C. M. Gomez and T. H. Plummer, *Biochemistry*, 24 (1985) 4665.

18. W. C. Baker and F. W. Putnam in F. W. Putnam (Editor), *"The Plasma Proteins"*, 2nd edition, Vol. 4, Academic Press, New York, 1984, p. 394.

19. F. W. Putnam, in F. W. Putnam (Editor), *"The Plasma Proteins"*, 2nd edition, Vol. 4, Academic Press, New York, 1984, pp. 74-76.

20. E. Chandrasekaran, M. Davila, D. Dixon and J. Mendicino, Cancer Res., 44 (1984) 1557.

21. D. Malamud and J. W. Drysdale, *Anal. Biochem.*, 86 (1978) 620.

22. I. Nicollet, J. Lebreton, M. Fontaine and M. Hiron, *Biochim. Biophys. Acta*, 668 (1981) 235.

23. J. Montreuil, S. Bouquelet, H. Debray, B. Fournet, G. Spik and G. Strecker, in M. F. Chaplin and J.F. Kennedy (Editors), *"Carbohydrate Analysis, a Practical Approach"*, IRL Press, Oxford,1986, p.161.

24. H. Yoshima, A. Matsumoto, T. Mizuochi, T. Kawasaki and A. Kobata, *J. Biol. Chem.*, 256 (1981) 8476.

25. R. Got, R. Bourrillon and P. Cornillot, *Biochim. Biophys. Acta*, 58 (1962) 126.

26. M. M. Bushey and J. W. Jorgenson, *J. Chromatogr.*, 480 (1989) 301.

27. C. J. Van Oss, *Sep. Purif. Mehtods*, 8 (1979) 119.

28. S. Honda, S. Iwase, A. Makino and S. Fujiwara, *Anal. Biochem.*, 176 (1989) 72.

29. R. A. Wallingford and A. G. Ewing, *J. Chromatogr.*, 441 (1988) 299.

30. H. L. Weith, J. L. Wiebers and P. T. Gilham, *Biochemistry*, 9 (1970) 4396.

CHAPTER VIII

CAPILLARY ZONE ELECTROPHORESIS OF LINEAR
AND BRANCHED OLIGOSACCHARIDES*

Abstract

The electrophoretic behavior of derivatized linear and branched oligosaccharides from various sources was examined in capillary zone electrophoresis with polyether coated fused-silica capillaries. Two UV absorbing (also fluorescent) derivatizing agents (2-aminopyridine and 6-aminoquinoline) were utilized for the electrophoresis and sensitive detection of neutral oligosaccharides, e.g., N-acetylchitooligosaccharides, high-mannose glycans and xyloglucan oligosaccharides. The oligosaccharides labelled with 6-aminoquinoline yielded eight times higher signal than those tagged with 2-aminopyridine. Plots of logarithmic electrophoretic mobilities of labelled N-acetylchitooligosaccharides with 6-aminoquinoline or 2-aminopyridine versus the number of sugar residues in the homologous series yielded straight lines in the size range studied, the slopes of which were independent of the tagging functions. The slopes of these lines are referred to as the N-acetylglucosaminyl group mobility decrement. The oligosaccharides were better resolved in the presence of tetrabutylammonium bromide in the running electrolyte. Furthermore, the electrophoretic mobilities of branched oligosaccharides were indexed with respect to linear homooligosaccharides, an approach that may prove valuable in correlating and predicting the mobilities of complex oligosaccharides.

Introduction

The separation of carbohydrates by electrophoresis have often required the *in situ* conversion of these compounds into charged species. Early investigations on carbohydrate electrophoresis described anionic complexes with sodium borate [1], sulphonated benzene boronic acid [2], sodium germanate [3], sodium stannate [1] or sodium tungstate [4]. Cationic complexes of carbohydrates with lead acetate [5], or cations of the alkali and alkaline earth metals [5] were also described for the electrophoresis of neutral carbohydrates. Furthermore, because of the ionization of the hydroxyl groups of the sugars at high pH, sodium hydroxide was also useful for the electrophoresis of neutral carbohydrates [6]. These buffer systems are expected to find their way to the capillary zone electrophoresis of sugars. In fact, very recently capillary zone electrophoresis systems based on borate complexes for mono- and oligosaccharides have been described [7,8].

Another difficulty in the analysis of sugars is the lack of chromophores in their structures. This can be overcomed by precolumn derivatization [7-11], or by indirect detection [12]. However, a precolumn derivatization that supplies both the charge and the chromophore for the electrophoresis and the sensitive detection, respectively, is preferred.

In recent reports from our laboratory, we have demonstrated the potential of CZE in the separation of 2-pyridylamino derivatives of maltooligosaccharides [9] and complex-type glycans cleaved from glycoproteins [10]. In the present article, the scope of applications of CZE was extended to the separation and determination of the homologous series of N-acetylchitooligosaccharides, the branched xyloglucan oligosaccharides form cotton cell walls, and the high-mannose glycans of ribonuclease B. The electrophoretic mobility of the 2-pyridylamino derivatives of xyloglucan fragments, was indexed to that of the homologous series, which permitted the evaluation of the contribution of sugar residues and degree of branching to the electrophoretic mobility of the derivatized

xyloglucan oligosaccharides. In addition, the potential of 6-aminoquinoline as a new tagging agent that provides both the charge and the center for detection was investigated.

Experimental

Instruments

The instrument for capillary electrophoresis was assembled in-house from commercially available components. It comprised two high-voltage power supplies of positive and negative polarity from Glassman High Voltage (Whitehouse Station, NJ, U.S.A.) and a Linear (Reno, NV, U.S.A.) Model 200 UV-Vis variable wavelength detector equipped with a cell for on-column capillary detection. The detection wavelength was set at 240 nm for sensing the derivatized oligosaccharides. The electropherograms were recorded with a Shimadzu computing integrator (Columbia, MD, U.S.A.) equipped with a floppy disk drive and a CRT monitor.

The absorption spectra of the derivatizing agents, i.e., 2-aminopyridine and 6-aminoquinoline were performed on a UV-Vis spectrophotometer (Model UV-160, Shimadzu) by scanning from 200 to 310 nm.

Capillary Columns

Fused-silica capillary columns of 50-μm I.D. and 365-μm O.D. were obtained from Polymicro Technology (Phoenix, AZ, U.S.A.). All capillaries used in this study were coated in-house with an interlocked polyether coating according to previously described procedures [13]. The running electrolyte was renewed after each run. To ensure reproducible separations the capillary column was flushed successively with fresh buffer, water, methanol, water, and again running buffer. The capillary was allowed to equilibrate for 10 minutes before each injection.

Reagents and Materials

Xyloglucan oligosaccharides were obtained from cotton cell walls as described earlier [14]. They were supplied as 2-pyridylamino derivatives by Dr. A. Mort from the Department of Biochemistry. N-acetylchitooligosaccharide standards having a degree of polymerization (d.p.) from 2 to 6 were from Seikagaku Kocyo Co. (Tokyo, Japan). High-mannose oligostandard, $(GlcNAc)_2$-Man_5, was purchased from Dionex (sunnyvale, CA, U.S.A.). Ribonuclease B (RNase B), TPCK-treated trypsin, N-acetylglucosamine (GlcNAc), 2-aminopyridine (2-AP), trizma base and Brij 35 were obtained from Sigma (St. Louis, MO, U.S.A.). Peptide-N-glycosidase F (PNGase F) from *Flavobacterium meningosepticum* was obtained from Boehringer Mannheim (Idianapolis, IN, U.S.A.). Mercaptoethanol, sodium cyanoborohydride, 6-aminoquinoline (6-AQ), trifluoroacetic acid (TFA) and tetrabutylammonium bromide (Bu_4N^+) were from Aldrich (Milwaukee, WI, U.S.A.). Reagent grade sodium phosphate monobasic and dibasic, phosphoric acid, hydrochloric acid, acetic acid, sodium hydroxide, calcium chloride, ethylenediaminetetraacetic acid disodium salt (EDTA), and HPLC grade methanol and acetonitrile were obtained from Fisher Scientific (Pittsburgh, PA, U.S.A.). Deionized water was used to prepare the running electrolyte. All solutions were filtered with 0.2-μm UniPrep syringeless filters obtained from Genex Corporation (Gaithersburg, MD, U.S.A.) to avoid column plugging.

Cleavage of High-Mannose Glycans

Bovine RNase B was first digested with TPCK-treated trypsin using a 10 mM Tris buffer containing 100 mM ammonium acetate and 0.1 mM calcium chloride, pH 8.3, at a trypsin substrate ratio of 1:100 and a temperature of 37 °C [15]. Trypsin was added again after 2 hours and the digestion was stopped after a total of 4 hours by addition of phosphoric acid. Thereafter, the whole digest was desalted by passing it on a Bakerbond

wide-pore octadecyl-silica column (250 x 4.6 mm) equilibrated with water at 0.05% (v/v) trifluoroacetic acid (TFA). The bound materials were eluted stepwise with 80% acetonitrile in water (v/v) at 0.05% TFA (v/v). The pooled fraction was evaporated to dryness using a SpeedVac Concentrator (from Savant Instrument Co., Farmingdale, NY, U.S.A.). The dried materials were then dissolved in 20 mM phosphate buffer containing 2 mM EDTA, 1% (v/v) mercaptoethanol, and 0.1% (w/v) Brij 35, pH 7.5. To this solution 3 units of peptide-N-glycosidase F were added, and the incubation was maintained at 37°C for 24 hours [16]. Thereafter, the mixture was evaporated to dryness with a Savant SpeedVac Concentrator. The dried materials containing the cleaved oligosaccharides, the peptide fragments, and other reagents employed in the incubation step was used as is without a sample clean up prior to the derivatization of its oligosaccharide components.

Derivatization of Oligosaccharides

Commercially available N-acetylchitooligosaccharides were tagged with 2-aminopyridine (2-AP) or 6-aminoquinoline (6-AQ) whereas the oligosaccharides cleaved from bovine ribonuclease B were derivatized with 2-AP, at their reducing termini *via* reductive amination according to the equations depicted in the next page, where N-acetylglucosamine is taken as a typical example. To that end a 0.26 M aqueous solution of 2-AP or 6-AQ was titrated to pH 5.8 with glacial acetic acid. Thereafter, sodium cyanoborohydride was added at a concentration of 20 mg/mL just prior to the addition of the carbohydrates. The reaction mixtures were incubated overnight at 70 °C. Following, the reaction mixtures containing the derivatized oligosaccharides were evaporated to dryness. The dried materials thus obtained were dissolved in water and then applied to capillary electrophoresis without any sample clean up from excess derivatizing agent and other components of the reaction mixture.
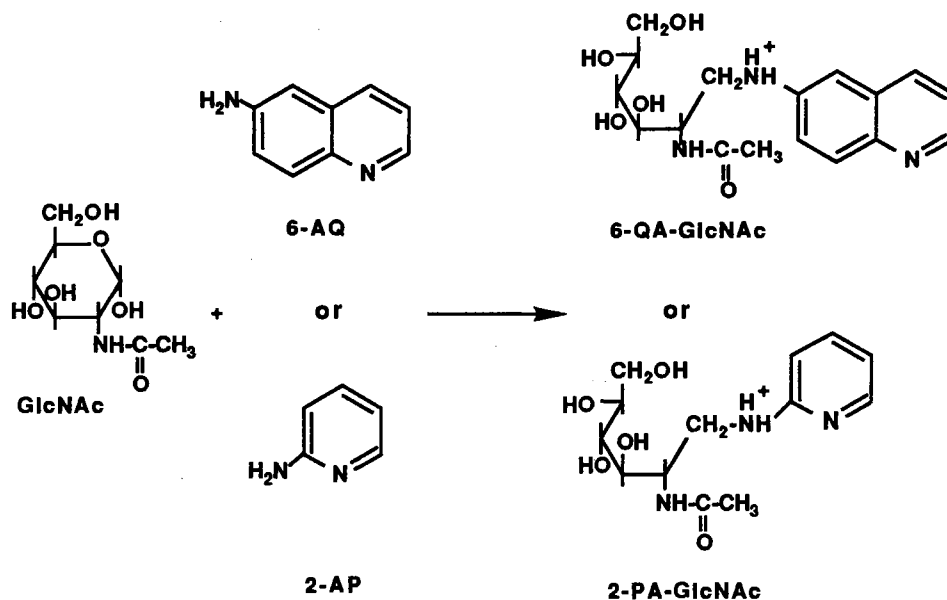
Results and Discussion

The electrophoretic behavior of derivatized linear and branched oligosaccharides from various sources was examined using fused-silica capillaries with hydrophilic coating. The results obtained with 2-pyridylamino derivatives were compared to those of 6-quinolylamino derivatives. A mobility indexing system for branched oligosaccharides was established with respect to linear homooligosaccharides.

CZE of Derivatized N-acetylchitooligosaccharides

N-Acetylglucosaminyl group mobility decrement. Figure 1A and B illustrates the high resolution separation of 2-pyridylamino and 6-quinolylamino derivatives of N-acetylchitooligosaccharides, respectively. It was brought about by adding tetrabutylammonium bromide (Bu_4N^+) to the running electrolyte, a medium that we have reported earlier for the separation of maltooligosaccharides [9] and complex glycans
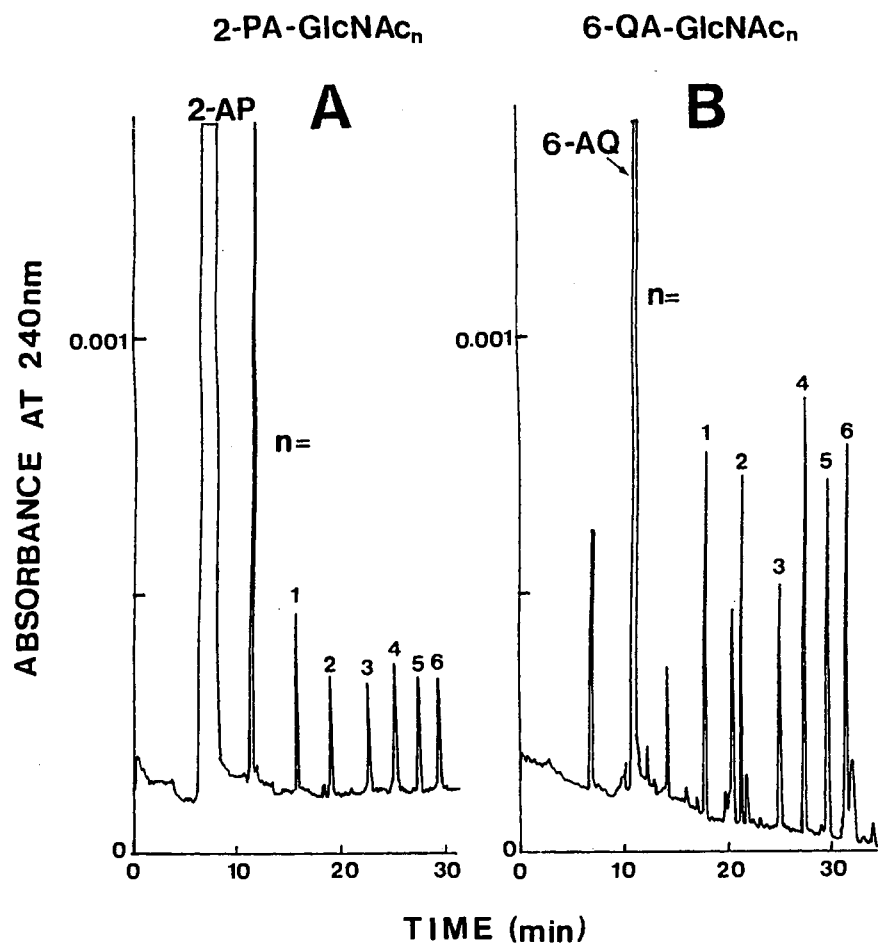
Figure 1. Electropherograms of 2-pyridylamino (A) and 6-quinolylamino (B) derivatives of N-acetylchitooligosaccharides. Capillary, fused-silica tube with polyether interlocked coating on the inner walls, 50 cm (to the detection point), 80 cm total length x 50 μm I.D.; electrolyte, 0.1 M phosphate solution containing 50 mM tetrabutylammonium bromide, pH 5.0; running voltage, 18 kV. Symbols: 2-AP, 2-aminopyridine; 6-AQ, 6-aminoquinoline.

cleaved from glycoproteins [10]. To further characterize the effect of the organic salt on the separation of derivatized oligosaccharides, the 2-pyridylamino derivatives of N-acetylchitooligosaccharides (2-PA-GlcNAc$_n$) were electrophoresed over a wide range of pH and Bu$_4$N$^+$ concentrations.

Figure 2 illustrates typical plots of the logarithmic electrophoretic mobility, log μ, of 2-AP-GlcNAc$_n$ versus the number of N-acetylglucosamine residues (GlcNAc) in the homologous series at different pH. These plots were linear in the size range studied. It has to be noted that the derivatized oligosaccharides carry the same net positive charge, and therefore the charge to size ratio decreases with the number of GlcNAc residues in the homologous series. As can be seen in Fig. 2, the electrophoretic mobility decreased with the pH as the derivatized oligosaccharides become less positively charged. As a result, the slope of the straight lines, which are referred to as the "N-acetylglucosaminyl group mobility decrement", δ_{GlcNAc}, increased in absolute value with increasing the pH in the range studied. However, the resolution between the homologs decreased as the pH increased due to an increase in the electroosmotic flow of the medium with increasing pH.

As expected, the 6-quinolylamino derivatives of N-acetylchitooligosaccharides (6-QA-GlcNAc$_n$) exhibited behavior similar to 2-PA-GlcNAc$_n$. Plots of log μ vs the number of GlcNAc residues of the homologous series labelled with 6-AQ, were also straight lines, and their slopes were identical to those obtained with 2-PA-GlcNAc$_n$ under otherwise identical conditions. This is to say that the δ_{GlcNAc} is the same regardless of the tagging functions. Note that both derivatizing agents have similar characteristic charges.

To study the effect of Bu$_4$N$^+$ on the electrophoretic behavior of derivatized N-acetylchitooligosaccharides, 2-PA-GlcNAc$_n$ were analyzed in the presence of various amounts of the organic salt in 0.1 M phosphate solutions, pH 5.0. Upon adding the salt to the running electrolyte, the migration time of the homologous series increased monotonically with increasing the salt concentration in the range studied. The plots of log μ versus the number of GlcNAc residues at different concentrations of Bu$_4$N$^+$ in the
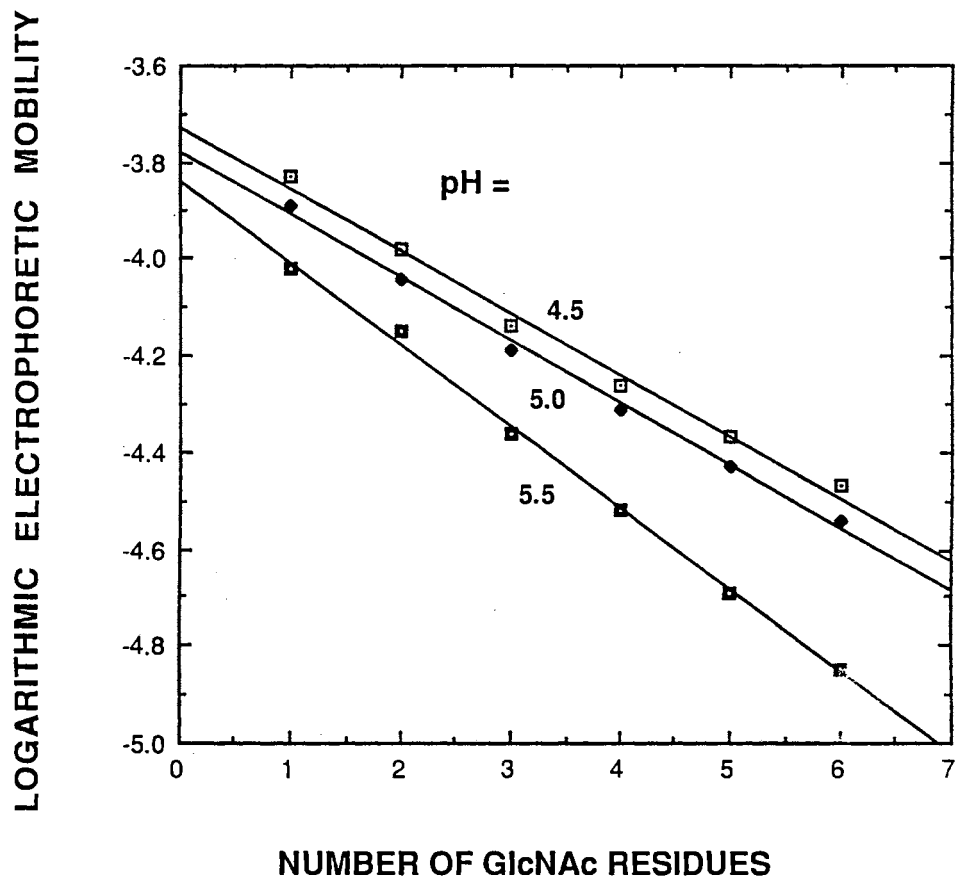
Figure 2. Plots of logarithmic electrophoretic mobility versus the number of GlcNAc residues in the 2-PA-GlcNAc$_n$ homologous series at various pH. Electrolytes, 0.1 M sodium phosphate solutions containing 50 mM tetrabutylammonium bromide. Other conditions are as in Fig. 1.

running electrolyte were also linear. Their slopes represent the " N-acetylglucosaminyl group mobility decrement", δ_{GlcNAc}, and are summarized in table I. The increase in the values of δ_{GlcNAc} with increasing Bu_4N^+ concentration reflects an increase in the resolution between the homologous series. It can be seen in table I that the addition of only 10 mM of the organic salt to the running electrolyte was enough to yield an absolute increase of about 28% in the value of δ_{GlcNAc}, while 50 mM Bu_4N^+ exhibited only 48% increase in the absolute value of δ_{GlcNAc}.

TABLE I.

LOGARITHMIC N-ACETYLGLUCOSAMINYL GROUP MOBILITY DECREMENT ,δ_{GlcNAc}, AS ESTIMATED FROM THE SLOPE OF THE LOGARITHMIC ELECTROPHORETIC MOBILITY VERSUS THE NUMBER OF GlcNAc RESIDUES 2-PA-GlcNAc$_n$ HOMOLOGOUS SERIES.

Electrolytes: 0.1 M phosphate solution, pH 5.0, at various tetrabutylammonium bromide concentration.

$[Bu_4N^+]$ mM	δ_{GlcNAc}	Correlation coefficient
0	-0.082	0.981
10.0	-0.105	0.990
30.0	-0.109	0.989
50.0	-0.122	0.990

To better assess the effect of the organic salt, the electroosmotic flow was measured at each salt concentration using methanol as the inert tracer. Typical results

obtained with N-acetylchitohexaose are depicted in Fig. 3 by plots of the overall and electrophoretic mobilities of this sugar as well as the electroosmotic flow versus the concentration of the organic salt in the running electrolyte. As shown in Fig. 3, the decrease in the net mobility of the various homologs could not be only accounted for by the slight decrease in the electroosmotic flow at higher salt concentration, but due to the continuous decrease in the electrophoretic mobilities of the 2-PA-GlcNAc$_n$ with increasing the ionic strength of the running buffer [17-19].

Comparison of the derivatizing agents. Although the derivatization with 2-aminopyridine is quite reproducible and allows the electrophoresis of carbohydrates by CZE, the 2-pyridylamino derivatives of mono- and oligosaccharides exhibited limited detection sensitivity in the UV. In search for a more sensitive tagging agent, the performance of 6-AQ, a UV absorbing and fluorescent tag, was investigated in this study and compared to that of 2-AP using an N-acetylchitooligosaccharides mixture ranging in size from N-acetylglucosamine to N-acetylchitohexaose as model sugar substrates.

Returning to Fig. 1A and B, the 6-quinolylamino derivatives of the oligosaccharides (6-QA-GlcNAc$_n$) exhibited slightly higher migration times than that of 2-PA-GlcNAc$_n$. This is attributed to the lower pK$_a$ value of 6-AQ (pK$_a$ = 5.64) as compared to 2-AP (pK$_a$ = 6.71). Also, 6-AQ has a slightly higher molecular size. As can be noted from Fig. 1A and B , the homologs tagged with 6-AQ showed almost 2 to 3 times higher detection signal than those labelled with 2-AP as estimated from peak height and area calculations from six consecutive runs.

To further characterize the derivatization reactions under investigation, spectral analysis was carried out on both tagging agents and their sugar derivatives. The absorption spectrum of 2-AP (see experimental) revealed two maxima at 229 and 290 nm with the most intense being at 229 nm, while the 6-AQ spectrum showed an absorption band with a maximum at 242 nm. Due to the difficulty of obtaining the derivatized
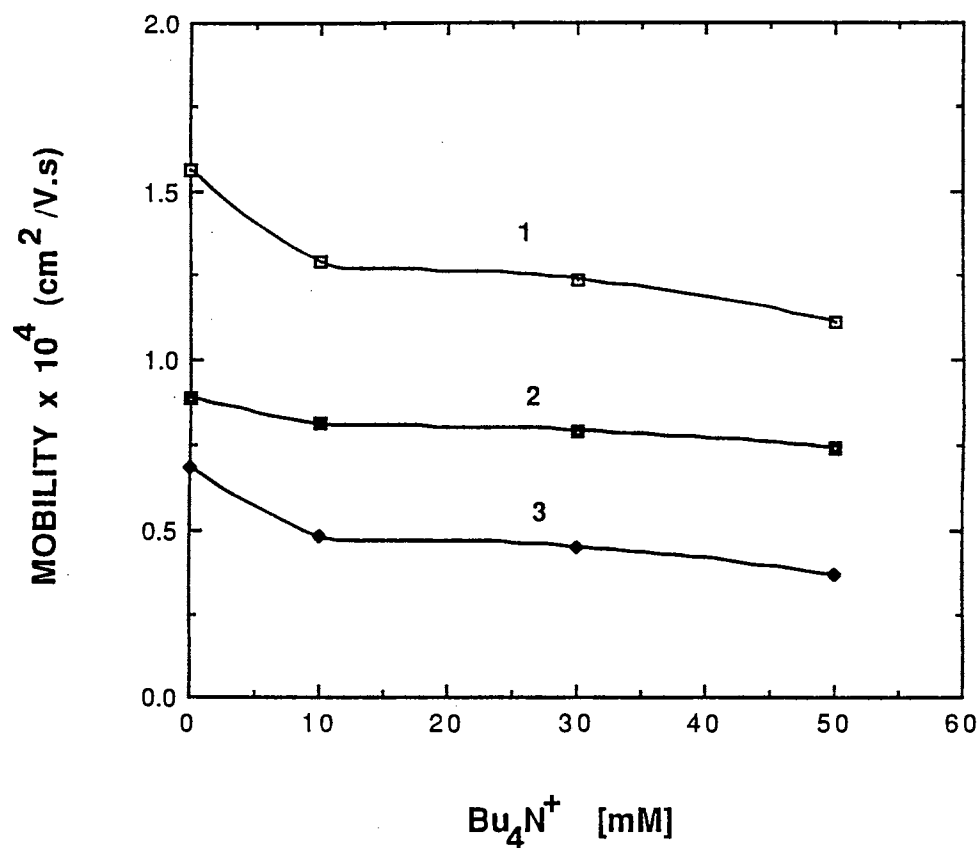
Figure 3. Plots of overall and electrophoretic mobilities of the 2-pyridylamino derivative of N-acetylchitohexaose as well as electroosmotic flow at various concentrations of tetrabutylammonium bromide in the running electrolyte, pH 5.0. Symbols: 1, overall; 2, electroosmotic; 3, electrophoretic. Other conditions are as in Fig. 1.

oligosaccharides in a highly pure form, their absorbance were measured from the electropherograms obtained from various electrophoretic runs. Typical results obtained with 2-PA-GlcNAc$_3$ and 6-QA-GlcNAc$_3$ are depicted in Fig. 4 by plots of the absorbance at maximum peak heights as a function of the detection wavelength in the range 210 to 280 nm in an increment of 10 nm. The λ_{max} for both the 2-pyridylamino and 6-quinolylamino derivatives shifted toward higher wavelengths than the pure derivatizing agents. The λ_{max} of 2-PA-GlcNAc$_n$ is around 240 nm and that of 6-AQ-GlcNAc$_n$ is at ca. 270 nm. As can be seen in Fig. 4, under the same electrophoretic conditions and in the wavelength range investigated, the 6-quinolylamino derivatives exhibited higher absorbance. When compared at their λ_{max}, 6-QA-GlcNAc$_n$ yielded a detection signal 8 times higher than that of the sugar tagged with 2-AP. The derivatization procedure described here may prove useful for fluorescence detection. In fact, 6-aminoquinoline possess ideal fluorescence properties [20] in the sense that its excitation wavelength (355 nm) is far removed from its emission wavelength (550 nm) and is therefore expected to give low detection limits with fluorescence detector.

CZE Mapping of 2-AP-Xyloglucan Oligosaccharides

Mapping. Xyloglucans are branched oligosaccharides having a backbone identical to that of cellulose (i.e. the $(1 \rightarrow 4)$ β-linked D-glucan) with various side chains comprising xylose, galactosyl-xylose, fucosyl-galactosyl-xylose and seldom arabinosyl-xylose. When digested with cellulase, the backbone of xyloglucans are cleaved after any glucosyl residue with no side chain linked to it. Therefore, the fragments obtained are reflective of xyloglucan branching.

The 2-pyridylamino derivatives of the xyloglucan fragments (2-PA-XG) obtained by cellulase digestion were first analyzed by reversed phase chromatography as reported earlier [14]. The collected fractions whose structures were assessed tentatively by liquid-secondary-ion mass spectrometry and previously proven structures were then analyzed by
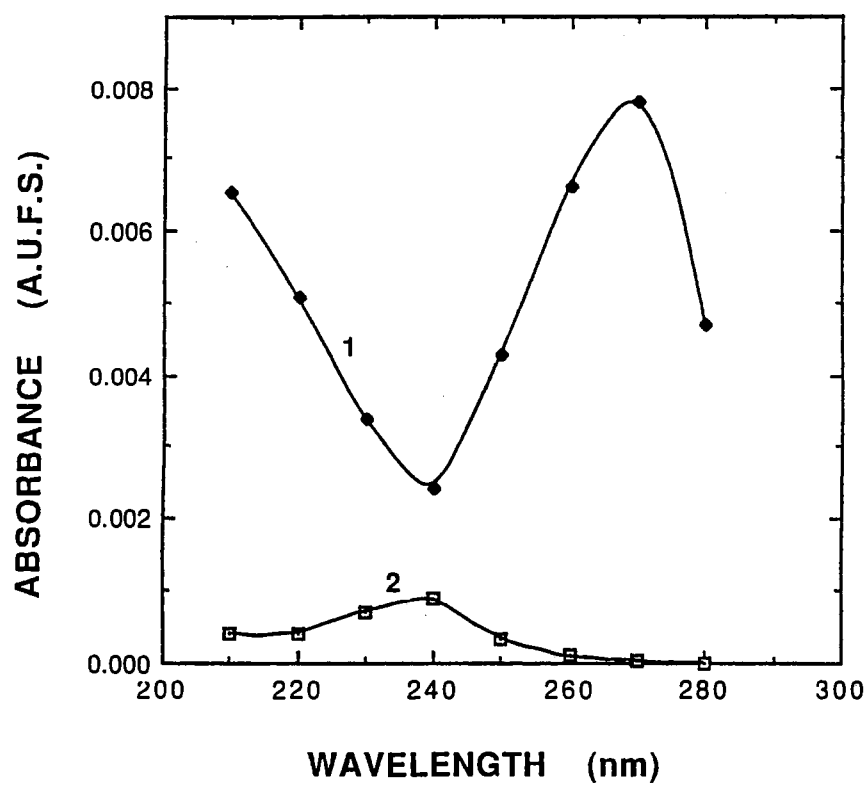
Figure 4. Plots of absorbance of 6-QA-GlcNAc$_3$ in (1) and 2-PA-GlcNAc$_3$ in (2) versus the detection wavelength. Conditions are as in Fig. 1, except electrolyte was 0.1 M sodium phosphate solution at pH 5.0.

CZE using the electrophoretic system described for the homologous series. Figure 5 is a typical electropherogram of a mixture reconstituted by mixing aliquots from selected RPC fractions. It was performed on a fused-silica capillary with a polyether interlocked coating using 0.1 M phosphate containing 50 mM Bu_4N^+ at pH 4.75. As expected the elution pattern in CZE was different from that in RPC. The peak numbering on the electropherogram (see Fig. 5) reflects the elution order obtained in RPC. In CZE the elution order was mainly governed by the number of sugar residues and the degree of branching, whereas in RPC the elution order was mainly influenced by the size of the oligosaccharide and the hydrophobic character of the sugar residues. For instance, fragment 4 which is smaller in size than fragment 3 was more retarded on the RPC column. This may be attributed to the presence of fucosyl residue in structure 3, which is more hydrophobic than any other sugar residues in the molecule. The same reasoning can explain the elution order for fragments 6 and 7. In CZE, due to the fact that all 2-PA-XG fragments possess the same charge they migrated in the order of increasing size as the charge to mass ratio decreased. However, for the same number of residues but with slight differences in molecular weight the less branched oligosaccharides eluted earlier than the more branched one. In fact, structure 4, which has a slightly higher molecular weight than structure 2 eluted first. This may be explained by the fact that structure 2 is doubly branched as opposed to fragment 4 which is singly branched. The same behavior was observed for fragments 7 (doubly branched) and 5 (triply branched). Thus, as the extent of oligosaccharide branching increased, the electrophoretic mobility decreased.

Figure 6 illustrates the high separation efficiency of acetylated xyloglucan oligosaccharides generated by a slightly different method [14] than that used to generate the fragments used in Fig. 5. The average plate count per meter was about 225,000 as calculated from the two major fragments 5 and 8. Both structures 8 and 8a are nonasaccharides with the same extent of branching. The only difference is that fragment 8a has an acetyl substitution at the galactosyl residue that is not present in structure 8. This
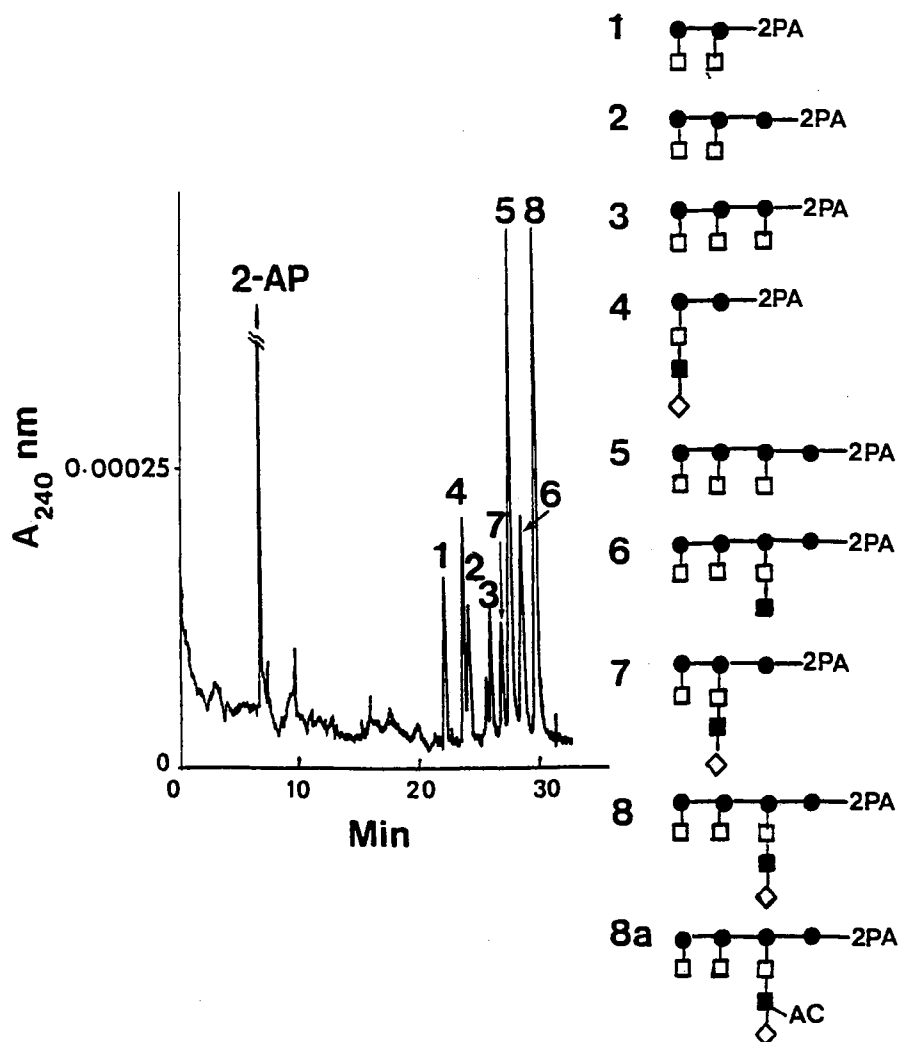
Figure 5. Capillary zone electrophoresis mapping of the 2-pyridylamino derivatives of xyloglucan oligosaccharides reconstituted by mixing aliquots from fractions collected during various chromatographic runs. Capillary, fused-silica tube with polyether interlocked coating on the inner walls, 50 cm (to the detection point), 80 cm total length x 50 μm I.D.; electrolyte, 0.1 M sodium phosphate solution containing 50 mM tetrabutylammonium bromide, pH 4.75; running voltage, 20 kV. Symbols: 2-AP, 2-aminopyridine; ●, glucose, □, xylose; ■, galactose;◇, fucose; Ac, acetyl group.
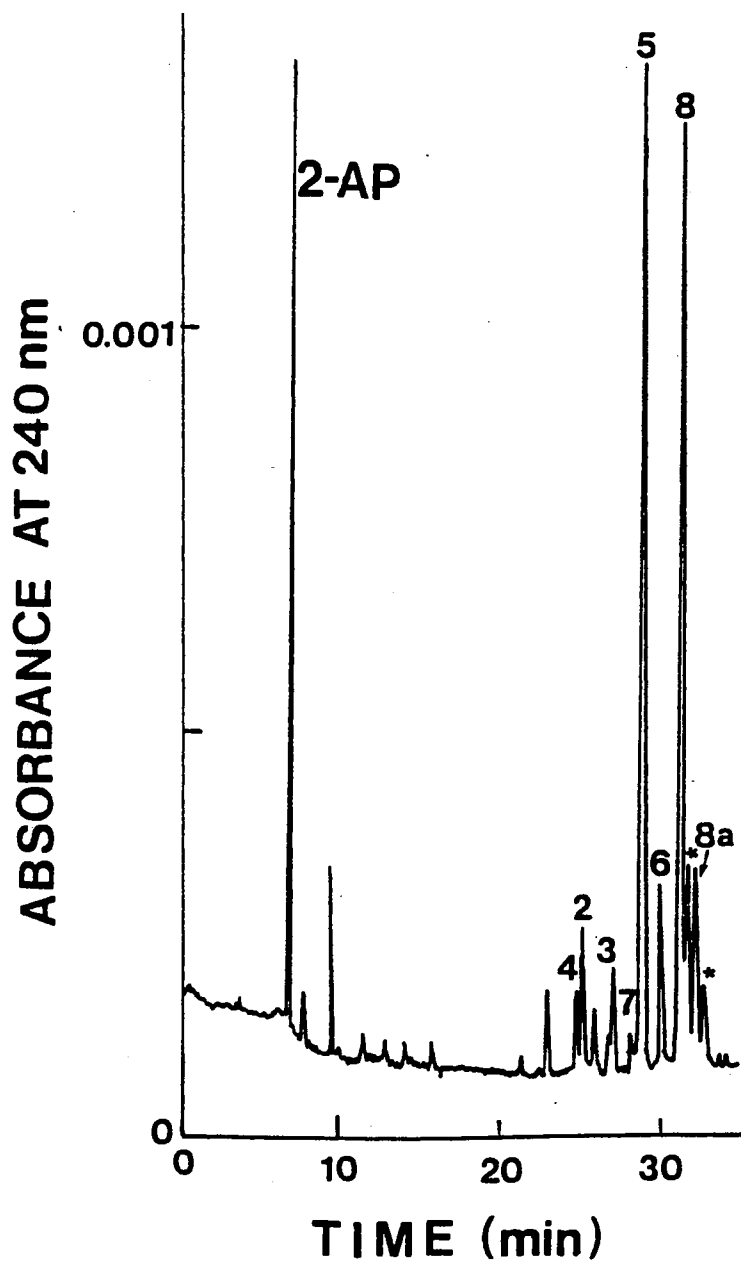
Figure 6 . Capillary zone electrophoresis mapping of 2-pyridylamino derivatives of acetylated xyloglucan oligosaccharides from cotton cell walls. For the structure of fragment 8a, see Fig. 5. Conditions are as in Fig. 5.

once more shows the high resolving power of CZE in recognizing small differences between the various xyloglucan fragments. The peaks labelled with asterisks may be attributed to other oligosaccharides present in the mixture.

Mobility indices. To interpret the electrophoretic behavior of the various 2-PA-XG and to quantitatively describe the effects of the various sugar residues on the electrophoretic mobility, we have attempted the indexing of the electrophoretic mobilities of the branched xyloglucan oligosaccharides with respect to the linear 2-PA-GlcNAc$_n$. In this regard, the mobility indices, M.I., of the 2-AP-XG fragments were calculated using the following equation:
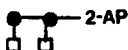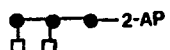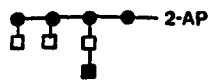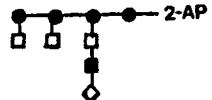
$$M.I.= 100n + 100\left(\frac{\log \mu_s - \log \mu_{n+1}}{\log \mu_n - \log \mu_{n+1}}\right)$$

where μ_s is the electrophoretic mobility of the 2-AP-XG solute, μ_n and μ_{n+1} are the electrophoretic mobilities for the two homologs with n and $n+1$ repetitive units which eluted before and after the xyloglucan fragment, respectively. This indexing is similar to that of Kovats retention indices for gas-liquid chromatography [21]. Table II compiles the values of mobility indices of selected 2-AP-XG fragments with respect to the homologous series, 2-AP-GlcNAc$_n$. In this table the mobility indices, M.I. were averaged over the pH range 4.5 to 5.25 and for Bu$_4$N$^+$ concentrations from 0 to 50 mM. The difference in mobility indices between an adjacent pair of 2-AP-XG fragments, ΔM.I., is referred to as the group mobility index decrement contributed by a sugar residue added to a parent oligosaccharide molecule. This value was practically the same over the pH range or salt concentrations studied for a given pair of derivatized xyloglucan fragments. Based on these findings, the M.I.'s were averaged as indicated in group III in Table II. As can be seen, the xyloglucan fragment 1 eluted between the homologs of d.p. 2 and 3, respectively. Fragment 2, which has an additional glucosyl residue in the backbone chain of the oligosaccharide, exhibited a mobility index decrement of 52 and eluted between the

TABLE II

MOBILITY INDICES (M.I.) AND GROUP MOBILITY INDEX DECREMENT (ΔM.I.) OF VARIOUS 2-PA-XG FRAGMENTS WITH RESPECT TO 2-PA-GlcNAc$_n$

See text for calculations. Group I, average values obtained with 0.1 M sodium phosphate solutions, pH 5.0, at 0, 10, 30 or 50 mM tetrabutylammonium bromide; group II, average values obtained with 0.1 M sodium phosphate solutions containing 50 mM tetrabutylammonium bromide at pH 4.50, 4.75, 5.00 or 5.25; group III, overall average. Symbols: ●, glucose, □, xylose; ■, galactose; ◇, fucose.

Xyloglucan	Group					
	I		II		III	
	M.I.	ΔM.I.	M.I.	ΔM.I.	M.I.	ΔM.I.
●●—2-AP (□□)	267.5 ± 5.6	51.5 ± 4.0	277.0 ± 7.8	53.5 ±4.0	272.3 ± 4.8	52.5 ± 2.8
●●●—2-AP (□□)	319.0 ± 9.0	57.1 ± 1.2	330.5 ± 10.9	53.7 ± 3.0	324.8 ± 7.1	55.4 ± 1.6
●●●—2-AP (□□□)	376.1 ± 9.0	53.3 ± 4.7	384.2 ± 10.0	54.6 ± 5.2	380.2 ± 6.7	54.0 ± 3.5
●●●●—2-AP (□□□)	429.4 ± 14.0	37.4 ± 4.1	438.8 ± 16.0	39.5 ± 5.0	434.1 ± 10.6	38.4 ± 3.2
●●●●—2-AP (□□□■)	466.8 ± 18.0	37.9 ± 4.0	478.3 ± 20.0	36.8 ± 5.6	472.5 ± 13.5	37.4 ± 3.4
●●●●—2-AP (□□□■◇)	504.7 ± 20.0		515.1 ± 20.0		509.8 ± 14.1	

homologs of d.p. 3 and 4, respectively. The presence of a xylosyl residue in structure 3 showed a similar change in the mobility index decrement. Furthermore, the addition of a glucosyl unit to the linear core chain imparted an identical increment in the migration time and xyloglucan fragment 5 eluted between the homologs of d.p. 4 and 5. It is therefore wise to say that a glucosyl residue in the backbone of the xyloglucan behaves as one half a GlcNAc residue in terms of its contribution to the electrophoretic mobility of the 2-AP-XG. The same can be stated about adding a xylosyl residue at the glucose loci. However, the addition of a galactosyl residue to an already branched xylosyl residue exhibited less retardation (almost 70%; see mobility index decrements in Table II) than the addition of a glucosyl or xylosyl unit to the backbone of the xyloglucan oligosaccharide. The same observation can be made about adding a fucosyl residue to a branched galactosyl residue. Thus, as the molecule becomes more branched, the addition of a sugar residue does impart a slightly less decrease in its mobility. Such indexing may prove valuable in correlating and predicting the mobilities of oligosaccharides.

CZE Mapping of Oligosaccharide Chains from Ribonuclease B

To further illustrate the resolving power of the electrophoretic system under investigation, high-mannose glycans were analyzed by CZE. In this regard, oligosaccharides from bovine RNase B were cleaved form the tryptic digest of the protein using peptide-N-glycosidase F, an endoglycosidase that cleaves all types of N-linked oligosaccharide chains between the asparagine and the carbohydrate units. The CZE mapping of the 2-pyridylamino derivatives of these oligosaccharides is portrayed in Fig. 7. It was performed on a capillary with a polyether interlocked coating using 0.1 M phosphate solution, pH 5.0, containing 50 mM tetrabutylammonium bromide as the running electrolyte. As can be seen in Fig. 7, the peak labelled with an arrow was identified as $(GlcNAc)_2-Man_5$ using an oligosaccharide standard. In fact, ribonuclease B is known as a source of high mannose oligosaccharides with only one glycosylation site. This results
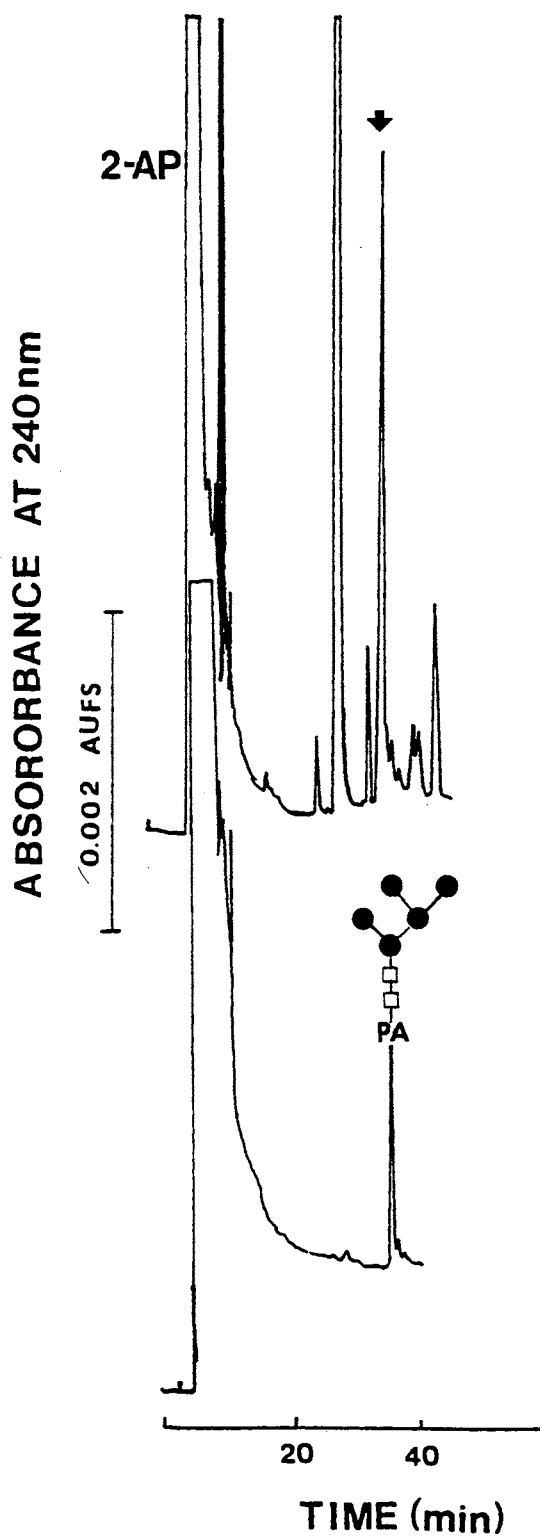
Figure 7. Capillary zone electrophoresis mapping of 2-pyridylamino derivatives of high mannose oligosaccharides cleaved from bovine ribonuclease B (top electropherogram), and of 2-PA-$(GlcNAc)_2$-Man_5 standard (lower electropherogram). Symbols: 2-AP, 2-aminopyridine; □ , GlcNAc; ●, Mannose. Conditions are as in Fig. 1.

in heterogeneous populations of structurally related oligosaccharides which renders RNase B, as most other glycoproteins, highly microheterogeneous. This may explain the presence of several peaks in the CZE map besides that of $(GlcNAc)_2\text{-}Man_5$ oligosaccharide which, according to Liang *et al* [22], is the most predominant carbohydrate moiety of bovine ribonuclease B.

Acknowledgements

References

1. E. M. Lees and H. Weigel, *J. Chromatogr.*, 16 (1964) 360.

2. P. J. Garegg and B. Lindberg, *Acta Chem. Scand.*, 15 (1961) 1913.

3. B. Lindberg and B. Swan, *Acta Chem. Scand.*, 14 (1960) 1043.

4. M. Weigel, *Adv. Carbohydr. Chem.*, 18 (1963) 61.

5. J. L. Frahn and J. A. Mills, *Aust. J. Chem.*, 12 (1959) 65.

6. G. Zweig and J.R. Whitaker, "Paper Chromatography and Electrophoresis," Academic press , New York, 1967, p. 233.

7. S. Honda, S. Iwase, A. Makino and S. Fujiwara, *Anal. Biochem.*, 176 (1989) 72.

8. S. Honda, A. Makino, S. Suzuki and K. Kakehi, *Anal. Biochem.*, 191 (1990) 228.

9. W. Nashabeh and Z. El Rassi, *J. Chromatogr.*, 514 (1990) 57.

10. W. Nashabeh and Z. El Rassi, *J. Chromatogr.*, 536 (1991) 31.

11. J. Liu, O. Shirota and M. Novotny, *Anal. Chem.*, 63 (1991) 413.

12. E. S. Yeung and W. G. Kuhr, *Anal. Chem.*, 63 (1991) 275 A.

13. W. Nashabeh and Z. El Rassi, *J. Chromatogr.*, 559 (1991) 367.

14. Z. El Rassi, D. Tedford, J. An and A. Mort, *Carbohydrate research*, 215(1991) 25.

15. C. B. Kasper, in S. B. Needleman (Editor), *"Protein Sequence Determination"*, Spring Verlag, Berlin, New York, 1975, p. 114.

16. A. L. Tarentino, C. M. Gomez and T. H. Plummer, *Biochemistry*, 24 (1985) 4665.

17. C. J. O. R. Morris and P. Morris, in *"Separation Methods in Biochemistry"*, Wiley, New York, 1976, p. 711.

18. K. D. Altria and C. F. Simpson, *Chromatographia,* 24 (1987) 527.

19. H. I. Issaq, I. Z. Atamna, G. M. Muschik and G. M. Janini, *Chromatographia,* 32 (1991) 155.

20. P. J. Brynes, P. Bevilacqua and A. Green, *Anal. Biochem.*, 116 (1981) 408.

21. E. sz. Kovats, in J. C. Giddings and R. A. Keller (Editors), *"Advances in Chromatography"*, Vol.1, Marcel Dekker, New York, 1965.

22. C. J. Liang, K. Yamashita, and A. Kobata, *J. Biochem.*, 88 (1980) 51.

CHAPTER IX

ENZYMOPHORESIS OF NUCLEIC ACIDS BY TANDEM CAPILLARY ENZYME REACTOR-CAPILLARY ZONE ELECTROPHORESIS*

Abstract

Enzymophoresis with coupled heterogeneous capillary enzyme reactors-capillary zone electrophoresis was developed and evaluated in the area of nucleic acids. Ribonuclease T_1, hexokinase and adenosine deaminase were successfully immobilized on the inner walls of short fused-silica capillaries through glutaraldehyde attachment. These open-tubular capillary enzyme reactors were quite stable for a prolonged period of use under operation conditions normally used in capillary zone electrophoresis. The capillary enzyme reactors coupled in series with capillary zone electrophoresis served as peak locator on the electropherogram, improved the system selectivity, and facilitated the quantitative determination of the analytes with good accuracy. Also, they allowed the on-line digestion and mapping of minute amounts of transfer ribonucleic acids, and the simultaneous synthesis and separation of nanogram quantities of oligonucleotides.

Introduction

Capillary zone electrophoresis (CZE) with its advanced instrumentation and unique

selectivity has become an important microseparation technique. In CZE, and for a given set of conditions, the migration of charged species depend primarily on the sign and magnitude of their net charge and to some extent on their shape and size. Therefore, when the analytes posses the same charge to mass ratio and differ only slightly in their size and shape, CZE is rather inadequate for their separation. In addition, as with other separation techniques, the identification of a given species in a mixture requires the use of additional means that can confirm its presence or absence, especially under coelution conditions or when no authentic standards are available. Enzymes, with their high stereospecificity in binding their substrates, are well suited to play this role.

In fact, the combination of enzymes with separation techniques has been a theme of research for many years. In 1970, Brown [1] pioneered the use of enzymes in free solution for sample pretreatment prior to chromatographic separation as a mean of peak identification, and coined the term enzymic peak-shift for the technique. On the other hand, the relative ease with which enzymes can be covalently attached or immobilized to various types of surfaces without substantial loss in their catalytic activity [2] has favored their use in solving many analytical problems [3]. One of the important applications of immobilized enzymes has been their use in pre- and post column derivatization devices with several high performance liquid chromatography techniques [3-8]. More recently, narrow bore packed-bed trypsin reactor was introduced for the nanogram digestion of proteins prior to microcolumn liquid chromatography and capillary zone electrophoresis tryptic peptide mapping [9].

This report is concerned with the miniaturization of immobilized enzyme reactors for use in tandem with CZE. In this regard, short fused-silica capillaries with immobilized enzymes on the inner wall were developed for tandem heterogeneous capillary enzyme reactors-capillary zone electrophoresis (HCER-CZE). This tandem format, which is referred to as enzymophoresis, was evaluated in both the qualitative and quantitative determinations of different nucleic acids. Various HCER-CZE systems were investigated

and characterized over a wide range of operation conditions including the design of the capillary enzyme reactor, the contact time of the substrates with the immobilized enzymes, the initial concentrations of the substrates, the nature of the background electrolyte and the pH. In addition, the effects of buffer additives as well as the immobilized enzymes on the magnitude and direction of the electroosmotic flow were investigated.

Experimental

Instrument

The instrument for capillary electrophoresis was assembled in-house from commercially available components, and resemble to previously reported systems [10, 11]. It comprised two high-voltage power supplies of positive and negative polarities Models MJ30P400 and MJ30N400, respectively, from Glassman High Voltage (Whitehouse Station, NJ, U.S.A.) and a Linear (Reno, NV, U.S.A.) Model 200 UV-Vis variable wavelength detector equipped with a cell for on-column capillary detection. The detection wavelength was set at 258 nm for sensing the various nucleic acids. The electropherograms were recorded with a Shimadzu (Columbia, MD, U.S.A.) computing integrator Model C-R3A equipped with a floppy disk drive Model FDD-1A and a CRT monitor.

Capillary Columns

Fused-silica capillary columns of 50-μm I.D. and 365-μm O.D. were obtained from Polymicro Technology (Phoenix, AZ, U.S.A.). All capillaries used in this study were coated in-house with either interlocked or fuzzy polyether chains according to previously described procedures [10].

Reagents and Materials

Ribonuclease T_1 (RNase T_1) from *Aspergillus oryzae* (EC 3.1.27.3), hexokinase (HK) from bakers yeast (EC 2.7.1.1), adenosine deaminase (ADA) from calf spleen (EC 3.5.4.4), transfer ribonucleic acid specific for phenylalanine (t-RNA^{Phe}) from brewers yeast, guanylyl-(3'→5')-adenosine (GpA), guanylyl-(3'→5')-uridine (GpU), guanylyl-(3'→5')-cytidine (GpC), uridylyl-(3'→5')-guanosine (UpG), guanosine-2':3'-cyclic monophosphate (G>p), guanosine-3'-monophosphate (Gp), adenosine-5'-triphosphate (ATP), adenosine-5'-diphosphate (ADP), adenosine (A), inosine (I), guanosine (G), uridine (U), cytidine (C), glucose and Trizma base were obtained from Sigma (St. Louis, MO, U.S.A.). L- Histidine (His), 2[N-morpholino]ethanesulfonic acid (MES), N,N'-bis[3-aminopropyl]-1,4 butanediamine tetrahydrochloride (Spermine) were from Aldrich (Milwaukee, WI, U.S.A.). γ-Aminopropyltriethoxysilane was purchased from Huls of America (Bristol, PA, U.S.A.). Reagent grade sodium phosphate monobasic and dibasic, magnesium chloride, ammonium hydrogen bifluoride, 1,3-naphthalenedisulfonic acid disodium salt, sodium acetate, phosphoric acid, hydrochloric acid, sodium hydroxide and HPLC grade methanol were obtained from Fisher Scientific (Pittsburgh, PA, U.S.A.). Deionized water was used to prepare the running electrolyte. All solutions were filtered with 0.2-μm UniPrep syringeless filters (Fisher Scientific) to avoid column plugging.

Enzyme Immobilization

Fused-silica capillaries of 15 to 25 cm long were first etched according to the procedure described by Onuska *et al* [12]. The etched capillaries were then reacted with 10% (v/v) solution of γ-aminopropyltriethoxysilane in water at 95°C for 30 minutes. This step was repeated twice. Following, a 1% (v/v) solution of glutaric dialdehyde in 50 mM phosphate, pH 7.0, was applied to the capillary and allowed to react at room temperature for one hour. Thereafter, a phosphate solution containing the enzyme of interest was

recycled through the aldehyde activated amino-fused-silica capillaries and allowed to stand overnight. Finally, residual aldehyde reactive functions were scavenged with 50 mM Tris-HCl at pH 7.5. All capillaries were stored in water at 5°C.

Other Procedures

In all experiments, the capillary enzyme reactors of 15 to 25 cm long were connected butt-to-butt to the separation capillaries having a polyether hydrophilic coating (i.e., CZE capillary) of 64 cm total length and 30 cm to the detection point using a teflon tube the inner diameter of which matched the outer diameters of the two capillary columns. The enzymic reactions were carried out on-line by allowing a thin plug of the substrates to flow through the tandem capillaries either by electromigration under the influence of an applied voltage or by hydrodynamic mode (i.e., gravity-flow) by raising the inlet reservoir to a certain height above the outlet reservoir. In both cases, the substrates first entered the capillary enzyme reactor and were converted to products. They were further separated in the separation capillary downstream the enzyme reactor. The time required for the substrates to traverse the enzyme reactor under hydrodynamic conditions, t_i, was estimated from the following equation [13]:

$$t_i = \frac{8\eta Ll}{\rho g r^2 \Delta h}$$

where η is the medium viscosity, L is the total length of the capillary, l is the distance traversed by the plug of the substrate, ρ is the electrolyte density, g is the gravitational constant, r is the inner radius of the capillary and Δh is the differential height between the electrolyte reservoirs. In all cases, the viscosity and density of the solutions were taken as that of water since the buffers used were dilute solutions of electrolytes. The calculations using the above equation agreed with the experimental migration time estimated from the chromatogram of the substrate that was allowed to flow by gravity through the tandem capillary enzyme reactor → CZE capillary. Therefore, in all the studies, the above equation

gave satisfactory results in terms of the time required for the species to reach a certain distance in the capillary by hydrodynamic flow.

The running electrolyte was renewed after each run. To ensure reproducible separations the separation capillary was flushed successively with fresh buffer, water, methanol, water, and again running buffer. The enzyme reactor was also flushed with fresh buffer solution after each run. Both capillaries were then equilibrated with the running electrolyte for 10 minutes before each injection.

Results and Discussion

Design of the Capillary Enzyme Reactor

Figure 1 is a schematic illustration of the capillary enzyme reactor. The walls of the fused-silica capillary were first roughened using a methanolic solution of ammonium bifluoride; see experimental. This etching step is to increase the specific surface area of the capillary wall in order to achieve higher enzyme loading of the reactor. This would yield capillary enzyme reactors with higher catalytic activity, and may increase the maximum velocity, V_{max}, of the enzymic reaction. The surface roughening by ammonium bifluoride at high temperature has been recently used in our laboratory for the preparation of octadecyl-capillaries for on-line preconcentration of dilute samples [14] and proved efficient in increasing the concentration of covalently attached hydrocarbonaceous ligands. Another function of the etching is to increase the surface wettability which permits the homogeneous spreading of the hydrophilic aminopropylsiliyl layer. This layer is to minimize solute-wall interactions and to provide the functional groups for the attachment of the enzyme. The heterogeneous capillary enzyme reactors (HCER) thus obtained were used in series with polyether coated capillaries.
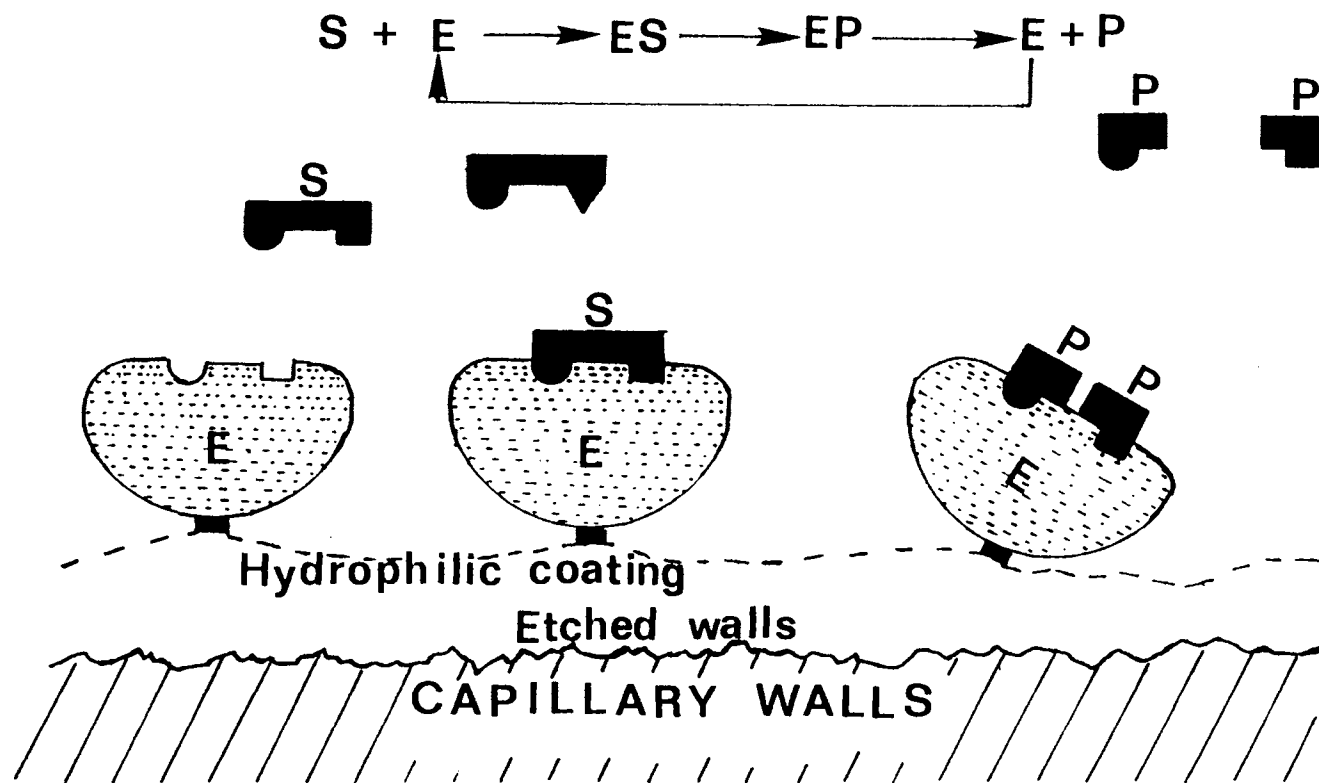
Figure 1. Schematic illustration of immobilized capillary enzyme reactor. Symbols: S, substrate; E, enzyme; P, product.

Operational and Basic Principles of Tandem Capillary Enzyme Reactor-CZE

The capillary consisted of two sections connected in series *via* a teflon tube. The first part is the capillary enzyme reactor and the second part is the separation capillary (i.e., CZE). In all cases, the substrate(s) is first introduced as a thin plug into the capillary enzyme reactor. The catalyzed reaction takes place as the substrate(s) migrate through the enzyme reactor either by hydrodynamic flow or electromigration. Following, the reaction mixture is further separated in the CZE capillary at the same or different applied voltage than in the precolumn enzymic derivatization reactor. To satisfy both the enzymic reaction and the separation, the background electrolyte for the reaction and separation processes can be either the same or different. Most importantly, the electrolyte for the enzymic reaction should minimize microenvironmental effects in the capillary enzyme reactor. These effects are related to electrostatic or hydrophobic interactions with the enzyme and/or the matrix [15].

Open tubular capillary enzyme reactors offer the convenience of repeated use of the enzyme without much loss of its activity, and provide enhanced storage and thermal stability for the enzyme. Furthermore, in contrary to packed-bed reactors where the substrate has to diffuse inside the pores of the packing to reach the immobilized enzyme, mass transfer in open tubular columns is of external nature (i.e., bulk diffusion). This would increase the effectiveness factor η, defined as the ratio of the actual reaction rate to that obtained under conditions where no diffusional mass transfer limitations are present (i.e., free solution). External mass transfer limitations, albeit small in a capillary tube, may still increase the apparent Michaelis constant K_M^{app} [16], which would result in increasing the linear dynamic range of the immobilized enzyme, and in turn benefit the analytical applications of capillary enzyme reactors.

Effect of Spermine on the Electroosmotic Mobility

The usefulness of the catalytic activities of the various HCERs was demonstrated in the separation, identification, quantitative determination, and synthesis of nucleic acid fragments and constituents. In order to bring about the migration and separation of the various nucleic acids under investigation with coated capillaries having moderate cathodal electroosmotic flow, a means for inverting the direction of the flow was necessary so that a negative polarity mode could be utilized. This was achieved by adding spermine to the running electrolyte at low concentration.

Spermine is a biogenic tetraamine that has been successfully used as a buffer additive in the CZE analysis of polycitidines [17] with polyacrylamide coated capillary tubes. In this study, it was thought that the spermine primary function is to reduce the net negative charge of the analytes and allow their migration and separation. To study its adsorption onto the capillary inner surface, we have measured the magnitude of the electroosmotic flow and examined its direction in the presence and absence of spermine over the pH range 3.5 to 7.0 using phenol as the inert tracer. The results of this study are summarized in Fig. 2. These studies were performed on an interlocked polyether coated capillary using a running electrolyte of 25 mM His and 25 mM MES, with or without 5mM spermine. In the presence of spermine, the direction of the electroosmotic flow was inverted from cathodal to anodal as shown in Fig. 2. The adsorption of spermine, which has a net positive charge of *ca* +4 below pH 7.0, onto the capillary inner surface changed the zeta potential of fused-silica from negative to positive. As can be seen in Fig. 2, the electroosmotic mobility slightly decreased upon increasing the pH in the range studied. This can be explained by both the slight decrease in the net positive charge of spermine and the increase in the ionization of surface silanols as the pH increased. Thus, spermine is a useful buffer adjunct for the analysis of negatively charged species in the negative polarity
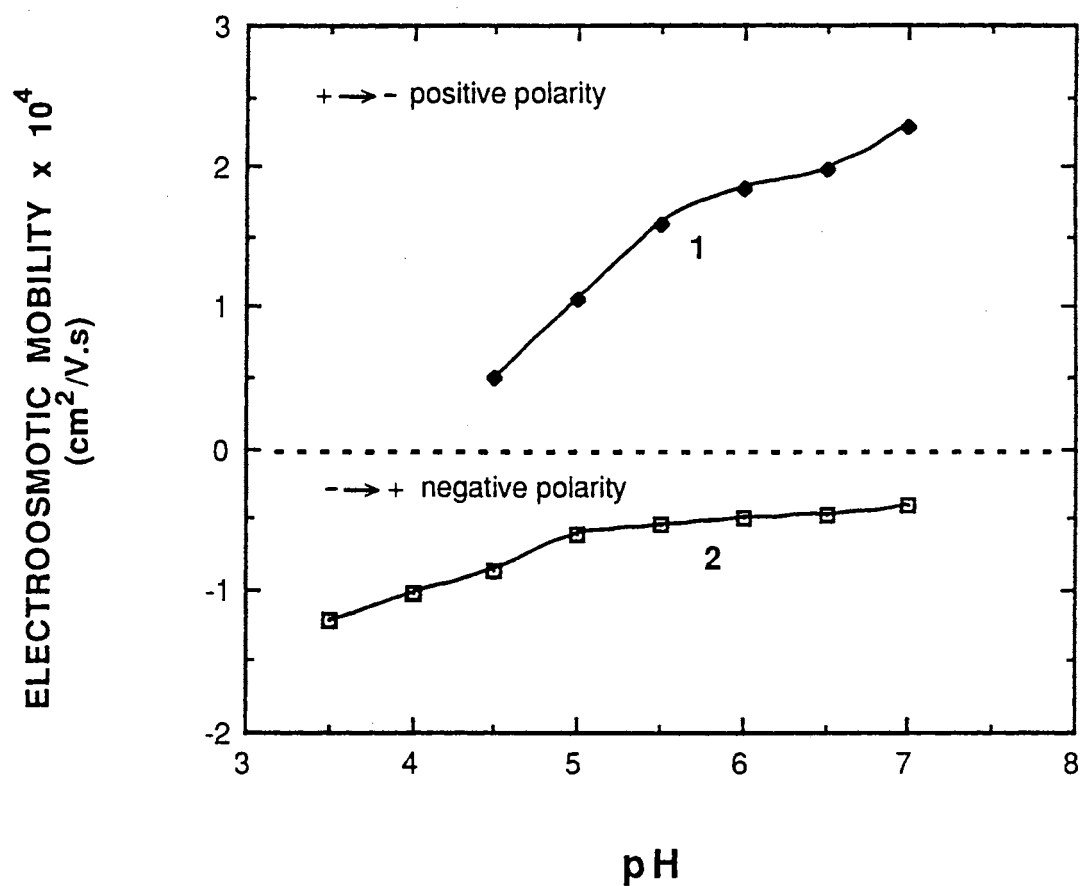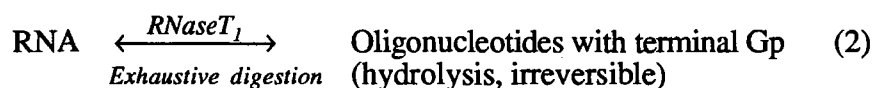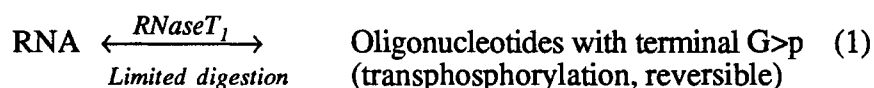
Figure 2. Plots of the electroosmotic mobility in the absence (1) or presence (2) of spermine in the running electrolyte as a function of pH. Capillary, interlocked polyether coating, 30 cm (to the detection point) 64 cm (total length) x 50 μm I.D. ; running voltage, 25 kV; background electrolyte, 25 mM His, 25 mM MES in the absence (1) or presence (2) of 5 mM spermine. Inert tracer, phenol.

mode, since it allows the separated analytes to migrate in the same direction as that of the electroosmotic flow which in turn would yield shorter separation time.

Ribonuclease T₁ Capillary Enzyme Reactor

Ribonuclease T_1 is a guanylic acid specific endoribonuclease that cleaves phosphodiester bonds between 3'-guanylic acid residues and the 5'-hydroxyl groups of adjacent nucleotidyl residues [18]. In addition, under certain conditions, the enzyme acts as a ligase catalyzing the esterification of G>p with the 5'-hydroxyl group of various nucleosides to yield the corresponding dinucleotides [18, 19]. Both catalytic functions of RNase T_1 were evaluated in the tandem RNase T_1-capillary enzyme reactor → CZE mode using an electrolyte system containing spermine as a buffer additive to facilitate the electrophoresis of negatively charged nucleotides, see above.

Immobilized ribonuclease T₁ as a hydrolytic enzyme. As mentioned above, RNase T_1 splits the internucleotide bonds specifically after guanylyl residues according to the following reaction schemes [18]:

$$RNA \xleftrightarrow[Limited\ digestion]{RNaseT_1} \text{Oligonucleotides with terminal G>p} \quad (1)$$
$$\text{(transphosphorylation, reversible)}$$

$$RNA \xleftrightarrow[Exhaustive\ digestion]{RNaseT_1} \text{Oligonucleotides with terminal Gp} \quad (2)$$
$$\text{(hydrolysis, irreversible)}$$

The above catalytic activity of the enzyme was demonstrated in the identification and quantitative determination of various dinucleotides using tandem RNase T_1-capillary enzyme reactor → CZE. In all experiments, the substrates were introduced as a thin plug and allowed to flow hydrodynamically through the enzyme reactor by raising the inlet reservoir to a height of 20 cm above the outlet reservoir. This corresponds to a contact time of ca. 16 min with the immobilized enzyme. As the plug of the reaction mixture

entered the separation capillary, the enzyme reactor was disconnected and the separation capillary was inserted into the electrolyte reservoir. Thereafter, the voltage was turned on to 25 kV to bring about the separation of the reaction mixture. As shown in Fig. 3a, a mixture of three dinucleotides namely GpU, GpA and GpC were not resolved by CZE alone using a buffer system containing 25 mM Histidine, 25 mM MES and 5 mM spermine at pH 5.0. This is because these dinucleotides have approximately the same charge to mass ratio. As shown in Fig. 3b, with the on-line RNase T_1-capillary enzyme reactor, the dinucleotide mixture was converted to more readily separated products. Each of the three dinucleotides GpA, GpU and GpC yielded the guanosine-2':3'-cyclic monophosphate and its corresponding nucleoside, i.e., adenosine, uridine and cytidine. Hence, the three dinucleotides that coeluted as a broad peak with CZE alone were transformed into four well resolved peaks, i.e., G>p, U, A and C, after a single pass through the 17 cm long RNase T_1-capillary enzyme reactor.

In another electrophoretic run, one of the three dinucleotides GpC, was replaced by UpG, a dinucleotide that is not digested by the enzyme. As expected, with CZE alone, this mixture exhibited the same electrophoretic behavior as the one in the preceding experiment, in the sense that its components could not be resolved as shown in Fig. 4a. However, after a single pass through the capillary enzyme reactor, UpG which is not split by the immobilized enzyme eluted intact, and was well resolved from the products of GpA and GpU. This feature of the capillary enzyme reactor has many practical significances. The tandem format can assess the identity of overlaping peaks and permits the simultaneous digestion and separation of the reaction mixture. Briefly, the capillary enzyme reactor functions as a peak locator by unmasking the analyte of interest on the electropherogram, and enhances the selectivity of the electrophoretic system by converting the substrates into more readily separated products.

The dinucleotide GpU, having the lowest relative rate of splitting by RNase T_1 among the other dinucleotides analyzed [20], was selected as a model substrate to evaluate
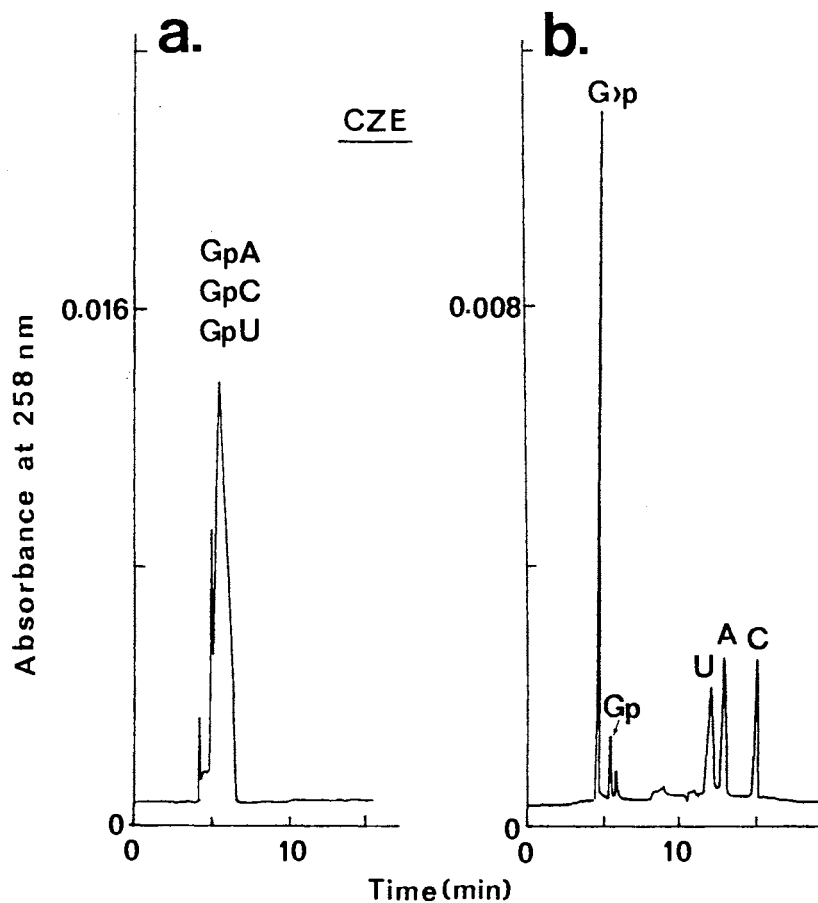
Figure 3. Typical electropherograms of dinucleotides and their RNase T₁ digest obtained by CZE alone (a) or by tandem RNase T₁-capillary enzyme reactor → CZE (b), respectively. Capillary enzyme reactor, 17 cm x 50 μm I.D.; separation capillary, interlocked polyether coating, 30 cm (to the detection point), 64 cm (total length) x 50 μm I.D.; substrate introduction, hydrodynamic mode; enzymic reaction was carried out using gravity-driven flow; separation step, as the plug of the reaction mixture entered the separation capillary, the enzyme reactor was disconnected and the voltage was turned on to 25 kV; background electrolyte, 25 mM His, 25 mM MES, 5 mM spermine, pH 5.0. Symbols: GpU, guanylyl-(3'→5')-uridine; GpA, guanylyl-(3'→5')-adenosine; GpC, guanylyl-(3'→5')-cytidine; G>p, guanosine-2':3'-cyclic monophosphate; Gp, guanosine-3'-phosphate; U, uridine; A, adenosine; C, cytidine.
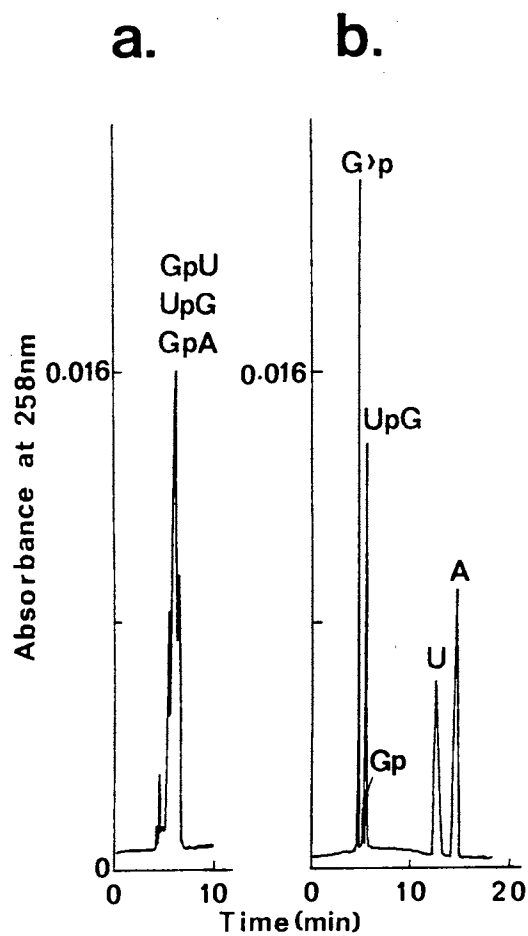
Figure 4. Typical electropherograms of dinucleotides and their RNase T₁ digest obtained by CZE alone (a) or by tandem RNase T₁-capillary enzyme reactor → CZE (b), respectively. Symbol: UpG, uridylyl-(3'→5')-guanosine. Other conditions and symbols are as in Fig. 3.

the stability of the RNase T_1-capillary enzyme reactor. The reactor showed steady behavior even after prolonged storage or repeated use. Over a period of more than 2 months, the RNase T_1-capillary enzyme reactor yielded complete conversion of GpU with the liberation of G>p and U as major peaks, suggesting that the enzymic reaction occurring at the wall of the HCER is primarily a limited digestion mechanism , see reaction 1.

Another important feature of the capillary enzyme reactor is its usefulness in the quantitative determination of the dinucleotides. To demonstrate this important application of HCER, typical calibration curves for G>p and some of the nucleosides were established using 1,3-naphthalenedisulfonic acid disodium salt as the internal standard. As shown in Fig. 5, these curves were linear in the concentration range investigated. In such measurements, the G>p peak can be used for the quantitative determination of the total concentration of the dinucleotides digested by the enzyme in a given mixture, while the peak of each nucleoside can be used to estimate the concentration of its corresponding dinucleotide. In the case of only one solute analyzed, both the G>p and the nucleoside peaks are equally useful in the quantitative determination of the analyte, thus increasing the reliability of the method. For instance, a thin plug of an unknown solution of GpU was analyzed with the coupled capillary enzyme reactor-capillary zone electrophoresis following the same operational schemes outlined above. The calibration curves revealed on the average a concentration of 0.90 μmol/mL for G>p and 1.00 μmol/mL for U. By averaging these two values, the concentration of GpU in the unknown solution was about 0.95 μmol/mL. This illustrates the use of the capillary enzyme reactor in enhancing the reliability of quantitative determination by CZE.

In addition, the RNase T_1-capillary enzyme reactor → CZE system proved very efficient in the on-line digestion and mapping of transfer ribonucleic acid specific for phenylalanine (t-RNA^{Phe}). The secondary structure of t-RNA^{Phe} is represented in Fig. 6. It comprises 76 nucleotide residues. The arrows in this figure indicate the 20 locations at
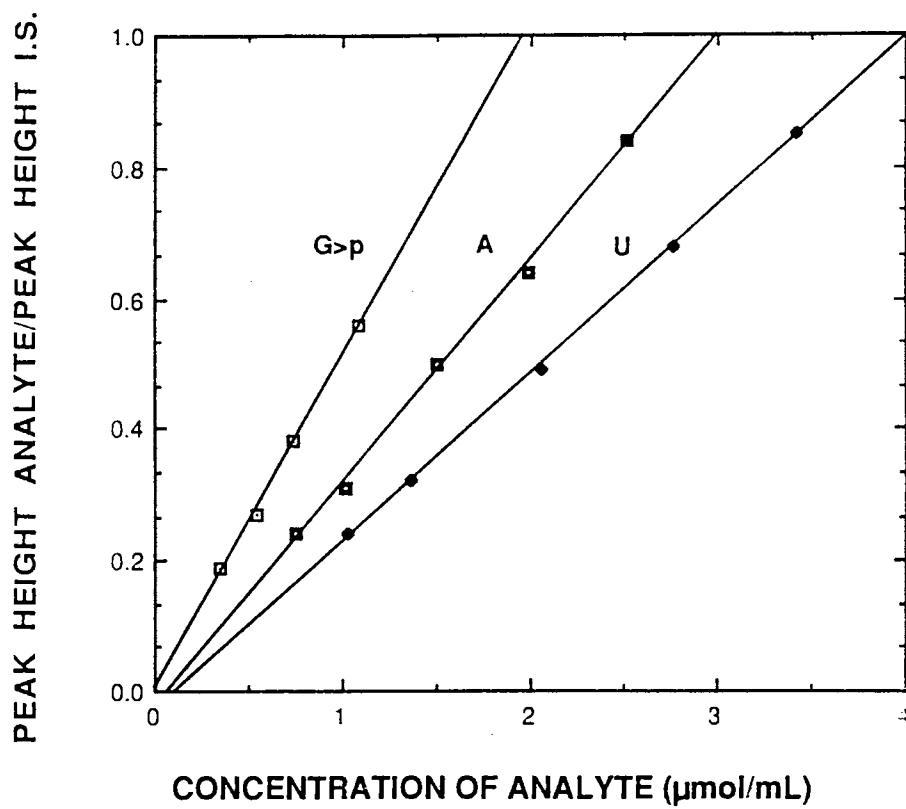
Figure 5. Plots of the ratio of the peak height of the analyte to that of the internal standard as a function of the analyte concentration. Internal standard, 1,3-naphthalenedisulfonic acid disodium salt. Other conditions and symbols are as in Fig. 2 and 3, respectively.

20 Cuts

16 Fragments

A—OH
C
C Acceptor
A stem
pG - C
C - G
G - C
G - U
A - U
U^{U} A

D loop

TψC loop

D^{G} A C U C m^{2}G A U A ╱ C U A ╱
D | | | | G A C A C G
G G A G C m^{5}C U G U G
G G A m$_2^2$G C U m^{7}G ↑T ψ
C - G A G

C - G A G ↖
C - G Variable
A - U loop
G - m$_5$C
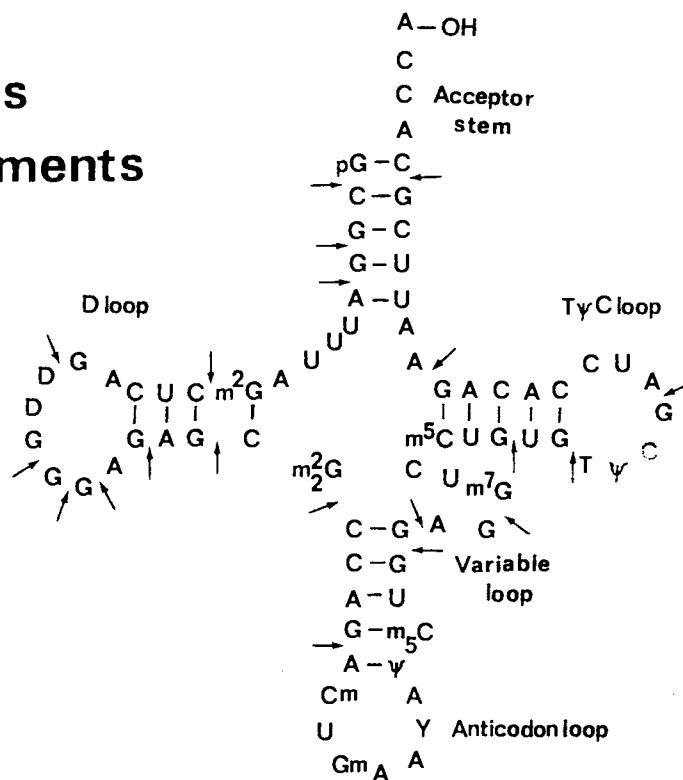A - ψ
Cm A
U Y Anticodon loop
Gm$_A$ A

Figure 6. Schematic representation of the secondary structure of transfer ribonucleic acid specific for phenylalanine (t-RNA^{Phe}). The arrows in this figure indicate the 20 locations at which RNase T$_1$ splits the internucleotide bonds.

which the enzyme splits the internucleotide bonds leading to the formation of 15 oligonucleotides and one guanosine monophosphate [21]. The digestion of t-RNA^{Phe} was carried out in a 20 cm long capillary enzyme reactor by allowing the substrate to contact the immobilized RNase T$_1$ for approximately 22 minutes while flowing hydrodynamically. Thereafter, the capillary enzyme reactor was disconnected and the RNase T$_1$ digest was mapped in the separation capillary using a running electrolyte of 0.1 M His, 0.1 M MES and 5 mM spermine, pH 7.0, see Fig. 7. In this experiment, the ionic strength of the running electrolyte was increased in order to minimize electrostatic interactions between the oligonucleotide fragments and the amino-silica matrix and/or the enzyme. It can be envisioned that such format can allow (i) the quick and reproducible mapping of other native or modified t-RNAs available only in minute quantities, and (ii) the conversion of ribonucleic acids to more electrophoretically manageable oligonucleotide fragments.

Immobilized ribonuclease T$_1$ as ligating enzyme. Another interesting feature of RNase T$_1$ is its ligating property. It can link cyclic G>p to a nucleoside and produce the corresponding dinucleotide. This aspect of the immobilized RNase T$_1$ has been previously investigated by El Rassi and Horvath using tandem packed bed enzyme reactor-high performance displacement chromatography [8]. To examine the effectiveness of tandem RNase T$_1$ capillary enzyme reactor $\rightarrow$ CZE in the synthesis and separation of ng quantities of dinucleotides, the following reaction was investigated:

$$G>p + U \quad \xleftarrow{\quad RNaseT_1 \quad}\rightarrow \quad GpU \qquad (3)$$
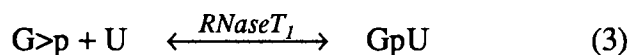
In contrary to the digestion reaction which occurs mostly in the forward direction, the ligation process requires the use of an excess of one of the reactants to drive the equilibrium towards the formation of the dinucleotide. Studies in free solution reveal that under appropriate conditions and 24 hrs incubation time, only 40 % of G>p is transformed into GpU [22]. Figure 8 a and b illustrates typical electropherograms of the reaction
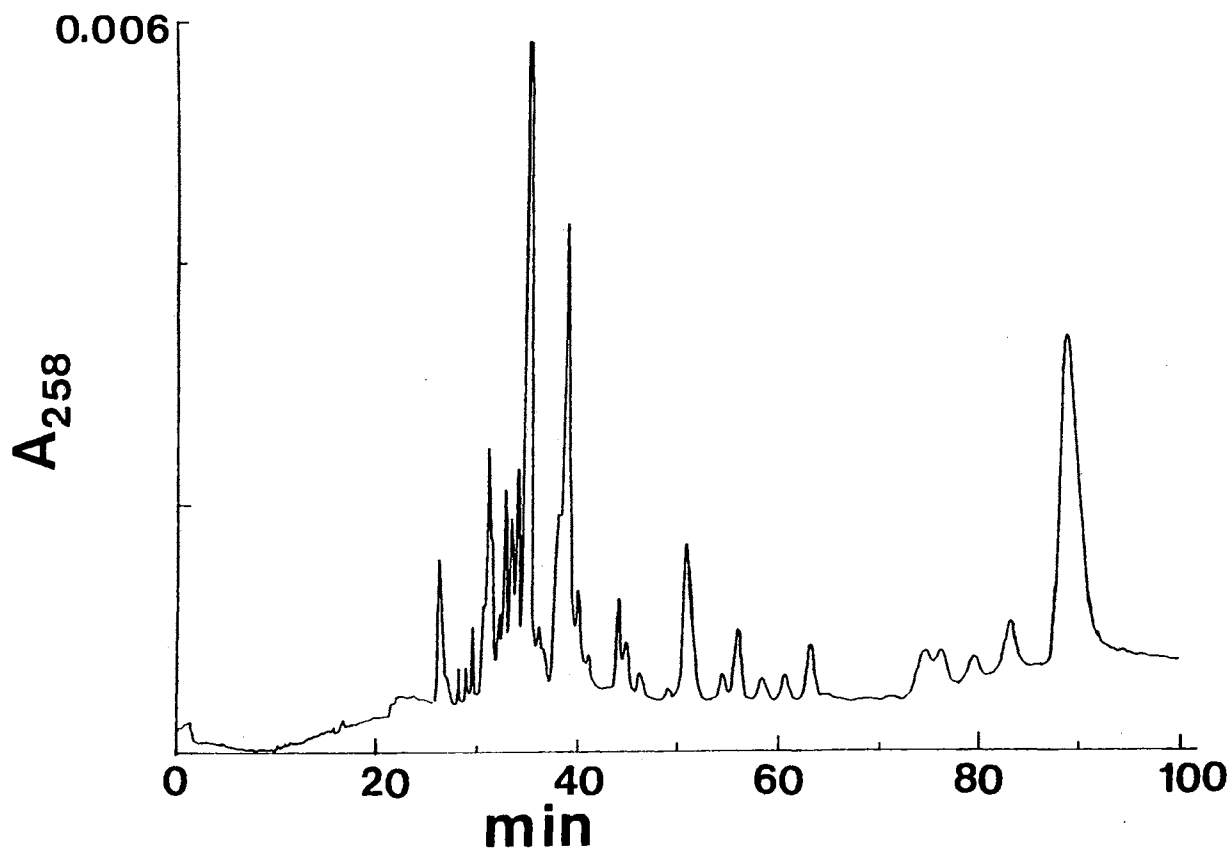
Figure 7. On-line digestion and mapping of t-RNA^{Phe} by tandem RNase T$_1$- capillary enzyme reactor → CZE. Capillary enzyme reactor, 20 cm x 50 μm I.D.; separation capillary, interlocked polyether coating, 50 cm (to the detection point), 80 cm (total length) x 50 μm I.D.; running voltage, 15 kV; background electrolyte, 0.1 M His, 0.1 M MES, 5 mM spermine, pH 7.0. Substrate introduction, enzymic reaction and separation steps are as in Fig. 3.
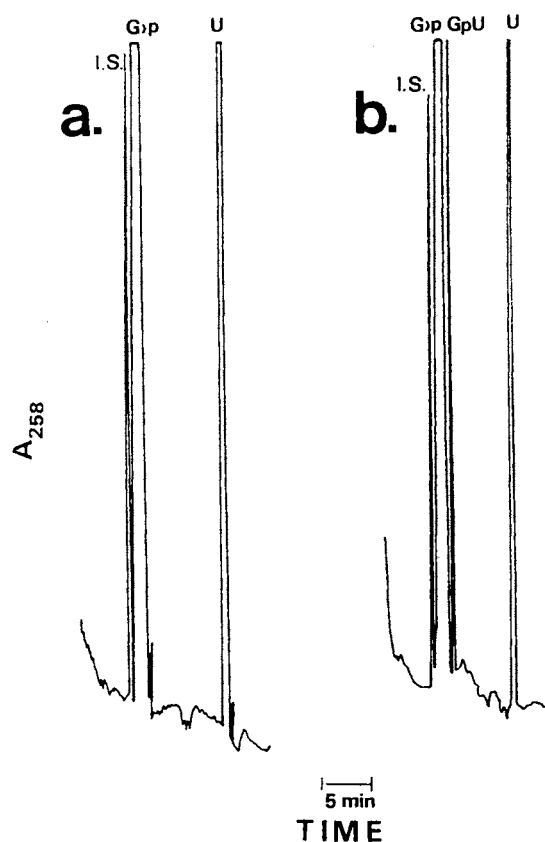
Figure 8. Typical electropherograms of the RNase T_1 synthetic reaction mixture in the absence, i.e., by CZE alone (a) or presence of RNase T_1-capillary enzyme reactor (b). Capillary enzyme reactor, 15 cm x 50 μm I.D.; separation capillary, interlocked polyether coating, 30 cm (to the detection point), 64 cm (total length) x 50 μm I.D.; substrate introduction, hydrodynamic mode; enzymic reaction was carried out using gravity-driven flow; separation step, as the plug of the reaction mixture entered the separation capillary, the enzyme reactor was disconnected and the voltage was turned on to 25 kV; background electrolyte, 25 mM His, 25 mM MES, 5 mM spermine, pH 5.5. Internal standard (I.S.), 1,3-naphthalenedisulfonic acid disodium salt. Initial concentration, [G>p] = 0.02 M, [U] = 0.10 M.

mixture obtained in the absence or presence of the RNase T_1-capillary enzyme reactor, respectively. Both the enzymic and separation processes were carried out in a buffer system of 25 mM His, 25 mM MES and 5 mM spermine, pH 5.5. The concentration of U was 5 times that of G>p and the condensation reaction was brought about by allowing a thin plug of both substrates to contact simultaneously the immobilized enzyme by gravity-driven flow. In such mode of bisubstrate enzymic reactions, where both substrates have different electrophoretic mobilities, the enzymic reaction was best achieved using hydrodynamic flow. In fact, under electromigration conditions, the negatively charged G>p would migrate downstream the enzyme reactor while uridine being neutral would migrate behind at a slower rate, and therefore both substrates are unable to get concurrently to the enzyme active sites.

The RNase T_1 catalyzed synthesis of GpU does not go to completion as manifested by the excess substrate peaks detected after the enzymic reaction; see Fig. 8b. It was then interesting to study the effect of various operational parameters on the yield of GpU. In that regard, a calibration curve was established for GpU using 1,3-naphthalenedisulfonic acid disodium salt as an internal standard. The plot of the peak height ratio of GpU to that of I.S. *vs* the concentration of GpU showed a linear behavior up to a concentration of 0.7 mg/mL of the analyte. This calibration curve was then used to estimate the amount of GpU produced. The % yield of GpU expressed in mol % of G>p converted into GpU was determined at various pH, initial substrate concentration and contact time using a thin plug of the substrate and a single pass reactor.

The effect of the electrolyte pH on the % yield of GpU was determined over the pH range 4.0 to 7.0 in an increment of 0.5 pH unit. The results obtained are illustrated in Fig. 9 by a plot of the % yield of GpU *vs* pH. In this study, the enzymic reaction was carried out using gravity-driven flow and buffers of same composition as the running electrolyte but at various pH. This means that both the capillary enzyme reactor and the separation capillary were first filled with the running electrolyte, pH 5.5 (i.e., the separation pH). As

the thin plug was introduced in the enzyme reactor, it was pushed through the immobilized capillary enzyme reactor with a buffer of the appropriate pH. When the reaction plug entered the separation capillary, the enzyme reactor was disconnected and the separation capillary was dipped into the separation buffer and the voltage was turned on to start the separation of the reaction mixture. Figure 9 shows that the % yield of GpU increased by a factor of 8 upon increasing the pH from 4.0 to 5.5. The optimum pH for the ligation reaction lies in the range 5.5 to 6.0 as opposed to 7.2 for the free enzyme [23]. This shift in the optimum activity of the immobilized enzyme toward more acidic pH values may be due to microenvironment effects and is in agreement with previous findings [24].

The effect of the initial substrate concentrations on the % yield of GpU was investigated at pH 5.5. The initial concentrations of G>p and U were varied while keeping the molar concentration ratio of U to that of G>p equal to 5.0. These results are reported in Fig. 10. Upon increasing the concentration of G>p from 0.001 to 0.01 M, the % yield of GpU increased from 1.2 to 4.7%. However, at G>p concentrations greater than 0.01 M the % yield of the synthesized GpU decreased monotonically. This may be explained by substrate inhibition due to system overloading. Experimental considerations such as peak overlaping limited the highest G>p concentration investigated to 0.04 M.

As mentioned above, the synthesis of GpU is a kinetically controlled process. Assuming Michaelis-Menten kinetics and under conditions of partial conversion, the integrated rate law can be written as [5]:

$$\frac{[P]}{[S_i]} = 1 - e^{-V_{max}t/K_m}$$

where $[P]$ is the product concentration at the outlet of the reactor, $[S_i]$ is the initial substrate concentration, V_{max} is the maximum velocity of the enzymic reaction, t is the residence time of the substrate and K_M is the Michaelis constant. According to this equation, the yield of the product should increase with increasing both V_{max} and t or decreasing K_M. V_{max} has already been improved through the etching process that
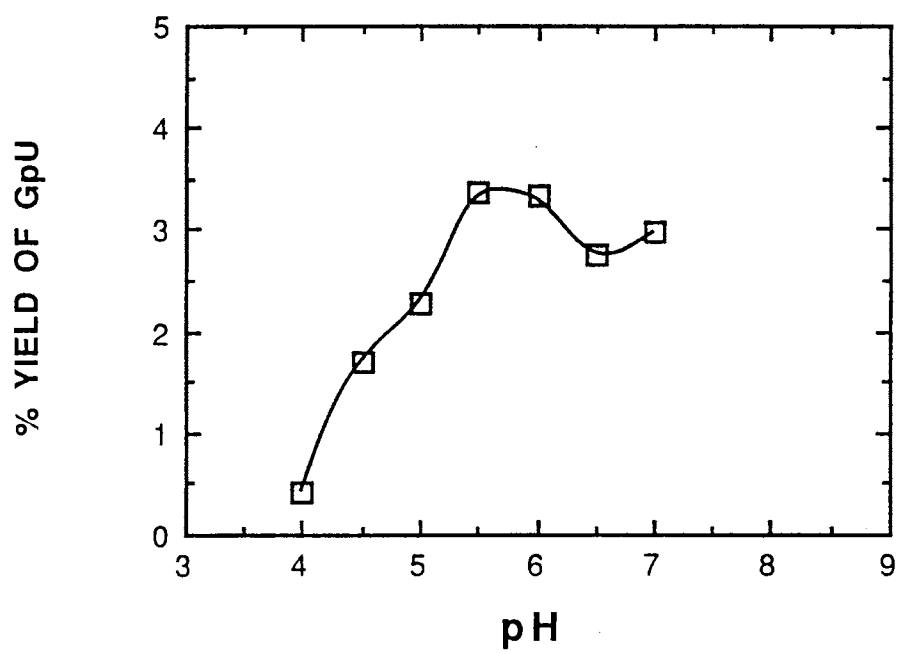
Figure 9. Plot of the % yield of GpU as a function of the pH of the enzymic reaction. Conditions are as in Fig. 8 except enzymic reaction was carried out with buffers of same composition as the running electrolyte but at various pH. See text for more details.
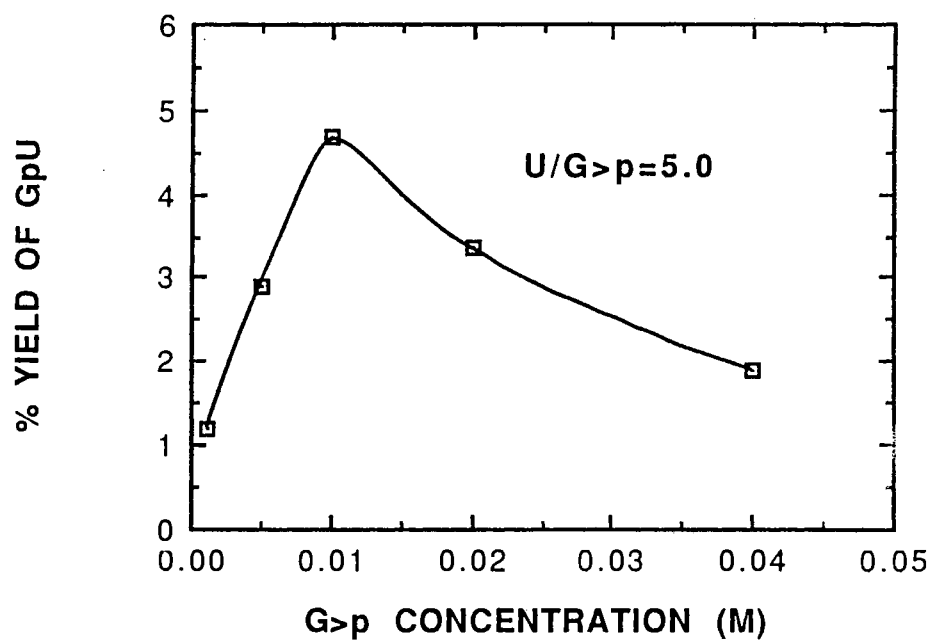
Figure 10. Plot of the % yield of GpU as a function of the initial G>p concentration. Conditions are as in Fig. 8.

increases the catalytic activity of the wall. A lower K_M value will decrease the linear dynamic range of the enzyme reactor and thus limits its analytical applications. In addition, K_M cannot be controlled systematically. Thus, the simplest alternative to enhance the product yield is to increase the contact time of the substrate with the immobilized enzyme. This can be accomplished by either using longer enzyme reactor or decreasing the flow-rate for a given length of enzyme reactor. In this study, the differential height between the two electrolyte reservoirs was varied in order to obtain different gravity driven flow-rates and consequently various contact times. Figure 11 shows the % yield of GpU versus the contact time of the substrates with the RNase T_1-capillary enzyme reactor. These results are in agreement with kinetic considerations. In fact, by increasing the contact time from 14 to 30 min, the % yield of GpU increased by a factor of 1.5 in almost a linear fashion and then levelled-off at higher contact times.

Besides the increase in the analysis time, a major concern of lower hydrodynamic flow velocity is its effect on the band width of the separated analytes. In open tubular systems, where longitudinal diffusion is the main source of bandspreading, longer residence time of the solute molecules leads to increased bandspreading. The number of theoretical plates of the GpU peak was measured at each contact time. These results are reported in Fig. 12 by a plot of the plate height as a function of the residence time in the enzyme reactor. As expected, the system efficiency decreased with increasing the contact time. However, increasing the contact time by a factor of 4 produced a decrease in the separation efficiency by a factor of 2 only.

It should be noted that under optimized conditions, approximately 10 ng of GpU can be produced from a single pass through the enzyme reactor. Such format employing simple CZE instrumentation can be easily automated and may prove useful in the micropreparative scale of important biochemicals, such as the synthesis of specific long oligonucleotides that are produced at low level by chemical synthesis methods. Such oligonucleotides are important in the study of mechanisms involving protein synthesis.
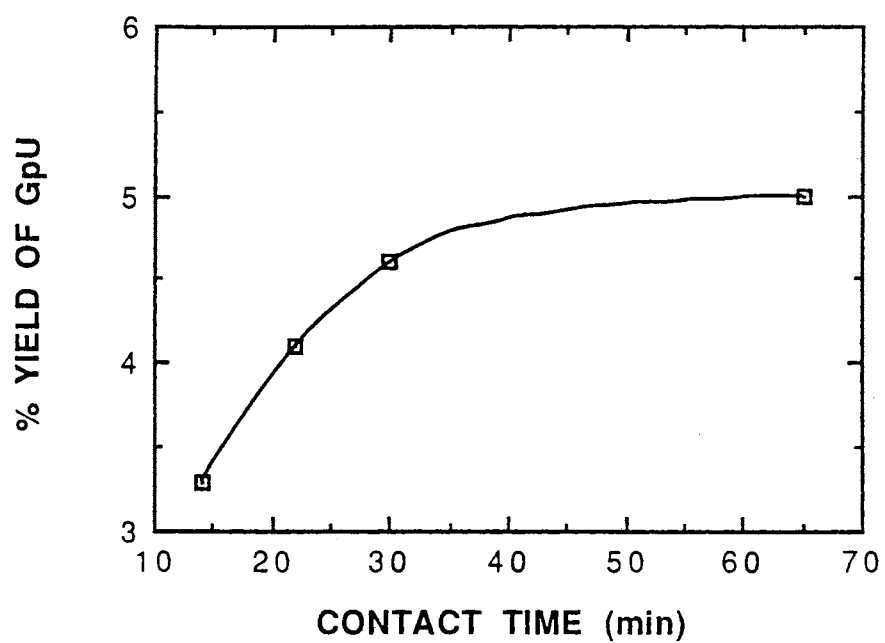
Figure 11. Plot of % yield of GpU as a function of the contact time with immobilized RNase T$_1$. Conditions are as in Fig. 8.
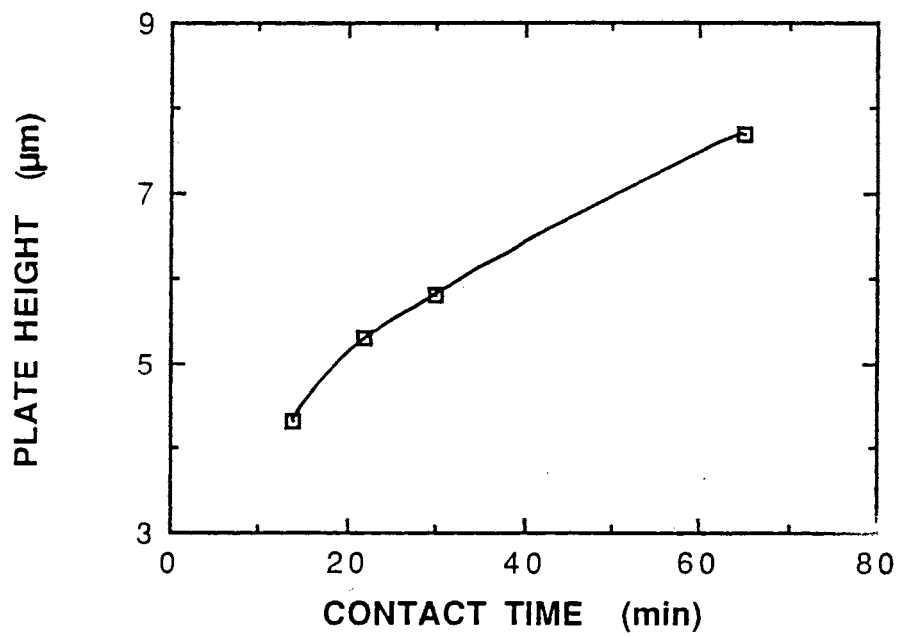
Figure 12. Plot of the plate height of the synthesized GpU peak as a function of the contact time with the immobilized RNase T_1 enzyme. Conditions are as in Fig. 8.

Hexokinase Capillary Enzyme Reactor

Hexokinase is a relatively nonspecific enzyme that catalyzes the phosphorylation of a wide variety of hexoses [25]. Its catalytic property was exploited in the HPLC separation and verification of the peak identities of ATP and ADP by treating the sample with the enzyme prior to the chromatographic separation [1]. This enzymatic reaction occurs *via* a random bi-bi mechanism in which the enzyme forms a ternary complex with glucose and Mg^{2+}-ATP before the start of the reaction [26]. Besides its orienting effect, the Mg^{2+} ions are thought to electrostatically shield the negative charges of the phosphate groups that would otherwise hinder the nucleophilic attack of the C(6)-OH group of glucose on the γ-phosphate of the Mg^{2+}-ATP complex. Thus, the overall net reaction is the transfer of a phosphoryl group from ATP to glucose to form glucose-6-phosphate (G6P) and ADP as follows [25]:

$$\text{glucose} + \text{ATP} \xleftrightarrow[Mg^{2+}]{HK} \text{glucose-6-phosphate} + \text{ADP} \qquad (4)$$
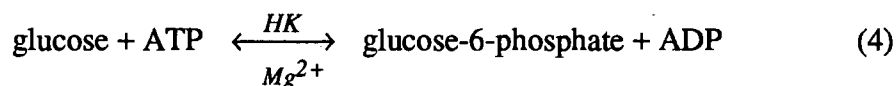
To evaluate the immobilized HK-capillary enzyme reactor, ATP was introduced as a thin plug into the tandem capillaries (i.e., capillary enzyme reactor → CZE), which were equilibrated with a buffer of 25 mM His, 25 mM MES and 5 mM spermine, pH 7.0, containing both glucose and Mg^{2+} so that the immobilized enzyme is in continuous contact with one of the substrate (i.e., glucose) and the metal ions required for the reaction. This allowed the reaction and separation to be carried out simultaneously at 25 kV. Under these conditions, the presence of spermine in the running electrolyte yielded an anodal electroosmotic flow and its effect on the magnitude and direction of the flow outweighed the influence of the immobilized enzyme on the wall of the capillary reactor. In the absence of spermine, one would expect that the electroosmotic flow to be affected primarily by the ionization of the immobilized enzyme (see below). Figure 13 illustrates a plot of the peak height ratio of ADP/ATP in arbitrary units as a function of the concentration of glucose or
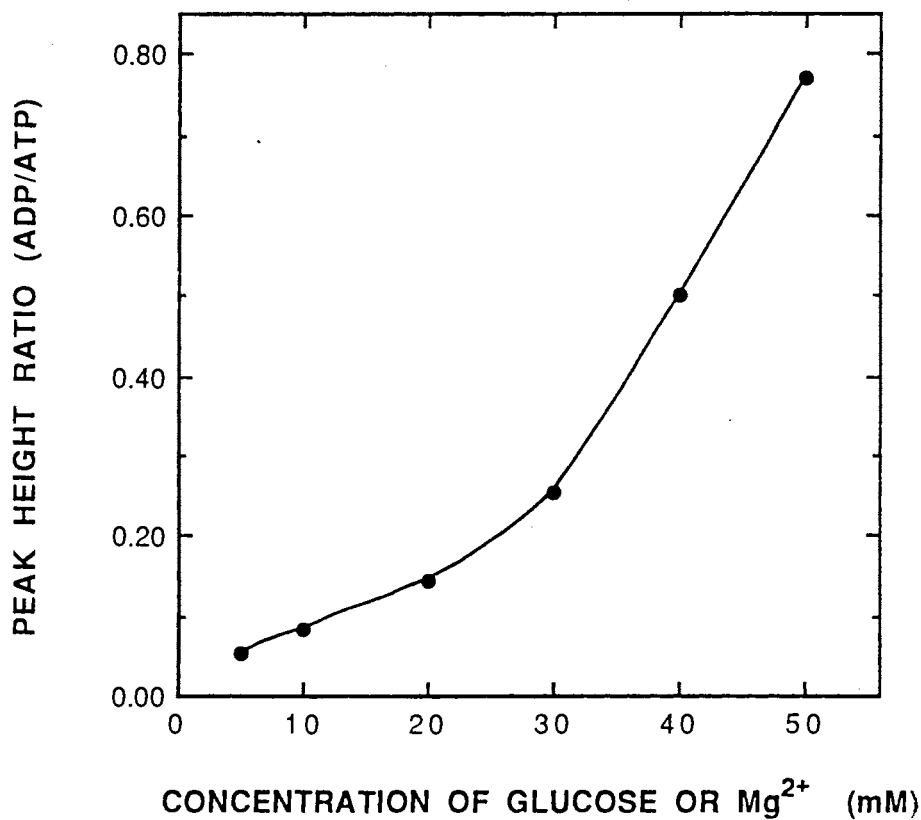
Figure 13. Plot of the peak height ratio of ADP/ATP in arbitrary units as a function of the concentration of glucose or Mg^{2+} in the running electrolyte. Capillary enzyme reactor, 15 cm x 50 µm I.D.; separation capillary, interlocked polyether coating, 30 cm (to the detection point), 64 cm (total length) x 50 µm I.D.; substrate introduction, electromigration mode; tandem enzymic reaction-CZE was carried out at the same voltage, 25 kV; background electrolyte, 25 mM His, 25 mM MES, 5 mM spermine, pH 7.0 at different concentration of glucose and Mg^{2+}.

Mg^{2+} in the running electrolyte. As expected, the magnitude of the conversion of ATP to ADP was a function of glucose and Mg^{2+} concentrations in the running electrolyte. As shown in Fig. 13, the peak height ratio of ADP/ATP increased by a factor of 16 upon increasing the concentrations of both glucose and Mg^{2+} by a factor of 10 (i.e., from 5 mM to 50 mM). However, due to the increase in the viscosity of the buffer system at high glucose concentrations, the electrophoretic system suffered from prolonged analysis time which resulted in poor efficiency.

In another set of experiments, ATP was allowed to migrate through the capillary enzyme reactor by a gravity-driven flow. This was aimed at studying the effect of contact time with the immobilized enzyme on the substrate conversion at constant temperature, a parameter that cannot be easily controlled when electromigration is used to vary the contact time of the substrates with the immobilized enzyme. Figure 14 illustrates typical electropherograms of the products of the enzymic reaction at various contact time. They were carried out on a fuzzy 2000 polyether coated capillary using 0.1 M acetate containing 20 mM glucose and 10 mM Mg^{2+}, pH 5.0, as the running electrolyte. Under these conditions, the electroosmotic flow was cathodal and its magnitude was relatively low. This is because the fuzzy polyether capillaries are characterized by relatively low electroosmotic flow [10], and the presence of heavy metal ions further reduced the flow [27]. This permitted the migration of the negatively charged nucleotides in the negative polarity mode without the inclusion of spermine in the background electrolyte. The electrophoretic velocity of the solutes was much greater than, and in opposite direction to, the electroosmotic flow. As can be noticed, at relatively low glucose concentration, the peak height ratio of ADP/ATP increased almost 3 times by increasing the contact time of the substrate with the immobilized enzyme from 10 to 52 minutes. As in the case of RNase T_1-capillary enzyme reactor, the increase in the residence time of ATP in the enzyme reactor from 10 to 52 min, led to a drop in the separation efficiency by a factor of 2.4 and 1.8 for ATP and ADP, respectively. The tandem format HK-capillary enzyme
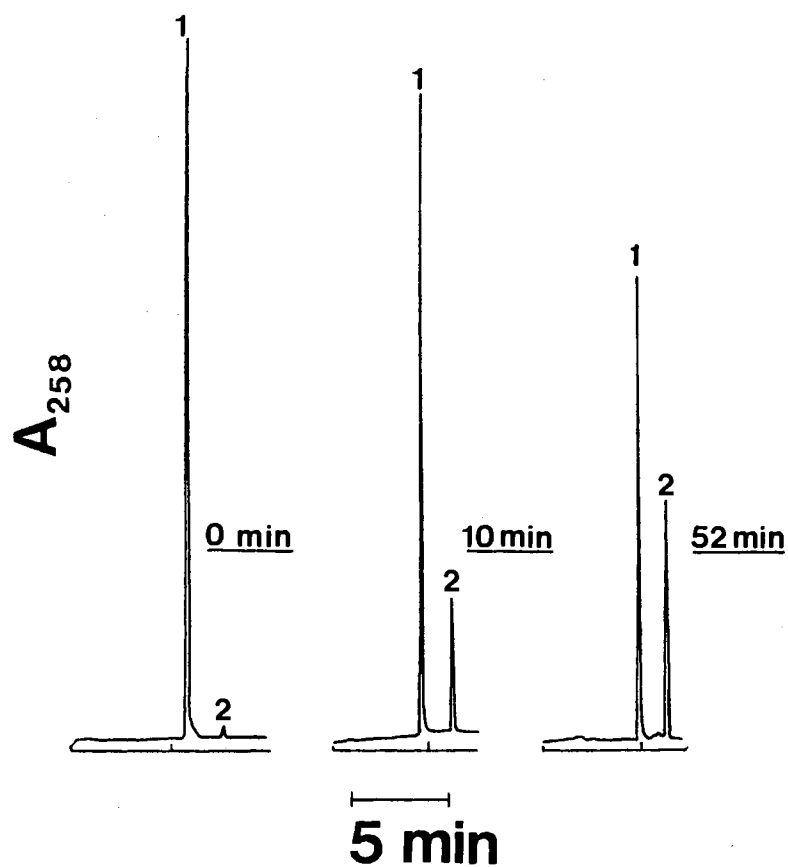
Figure 14. Typical electropherograms of ATP and ADP at various contact time with the hexokinase capillary enzyme reactor. Capillary enzyme reactor, 15 cm x 50 μm I.D.; separation capillary, fuzzy polyether coating, 30 cm (to the detection point), 64 cm (total length) x 50 μm I.D.; substrate introduction, hydrodynamic mode; enzymic reaction was carried out using gravity driven flow; separation step, as the plug of the reaction mixture entered the separation capillary, the enzyme reactor was disconnected and the voltage was turned on to 20 kV; background electrolyte, 0.1 M acetate containing 20 mM glucose and 10 mM Mg^{2+}, pH 5.0.

reactor --> CZE can be used to locate the ATP peak through its partial conversion to ADP and therefore can serve to confirm the presence or absence of ATP in a complex biological matrix.

Adenosine Deaminase Capillary Enzyme Reactor

Adenosine deaminase is a highly specific enzyme that catalyzes the deamination of adenosine to inosine with the liberation of NH3 as follows [28]:

$$\text{adenosine} + H_2O \xleftrightarrow{\quad ADA \quad} \text{inosine} + NH_3 \qquad (5)$$
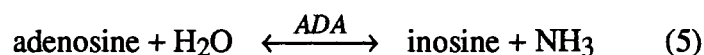
It was successfully immobilized on the inner walls of a 15 cm long fused-silica capillaries as described in experimental. The enzymic reaction was examined with a thin plug of an equimolar mixture of adenosine and inosine using 0.1 M phosphate, pH 6.5, as the background electrolyte. Figure 15 a and b illustrates the electropherograms of this mixture obtained on an interlocked polyether capillary in the absence or presence of the ADA-capillary enzyme reactor, respectively. The enzymic reaction and the separation were carried out simultaneously at a field strength of 190 V/cm without disconnecting the enzyme reactor. Thus, the higher retention time of the inosine solute in Fig. 15b is simply the result of the extra length of the capillary enzyme reactor that the solute has to migrate. As can be seen in Fig. 15, for a short contact time of ca. 10 min, complete conversion of adenosine to inosine was obtained from a single pass through the reactor as manifested by the disappearance of the adenosine peak and a proportional increase in the peak height of inosine.

Since the enzymic reaction and separation were carried out simultaneously using tandem ADA-capillary enzyme reactor → CZE, it was necessary to determine the effects of coupling a capillary enzyme reactor to a separation capillary both having different magnitude and sign of zeta potentials. Unlike in the case of HK-capillary enzyme reactor→ CZE where the direction and magnitude of the flow was mostly determined by spermine,
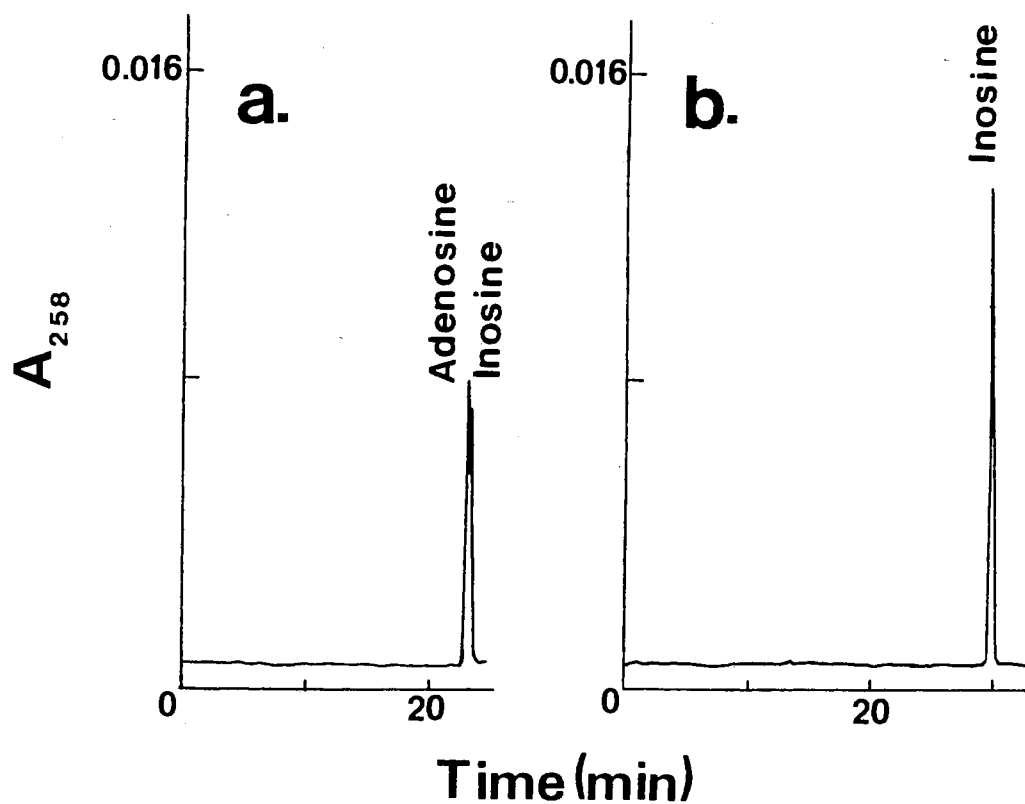
Figure 15. Typical electropherograms of an equimolar mixture of adenosine and inosine obtained by CZE alone (a) or by tandem ADA-capillary enzyme reactor → CZE (b). Capillary enzyme reactor, 15 cm x 50 μm I.D.; separation capillary, interlocked polyether coating, 30 cm (to the detection point), 64 cm (total length) x 50 μm I.D.; substrate introduction, electromigration mode; tandem enzymic reaction-CZE was carried out at the same field strength, 190 V/cm; background electrolyte, 0.1 M phosphate, pH 6.5.

in the case of ADA-capillary enzyme reactor cum CZE, the buffer did not contain any additive that would almost exclusively control the magnitude and direction of the flow. When operating the tandem capillary enzyme reactor → CZE under electromigration mode, the net electroosmotic flow of the tandem system was a function of the isoelectric point of the immobilized enzyme. In fact, as shown in table I, at pH 6.5, i.e., at pH higher than the isoelectric point of ADA (pI = 4.50-5.05), no significant change in the magnitude of the electroosmotic flow was observed upon connecting the capillary enzyme

TABLE I.

VALUES OF THE ELECTROOSMOTIC FLOW-RATE, EOF, AND PLATE HEIGHT, H, MEASURED FROM PHENOL PEAK.

The measurements were performed on interlocked polyether capillaries, I-200, and tandem ADA capillary enzyme reactor-interlocked polyether capillary, ADA → I-200, at various pH of the running electrolyte. ADA-capillary enzyme reactor; 15 cm total length x 50 μm I.D., connected to an interlocked polyether capillary of 64 cm (total length) and 30 cm to the detection point; I-200 capillary, two connected interlocked polyether capillaries of 15 and 64 cm in length, respectively; electrolytes, 0.1 M phosphate at different pH; field strength, 190 V/cm.

Capillary type	pH 6.50		pH 5.50		pH 5.00		pH 4.50	
	EOF (nL/min)	H (μm)	EOF (nL/min)	H (μm)	EOF (nL/min)	H (μm)	EOF (nL/min)	H (μm)
I-200	37.5	8.47	29.9	10.1	17.7	12.8	8.0	19.0
ADA-->I-200	36.3	8.18	30.4	10.3	12.6	18.6	--	--

reactor to the separation capillary in series. However, as the pH of the running electrolyte approached the isoelectric point of the immobilized protein, a continuous drop in the electroosmotic flow was detected. The electroosmotic flow was reduced by 30% at pH 5.0 and at pH 4.5 there was practically no flow. This can be attributed in part to the fact that the net charge of the immobilized protein becomes positive at a pH lower than its isoelectric point. It should be noted that the unreacted amino groups of the aminopropylsilyl coating could also contribute to the reduction of the flow and inverting its direction at pH 4.5. As can be seen in Table I, the plate height measured from the peak of phenol increased from 10.3 to 18.6 μm upon decreasing the pH of the running electrolyte from 5.5 to 5.0, respectively. This is because the solute stayed longer time in the capillary. These study revealed interesting fundamental points concerning the operation of capillary with immobilized enzymes on the inner walls in tandem with CZE. Since the flow was unaffected at the pH of maximum enzyme activity (i.e., pH 6.5), such an arrangement can be exploited without any adverse effects on separation.

The ADA-capillary enzyme reactor converted its substrate to a product that is more readily separated from other nucleosides. Figure 16a depicts the electropherogram of a mixture of 3 nucleosides, namely cytidine, adenosine and inosine. Under these conditions both cytidine and adenosine practically coeluted but were resolved from inosine. However, after passing the mixture through the ADA-capillary enzyme reactor, two well resolved peaks for cytidine and inosine were obtained, see Fig. 16b. Besides playing the role of peak locator, the ADA-capillary enzyme reactor can facilitate the quantitative determination of the analyte of interest. For instance, in situations similar to Fig. 16, the cytidine solute can be determined with good accuracy, since the previously overlaping peak of adenosine has been completely converted to inosine. In addition, the increase in the peak height of inosine can be used for the quantitative determination of adenosine.

It should be noted that the conversion of adenosine to inosine was complete even when the ADA-capillary enzyme reactor was shortened to 3 cm, which correspond to a
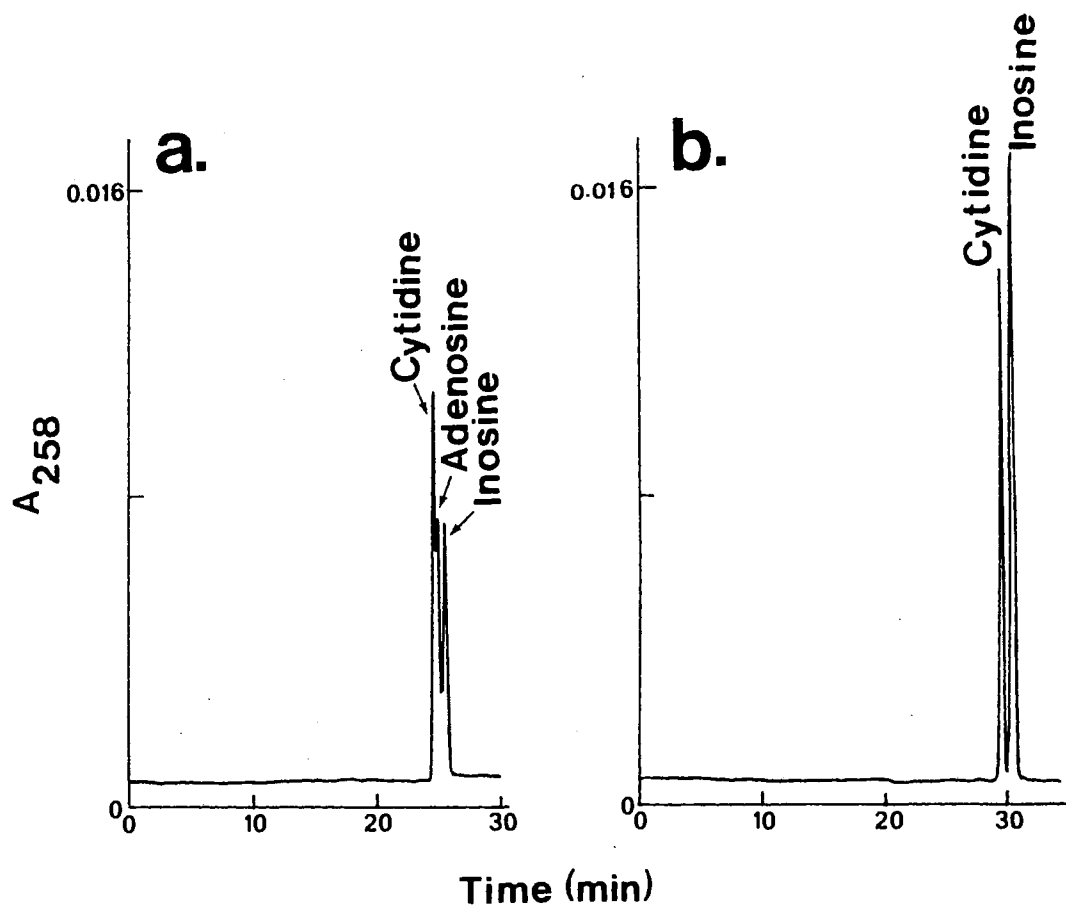
Figure 16. Typical electropherograms of a mixture of cytidine, adenosine and inosine obtained by CZE alone (a) or by tandem ADA-capillary enzyme reactor → CZE (b). Other conditions are as in Fig. 15.

contact time of ca. 2 min with the enzyme reactor. From this finding, and provided that the enzymic reactions are kinetically favored, various short capillary enzyme reactors having different immobilized enzymes can be connected in series at the inlet of a separation capillary and may prove useful in the specific analysis of different solutes in a complex biological mixture.

Conclusions

In summary, the coupling of immobilized capillary enzyme reactors to capillary zone electrophoresis has proved suitable in the area of nucleic acids. The coupled format, which we refer to as enzymophoresis can be regarded as separation-based sensors with superimposed selectivities. While the enzyme provides the selective conversion of the substrates, CZE with its unique selectivity separates and detects the products. The various concepts developed and tested in this report can be transposed to electrophoretic systems involving other types of species of relevance to many areas of the life sciences and biotechnology. The enzymophoresis systems in miniature have provided the following: (i) repeated use and long term stability of enzymes, (ii) conversion of unseparable analytes to well resolved products, (iii) peak identification of the analyte of interest, (iv) simultaneous synthesis and separation of ng quantities of biological species, (v) improved the reliability of CZE in the quantitative determination of analytes, and (vi) on-line digestion and mapping of biopolymers. The fact that enzymophoresis involving coupled HCER-CZE lends itself to automation will add another dimension to the capability of CZE in many areas of the life sciences.

Acknowledgements

References

1. P. R. Brown, *J. Chromatogr.*, 52 (1970) 257.

2. P. Manson and D. Combes, *Methods Enzymol.*, 137 (1988) 584.

3. L. D. Bowers, *Anal. Chem.*, 58 (1976) 513A.

4. L.D. Bowers and W.D. Bostick in F. Frei and J.F. Lawrence (eds), *Chemical Derivatization in Analytical Chemistry*, Vol 2, Plenum Press, New York, 1982, p.97.

5. L. Dalgaard, *Trends Anal. Chem.*, 5 (1986) 185.

6. K. Shimada, T. Oe, and T. Nambara, *J. Chromatogr.*, 492 (1989) 345.

7. L. D. Bowers and P. R. Johnson, *Biochim. Biophys. Acta*, 161 (1981) 111.

8. Z. El Rassi and C. Horvath, *J. Chromatogr.*, 266 (1983) 319.

9. K. A. Cobb and M. Novotny, *Anal. Chem.*, 61 (1989) 2226.

10. W. Nashabeh and Z. El Rassi, *J. Chromatogr.*, 536 (1991) 31.

11. W. Nashabeh and Z. El Rassi, *J. Chromatogr.*, 600 (1992) 279.

12. F. I. Onuska, M. E. Comba, T. Bistricki and R. J. Wilkinson, *J. Chromatogr.*, 142 (1977) 117.

13. R.A. Wallingford and A.G. Ewing, *Adv. Chromatogr.*, 29 (1989) 1.

14. J. Cai and Z. El Rassi, *J. Liq. Chromatogr.*, 15 (1992) 1179.

15. A. D. McLaren and L. Packer, *Adv. Enzymol.*, 28 (1975) 61.

16. C. Horvath and J. M. Engasser, *Biotechnol. Bioeng.*, 16 (1974) 909.

17. V. Dolnik, J. Liu, J. F. Banks, Jr and M. Novotny, *J. Chromatogr.*, 480 (1989) 321.

18. T. Uchida and F. Egami, *Methods Enzymol.*, 12 (1967) 228.

19. H. Hayashi and F. Egami, *J. Biochem.*, (tokyo) 53 (1963) 176.

20. P. R. Whitfield and H. Witzel, *Biochim. Biophys. Acta*, 72 (1963) 338.

21. L. W. Mclaughlin and E. Craesen, *J. Liq. Chromatogr.*, 5 (1982) 2061.

22. K. Sato-Asano, *J. Biochem. (Tokyo)*, 48 (1960) 284.

23. S. Irie, T. Itoh, T. Ueda, and F. Egami, *J. Biochem. (Tokyo)*, 68 (1970) 163.

24. H. Ito, M. Hagiwara, K. Takahashi and I. Ichikizaki, *J. Biochem.,(Tokyo)*, 82 (1977) 877.

25. W. Lamprecht and I. Trantschold in H.U. Bergmeyer (ed), *Methods of Enzymatic Analysis*, Academic Press, New York, 1963, pp. 543-551.

26. D. Voet and J.G. Voet, *Biochemistry*, Wiley, New York, 1990, pp. 430-431.

27. C.J.O.R. Morris and P. Morris, *Separation Methods in Biochemistry*, 2nd edition, Wiley, New York, 1976, p. 721.

28. H. Mollering and H.U. Bergmeyer in H.U. Bergmeyer (ed), *Methods of Enzymatic Analysis,* Academic Press, New York, 1965, pp. 491-494.

VITA

WASSIM ABDEL-HAMID NASHABEH

Candidate for the Degree of

Doctor of Philosophy

Thesis: NEW APPROACHES IN HIGH PERFORMANCE CAPILLARY ELECTROPHORESIS OF BIOLOGICAL SUBSTANCES

Major Field: Chemistry

Biographical:

Personal Data: Born in Tripoli, Lebanon, January 01, 1968, the son of Abdel-Hamid Nashabeh and Jamile Chafic.

Education: Graduated fron College des Freres High School, Tripoli, Lebanon; received Bachelor of Science Degree in Chemistry from the American University of Beirut, Beirut, Lebanon in 1988; completed requirements for the Doctor of Philosophy degree at Oklahoma State University in May, 1993.

Professional Experience: August 1989 to present, graduate research and teaching assistant, Oklahoma State University.

Professional Organization: American Chemical Society, Phi Lambda Upsilon.